

# Internally Contracted Multireference Coupled Cluster Method and Normal-Order-Based Automatic Code Generator

by

Liguo Kong

A thesis  
presented to the University of Waterloo  
in fulfilment of the  
thesis requirement for the degree of  
Doctor of Philosophy  
in  
Chemistry

Waterloo, Ontario, Canada, 2009

©Liguo Kong 2009

I hereby declare that I am the sole author of this thesis.

This is a true copy of the thesis, including any required final revisions, as accepted by my examiners. I understand that my thesis may be made electronically available to the public.

## Abstract

Single reference coupled cluster theory has been established as the method of choice for calculating electronic properties of small-to-medium size molecules. However, in typical multireference cases, such as bond breaking processes, biradicals, excited states, very high order excitations may be needed in the cluster operator to obtain reliable and accurate results, which is not practical due to the rapidly growing computational costs. Although there has been much effort to extend the applicability of single reference methods, there is little doubt that genuine multireference methods are indispensable.

The method we are developing, the State Specific Equation of Motion Coupled Cluster (SS-EOMCC) method, generalizes the state universal Equation of Motion Coupled Cluster (EOMCC) methods to a state specific version. SS-EOMCC works for both ground states and excited states. It is rigorously spin-adapted. The cluster operator amplitudes are solved, taking the complete-active-space self-consistent-field function as the reference function. The differential relaxation effects are taken into account by diagonalizing the transformed Hamiltonian in the multireference configuration interaction singles (MRCIS) space. To implement the method, we developed an automatic program generator, the details of which are presented.

The strategy used in approximating residual equations in SS-EOMCC is based on a novel normal order theory, which is a generalization of traditional particle-hole formalism based normal order theory. We discuss normal order theory in a general context, start with the version developed by Mukherjee and Kutzelnigg, and we furnish an algebraic proof for the corresponding contraction rules. Then we proceed to show how our normal order theory works.

Finally we present the benchmark results to gauge the SS-EOMCC method. We calculate the  $^3\Sigma_u^-$  state of  $F_2$  to examine the behavior of the method for single reference systems, and study the singlet states of  $H_2O$ ,  $CO$  and  $N_2$  to test its performance for multireference systems. In addition, we illustrate the effect of a perturbative correction, which attempts to alleviate the redundancy issue. We also apply the method to study the energetics of end-on and side-on peroxide coordination in ligated  $Cu_2O_2$  models, where SS-EOMCC[+2] employing a small active space achieves quite accurate results.

The final diagonalization of the transformed Hamiltonian in the MRCIS space is expensive and limits the applicability of the method. We attempt to develop a cheaper internally contracted multireference coupled cluster method by introducing semi-internal excitation operators in the cluster operator such that the final diagonalization can be confined within the active space, but the results are not satisfactory yet.

The Jeziorski-Monkhorst (JM) ansatz has been studied extensively, and different ways to resolve the redundancy issue have been explored. We analyze these JM-ansatz based methods, derive them in a simple way to disclose their connections transparently, and point out some problem in these methods. Another issue of general interest which is examined in the thesis is orbital invariance. For single reference methods the invariance property is usually clear, but this is not always the case for multireference methods. We analyze this problem from the tensor theory point of view, and propose a practical self-consistency-checking algorithm to determine whether a method is orbital invariant or not. We apply the algorithm to different methods, in particular, demonstrating the lack of the invariance property for JM-ansatz based methods.

## Acknowledgements

The four years I spent at Waterloo as a graduate student were the happiest time of my life. Fighting with fundamental problems and struggling to understand motions of electrons certainly gives me enormous pleasure. However, the foremost happiness comes from communicating with good people that I had such good luck to get to know.

I am deeply grateful to my supervisor Professor Marcel Nooijen for uncountable reasons. He brought me to the fascinating field of electronic structure theory and walked me through the very beginnings, when I was just as much worried as ignorant. He always helps me out without reservation when I have difficulties, whether scientific or personal. If I were to single out two aspects I appreciate the most, I must say: freedom and encouragement. I am encouraged and given the freedom to pursue ideas in which I am interested, whether they are project-related or not. I am never pushed to finish something quickly; rather I am given ample time to think through and think independently until I find the way by myself. Whenever I get some new idea and rush to his office, Marcel unfailingly shows enthusiasm and tries to find something meaningful, even when my idea is not entirely correct. This is one of his “invariant” properties. He is willing to discuss at all times, he can grasp the points you are striving to make and analyze them very clearly. I thoroughly enjoyed these informal conversations, which become an invaluable channel of learning. I learned so much from Marcel: fight to get to the bottom of questions, look at the same problem from different angles, never take things for granted, be ready to listen carefully even on issues with which you are thoroughly familiar, and the most important, have the utmost dedication to science.

In the theory group, Professors Robert Le Roy and Fred McCourt are our constant source of strength. In addition to the scientific consultations they provided, I have great gratitude to them also because they give precious advice on career choices and are ready to share their wisdom whenever needed. Along with Marcel and other people, they are welcoming, they show us around, and they work hard to make this area comfortable and an ideal place for scientific research. I am also delighted to meet the recently arrived group of Professor Pierre-Nicholas Roy, and greatly enjoyed conversations with them.

I thank Professor John Goddard and Josef Paldus for accepting to serve on my Ph.D. committee. I had the pleasure of talking with Professor Paldus a few times, and the communications are always inspiring to me. I also thank Professor Norbert Lütkenhaus and Dr. Karol Kowalski for their careful review of the thesis.

Interacting with excellent colleagues is another great source of happiness. I admire K. R. Shamasundar for his knowledge, and was eager to seek his opinion when I found something interesting. Dominika Zgid was with me for most of my Ph.D. period. She accompanied me through all the ups and downs, and helped me to adjust myself at different stages of my life. I also had a lot of interesting discussions with Ondrej Demel and Bijoy Dey. Ondrej is a man in peace, and he helped me to form a more healthy attitude towards life. Hui Li came to Waterloo at the same time as me, and we have worked and played together since then. Our friendship is forged as time goes on. I thank Yiye Huang for helping me with various computer problems. By luck I got to know many talented younger colleagues: Mukto Akash, Mathew Anthony Badali, Nikesh Dattani, Robert Henderson, Lee Huntington, Christopher Leon and David Pitkanen. We share reading experience and exchange views on a broad range of topics, and it has been a great joy to talk with them.

I am thankful to Cathy van Esch, our departmental secretary. This forever warm-hearted lady does a wonderful organizational job and helps people wholeheartedly. Indeed, she is so nice that sometimes I even approach her with personal problems, and she again tries her best to help me out.

I had the pleasure to meet Professor Debashis Mukherjee in 2007, and since then we have been talking extensively. His short stays in Waterloo proved especially beneficial to me. After every occasion of talking with him, I feel refreshed. Although burdened with administrative responsibilities, he manages to talk to me whenever I approach him with questions. He was also extremely hospitable in inviting me to Kolkata and making me feel at home there, an experience that I will never forget.

I shall thank my family for their love, understanding and support. I also thank Hong, my wife. It is my great fortune to meet and marry her; she brings a different meaning to my life.

This thesis is dedicated to Professor Debashis Mukherjee  
who greatly encouraged and inspired me.

# Contents

<b>List of Tables</b>	<b>xii</b>
<b>List of Figures</b>	<b>xiii</b>
<b>1 Introduction</b>	<b>1</b>
1.1 Coupled cluster theory . . . . .	1
1.2 Scope of the thesis . . . . .	8
<b>2 Jeziorski-Monkhorst ansatz</b>	<b>12</b>
2.1 Grouping . . . . .	13
2.1.1 H1E1 . . . . .	17
2.1.2 H1E2 . . . . .	18
2.1.3 H2E1 . . . . .	19
2.1.4 H2E2 . . . . .	19
2.2 Transformation of Projection Manifold . . . . .	19
2.3 A Problem with These Methods, and Comparisons with MRexpT . . . . .	21
2.4 Conclusion . . . . .	24
<b>3 Orbital invariance issue</b>	<b>26</b>
3.1 Hartree-Fock, Single Reference CI and CC . . . . .	32
3.2 CASSCF and MRCI . . . . .	36
3.3 CASCC and CCSDt . . . . .	39



3.4	MRCC: JM-ansatz based methods . . . . .	44
3.4.1	Residual equation . . . . .	44
3.4.2	Wavefunction and Energy . . . . .	46
3.5	Conclusion . . . . .	49
<b>4</b>	<b>State Specific Equation of Motion Coupled Cluster Method</b>	<b>50</b>
4.1	General framework . . . . .	50
4.2	Appearance of density matrices . . . . .	55
4.3	Convergence Scheme . . . . .	58
4.3.1	Solving the near-singular non-linear equations . . . . .	58
4.3.2	Orbital energies in the zeroth order Hamiltonian . . . . .	60
4.3.3	Singular perturbative correction . . . . .	63
<b>5</b>	<b>Normal order and generalized Wick theorem</b>	<b>66</b>
5.1	Antisymmetrization operator . . . . .	69
5.2	$\lambda$ -normal order . . . . .	73
5.3	Generalized Wick Theorem . . . . .	75
5.4	Proof . . . . .	77
5.4.1	$T_2 + T_3 - T_4$ . . . . .	79
5.4.2	$T_1$ . . . . .	81
5.4.3	$T_{1a} + T_{1b}$ . . . . .	83
5.5	Extension . . . . .	84
5.6	$\gamma$ -normal order . . . . .	85
<b>6</b>	<b>Automatic program generator</b>	<b>92</b>
6.1	Obtain Equations from Normal Order Theory . . . . .	93
6.2	Equation Derivation . . . . .	94
6.2.1	Term representation: hierarchical <i>class</i> structure . . . . .	94
6.2.2	Generalized Wick Theorem . . . . .	95
6.2.3	Canonicalization . . . . .	100

6.3	Generating Fortran Codes . . . . .	103
6.3.1	Factorization . . . . .	103
6.3.2	Multiplication and addition subroutines . . . . .	108
6.3.3	Minimize the number of intermediates . . . . .	112
6.4	Conclusion . . . . .	112
<b>7</b>	<b>Benchmark results</b>	<b>114</b>
7.1	Triplet state of $F_2$ . . . . .	115
7.2	General active spaces: $N_2$ , $H_2O$ and $CO$ . . . . .	115
7.3	Effect of a perturbative correction . . . . .	124
7.4	Conclusions . . . . .	128
<b>8</b>	<b>Ligated <math>Cu_2O_2</math> models</b>	<b>134</b>
8.1	Computational Details . . . . .	136
8.2	$^1A_g$ states of $Cu_2O_2^{2+}$ ( <b>0</b> ) and $\{(H_3N)Cu\}_2O_2^{2+}$ ( <b>1</b> ). . . . .	137
8.3	Effect of Brueckner orbitals. . . . .	140
8.4	Convergence of EOMCC[+2] w.r.t. reference space . . . . .	141
8.5	Neighboring states . . . . .	142
8.6	mrSF-EOMCC. . . . .	146
8.7	Conclusions . . . . .	146
<b>9</b>	<b>Beyond SS-EOMCC: more cost-effective solutions</b>	<b>148</b>
9.1	Internally contracted multireference coupled cluster method (ic-MRCC): ansatz . . . . .	149
9.2	ic-MRCC: residual equation . . . . .	151
9.3	ic-MRCC: $h$ -normal order . . . . .	153
9.4	ic-MRCC: $\gamma$ -normal order . . . . .	153
9.5	Final remarks . . . . .	156
	<b>APPENDICES</b>	<b>158</b>
<b>A</b>	<b>Supporting information</b>	<b>159</b>



# List of Tables

4.1	The excitation energies of the first four singlet and triplet states of ozone in the PBS basis set . . . . .	63
7.1	MAE's and NPE's for different methods . . . . .	124
8.1	Absolute energy (Hartree) of $\mathbf{0}_F$ structures with BS1 . . . . .	138
8.2	$^1A_g$ state relative energy (kcal·mol <sup>-1</sup> ) of $\mathbf{0}_F$ structures with BS1 . . . . .	139
8.3	Absolute energy (Hartree) of $\mathbf{1}_F$ structures with BS1 . . . . .	139
8.4	$^1A_g$ state relative energy (kcal·mol <sup>-1</sup> ) of $\mathbf{1}_F$ structures with BS1 . . . . .	140
8.5	$^3B_g$ state relative energy (Hartree) of $\mathbf{0}_F$ and $\mathbf{1}_F$ structures with BS1 . . . . .	145
A.1	Comparison with UCCSD(T) for F <sub>2</sub> $^3\Sigma_u^-$ state in the cc-pVTZ basis set . . . . .	160
A.2	Comparison with MRCI+Q for the N <sub>2</sub> $^1\Sigma_g$ state in the cc-pVDZ basis set . . . . .	161
A.3	Comparison with MRCI+Q for the N <sub>2</sub> $^1\Sigma_g$ state in the cc-pVTZ basis set . . . . .	162
A.4	Comparison with MRCI+Q for the H <sub>2</sub> O $^1A_1$ state in the cc-pVDZ basis set . . . . .	163
A.5	Comparison with MRCI+Q for the H <sub>2</sub> O $^1A_1$ state in the cc-pVTZ basis set . . . . .	164
A.6	Comparison with MRCI+Q for the CO $^1A_1$ state in the cc-pVDZ basis set . . . . .	165
A.7	Comparison with MRCI+Q for the CO $^1A_1$ state in the cc-pVTZ basis set . . . . .	166

# List of Figures

5.1	Illustrative diagrams . . . . .	80
6.1	$A_{wx}^{rz} \times B_{vy}^{wx} \times C_{su}^{vt} \times D_{tr}^{qs}$ contraction pattern . . . . .	107
7.1	Energy difference from CCSD(T) for $F_2$ $^3\Sigma_u^-$ state . . . . .	116
7.2	Illustration of certain triple excitations present in SS-EOMCC[+2] . . . . .	117
7.3	Comparison with MRCI+Q for $N_2$ ground state in the cc-pVDZ basis set . . . . .	118
7.4	Comparison with MRCI+Q for $N_2$ ground state in the cc-pVTZ basis set . . . . .	119
7.5	Comparison with MRCI+Q for CO ground state in the cc-pVDZ basis set . . . . .	120
7.6	Comparison with MRCI+Q for CO ground state in the cc-pVTZ basis set . . . . .	121
7.7	Comparison with MRCI+Q for $H_2O$ ground state in the cc-pVDZ basis set . . . . .	122
7.8	Comparison with MRCI+Q for $H_2O$ ground state in the cc-pVTZ basis set . . . . .	123
7.9	MAE's of different methods for different systems . . . . .	125
7.10	NPE's of different methods for different systems . . . . .	126
7.11	Test of the effect of perturbative correction for $N_2$ in the cc-pVDZ basis set: discarded t2-amplitudes for different thresholds . . . . .	129
7.12	Test of the effect of perturbative correction for $N_2$ in the cc-pVDZ basis set: deviations for different thresholds . . . . .	130
8.1	Binding motifs for $Cu_2O_2$ . . . . .	136
8.2	Model compounds . . . . .	136

8.3	$^1A_g$ state relative energy vs F for <b>0</b> at selected levels of theory . . . . .	138
8.4	$^1A_g$ state relative energy vs F for <b>1</b> at select levels of theory . . . . .	139
8.5	$^1A_g$ state relative energy vs F for <b>0</b> from SS-EOMCC . . . . .	141
8.6	Absolute energy vs F for different states of <b>0</b> . . . . .	142
8.7	Absolute energy vs F for different states of <b>1</b> . . . . .	143
8.8	Relative energy vs F for $^3B_g$ state of <b>0</b> . . . . .	144
8.9	Relative energy vs F for $^3B_g$ state of <b>1</b> . . . . .	145
9.1	Comparison with FCI for HF $^1\Sigma^+$ state in the 6-31G** basis set. . . . .	156
9.2	Comparison with MRCI+Q for the N <sub>2</sub> ground state in the cc-pVDZ basis set. . . . .	157

# Chapter 1

## Introduction

### 1.1 Coupled cluster theory

*ab initio* quantum chemistry methods aim to solve the Schrödinger equation

$$\hat{H}|\Psi\rangle = E|\Psi\rangle. \quad (1.1)$$

The full Hamiltonian includes the kinetic and potential energies of the nuclei and electrons:

$$\hat{H} = \sum_{\alpha} -\frac{1}{2m_{\alpha}}\nabla_{\alpha}^2 + \sum_i \left(-\frac{1}{2}\nabla_i^2 - \sum_{\alpha} \frac{Z_{\alpha}}{r_{\alpha i}}\right) + \sum_{\alpha < \beta} \frac{Z_{\alpha}Z_{\beta}}{r_{\alpha\beta}} + \sum_{i < j} \frac{1}{r_{ij}}, \quad (1.2)$$

where  $\alpha$  and  $\beta$  are nucleus indices,  $i$  and  $j$  are electron indices,  $Z_{\alpha}$  and  $Z_{\beta}$  are nuclear charges,  $r_{\alpha\beta}$  is the distance between nuclei  $\alpha$  and  $\beta$ , and  $r_{ij}$  is the distance between electrons  $i$  and  $j$ .

It is difficult to solve the full Schrödinger equation for both nuclei and electrons. Mostly, the Born-Oppenheimer approximation is employed, and at each nuclear configuration, we solve the electronic Schrödinger equation and obtain the electronic state energies (the energies at different nuclear configurations provide a potential energy hyper-surface on which the nuclei move and nuclear dynamics can then be studied).

The electronic Schrödinger equation has the form:

$$\hat{H}_{\text{elec}}|\Psi_{\text{elec}}\rangle = E_{\text{elec}}|\Psi_{\text{elec}}\rangle, \quad (1.3)$$

where

$$\hat{H}_{\text{elec}} = \sum_i \left( -\frac{1}{2}\nabla_i^2 - \sum_{\alpha} \frac{Z_{\alpha}}{r_{\alpha i}} \right) + \sum_{i<j} \frac{1}{r_{ij}}. \quad (1.4)$$

Since in the thesis we only deal with the electronic Schrödinger equation, we drop the subscripts in the above equation to simply notation. That is, the electronic Schrödinger equation itself is also written as

$$\hat{H}|\Psi\rangle = E|\Psi\rangle, \quad (1.5)$$

and there should be no confusion arising.

Suppose that we have obtained a set of molecular orbitals  $\{\phi_1, \phi_2, \dots, \phi_k\}$  for a system of  $n$  electrons (e.g., from a Hartree-Fock calculation). Then we can construct a many-electron determinantal basis  $\{\Phi_0, \Phi_1, \Phi_2, \dots\}$  by distributing the  $n$  electrons over the  $k$  spin orbitals  $\{\phi_1, \phi_2, \dots, \phi_k\}$  (to simplify the discussion, here we neglect the spin and spatial symmetry constraints). Therefore the dimension of the many-electron basis is  $\binom{k}{n}$ . In principle an infinite number of orbitals are needed to get a complete orbital basis, and correspondingly a complete many-electron basis, but for practical reasons we always adopt a finite orbital basis in numerical computations. Mostly, the larger the basis (the more orbitals), the more expensive the computations, the more accurate the results. To obtain computational results converged with respect to the basis is a non-trivial issue, and developing fast convergent basis sets is so far a topic under active study.

In *ab initio* quantum chemistry, second-quantization is carried out within the finite orbital basis, and we use *finite* representations of second-quantized operators (therefore the representations are approximate). With this orbital basis, we can rewrite the (electronic) Hamiltonian and the



determinants in the second-quantization language, using creation and annihilation operators [1],

$$\hat{H} = \sum_{p,q} h_p^q \hat{a}_q^p + \frac{1}{4} \sum_{p,q,r,s} V_{pq}^{rs} \hat{a}_{rs}^{pq}, \quad (1.6)$$

with

$$\hat{a}_q^p = \hat{a}_p^+ \hat{a}_q, \quad (1.7)$$

$$\hat{a}_{rs}^{pq} = \hat{a}_p^+ \hat{a}_q^+ \hat{a}_s \hat{a}_r, \quad (1.8)$$

$$h_p^q = \int \phi_p^*(\mathbf{x}) \left( -\frac{1}{2} \nabla^2 - \sum_I \frac{Z_I}{r_I} \right) \phi_q(\mathbf{x}) d\mathbf{x},$$

$$g_{pq}^{rs} = \int \frac{\phi_p^*(\mathbf{x}_1) \phi_q^*(\mathbf{x}_2) \phi_s(\mathbf{x}_2) \phi_r(\mathbf{x}_1)}{r_{12}} d\mathbf{x}_1 d\mathbf{x}_2,$$

$$V_{pq}^{rs} = g_{pq}^{rs} - g_{pq}^{sr}, \quad (1.9)$$

where  $Z_I$  is the nuclear charge,  $r_I$  the electron-nuclear separation,  $r_{12}$  the electron-electron separation and  $\mathbf{x}$  the electron coordinate including spin.

For any determinant  $|\Phi\rangle = |\phi_{i_1} \phi_{i_2} \cdots \phi_{i_n}\rangle$ , it can be written as a product of creation operators acting on the true vacuum  $|\rangle$ :

$$|\Phi\rangle = \hat{a}_{i_1}^+ \hat{a}_{i_2}^+ \cdots \hat{a}_{i_n}^+ |\rangle. \quad (1.10)$$

The antisymmetry of determinants is automatically taken into account, due to the commutation and anticommutation relations for fermions:

$$[\hat{a}_p^+, \hat{a}_q^+] \equiv \hat{a}_p^+ \hat{a}_q^+ + \hat{a}_q^+ \hat{a}_p^+ = 0, \quad (1.11)$$

$$[\hat{a}_p, \hat{a}_q] \equiv \hat{a}_p \hat{a}_q + \hat{a}_q \hat{a}_p = 0, \quad (1.12)$$

$$[\hat{a}_p^+, \hat{a}_q]_+ \equiv \hat{a}_p^+ \hat{a}_q + \hat{a}_q \hat{a}_p^+ = \delta_q^p. \quad (1.13)$$

In this thesis, we still speak of *determinants* for convenience at certain places, but in practice, all the work is done with the use of the second-quantization language, and in principle we can avoid

using the term *determinants*.

Now we briefly discuss the concepts of dynamical and non-dynamical correlation effects. We expand the wavefunction in this many-electron basis:

$$|\Psi\rangle = c_0|\Phi_0\rangle + c_1|\Phi_1\rangle + c_2|\Phi_2\rangle + \dots \quad (1.14)$$

According to the characteristic of the wavefunction, we can categorize wavefunctions into two classes: single reference wavefunctions and multireference ones. If there is one particular determinant, for example,  $|\Phi_0\rangle$ , which makes a major contribution, that is,  $|c_0|^2 \gg |c_i|^2, \forall i \neq 0$ , we call  $|\Psi\rangle$  a single reference (SR) wavefunction.<sup>1</sup> The ground states of closed-shell organic molecules are the most usual SR systems. In contrast, if more than one determinant make major contributions, we call  $|\Psi\rangle$  a multireference (MR) wavefunction. Excited states, biradicals, and transition metal compounds are typical MR systems. Mean field theories (such as the Hartree-Fock method) take account of the instantaneous interaction between every pair of electrons in an average way. We refer to the effects of the electron-electron interaction (other than this average portion) on the wavefunction as correlation effects. Roughly, we define the correlation effects contained in the few dominant determinants as non-dynamical correlations effects, and the others as dynamical correlation effects.

Usually the Hartree-Fock (HF) determinant is a fairly good approximation to the exact wavefunction, but to predict chemistry, higher accuracy is required. More sophisticated methods taking account of dynamical correlations have been developed. These methods are called correlation methods or post-Hartree-Fock (post-HF) methods. Typically an ansatz for the wavefunction is defined at first which contains unknown parameters. Then a set of equations (the so called *residual equations*) are obtained in some way for the parameters. Solving the residual equations give the parameters, and thus the wavefunction.

---

<sup>1</sup>To be precise, for a SR wavefunction, it may well happen that the contribution from  $|\Phi_0\rangle$  is smaller than the *collective* contributions from all the other determinants. That is,

$$|c_0|^2 < \sum_{i \neq 0} |c_i|^2,$$

although  $|c_0|^2 \gg |c_i|^2, \forall i \neq 0$ .

Coupled cluster (CC) theory is one of the most successful post-HF theories. For SR systems, coupled cluster theory employs an exponential ansatz for the wavefunction:

$$|\Psi\rangle = e^{\hat{T}}|\psi_{\text{ref}}\rangle, \quad (1.15)$$

where the reference function  $|\psi_{\text{ref}}\rangle$ , which takes care of non-dynamical correlation effects, is usually the mean-field Hartree-Fock determinant, and  $\hat{T}$  is the excitation operator, which takes care of dynamical correlation effects. SRCC theory [2, 3, 4, 5] has been firmly established as the method of choice for high-accuracy computations of small-to-medium size molecules [6, 7, 8, 9, 10, 11, 12, 13]. Since the implementation of the coupled cluster singles and doubles (CCSD) method [6, 14], the theory has been extended to increasingly higher order, and now there are implementations of arbitrary order excitation coupled cluster methods [15, 16, 17]. In principle, the theory can treat both single reference and multireference systems satisfactorily if sufficiently high order excitations are included, but the rapid increase of computational cost hinders the application of high level coupled cluster methods. The popular CCSD(T) [10] method represents a nice compromise between computational expense and accuracy. However, coupled cluster methods truncated at low orders have difficulties in treating multireference systems. To extend the applicability of the coupled cluster approach within the single reference framework, various possibilities have been explored. It is possible to obtain cluster amplitudes from a different source, for example, singles and doubles in Ref. [18], triples and quadruples in Refs. [19, 20]. The energy functional can be modified as in the renormalized CC approaches [21, 22, 23, 24], or the most important higher excitations can be included in the cluster operator [25, 26, 27]. Other approaches essentially change the projection manifold in obtaining the amplitude equations, as in variants of extended coupled cluster, unitary coupled cluster and expectation value coupled cluster approaches [28, 29, 30, 31, 32, 33, 34, 35, 36].

Apart from the development in this direction, theories designed explicitly to treat multireference systems have been under development since the early stage of coupled cluster theory [37, 38, 39]. In Fock Space coupled cluster theories [40, 41, 42, 43, 44, 45, 46, 47, 48, 49, 50, 51, 52, 53, 54], one universal wave operator is used for all sectors of Fock space. Starting with a parent state which has a closed-shell reference determinant, the open-shell systems are reached by chang-

ing the number of electrons from the reference state. This method is suitable for computing energy differences, such as ionization potentials and excitation energies. A second class of multi-reference coupled cluster (MRCC) methods are Jeziorski-Monkhorst (JM) ansatz based methods [55, 56, 57, 58]. This ansatz has a set of excitation operators for every determinant in the reference space. The current consensus is that for general open shell problems, the JM ansatz should be employed in a state specific fashion, which introduces a redundancy problem. Attempts to solve this problem have led to the development of different methods [59]: the Brillouin-Wigner coupled cluster method [60, 61, 62], the Mk-MRCC method [63, 64, 65, 66, 67, 68, 69, 70], and the MR-expT method [71, 72]. These methods are suitable for computing potential energy surfaces, and encouraging results have been obtained. The major issues [59] include the lack of spin-adaptation and orbital invariance [73].

To treat dynamical and non-dynamical correlation in a balanced way, it is conceptually attractive to include the dominant determinants in the reference function, which takes care of non-dynamical correlation effects, and then to build up dynamical correlation effects for each determinant, as is done in JM ansatz-based methods. The computational scaling, however, is not favorable if the number of the reference determinants is large. In contrast, the ansatz for internally contracted coupled cluster methods is more compact, which usually assumes the following form:

$$|\Psi\rangle = e^{\hat{S}}|R\rangle, \quad (1.16)$$

where  $|R\rangle$  is the reference function, and  $\hat{S}$  is the cluster operator which takes care of dynamical correlation and orbital relaxation effects. Using one universal cluster operator on the whole reference function has certain limitations. One of the major problems is the potentially unsatisfactory treatment of differential orbital relaxation effects, unless sufficiently high order semi-internal and internal excitation operators are included in  $\hat{S}$ . Here the *differential* orbital relaxation effects refer to the effects of orbital rotation of each individual active space determinant. Another drawback is that the equations for the s-amplitudes (residual equations) can be ill-defined. This problem may emerge in all methods adopting the above ansatz, and it may affect the stability and accuracy of this type of method.

In the multiconfiguration reference state coupled cluster method developed by Banerjee and Simons [74, 75], only excitations from occupied orbitals to inactive virtual orbitals are included in the cluster operator, so that the excitation operators are commutative. Therefore the differential orbital relaxation effects are not properly accounted for. In the early effort of Hoffman and Simons [76], an anti-Hermitian cluster operator  $\hat{S}$  is employed, which contains internal and semi-internal excitations, and the residual equation is defined by the stationary condition of the energy. In their approach, the energy expression  $\langle R|e^{-\hat{S}}\hat{H}e^{\hat{S}}|R\rangle$  is approximated by keeping up to quadratic terms in s-amplitudes. Mukherjee proposed an ansatz [63, 64] which is based on a multireference normal order theory [77, 78]. Physically important semi-internal excitation operators are included, and the normal order exponential ansatz leads to a particularly attractive feature of this method: residual equations automatically truncate at the quartic power of the excitation amplitudes. The more recent canonical transformation (CT) [79, 80] method by Chan and Yanai and the closely related anti-Hermitian contracted Schrödinger equation [81, 82] method by Mazziotti also use an anti-Hermitian  $\hat{S}$ , and the residual equation is obtained from projections. In addition, in the residual equation, the many-body operators from the commutator expansion of the transformed Hamiltonian  $e^{-\hat{S}}\hat{H}e^{\hat{S}}$  are approximated by one- and two-body operators by utilizing the cumulant techniques [83, 84, 85, 86, 87, 88, 89, 90, 91] at each order of the commutator expansion. Another interesting internally contracted approach is the blocked correlated coupled cluster (BCCC) method by Fang, Shen and Li [92, 93]. In BCCC, instead of orbitals, the basic construction units of the wavefunction are so called *block states*, which can be multi-determinantal functions. The relaxation and dynamical correlation effects are taken care of by  $\hat{S}$ , which includes excitations between block states. The Fock space feature of the method bears certain similarity to the density matrix renormalization group (DMRG) approach [94, 95, 96, 97, 98, 99].

EOMCC methods [100, 101, 102, 103, 104, 105] (and closely related coupled cluster linear response theory [106, 107, 108, 109, 110, 111, 112, 113], SAC-CI method [114, 115, 116], and coupled cluster Green's function method [117, 118, 119]) have been very useful for computing energy differences. Here the cluster operator is obtained for a single reference parent state, which accounts for dynamical correlation. The cluster operator is then used to transform the

Hamiltonian. Finally, the transformed Hamiltonian is diagonalized over a suitable manifold to obtain excited state energies and wavefunctions. Conceptually, the success of EOMCC methods relies on the transferability of dynamical correlation. Many extensions of excited state EOMCC (EE-EOMCC) methods have been developed, such as EA-EOMCC [120, 121], IP-EOMCC [122] (and closely related coupled cluster Green’s function method [117, 118, 119]), DIP-EOMCC [123, 124] and SF-EOMCC [125, 126]. Most of these methods generalize the definition of the single reference parent state. There are limitations to the concept, however, as it is not always possible to define a single reference parent state which is reasonably close to the target state of interest. Another issue is that EOMCC is not size-extensive, although it does satisfy the important property of core-extensivity [127] and relatedly size-intensivity [128, 129].

To summarize, different approaches have been introduced in attempting to treat MR systems, but none has been established as the method of choice which has all the desired properties: spin-adapted, size-extensive, orbital invariant, effective inclusion of orbital relaxation and differential orbital relaxation effects, and ease of convergence. In addition, computational cost is an important factor, and it can severely limit the applicability of a method. If our goal is to construct accurate potential energy surfaces, we need a method which is accurate for both SR systems and MR systems. With the consideration of the essentially different features of SR and MR wavefunctions, this requirement, which is essential for predicting chemistry, is not trivial.

## 1.2 Scope of the thesis

In the last few years we have been developing a generalization of EOMCC methods. In the State Specific Equation of Motion Coupled Cluster (SS-EOMCC) approach both orbitals and dynamical correlation are optimized for the target state, so the method is state specific. The main idea is to fold the major dynamical correlation into the transformed Hamiltonian, and to take care of non-dynamical correlation by a final diagonalization. The SS-EOMCC method is an internally-contracted multireference approach, applicable to both ground and excited states. Attractive features of the method are: (1) the SS-EOMCC wavefunction is qualitatively correct

and rigorously spin-adapted, (2) both orbitals and dynamical correlation are optimized for the target state, (3) non-dynamical correlation and differential orbital relaxation effects are taken care of by a diagonalization of the transformed Hamiltonian in the multireference configuration-interaction singles (MRCIS) space, (4) only one- and two-particle density matrices of a CASSCF reference state are needed to define equations for the cluster amplitudes, and (5) the method is invariant with respect to orbital rotations in core, active and virtual subspaces.

Properly defined equations and orbital invariance are not conditions trivially satisfied for multireference methods. In Chapter 2, we first discuss a class of important MRCC methods: Jeziorski-Monkhorst (JM)-ansatz based methods. These methods are unified according to how to group terms to eliminate the so called redundancy problem. It is found that some seemingly different methods are equivalent. It is argued that the various defining equations are not entirely proper, in the sense that the *proper residual condition* is not satisfied. This may partially rationalize the unsatisfactory performance of the various methods for single reference systems. In contrast, the MRexpT method satisfies the proper residual condition, and it is expected to outperform other JM-ansatz based methods in single reference cases.

In Chapter 3, we examine the orbital invariance issue in a general context from a tensor theory point of view. By utilizing the transformation property of second-quantized operators, and thus also of determinants, we analyze the orbital invariance property of various methods by examining the tensor property of residuals. A simple self-consistency-checking algorithm is proposed. To reveal the essential transformation property of tensors, the antisymmetry property of certain tensors is extensively used to rewrite them in contracted forms. We first establish the orbital invariance of the Hartree-Fock, single reference configuration interaction (SRCI), coupled cluster, complete-active-space self-consistent-field (CASSCF), and multireference configuration interaction (MRCI) methods, and then discuss the invariance properties of the CASCC and CCSDt methods. Finally, we demonstrate the lack of orbital invariance for JM-ansatz based methods. It appears necessary to modify the ansatz if orbital invariance is desired for this class of methods, and internal-contraction serves as one possible solution. From these discussions, the orbital invariance property for SS-EOMCC can easily be established, as is discussed briefly in Chapter 4.

Starting with Chapter 4, we elaborate on the theory of the SS-EOMCC method, how to approximate the residual equation, and the practical convergence scheme. Since we have developed a novel normal order theory ( $\gamma$ -normal order) for approximating the residual equation, and this particular normal order is closely related to traditional normal order theory and a more general one ( $\lambda$ -normal order) developed by Mukherjee and Kutzelnigg [63, 77, 78], it is desirable to have a full-fledged discussion of normal order theory, which is the content of Chapter 5. We demonstrate the relationships among different versions of normal order theory. In addition, we give an algebraic proof of the generalized Wick theorem corresponding to  $\lambda$ -normal order.

In Chapter 6, we discuss the details of the implementation of the SS-EOMCC method. Since manual implementation would be extremely tedious and prone to error, we wrote an automatic program generator (APG) in Python to facilitate the implementation. Both equation derivation and Fortran code generation mechanisms are expounded. We discuss the basic structure of the code, how different versions of generalized Wick theorems are implemented, how equations are canonicalized, how Fortran subroutines are called automatically, the factorization algorithm, and possible further improvements. A major ingredient of SS-EOMCC in general active spaces is the diagonalization of a non-Hermitian Hamiltonian in a MRCIS space. The CASSCF and MRCI programs were implemented by K. R. Shamasundar, and the code to calculate three-body density matrices and diagonalize the three-body transformed Hamiltonian was written by Ondrej Demel.

Prior applications of SS-EOMCC focused on biradical-like systems or singly bonded species, in which only one extra orbital is needed to construct the active space. SS-EOMCC has been applied to study the ground and excited states of  $O_2$  and  $F_2$ , the dissociation of LiF, and organic biradicals, such as the automerization barrier of cyclobutadiene, singlet-triplet gaps of trimethylmethylene, and the activation and reaction energies of Bergman reaction. Now the applicability of the method is extended to systems with general active spaces, and benchmark results are presented in Chapter 7. The  $^3\Sigma_u^-$  state of  $F_2$  is calculated to examine the behavior of the SS-EOMCC method for single reference systems. The singlet states of  $H_2O$ ,  $CO$  and  $N_2$  are computed to gauge the accuracy for systems with somewhat large active spaces. In addition, the effect of a perturbative correction, which attempts to alleviate the near singularity issue, is illustrated.



In Chapter 8, the method is applied to study the relative energetics of  $\mu$ -1:2(trans end-on) and  $\mu$ - $\eta^2$  :  $\eta^2$ (side-on) peroxo isomers of  $\text{Cu}_2\text{O}_2$  fragments with 0 and 2 ammonia ligands. These model systems had been shown to be problematic for multireference perturbation theory (MRPT) and density functional theory (DFT) methods. In spite of the small reference space used, SS-EOMCC gives much improved results by comparison to benchmark CR-CC results. In addition to the fully symmetric  $^1\text{Ag}$  state, the  $^1\text{Bg}$  and  $^3\text{Bg}$  states are also computed, demonstrating the complexity of the systems under study, as seen from the energy crossing at intermediate geometries. The so called spin-flip idea introduced by Krylov is tested for the model systems, and Brueckner orbitals are compared with B-CI orbitals.

In SS-EOMCC, the final diagonalization of the transformed Hamiltonian in the MRCIS space takes account of the semi-internal excitations and differential orbital relaxation effects which are missing from the cluster operator. This diagonalization is expensive, which limits the applicability of the method. In Chapter 9, we describe our endeavor to develop a cheap internally contracted MRCC (ic-MRCC) method. In ic-MRCC, semi-internal excitation operators are introduced into the cluster operator to partially compensate for the missing effects, and the final diagonalization is confined within the active space. Both  $h$ -normal order and  $\gamma$ -normal order has been attempted, and the renormalization idea has been tested. The near-singularity issue and convergence issue prove to be difficult to resolve, and the results are not satisfactory yet.

## Chapter 2

# Jeziorski-Monkhorst ansatz

In this chapter, we carry out a detailed examination of the Jeziorski-Monkhorst (JM) ansatz-based methods.<sup>1</sup> In the JM ansatz, the wave operator assumes the form:

$$\hat{\Omega} = \sum_{\mu} e^{\hat{T}_{\mu}} |\mu\rangle \langle \mu|,$$

where  $|\mu\rangle$  is any determinant in the reference function, and  $\hat{T}_{\mu}$  is the cluster operator associated with the reference determinant (in the following discussion we assume a complete active space of dimension  $M$ ). The wavefunction has the form:

$$|\Psi\rangle = \hat{\Omega} \sum_{\mu} c_{\mu} |\mu\rangle = \sum_{\mu} e^{\hat{T}_{\mu}} c_{\mu} |\mu\rangle,$$

where  $\sum_{\mu} c_{\mu} |\mu\rangle$  is the reference function. Balanced treatment of every reference determinant is among the most attractive features of the JM ansatz, in the sense that every determinant is associated with its own cluster excitation operator to take care of differential correlation and dynamical correlation effects, instead of applying one universal operator to the whole reference function, as in FSCC, EOMCC and internally contracted methods.

---

<sup>1</sup>Contents of this chapter were published in *Int. J. Quant. Chem.* **109**, 441(2009).

Inserting the ansatz into the Schrödinger equation yields:

$$\hat{H} \sum_{\mu} e^{\hat{T}_{\mu}} c_{\mu} |\mu\rangle = E \sum_{\mu} e^{\hat{T}_{\mu}} c_{\mu} |\mu\rangle$$

that is,  $\sum_{\mu} (\hat{H} - E) e^{\hat{T}_{\mu}} c_{\mu} |\mu\rangle = 0.$  (2.1)

If all the parameters are independent, there is redundancy in the ansatz in the sense that some excited determinants can be reached in multiple ways by the linear excitation of some reference determinants. The problem is how to define equations *properly* to fix the redundancy problem. There are different ways to tackle the obstacle. In this work, various JM-ansatz based methods are cast in a vector form and unified from the *grouping* point of view. It is hoped that the *hindsight reflection* may reveal the connection between different methods more transparently. This chapter is organized in the following order: Section 2.1 unifies a few JM-ansatz based methods; Section 2.2 discusses the transformed projection idea; Section 2.3 points out a possible problem present in some methods; Section 2.4 presents our conclusions.

## 2.1 Grouping

In determinantal basis,

$$|\Lambda\rangle = \sum_{\nu} (\hat{H} - E) e^{\hat{T}_{\nu}} c_{\nu} |\nu\rangle = \mathbf{0} \quad (2.2)$$

is a vector. In the following, we use  $\mu, \nu, \rho, \sigma$  ( $\ell, \kappa$ ) to denote determinants in the active (external) space and  $u$  ( $l, k$ ) to denote the *projection coefficients* of active (external) space determinants in  $|\Lambda\rangle$ . In vector form, the above equation becomes

$$\vec{\Lambda} = \begin{pmatrix} \mathbb{U}_1 \\ \mathbb{U}_2 \\ \vdots \\ \mathbb{U}_M \\ \mathbb{L}_1 \\ \mathbb{L}_2 \\ \vdots \\ \mathbb{L}_K \\ \vdots \end{pmatrix} = \begin{pmatrix} \langle \mu_1 | \sum_{\nu} (\hat{H} - E) e^{\hat{T}_{\nu}} c_{\nu} | \nu \rangle \\ \langle \mu_2 | \sum_{\nu} (\hat{H} - E) e^{\hat{T}_{\nu}} c_{\nu} | \nu \rangle \\ \vdots \\ \langle \mu_M | \sum_{\nu} (\hat{H} - E) e^{\hat{T}_{\nu}} c_{\nu} | \nu \rangle \\ \langle \ell_1 | \sum_{\nu} (\hat{H} - E) e^{\hat{T}_{\nu}} c_{\nu} | \nu \rangle \\ \langle \ell_2 | \sum_{\nu} (\hat{H} - E) e^{\hat{T}_{\nu}} c_{\nu} | \nu \rangle \\ \vdots \\ \langle \ell_K | \sum_{\nu} (\hat{H} - E) e^{\hat{T}_{\nu}} c_{\nu} | \nu \rangle \\ \vdots \end{pmatrix} = \mathbf{0}. \quad (2.3)$$

Let us assume that no pure active-active excitation operator is included, that is,

$$\langle \nu | \hat{T}_{\mu}^{(i)} | \mu \rangle = 0, \quad \forall \mu, \nu, i.$$

From

$$\mathbb{U}_i = 0 \quad (i = 1, 2, \dots, M),$$

we naturally get M equations which define the  $c_{\mu}$  coefficients:

$$\sum_{\nu} \tilde{H}_{\mu\nu} c_{\nu} = E c_{\mu}, \quad (2.4)$$

where  $\tilde{H}_{\mu\nu} = \langle \mu | e^{-\hat{T}_{\nu}} \hat{H} e^{\hat{T}_{\nu}} | \nu \rangle$ . The above is an eigenvalue equation and is adopted in all the following methods. Once the t-amplitudes are determined, the reference function can be updated by diagonalization of the matrix  $\tilde{H}_{\mu\nu}$  and thus a self-consistent procedure is obtained.

We emphasize that the above equation holds because no pure active-active excitation operator is included, so we have

$$\langle \mu | \hat{H} e^{\hat{T}_{\nu}} | \nu \rangle = \langle \mu | e^{-\hat{T}_{\nu}} \hat{H} e^{\hat{T}_{\nu}} | \nu \rangle = \tilde{H}_{\mu\nu} \quad (2.5)$$

$$\text{and } E \langle \mu | e^{\hat{T}_{\nu}} | \nu \rangle = E \delta_{\mu\nu}. \quad (2.6)$$

The problem is the fact that the projection over the linear excitation manifolds

$$\mathbb{L}_i = \langle \ell_i | \sum_{\nu} (\hat{H} - E) e^{\hat{T}_{\nu}} c_{\nu} | \nu \rangle = 0, \quad (2.7)$$

does not furnish enough equations for  $t$ -amplitudes, because some excited determinants can be reached by the linear excitation of reference determinants in multiple ways. In other words, it may happen that

$$|\ell_i\rangle = \hat{T}_{\mu}^{(j)} |\mu\rangle = \hat{T}_{\nu}^{(k)} |\nu\rangle \quad (\mu \neq \nu). \quad (2.8)$$

The usual resolution is as follows. Since  $\mathbb{L}_i$  contains contributions from all  $t_{\mu}$  and  $c_{\mu}$ , the equations are defined naturally if we could group contributions to  $\mathbb{U}$  into classes which can be *labeled* (meaning will be clear below) by reference determinants

$$\mathbb{L} = \sum_{\mu} \mathbb{L}^{\mu}, \quad (2.9)$$

and we set

$$\mathbb{L}^{\mu} = 0, \quad \forall \mu \quad (2.10)$$

(in the above equations, the subscript  $i$  for  $l$  is dropped for notational simplicity).

Following the same grouping procedure, we can correspondingly group  $\mathbb{U}$  terms into classes  $\mathbb{U} = \sum_{\mu} \mathbb{U}^{\mu}$ . Therefore the problem is converted to *how to group terms* (the MRexpT method [71, 130], which follows a different route, is discussed in Section IV). The form of  $\mathbb{L}$  itself usually presents a natural way to group terms, or we can reshuffle terms to achieve different groupings. The basic idea is to change a single summation to a double summation, and then interchange them [66].

Let us look at a few ways of grouping terms.

$$\mathbb{L} = \langle \ell | \sum_{\nu} (\hat{H} - E) e^{\hat{T}_{\nu}} c_{\nu} | \nu \rangle = \langle \ell | \sum_{\nu} \hat{H} e^{\hat{T}_{\nu}} c_{\nu} | \nu \rangle - \langle \ell | \sum_{\nu} E e^{\hat{T}_{\nu}} c_{\nu} | \nu \rangle = 0. \quad (2.11)$$

For E terms:

$$\mathbb{L} = -\langle \ell | \sum_{\mu} E e^{\hat{T}_{\mu}} c_{\mu} | \mu \rangle + \text{terms containing H} \quad (2.12)$$

$$= \sum_{\mu} -E c_{\mu} \langle \ell | e^{\hat{T}_{\mu}} | \mu \rangle + \dots$$

$$= \sum_{\mu} -E c_{\mu} \langle \ell | e^{\hat{T}_{\mu}} | \mu \rangle + \dots$$

$$= \sum_{\mu} l^{\mu} + \dots \quad (\mathbf{E1}), \quad (2.13)$$

or

$$\mathbb{L} = \sum_{\mu} -E c_{\mu} \langle \ell | e^{\hat{T}_{\mu}} | \mu \rangle + \text{terms containing H}$$

$$= \sum_{\mu\nu} -\tilde{H}_{\mu\nu} c_{\nu} \langle \ell | e^{\hat{T}_{\mu}} | \mu \rangle + \dots$$

$$= \sum_{\nu} (-c_{\nu} \sum_{\mu} \tilde{H}_{\mu\nu} \langle \ell | e^{\hat{T}_{\mu}} | \mu \rangle) + \dots$$

$$= \sum_{\mu} (-c_{\mu} \sum_{\nu} \tilde{H}_{\nu\mu} \langle \ell | e^{\hat{T}_{\nu}} | \nu \rangle) + \dots$$

$$= \sum_{\mu} l^{\mu} + \dots \quad (\mathbf{E2}). \quad (2.14)$$

In this manipulation the assumption is made again that no active-active excitation operator is included, because the relation  $E c_{\mu} = \sum_{\nu} \tilde{H}_{\mu\nu} c_{\nu}$  has been used.

For terms containing H, the above trick doesn't apply.

$$\mathbb{L} = \sum_{\mu} c_{\mu} \langle \ell | \hat{H} e^{\hat{T}_{\mu}} | \mu \rangle + \text{terms containing E} \quad (2.15)$$

$$= \sum_{\mu} l^{\mu} + \dots \quad (\mathbf{H1}) \quad (2.16)$$

Another way is to insert resolution identity:

$$\begin{aligned}
\mathbb{L} &= \sum_{\nu} c_{\nu} \langle \ell | \hat{H} e^{\hat{T}_{\nu}} | \nu \rangle + \text{terms containing E} \\
&= \sum_{\nu} c_{\nu} \langle \ell | e^{\hat{T}_{\nu}} \hat{\mathbf{1}} e^{-\hat{T}_{\nu}} \hat{H} e^{\hat{T}_{\nu}} | \nu \rangle + \dots \\
&= \sum_{\nu} c_{\nu} \langle \ell | e^{\hat{T}_{\nu}} \mathbf{Q} e^{-\hat{T}_{\nu}} \hat{H} e^{\hat{T}_{\nu}} | \nu \rangle + \sum_{\nu} c_{\nu} \langle \ell | e^{\hat{T}_{\nu}} \sum_{\mu} | \mu \rangle \langle \mu | e^{-\hat{T}_{\nu}} \hat{H} e^{\hat{T}_{\nu}} | \nu \rangle + \dots \\
&= \sum_{\mu} c_{\mu} \langle \ell | e^{\hat{T}_{\mu}} \mathbf{Q} e^{-\hat{T}_{\mu}} \hat{H} e^{\hat{T}_{\mu}} | \mu \rangle + \sum_{\mu} \left( \sum_{\nu} c_{\nu} \langle \ell | e^{\hat{T}_{\nu}} | \mu \rangle \tilde{H}_{\mu\nu} \right) + \dots \\
&= \sum_{\mu} \left( c_{\mu} \langle \ell | e^{\hat{T}_{\mu}} \mathbf{Q} e^{-\hat{T}_{\mu}} \hat{H} e^{\hat{T}_{\mu}} | \mu \rangle + \sum_{\nu} c_{\nu} \langle \ell | e^{\hat{T}_{\nu}} | \mu \rangle \tilde{H}_{\mu\nu} \right) + \dots \\
&= \sum_{\mu} l^{\mu} + \dots \quad (\mathbf{H2}) \tag{2.17}
\end{aligned}$$

The different ways of grouping are denoted by E1, E2, H1, H2. Now we can combine contributions from E terms and H terms in four ways, which correspond to four different methods, which are denoted by H1E1, H2E1, H1E2 and H2E2, respectively. The linear combination of them may also be worth trying [131, 132]. Although this may turn out to be numerically advantageous, the physical meaning or motivation of the subsequent t-amplitude equations becomes unclear. Furthermore, the exactness of the corresponding theory in the full limit deserves attention in that case.

### 2.1.1 H1E1

The simplest way to group terms is the H1E1 combination:

$$\mathbb{L}^{\mu} = c_{\mu} \langle \ell | \hat{H} e^{\hat{T}_{\mu}} | \mu \rangle - c_{\mu} E \langle \ell | e^{\hat{T}_{\mu}} | \mu \rangle = 0, \tag{2.18}$$

$$\text{that is,} \quad \langle \ell | \hat{H} e^{\hat{T}_{\mu}} | \mu \rangle = E \langle \ell | e^{\hat{T}_{\mu}} | \mu \rangle. \tag{2.19}$$

This gives the BWCC method [61, 132, 62, 133, 134, 135]. The state-specificity comes only from the dependence on energy, which is specific for a particular state. Hence the state-specificity is ‘weak’ in the sense that the residual equations are nearly decoupled. The equation is formally

close to a single reference coupled cluster equation. This method is not size-extensive.

### 2.1.2 H1E2

The H1E2 combination gives:

$$\begin{aligned}\mathbb{L}^\mu &= c_\mu \langle \ell | \hat{H} e^{\hat{T}^\mu} | \mu \rangle - c_\mu \sum_\nu \tilde{H}_{\nu\mu} \langle \ell | e^{\hat{T}^\nu} | \nu \rangle \\ &= 0,\end{aligned}\tag{2.20}$$

$$\text{that is,} \quad \langle \ell | \hat{H} e^{\hat{T}^\mu} | \mu \rangle = \sum_\nu \tilde{H}_{\nu\mu} \langle \ell | e^{\hat{T}^\nu} | \nu \rangle.\tag{2.21}$$

The size-extensivity of this method is not obvious, but it will be shown below that the above equation is *equivalent to the residual equation in the State Universal MRCC (SU-MRCC) method* [55, 57, 58], so the method is size-extensive. As for SU-MRCC, this method is state-universal because the t-amplitude equation (residual equation) does not depend on any particular state (no  $c_\mu$  appears in the equation).

For later use, we give here an example of grouping  $\mathbb{U}$  terms in the ‘H1E2’ manner.  $\mathbb{U}_\rho = \sum_\mu \mathbb{U}_\rho^\mu$  :

$$\begin{aligned}\mathbb{U}_\rho &= \langle \rho | \sum_\mu (\hat{H} - E) e^{\hat{T}^\mu} c_\mu | \mu \rangle \\ &= \sum_\mu (c_\mu \langle \rho | \hat{H} e^{\hat{T}^\mu} | \mu \rangle - c_\mu \sum_\nu \tilde{H}_{\nu\mu} \langle \rho | e^{\hat{T}^\nu} | \nu \rangle) \\ &= \sum_\mu \mathbb{U}_\rho^\mu.\end{aligned}\tag{2.22}$$

In this case,

$$\begin{aligned}\mathbb{U}_\nu^\rho &= (c_\mu \langle \rho | \hat{H} e^{\hat{T}^\mu} | \mu \rangle - c_\mu \sum_\nu \tilde{H}_{\nu\mu} \langle \rho | e^{\hat{T}^\nu} | \nu \rangle) \\ &= c_\mu (\tilde{H}_{\rho\mu} - \sum_\nu \tilde{H}_{\nu\mu} \delta_{\rho\nu}) \\ &= 0.\end{aligned}\tag{2.23}$$



### 2.1.3 H2E1

The H2E1 combination gives:

$$\begin{aligned}\mathbb{L}^\mu &= (c_\mu \langle \ell | e^{\hat{T}_\mu} \mathbf{Q} e^{-\hat{T}_\mu} \hat{H} e^{\hat{T}_\mu} | \mu \rangle + \sum_\nu c_\nu \langle \ell | e^{\hat{T}_\nu} | \mu \rangle \tilde{H}_{\mu\nu}) - c_\mu E \langle \ell | e^{\hat{T}_\mu} | \mu \rangle \\ &= 0.\end{aligned}\tag{2.24}$$

This equation looks disconnected, but it will be shown that it is *equivalent to the residual equation used in the Mk-MRCC method* [63, 64, 66, 68, 65, 136, 67, 69, 70, 137], so the method is also size-extensive. Compared to BWCC, this method (or equivalently, the Mk-MRCC method) has a stronger state-specific character in the sense that every residual equation explicitly depends on all the reference determinants.

### 2.1.4 H2E2

The H2E2 combination defines another method:

$$\begin{aligned}\mathbb{L}^\mu &= (c_\mu \langle \ell | e^{\hat{T}_\mu} \mathbf{Q} e^{-\hat{T}_\mu} \hat{H} e^{\hat{T}_\mu} | \mu \rangle + \sum_\nu c_\nu \langle \ell | e^{\hat{T}_\nu} | \mu \rangle \tilde{H}_{\mu\nu}) - c_\mu \sum_\nu \tilde{H}_{\nu\mu} \langle \ell | e^{\hat{T}_\nu} | \nu \rangle \\ &= 0.\end{aligned}\tag{2.25}$$

$$\tag{2.26}$$

This method has not previously been reported in the literature.

## 2.2 Transformation of Projection Manifold

Another way of defining equations is introduced by the transformation of the projection manifold [66]:

$$\langle l | \rightarrow \langle \tilde{l} | = \langle l | e^{-\hat{T}_\mu}.$$

(assume  $\langle \tilde{l} |$  is obtained from the excitation of  $\langle \mu |$ ).  $\hat{T}_\mu$  acts on the bra state  $\langle l |$  as an de-excitation operator. Let us denote by  $S_{\text{active}}$  the space spanned by the bra states corresponding to the reference determinants, and denote by  $S_\mu$  the space spanned by the bra state corresponding to

determinants from all possible excitations in  $\hat{T}_\mu$  of  $|\mu\rangle$ . It is not hard to see that  $\langle \tilde{l} |$  can be expanded in  $S_{\text{active}}$  and  $S_\mu$ . In particular,  $\langle \tilde{l} |$  contains contribution from  $\langle \nu |$  ( $\nu \neq \mu$ ); this is where the subtle difference between using  $\langle l |$  and  $\langle \tilde{l} |$  to define the equations arises, as will be clear below.

$$\langle \tilde{l} | = \langle l | e^{-\hat{T}_\mu} = \sum d_\nu \langle \nu | + \sum_k d_k \langle k | \quad (2.27)$$

where  $|k\rangle \in S_\mu$ .

By replacing  $\langle l |$  with  $\langle \tilde{l} |$ , the  $l^\mu$  equations are transformed into

$$\tilde{\mathbb{L}}^\mu = \sum d_\nu u_\nu^\mu + \sum_k d_k l_k^\mu. \quad (2.28)$$

We will certainly have

$$\tilde{\mathbb{L}}^\mu = 0, \quad (2.29)$$

if

$$\mathbb{U}_\nu^\mu = 0, \quad (2.30)$$

$$\text{and } \mathbb{L}_k^\mu = 0. \quad (2.31)$$

From the direct projection, we defined  $\mathbb{L}_k^\mu = 0$  (in truncated schemes, this equation still holds, again, because  $|k\rangle$  falls within the set of determinants  $\{\hat{T}_\mu^i|\mu\rangle, \forall i\}$ ). Thus if  $\mathbb{U}_\nu^\mu = 0$  is automatically satisfied, the direction projection method is theoretically equivalent to the corresponding transformed projection method.

Examining the above four ways to define equations, we find that following either H2E1, or H1E2, we automatically have

$$\mathbb{U}_\nu^\mu = 0, \quad (2.32)$$

using  $\langle \nu | e^{\hat{T}} |\mu\rangle = \delta_{\nu\mu}$  or  $\sum_\nu \tilde{H}_{\mu\nu} c_\nu = E c_\mu$  (refer to the example in the H1E2 section). Hence

using projections directly or using transformed projections are equivalent for the H2E1 and H1E2 methods. (this is not the case for the H2E2 method).

With transformed projections, we get a few ways to define equations, which might be denoted by t-H1E2, t-H2E1 and t-H2E2 (t means ‘transform’); t-H1E1 leads to unreasonable equation, so it is discarded. Due to the above argument, only t-H2E2 is different from the corresponding untransformed method.

t-H2E1 defines the Mk-MRCC method and t-H1E2 defines the SU-MRCC method. Since it has been shown that H2E1 and H1E2 are equivalent to t-H2E1 and t-H1E2, respectively, this establishes the equivalence between H2E1/H1E2 and Mk-MRCC/SU-MRCC, respectively, as claimed in previous sections. The t-H2E2 method ((Eq. (22) in Ref. [66])) has nearly the same first order expression for t-amplitudes as does the Mk-MRCC method, since the denominator is the same, so it should be free from the intruder state problem. The method is also size-extensive.

## 2.3 A Problem with These Methods, and Comparisons with MRexpT

Let us denote by  $L_\mu$  the set of excited determinants which can be reached by  $\hat{T}_\mu$  (it contains a set of excitation operators), and the union of the sets by  $L$ , that is,

$$L = \bigcup L_\mu \bigcup L_\nu \bigcup \dots$$

The number of elements in  $L$  is much larger than the number of elements in any particular subset  $L_\mu$ . Considering that excitations involving only core and virtual orbitals are far larger in number than those involving active orbitals (unless the number of active orbitals is comparable to that of core orbitals), we approximately have

$$|L| \approx M \times |L_\mu|,$$

where  $|L|$  denotes the number of elements in  $L$ , and  $M$  is the dimension of the active space. This is approximately the number of all independent  $t$ -amplitudes.

So far, formally it seems that we apply the projection to every  $|\ell\rangle \in L$  and decompose

$$\begin{aligned}\mathbb{L} &= \langle \ell | \sum_{\nu} (\hat{H} - E) e^{\hat{T}_{\nu}} c_{\nu} | \nu \rangle \\ &= \sum_{\nu} \mathbb{L}^{\nu},\end{aligned}\tag{2.33}$$

$$\text{and then set} \quad \mathbb{L}^{\nu} = 0, \quad \forall \nu.\tag{2.34}$$

However, this is only for formal simplicity, and it is far from reality. Given the requirement that the number of independent  $t$ -amplitudes must equal the number of equations, the following cannot be true:

$$\mathbb{L}^{\nu} = 0, \quad \forall \nu, \mathbb{L}\tag{2.35}$$

because the total number of equations of this type is roughly  $M \times |L|$ , whereas the number of independent  $t$ -amplitudes is about  $|L|$ . We only have  $\mathbb{L}^{\nu} = 0$  for those  $\nu$  which can be excited to  $|\ell\rangle$  by an excitation operator in  $\hat{T}_{\nu}$ . Understanding this, let us examine two cases.

- First, consider the case in which  $|\ell\rangle$  can only be reached by the linear excitation of a particular reference determinant  $|\mu\rangle$ , for example (in singles and doubles truncation schemes) where  $|\ell\rangle$  is from the double excitation of  $|\mu\rangle$  from two core orbitals to two virtual orbitals. From the above methods, we only have  $\mathbb{L}^{\nu} = 0$  for the particular  $\nu = \mu$ . For  $\nu \neq \mu$ , we have  $\mathbb{L}^{\nu} \neq 0$ . We illustrate this by the SU-MRCC method (the conclusion holds equally for the BWCC and Mk-MRCC methods):

$$\begin{aligned}\mathbb{L}^{\nu} &= c_{\nu} \langle \ell | \hat{H} e^{\hat{T}_{\nu}} | \nu \rangle - c_{\nu} \sum_{\rho} \tilde{H}_{\rho\nu} \langle \ell | e^{\hat{T}_{\rho}} | \rho \rangle \\ &\neq 0, \quad \forall \nu \neq \mu.\end{aligned}\tag{2.36}$$

The Schrödinger equation requires that

$$\mathbb{L} = \langle \ell | (\hat{H} - E) | \Psi \rangle = \langle \ell | \sum_{\nu} (\hat{H} - E) e^{\hat{T}_{\nu}} c_{\nu} | \nu \rangle.$$

Let us define  $\mathbb{L}$  as the *proper residual* and  $\mathbb{L} = 0$  as the *proper residual condition*. After we eliminate the redundancy problem and modify the definition equation to  $\mathbb{L}^{\mu} = 0$ , the proper residual does not vanish:

$$\begin{aligned} \mathbb{L} &= \sum_{\rho} \mathbb{L}^{\rho} \\ &= \mathbb{L}^{\mu} + \sum_{\rho \neq \mu} \mathbb{L}^{\rho} \\ &= \sum_{\rho \neq \mu} \mathbb{L}^{\rho} \\ &\neq 0. \end{aligned} \tag{2.37}$$

$\mathbb{L}$  may even be far from zero, based on the consideration of the numerous non-zero *component residuals*  $\mathbb{L}^{\rho}$  ( $\rho \neq \mu$ ).

- For the other cases, suppose  $|\ell\rangle$  can be reached by linear excitations of  $|\mu_1\rangle, |\mu_2\rangle, \dots, |\mu_W\rangle$ ,  
 . Using a similar argument we arrive at

$$\begin{aligned} \mathbb{L} &= \sum_{\rho} \mathbb{L}^{\rho} \\ &= \mathbb{L}^{\mu_1} + \mathbb{L}^{\mu_2} + \mathbb{L}^{\mu_W} + \sum_{\rho \neq \mu_1, \mu_2, \dots, \mu_W} \mathbb{L}^{\rho} \\ &= \sum_{\rho \neq \mu_1, \mu_2, \dots, \mu_W} \mathbb{L}^{\rho} \\ &\neq 0 \end{aligned} \tag{2.38}$$

As a result the proper residual, which is supposed to vanish according to the Schrödinger equation, is non-zero now. In fact, even the redundant  $|\ell\rangle$ 's can be reached only by a small portion of  $\{|\mu\rangle\}$ ; thus, it is unclear how far  $\mathbb{L}$  is from zero, given the large number of non-zero *component residuals*.

Therefore, in spite of the over-parameterization of the ansatz, almost none of the *proper residuals* are zero. Similar arguments hold for the transformed projection method: the proper residuals are non-zero.

In traditional CC methods, the proper residual condition provides a natural way to define t-amplitude equations. While for the various (truncated) JM-ansatz based methods, there is a conflict between the sufficiency condition and the proper residual condition. In general, it may be hard to judge how reasonable the various sufficiency conditions are. Particularly in single reference (SR) cases, we believe that the traditional way of doing CC, which utilizes the proper residual condition, is rather reasonable. With this understanding, we may take ‘failing to fulfill the proper residual condition’ as one unsatisfactory aspect of the various JM-ansatz based methods. (It is another question how serious the drawback is.) The above argument may give a clue as to why, say, the Mk-MRCC method is outperformed by single reference coupled cluster methods [69] for SR systems.

The discussion naturally leads to the MRexpT method [71, 130] as a relevant comparison. In MRexpT, the redundancy problem is removed by exerting some constraints on redundant t-amplitudes so that they become dependent, and there is a one to one correspondence between the excited determinant and the independent t-amplitudes. Then the proper residual condition is invoked:

$$\langle \ell | \sum_{\nu} (\hat{H} - E) e^{\hat{T}_{\nu}} c_{\nu} | \nu \rangle = 0. \quad (2.39)$$

From the proper residual condition argument, the MRexpT method is expected to outperform other methods for SR systems in general. It will be interesting to see more extensive tests (beyond the model systems studied, which are typically very small [71, 69]).

## 2.4 Conclusion

Different JM-ansatz based methods are unified according to how to group terms  $\mathbb{L} = \sum_{\mu} \mathbb{L}^{\mu}$ . The transformed projection provides extra flexibility; for example, t-H2E2 differs from H2E2. It has

been shown that some seemingly different methods are indeed equivalent: H2E1 is equivalent to Mk-MRCC (t-H2E1), and H1E2 is equivalent to SU-MRCC (t-H1E2). It is nontrivial to show the size-extensivity in the untransformed forms (H2E1 and H1E2), while the transformation renders the size-extensivity proof simpler.

Although different sufficiency conditions are proposed, the underlying physical meaning still evades a clear understanding. It is argued that the defining equations are not entirely proper, in the sense that the proper residual condition is broken. This may partially rationalize the unsatisfactory performance of the various methods for SR systems. In contrast, the MRexpT method fulfills the proper residual condition, and it is expected to outperform other methods in SR cases. More extensive tests are needed to verify the statement.

## Chapter 3

# Orbital invariance issue

For *ab initio* methods, the solutions to molecular orbitals are often not unique unless extra conditions are imposed, such as canonical orbitals for the Hartree-Fock (HF) method and natural orbitals for the complete-active-space self-consistent-field (CASSCF) method. Different sets of orbitals are often related by unitary transformations. It is certainly desired that energy and other properties not be affected by the choice of orbitals. The sensitivity to orbitals introduces a certain degree of arbitrariness into the solutions. If the energy does not change upon orbital rotations in certain orbital spaces, we say that the method is orbital invariant. The orbital rotation spaces are usually clear from the context. The transformation property of the energy is closely related to that of the wavefunction, and we will discuss them together.

The orbital invariance issue generally does not pose a problem for single reference methods (the single reference coupled electron pair (CEPA) approach [138, 139, 140, 141, 142] are among the possible exceptions), but this issue is not well addressed yet for multireference methods. In this chapter, we will use tensor theory as the tool to examine the orbital invariance property.<sup>1</sup> The technique developed here is general and convenient to investigate the invariance issue for a large class of methods. The invariance property of the Hartree-Fock, single reference and multireference configuration interaction, single reference coupled cluster and complete-active-space

<sup>1</sup>The contents of this chapter are submitted to J. Chem. Phys. for publication



self-consistent-field methods are well known. There are simpler approaches to establish their invariance property. In comparison, the approach adopted in this work may appear tedious and unwieldy at some places. In that case, the point of the analysis is not in the conclusion itself, but mainly to develop and demonstrate a generally applicable technique, and to provide an alternative route to establish the invariance property. In addition, the excitation amplitudes or the determinant coefficients in the wavefunction are given explicitly in tensor form, therefore how they transform upon orbital rotations is explicitly known, and thus the proof is constructive.

To define notation and draw the analogy between coordinate transformations and orbital transformations, we summarize the basics of tensor theory [143]. For an (admissible) coordinate transformation:

$$T : y^i = y^i(x^1, x^2, \dots, x^n), \quad i = 1, 2, \dots, n, \quad (3.1)$$

a covariant tensor of rank one is the entire class of sets of quantities  $\{A_\alpha(x)\}, \{B_i(y)\}, \dots$  related to one another by the transformation of the form:

$$B_i(y) = \sum_{\alpha=1}^n \frac{\partial x^\alpha}{\partial y^i} A_\alpha(x), \quad i = 1, 2, \dots, n, \quad (3.2)$$

where  $\{A_\alpha(x)\}$  is the representation of the tensor in the X-coordinate system, and  $\{B_i(y)\}$  is its representation in the coordinate system Y, which is related to the X-system by the transformation T. A contravariant tensor of rank one is the entire class of quantities such as  $\{A^\alpha(x)\}, \{B^i(y)\}, \dots$  related to one another by the transformation of the form

$$B^i(y) = \sum_{\alpha=1}^n \frac{\partial y^i}{\partial x^\alpha} A^\alpha(x), \quad i = 1, 2, \dots, n. \quad (3.3)$$

The generalization to tensors of higher rank is straightforward [143]. A set of  $n^r$  quantities  $A_{i_1 i_2 \dots i_r}(x)$ , associated with the X-coordinate system, represents the components of a covariant tensor of rank r if the corresponding set of  $n^r$  quantities  $B_{i_1 i_2 \dots i_r}(y)$ , associated with the Y-

coordinate system, is given by

$$B_{i_1 i_2 \dots i_r} = \sum_{\alpha_1, \dots, \alpha_r} \frac{\partial x^{\alpha_1}}{\partial y^{i_1}} \frac{\partial x^{\alpha_2}}{\partial y^{i_2}} \dots \frac{\partial x^{\alpha_r}}{\partial y^{i_r}} A_{\alpha_1 \alpha_2 \dots \alpha_r}. \quad (3.4)$$

A set of  $n^r$  quantities  $A^{i_1 i_2 \dots i_r}(x)$ , associated with the X-coordinate system, represents the components of a contravariant tensor of rank  $r$  if the corresponding set of  $n^r$  quantities  $B^{i_1 i_2 \dots i_r}(y)$ , associated with the Y-coordinate system, is given by

$$B^{i_1 i_2 \dots i_r} = \sum_{\alpha_1, \dots, \alpha_r} \frac{\partial y^{i_1}}{\partial x^{\alpha_1}} \frac{\partial y^{i_2}}{\partial x^{\alpha_2}} \dots \frac{\partial y^{i_r}}{\partial x^{\alpha_r}} A^{\alpha_1 \alpha_2 \dots \alpha_r}. \quad (3.5)$$

A set of  $n^{r+s}$  quantities, typified in the X-coordinate system by the expressions  $A^{j_1 j_2 \dots j_s}_{i_1 i_2 \dots i_r}(x)$ , is a mixed tensor, covariant of rank  $r$  and contravariant of rank  $s$ , provided that the corresponding quantities  $B^{j_1 j_2 \dots j_s}_{i_1 i_2 \dots i_r}(y)$  in the Y-coordinate system are given by the law

$$B^{j_1 j_2 \dots j_s}_{i_1 i_2 \dots i_r} = \sum_{\alpha_1, \dots, \alpha_r}^{\beta_1, \dots, \beta_s} \frac{\partial x^{\alpha_1}}{\partial y^{i_1}} \frac{\partial x^{\alpha_2}}{\partial y^{i_2}} \dots \frac{\partial x^{\alpha_r}}{\partial y^{i_r}} \frac{\partial y^{j_1}}{\partial x^{\beta_1}} \frac{\partial y^{j_2}}{\partial x^{\beta_2}} \dots \frac{\partial y^{j_s}}{\partial x^{\beta_s}} A^{\beta_1 \beta_2 \dots \beta_s}_{\alpha_1 \alpha_2 \dots \alpha_r}. \quad (3.6)$$

In this work, we follow the convention of using superscripts to denote contravariant indices and using subscripts to denote covariant indices. The Einstein convention is not adopted herein, as understandably it is not suitable to discuss equations that are *not* invariant.

In the context of studying orbital invariance, we examine the relation of the energy and/or wavefunction to orbital rotations instead of coordinate transformations [144]. Without loss of generality, we focus on a unitary transformation of a set of orthonormal molecular orbitals  $\{\phi_i\}$ :

$$\tilde{\phi}_i = \sum_j \mathbb{U}_j^i \phi_j, \quad \forall i, \quad (3.7)$$

and correspondingly, the inverse transformation:

$$\phi_i = \sum_j \bar{\mathbb{U}}_j^i \tilde{\phi}_j, \quad \forall i, \quad (3.8)$$

where

$$\bar{\mathbb{U}} = \mathbb{U}^{-1} = \mathbb{U}^\dagger. \quad (3.9)$$

Tensor analysis is carried out with respect to this type of transformation (see Ref. [144] for an interesting discussion of a tensor formulation of many-electron theory in a nonorthogonal single-particle basis). Under these circumstances, creation operators behave like contravariant tensors, and annihilation operators behave like covariant tensors [1]. The transformation properties of molecular integrals are also straightforward to demonstrate. We will use these results directly, and adopt proper tensor notations accordingly. One important result from tensor analysis is that tensor contraction operations reduce tensor ranks. In other words, the contracted indices are invariant, and we do not have to pay attention to them when examining transformation properties (more precisely, if the contracted indices are within a certain class, the invariance of contracted indices is limited to transformations within that class). With this knowledge, we readily see the invariance of the Hamiltonian:

$$\hat{H} = \sum_{p,q} F_p^q \hat{a}_q^p + \frac{1}{4} \sum_{p,q,r,s} V_{pq}^{rs} \hat{a}_{rs}^{pq}, \quad (3.10)$$

with

$$F_p^q = \int \phi_p^*(\mathbf{x}) \left( -\frac{1}{2} \nabla^2 - \sum_I \frac{Z_I}{r_I} \right) \phi_q(\mathbf{x}) d\mathbf{x}, \quad (3.11)$$

$$g_{pq}^{rs} = \int \frac{\phi_p^*(\mathbf{x}_1) \phi_q^*(\mathbf{x}_2) \phi_s(\mathbf{x}_2) \phi_r(\mathbf{x}_1)}{r_{12}} d\mathbf{x}_1 d\mathbf{x}_2, \quad (3.12)$$

$$V_{pq}^{rs} = g_{pq}^{rs} - g_{pq}^{sr}, \quad (3.13)$$

where  $Z_I$  is the nuclear charge,  $r_I$  the electron-nuclear separation,  $r_{12}$  the electron-electron separation, and  $\mathbf{x}$  the electron coordinate including spin. In addition, the true vacuum  $|\rangle$  (not the Fermi vacuum) is a physical state which does not depend on orbitals. It therefore behaves like a scalar, and is invariant to orbital rotations. Combining all the established results, we can write a

determinant in the following form, revealing the tensor property explicitly:

$$|\phi_{i_1} \phi_{i_2} \cdots \phi_{i_{s-1}} \phi_{i_s}\rangle = \hat{a}_{i_1}^\dagger \hat{a}_{i_2}^\dagger \cdots \hat{a}_{i_{s-1}}^\dagger \hat{a}_{i_s}^\dagger | \rangle = \hat{a}^{i_1} \hat{a}^{i_2} \cdots \hat{a}^{i_{s-1}} \hat{a}^{i_s} | \rangle = \hat{a}^{i_1 i_2 \cdots i_{s-1} i_s} | \rangle \quad (3.14)$$

by defining

$$\hat{a}^{i_k} = \hat{a}_{i_k}^\dagger \quad \text{and} \quad \hat{a}^{i_1 i_2 \cdots i_k i_s} = \hat{a}^{i_1} \hat{a}^{i_2} \cdots \hat{a}^{i_{s-1}} \hat{a}^{i_s}. \quad (3.15)$$

The tensor property is now explicit, since the creation operator  $\hat{a}^{i_k}$  is a contravariant tensor. Being able to write determinants in tensor form is one key element of the analysis in this chapter, and its advantages will be made clear.

To be precise, when we discuss orbital invariance, we should always clarify the space in which the orbital transformation is performed. Depending on the method, usually the orbitals are naturally divided into a few classes, and we always refer to the transformations within each class. For single reference theories, we have usually two classes: occupied orbitals and unoccupied (virtual) orbitals.

Now we outline the general algorithm to determine the transformation property (invariant or not) of various methods. In summary, the algorithm is a self-consistency-checking procedure:

Firstly, we *assume* that residual equations have been solved, and that all quantities (particularly excitation amplitudes) appearing in residual equations are tensors. The ranks of the tensors are denoted by the numbers of superscripts and subscripts. Following these assumptions, usually we can show that energy is invariant, because it has a scalar form in the sense that all indices in the energy expression are contracted or energy is expressed completely in terms of invariant quantities (complication with respect to the invariance of energy may arise in some cases, to which we will pay due attention). Then we carry out an arbitrary unitary transformation of orbitals, and check whether the residuals remain zero. If it is, then the self-consistency-checking is passed, and the theory is orbital invariant. Otherwise, a contradiction is reached, and the theory does not have the property of orbital invariance.

Thus, the main job is to check whether the residuals remain zero upon orbital transformations

(supposing the energy expression behaves like a scalar, and does not pose a problem for invariance). More precisely, we are looking at any *infinitesimal* unitary transformation (a finite transformation can be taken as a succession of infinitesimal transformations), and for various methods to be invariant, the residuals need to remain zero for such transformations. This is a rather strong constraint. Residual equations are expressed in terms of tensor quantities (such as  $V_{pq}^{rs}$  and determinants) and excitation amplitudes, and tensor equations are known to be invariant, so we feel justified to assume that these amplitudes are tensors (and thus that residual equations become *formally* tensor equations), as stated in the above procedure.

Whether or not a method is invariant depends on the ansatz and the amplitude equations. The procedure developed in this chapter only helps to reveal this property mathematically. To show that a method is orbital invariant, we seek tensor expressions for the wavefunction and residual equation to make the invariance explicit (see Section 3.2 on MRCI for an example). For a method which is not invariant or whose invariance property is unclear, we first assume that the method is invariant and strive to establish the tensor character of the amplitudes. Then we employ the above procedure to check the self-consistency to determine whether the method is invariant or not (see Section 3.3 on CASCC for an example). It can be tricky to establish the tensor character of the amplitudes. If we fail to do this, the technique does not work (see Section 3.3 on MRCI in the linearized CASCC ansatz for an example).

Single reference methods are examined in Section II. Then the complete-active-space self-consistent-field (CASSCF) and multireference configuration interaction (MRCI) [145, 146, 147, 148] methods are scrutinized. The complete-active-space coupled cluster (CASCC) [25, 26] and CCSDt [149, 27] methods are discussed afterwards. Subsequently the Jeziorski-Monkhorst (JM) ansatz-based methods [55, 59] are analyzed. For simplicity, spatial and spin symmetries are not considered in these discussions.

### 3.1 Hartree-Fock, Single Reference CI and CC

Let us start with the Hartree-Fock method. There is the well-known result that for any determinant

$$\begin{aligned} |\psi\rangle &= |\phi_{i_1} \cdots \phi_{i_r}\rangle \\ &= \hat{a}^{i_1 \cdots i_r} | \rangle, \end{aligned} \quad (3.16)$$

upon a unitary orbital transformation within the set of orbitals occupied in the determinant  $\mathcal{G} = \{\phi_{i_1}, \dots, \phi_{i_r}\}$ ,  $|\psi\rangle$  only changes by a phase factor  $e^{i\theta}$  [1, 150]. Thus, the Hartree-Fock determinant  $|\psi_{\text{HF}}\rangle$  changes by a phase factor upon an orbital rotation. The Hartree-Fock energy  $E_{\text{HF}} = \langle \psi_{\text{HF}} | \hat{H} | \psi_{\text{HF}} \rangle$  is invariant because  $\hat{H}$  is invariant, and the phase factors from the ket state and that from the bra state multiply to yield a factor of unity.

The result that  $\hat{a}^{i_1 \cdots i_r}$  changes by a phase factor  $\det(\mathbf{U})$  is not so much related to the fact that it is a product of second-quantized operators; rather it is based only on the assumption that  $\hat{a}^{i_1 \cdots i_r}$  is an antisymmetric tensor. Here we prove the result.

Suppose  $X^{i_1 \cdots i_n}$  is an antisymmetric tensor in the orbital basis  $\{\phi_i\}$  and  $Y^{i_1 \cdots i_n}$  is the corresponding tensor in the orbital basis  $\{\tilde{\phi}_i\}$ . The two orbital bases are related by the unitary transformation:

$$\tilde{\phi}_i = \sum_j \mathbb{U}_j^i \phi_j, \forall i. \quad (3.17)$$

The result we will prove is that

$$Y^{i_1 \cdots i_n} = \det(\mathbf{U}) X^{i_1 \cdots i_n}, \quad (3.18)$$

( $\det(U) = e^{i\theta}$ ). From the transformation property of contravariant tensors:

$$\begin{aligned}
Y^{i_1 \cdots i_n} &= \sum_{j_1 \cdots j_n} U_{j_1}^{i_1} \cdots U_{j_n}^{i_n} X^{j_1 \cdots j_n} \\
&= \sum_{j_1 \cdots j_n} [U_{j_1}^{i_1} \cdots U_{j_n}^{i_n} \frac{1}{n!} (\sum_{k_1 \cdots k_n} \delta_{k_1 \cdots k_n}^{j_1 \cdots j_n} X^{k_1 \cdots k_n})] \\
&= \frac{1}{n!} \sum_{\substack{j_1 \cdots j_n \\ k_1 \cdots k_n}} (U_{j_1}^{i_1} \cdots U_{j_n}^{i_n} \delta_{k_1 \cdots k_n}^{j_1 \cdots j_n} X^{k_1 \cdots k_n}) \\
&= \frac{1}{n!} \sum_{\substack{j_1 \cdots j_n \\ k_1 \cdots k_n}} [U_{j_1}^{i_1} \cdots U_{j_n}^{i_n} (\delta_{i_1 \cdots i_n}^{j_1 \cdots j_n} \delta_{k_1 \cdots k_n}^{i_1 \cdots i_n}) X^{k_1 \cdots k_n}] \\
&= \frac{1}{n!} \sum_{k_1 \cdots k_n} [(\sum_{j_1 \cdots j_n} U_{j_1}^{i_1} \cdots U_{j_n}^{i_n} \delta_{i_1 \cdots i_n}^{j_1 \cdots j_n}) \delta_{k_1 \cdots k_n}^{i_1 \cdots i_n} X^{k_1 \cdots k_n}] \\
&= \frac{1}{n!} \sum_{k_1 \cdots k_n} (\det(U) \delta_{k_1 \cdots k_n}^{i_1 \cdots i_n} X^{k_1 \cdots k_n}) \\
&= \det(U) \frac{1}{n!} \sum_{k_1 \cdots k_n} (\delta_{k_1 \cdots k_n}^{i_1 \cdots i_n} X^{k_1 \cdots k_n}) \\
&= \det(U) X^{i_1 \cdots i_n}, \tag{3.19}
\end{aligned}$$

in which  $\delta_{i_1 \cdots i_n}^{j_1 \cdots j_n}$  is a generalized Kronecker delta tensor [151]. Such a tensor is antisymmetric in superscripts and subscripts, and whose value is non-zero only if the superscripts are distinct from each other, and the subscripts are the same set of numbers as the superscripts, being +1 or -1 according as an even or odd number of transpositions is required to arrange the superscripts in the same order as the subscripts). In this derivation, we have used the identity that

$$X^{j_1 \cdots j_n} = \frac{1}{n!} \sum_{k_1 \cdots k_n} \delta_{k_1 \cdots k_n}^{j_1 \cdots j_n} X^{k_1 \cdots k_n}, k_i = 1, 2, \dots, n, \forall i, \tag{3.20}$$

due to the antisymmetry of the tensor  $X$ . Additionally, to factorize out  $\det(U)$  we use the identity

$$\delta_{k_1 \cdots k_n}^{j_1 \cdots j_n} = \delta_{i_1 \cdots i_n}^{j_1 \cdots j_n} \delta_{k_1 \cdots k_n}^{i_1 \cdots i_n}. \tag{3.21}$$

The identity holds when there is no repeated index in  $\{i_1, \dots, i_n\}$ , which is the case here. The validity of the identity is clear since: (1) when there are repeated indices in either  $\{j_1, \dots, j_n\}$  or

$\{k_1, \dots, k_n\}$ , both sides are zero (the generalized Kronecker delta tensor is antisymmetric), (2)  $\delta_{k_1 \dots k_n}^{j_1 \dots j_n}$  is determined by the parity of the permutation of  $(j_1 \dots j_n)$  to  $(k_1 \dots k_n)$ , (3) the parity does not depend on the specific way that the permutation is carried out, so the parity of the permutation of  $(j_1 \dots j_n)$  to  $(k_1 \dots k_n)$  is the same as that of the permutation of  $(j_1 \dots j_n)$  to  $(i_1 \dots i_n)$ , then to  $(k_1 \dots k_n)$ , while the parity of the latter equals  $\delta_{i_1 \dots i_n}^{j_1 \dots j_n} \delta_{k_1 \dots k_n}^{i_1 \dots i_n}$ .

Formally it may be advantageous to modify the form of the Hartree-Fock wavefunction to make it explicitly invariant, that is, to eliminate the phase factor:

$$|\tilde{\psi}_{\text{HF}}\rangle = \frac{1}{n!} \sum_{i_1, \dots, i_n} C_{i_1 \dots i_n} \hat{a}^{i_1 \dots i_n} | \rangle. \quad (3.22)$$

where  $C_{i_1 \dots i_n}$  is an antisymmetric tensor. Suppose every index in  $\{i_1, \dots, i_n\}$  goes from 1 to n. To normalize the wavefunction, we can set  $C_{12 \dots n} = 1$ . Whether to use  $|\psi_{\text{HF}}\rangle$  or  $|\tilde{\psi}_{\text{HF}}\rangle$  as the Hartree-Fock determinant does not affect the invariance of the energy for the methods to be discussed in this section, but using  $|\tilde{\psi}_{\text{HF}}\rangle$  also makes the wavefunction invariant. Hereafter, we assume that  $|\tilde{\psi}_{\text{HF}}\rangle$  is used in the following discussions of single reference configuration interaction (SRCI) and single reference coupled cluster (SRCC) methods, so that the wavefunction is explicitly invariant. For notational simplicity, we drop the ‘ $\tilde{\cdot}$ ’ and simply write the invariant HF determinant as  $|\psi_{\text{HF}}\rangle$ .

For SRCI methods, we take the configuration interaction doubles (CID) method as an example for the sake of simplicity, assuming intermediate normalization.

$$\hat{\Omega} = 1 + \hat{C} = 1 + \frac{1}{(2!)^2} \sum_{i_1, i_2, b_1, b_2} c_{ab}^{ij} \hat{a}_{i_1 i_2}^{b_1 b_2}, \quad (3.23)$$

$$|\psi_{\text{CID}}\rangle = \hat{\Omega} |\psi_{\text{HF}}\rangle = \hat{\Omega} |\phi_{i_1} \phi_{i_2} \phi_{i_3} \dots \phi_{i_r}\rangle, \quad (3.24)$$

$$\hat{H} \hat{\Omega} |\psi_{\text{HF}}\rangle = E \hat{\Omega} |\psi_{\text{HF}}\rangle, \quad (3.25)$$

$$E = \langle \psi_{\text{HF}} | \hat{H} \hat{\Omega} | \psi_{\text{HF}} \rangle, \quad (3.26)$$

$$\langle \phi_{b_1} \phi_{b_2} \phi_{i_3} \dots \phi_{i_r} | (\hat{H} - E) \hat{\Omega} | \phi_{i_1} \phi_{i_2} \phi_{i_3} \dots \phi_{i_r} \rangle = 0, \quad (3.27)$$

$$\langle \hat{a}_{b_1 b_2 i_3 \dots i_r} (\hat{H} - E) \hat{\Omega} \hat{a}^{i_1 i_2 i_3 \dots i_r} | \rangle = 0, \quad (3.28)$$

where  $i_1, i_2, \dots$  denote occupied orbitals, and  $b_1, b_2, \dots$  denote unoccupied orbitals. From the



algorithm outlined in Section I, we first assume that t-amplitudes are tensors covariant of rank 2 and contravariant of rank 2. Then it follows that: (1)  $\hat{C}$  and  $\hat{\Omega}$  are invariant due to tensor contractions, (2) energy is invariant, and (3) the composite operator  $\hat{Z}$  is invariant if we define

$$\hat{Z} = (\hat{H} - E)\hat{\Omega}. \quad (3.29)$$

Since  $\hat{Z}$  is invariant, the tensor character of the residual is determined by  $\hat{a}_{b_1 b_2 i_3 \dots i_r}$  and  $\hat{a}^{i_1 i_2 i_3 \dots i_r}$ . Thus we can write the residual in tensor notation:

$$\mathbb{R}_{b_1 b_2 i_3 \dots i_r}^{i_1 i_2 i_3 \dots i_r} = \langle \hat{a}_{b_1 b_2 i_3 \dots i_r} (\hat{H} - E) \hat{\Omega} \hat{a}^{i_1 i_2 i_3 \dots i_r} | \rangle = \langle \hat{a}_{b_1 b_2 i_3 \dots i_r} \hat{Z} \hat{a}^{i_1 i_2 i_3 \dots i_r} | \rangle. \quad (3.30)$$

Although we can prove orbital invariance using the residual in this form, we prefer to rewrite  $\mathbb{R}$  to reveal its fundamental transformation property:

$$\mathbb{R}_{b_1 b_2 i_3 \dots i_r}^{i_1 i_2 i_3 \dots i_r} = \frac{1}{(r-2)!} \sum_{i_3, \dots, i_r} \mathbb{R}_{b_1 b_2 i_3 \dots i_r}^{i_1 i_2 i_3 \dots i_r} = \mathbb{R}_{b_1 b_2}^{i_1 i_2}. \quad (3.31)$$

The above equations hold because  $\mathbb{R}$  is an antisymmetric tensor. Utilizing antisymmetry of some tensors to rewrite uncontracted quantities in contracted forms is another key element of the analysis in this chapter. The tensor rank of  $\mathbb{R}$  is reduced due to tensor contraction operations indicated by the explicit summations. This is the form we often see in the literature. Now we can prove orbital invariance easily by showing that the residual remains zero upon orbital rotations. Suppose that

$$\mathbb{R}_{b_1 b_2}^{i_1 i_2} = 0, \forall i_1, i_2, b_1, b_2. \quad (3.32)$$

Upon orbital rotations, the residual remain zero:

$$\mathbb{R}_{\tilde{b}_1 \tilde{b}_2}^{\tilde{i}_1 \tilde{i}_2} = \sum_{i_1, i_2, b_1, b_2} \mathbb{U}_{i_1}^{\tilde{i}_1} \mathbb{U}_{i_2}^{\tilde{i}_2} \bar{\mathbb{U}}_{b_1}^{b_1} \bar{\mathbb{U}}_{b_2}^{b_2} \mathbb{R}_{b_1 b_2}^{i_1 i_2} = 0. \quad (3.33)$$

Thus we have proved that the CID method is invariant.

This line of arguments clearly can be extended to general single reference CI methods, irrespective of the level of truncation in  $\hat{C}$ . The same arguments hold for single reference coupled cluster (SRCC) methods, by redefining

$$\hat{Z} = e^{-\hat{T}} \hat{H} e^{\hat{T}}, \quad (3.34)$$

where  $\hat{T}$  is the excitation cluster operator. SRCC is orbital invariant with respect to separate rotations within the occupied orbital space and within the unoccupied orbital space (in comparison,  $\hat{H}$  is invariant with respect to rotations within the space spanned by all orbitals). We emphasize the restricted invariance because it will play a role in Sections III and IV.

The line of reasoning presented above will be used henceforth. Usually we can write the residual equation in the form  $\langle \phi_\lambda | \hat{Z} | \phi \rangle$ , in which  $|\phi_\lambda\rangle$  is an excited determinant,  $|\phi\rangle$  is a reference determinant and  $\hat{Z}$  is an orbital invariant operator, due to explicit summations of all indices in it. We then identify the tensor character of the residual from  $\langle \phi_\lambda |$  and  $|\phi\rangle$ . Finally, we draw conclusions, depending on whether the residual remains zero upon orbital rotations. This is a simplification of the self-consistency-checking algorithm introduced in Section I.

## 3.2 CASSCF and MRCI

For the CASSCF method, upon convergence, the wavefunction has the form

$$\begin{aligned} |\psi_{\text{CASSCF}}\rangle &= \sum_{\mu} C_{\mu} |\mu\rangle \\ &= \sum_{i'_1 < i'_2 < \dots < i'_k, m_1 < m_2 < \dots < m_s} C_{i'_1 \dots i'_k m_1 \dots m_s} |\phi_{i'_1} \dots \phi_{i'_k} \phi_{m_1} \dots \phi_{m_s}\rangle \\ &= \sum_{i'_1 < i'_2 < \dots < i'_k, m_1 < m_2 < \dots < m_s} C_{i'_1 \dots i'_k m_1 \dots m_s} \hat{a}^{i'_1 \dots i'_k m_1 \dots m_s} | \rangle, \end{aligned} \quad (3.35)$$

where  $i'_1, \dots, i'_k$  denote core orbitals and  $m_1, \dots, m_s$  denote active orbitals. Since the summations of indices are restricted, it will be awkward to demonstrate the invariance in this form. Let us

rewrite the wavefunction:

$$\begin{aligned}
|\psi_{\text{CASSCF}}\rangle &= \sum_{i'_1 < i'_2 < \dots < i'_k, m_1 < m_2 < \dots < m_s} C_{i'_1 \dots i'_k m_1 \dots m_s} \hat{a}^{i'_1 \dots i'_k m_1 \dots m_s} | \rangle \\
&= \frac{1}{k!} \sum_{i'_1, \dots, i'_k, m_1 < m_2 < \dots < m_s} C_{i'_1 \dots i'_k m_1 \dots m_s} \hat{a}^{i'_1 \dots i'_k m_1 \dots m_s} | \rangle \\
&= \frac{1}{k!s!} \sum_{i'_1, \dots, i'_k, m_1, \dots, m_s} C_{i'_1 \dots i'_k m_1 \dots m_s} \hat{a}^{i'_1 \dots i'_k m_1 \dots m_s} | \rangle. \tag{3.36}
\end{aligned}$$

The amplitudes  $C_{i'_1 \dots i'_k m_1 \dots m_s}$ 's are assumed to be antisymmetric (if not, we can rewrite the wavefunction expression to make the  $C$ 's antisymmetric). In Eq. (3.36), utilizing the antisymmetry of  $\hat{a}^{i'_1 \dots i'_k m_1 \dots m_s}$  and  $C_{i'_1 \dots i'_k m_1 \dots m_s}$ , we lift the restrictions on the indices, and modify the restricted summations to free summations. The free summations make the orbital invariance of  $|\psi_{\text{CASSCF}}\rangle$  explicit (assuming the self-consistency-checking is passed). (Let us mention a related point: if  $|\mu\rangle$ 's span the complete active space, we can show, using the above summation technique, that the projection operator in the active space, which has the form

$$\hat{P}_{\text{act}} = \sum_{\mu} |\mu\rangle\langle\mu|,$$

is invariant to orbital rotations in active space.) The orbital invariance of the energy follows, since

$$E = \langle\psi_{\text{CASSCF}}|\hat{H}|\psi_{\text{CASSCF}}\rangle, \tag{3.37}$$

and every quantity in the expression is invariant with respect to separate rotations in core orbital space, in active orbital space and in non-active virtual orbital space. Once the C-amplitudes are converged, the final residual equation has the form:

$$\langle\phi_{i'_1} \dots \phi_{i'_k} \phi_{m_1} \dots \phi_{m_s} | \left( (\hat{H} - E) |\psi_{\text{CASSCF}}\rangle \right) = 0, \tag{3.38}$$

$$\langle \hat{a}_{i'_1 \dots i'_k m_1 \dots m_s} \left( (\hat{H} - E) |\psi_{\text{CASSCF}}\rangle \right) = 0, \tag{3.39}$$

$$\mathbb{R}_{i'_1 \dots i'_k m_1 \dots m_s} = \langle \hat{a}_{i'_1 \dots i'_k m_1 \dots m_s} \left( (\hat{H} - E) |\psi_{\text{CASSCF}}\rangle \right) = 0, \forall i'_1, \dots, i'_k, m_1, \dots, m_s. \tag{3.40}$$

Additionally, the wavefunction satisfies the stationary condition:

$$\begin{aligned}\bar{\mathbb{R}}_{b_y}^{m_x} &= \langle \psi_{\text{CASSCF}} | \hat{a}_{b_y}^{m_x} \hat{H} | \psi_{\text{CASSCF}} \rangle \\ &= \langle \psi_{\text{CASSCF}} | \hat{a}_{b_y}^{m_x} \left( \hat{H} | \psi_{\text{CASSCF}} \right) \rangle = 0, \forall m_x, b_y,\end{aligned}\quad (3.41)$$

$$\begin{aligned}\ddot{\mathbb{R}}_{m_y}^{i'_x} &= \langle \psi_{\text{CASSCF}} | \hat{a}_{m_y}^{i'_x} \hat{H} | \psi_{\text{CASSCF}} \rangle \\ &= \langle \psi_{\text{CASSCF}} | \hat{a}_{m_y}^{i'_x} \left( \hat{H} | \psi_{\text{CASSCF}} \right) \rangle = 0, \forall i'_x, m_y,\end{aligned}\quad (3.42)$$

where ‘ $b_y$ ’ denotes any non-active virtual orbital.

We have grouped orbital invariant quantities in parentheses, so that the tensor character of the residual is clearly fully determined by the determinant on the left. Upon separate orbital rotations in core orbital space and in active orbital space, the residual remains zero:

$$\begin{aligned}\mathbb{R}_{\tilde{i}'_1 \dots \tilde{i}'_k \tilde{m}_1 \dots \tilde{m}_s} &= \sum_{j'_1, \dots, j'_k, n_1, \dots, n_s} \bar{\mathbb{U}}_{\tilde{i}'_1}^{j'_1} \dots \bar{\mathbb{U}}_{\tilde{i}'_k}^{j'_k} \bar{\mathbb{U}}_{\tilde{m}_1}^{n_1} \dots \bar{\mathbb{U}}_{\tilde{m}_s}^{n_s} \mathbb{R}_{j'_1 \dots j'_k n_1 \dots n_s} \\ &= 0, \forall \tilde{i}'_1, \dots, \tilde{i}'_k, \tilde{m}_1, \dots, \tilde{m}_s.\end{aligned}\quad (3.43)$$

Similarly, we can demonstrate that  $\bar{\mathbb{R}}_{b_y}^{m_x}$  and  $\ddot{\mathbb{R}}_{m_y}^{i'_x}$  remain zero upon orbital rotations in core and active subspaces. Thus, we conclude that the CASSCF wavefunction and energy are orbital invariant.

The arguments for the multireference configuration interaction (MRCI) method are similar. The wavefunction has the form:

$$\begin{aligned}|\psi_{\text{MRCI}}\rangle &= \sum_{x+y+z=N} \sum_{\substack{i'_1 < \dots < i'_x \\ m_1 < \dots < m_y \\ b_1 < \dots < b_z}} C_{i'_1 \dots i'_x m_1 \dots m_y b_1 \dots b_z} \hat{a}^{i'_1 \dots i'_x m_1 \dots m_y b_1 \dots b_z} | \rangle \\ &= \frac{1}{x!y!z!} \sum_{x+y+z=N} \sum_{i'_1, \dots, i'_x, m_1, \dots, m_y, b_1, \dots, b_z} C_{i'_1 \dots i'_x m_1 \dots m_y b_1 \dots b_z} \hat{a}^{i'_1 \dots i'_x m_1 \dots m_y b_1 \dots b_z} |\mathfrak{B}, 44\rangle\end{aligned}$$

where  $b_1, \dots, b_z$  are virtual orbital indices,  $x, y$  and  $z$  are the numbers of electrons occupying core, active and virtual orbitals, respectively, and  $N$  is the total number of electrons. For the MRCI

method truncated at some level, there are restrictions on the values of  $x$ ,  $y$  and  $z$ , but this issue does not affect the orbital invariance analysis, once we group terms/determinants into classes according to the values of  $x$ ,  $y$ , and  $z$ . With the above notation, we see that the wavefunction, and hence also the energy, are orbital invariant with respect to separate orbital rotations in three subspaces. The residual has the form

$$\langle \phi_{i'_1} \cdots \phi_{i'_x} \phi_{m_1} \cdots \phi_{m_y} \phi_{b_1} \cdots \phi_{b_z} | \left( (\hat{H} - E) | \psi_{\text{MRCI}} \right) \rangle = 0, \quad (3.45)$$

$$\langle | \hat{a}_{i'_1 \cdots i'_x m_1 \cdots m_y b_1 \cdots b_z} \left( (\hat{H} - E) | \psi_{\text{MRCI}} \right) \rangle = 0, \quad (3.46)$$

$$\mathbb{R}_{i'_1 \cdots i'_x m_1 \cdots m_y b_1 \cdots b_z} = 0 \quad \forall i'_1, \dots, i'_x, m_1, \dots, m_y, b_1, \dots, b_z. \quad (3.47)$$

Again, we group orbital invariant quantities together, and exhibit the tensor character of the residual explicitly. It is almost the same as for CASSCF to demonstrate that the residual remains zero after orbital rotations.

At this point it should be clear that orbital invariance is formally induced by orbital index summations (tensor contractions) and is limited by the space of orbital index summations. If the summation is confined to separate summations within space X and within space Y, then orbital invariance of the method, if it exists, can hold at most for separate rotations in the same space.

### 3.3 CASCC and CCSDt

Once understanding the invariance property of MRCI, we can easily see the lack of invariance of the CAS(2, 2)CCSD [152] and CCSDt [26, 149, 27] methods with respect to orbital rotations in the whole active space. We analyze the two specific variants instead of the general formulations because they are the representatives of the corresponding two classes of methods. Focusing on the two special cases facilitates a concrete analysis.

The CAS(2, 2)CCSD method deal with the multireference systems with two active electrons in two active orbitals. We focus on the version in which orbitals are obtained from a prior CASSCF calculation [26]. The determinant  $|0\rangle$  which makes the largest contribution to the CAS reference

function is singled out as the reference function to define occupied and virtual orbitals. Thus, the active orbitals are classified as active occupied or active virtual orbitals according to whether or not they are occupied in  $|0\rangle$ . The wavefunction has the form:

$$\begin{aligned}
|\psi\rangle &= e^{\hat{T}_1 + \hat{T}_2 + \hat{T}_3(\mathbf{A}_1 a_1 a_2)_{i_1 i_2 \mathbf{I}_1}} + \hat{T}_4(\mathbf{A}_1 \mathbf{A}_2 a_1 a_2)_{i_1 i_2 \mathbf{I}_1 \mathbf{I}_2} (1 + \hat{C}_1 + \hat{C}_2) |0\rangle \\
&= e^{\hat{T}^{\text{ext}}} (1 + \hat{C}_1 + \hat{C}_2) |0\rangle \\
&= e^{\hat{T}^{\text{ext}}} e^{\hat{T}^{\text{int}}} |0\rangle \\
&= e^{\hat{T}^{\text{ext}} + \hat{T}^{\text{int}}} |0\rangle,
\end{aligned} \tag{3.48}$$

where  $i_1, i_2$  ( $a_1, a_2$ ) denote occupied (virtual) orbitals, both active and inactive, and  $\mathbf{I}_1, \mathbf{I}_2$  ( $\mathbf{A}_1, \mathbf{A}_2$ ) denote active occupied (active virtual) orbitals. For later use, we define

$$\hat{T}^{\text{ext}} = \hat{T}_1 + \hat{T}_2 + \hat{T}_3(\mathbf{A}_1 a_1 a_2)_{i_1 i_2 \mathbf{I}_1} + \hat{T}_4(\mathbf{A}_1 \mathbf{A}_2 a_1 a_2)_{i_1 i_2 \mathbf{I}_1 \mathbf{I}_2}, \tag{3.49}$$

and  $\hat{T}^{\text{int}}$  is extracted from  $\hat{C}_1 + \hat{C}_2$ . The superscript ‘ext’ means that in each  $\hat{T}$  operator there is at least one inactive (core or virtual) orbital index. The superscript ‘int’ means that all indices are in the active space.

Now there are four subsets of orbitals: core orbitals, active occupied orbitals, active virtual orbitals, and inactive virtual orbitals. All the summations (tensor contractions) in  $\hat{T}$  can be explicitly classified according to the subset to which each index belongs. Since the invariance is induced by tensor contractions, the energy of CAS(2,2)CCSD,

$$E = \langle 0 | \hat{H} e^{\hat{T}^{\text{ext}} + \hat{T}^{\text{int}}} | 0 \rangle, \tag{3.50}$$

is invariant with respect to orbital rotations within the four subspaces, following reasoning similar to that used for SRCC.

In CCSDt [27], there are also four subsets of orbitals, as in CASCC. The wavefunction has the

form:

$$|\psi\rangle = e^{\hat{T}_1 + \hat{T}_2 + \hat{T}_3} \binom{\mathbf{A}_1 a_1 a_2}{i_1 i_2 \mathbf{I}_1} |0\rangle. \quad (3.51)$$

To be clear,  $\hat{T}_1$  and  $\hat{T}_2$  here include all internal and external single and double excitations. Without much difficulty, we can demonstrate that the energy is invariant with respect to orbital rotations within the four subsets.

Although we have argued that restricted orbital invariance exists for these methods, the full invariance in the whole active orbital space is certainly desired. However, the restricted index summations break this more general invariance, which we now proceed to demonstrate explicitly. For simplicity, we take the case of CAS(2,2)CCSD, in which  $\hat{T}^{\text{int}}$  is fixed from the previous CASSCF calculation, such that we can write the CASCC wavefunction as:

$$|\psi\rangle = e^{\hat{T}^{\text{ext}}} |\psi_{\text{CASSCF}}\rangle = e^{\hat{T}_1 + \hat{T}_2 + \hat{T}_3} \binom{\mathbf{A}_1 a_1 a_2}{i_1 i_2 \mathbf{I}_1} + \hat{T}_4 \binom{\mathbf{A}_1 \mathbf{A}_2 a_1 a_2}{i_1 i_2 \mathbf{I}_1 \mathbf{I}_2} |\psi_{\text{CASSCF}}\rangle. \quad (3.52)$$

For  $|\psi\rangle$  to be invariant,  $\hat{T}^{\text{ext}}$  must be invariant since  $|\psi_{\text{CASSCF}}\rangle$  is invariant. Thus, every component excitation operator must be invariant. For simplicity, we look at one particular class of  $\hat{T}_2$  operators:

$$\hat{T}_\alpha = \sum_{\mathbf{A}_1, b_1, i'_1, \mathbf{I}_1} t(\mathbf{A}_1 b_1; i'_1 \mathbf{I}_1) \hat{a}_{i'_1 \mathbf{I}_1}^{\mathbf{A}_1 b_1},$$

where ‘ $b_1$ ’ denotes any non-active virtual orbital, although the conclusion applies to any external excitation operator. The restricted summation of the indices already indicates that the operator can not be invariant, but we still present the detailed analysis for completeness.

For this operator to be invariant, the amplitude  $t(\mathbf{A}_1 b_1; i'_1 \mathbf{I}_1)$  must transform like a tensor covariant of rank 2 and contravariant of rank 2,  $t_{\mathbf{A}_1 b_1}^{i'_1 \mathbf{I}_1}$ , because the tensor property of the corresponding operator  $\hat{a}_{i'_1 \mathbf{I}_1}^{\mathbf{A}_1 b_1}$  is already known. Thus, we can write the operator in tensor form:

$$\hat{T}_\alpha = \sum_{\mathbf{A}_1, b_1, i'_1, \mathbf{I}_1} t_{\mathbf{A}_1 b_1}^{i'_1 \mathbf{I}_1} \hat{a}_{i'_1 \mathbf{I}_1}^{\mathbf{A}_1 b_1}.$$

We will show that the operator is not invariant with respect to orbital rotations in the whole active space; hence a contradiction is reached, and the lack of invariance is demonstrated. In other words, we will demonstrate that

$$\tilde{T}_\alpha \neq \hat{T}_\alpha,$$

where  $\tilde{T}_\alpha$  denotes the operator in the rotated orbital basis.

Following the transformation property implied by the tensor form, upon orbital rotations in the whole active space, we get:

$$\begin{aligned} \tilde{T}_\alpha &= \sum_{\tilde{\mathbf{A}}_1, b_1, i'_1, \tilde{\mathbf{I}}_1} t_{\tilde{\mathbf{A}}_1, b_1}^{i'_1 \tilde{\mathbf{I}}_1} \hat{a}_{i'_1 \tilde{\mathbf{I}}_1}^{\tilde{\mathbf{A}}_1 b_1} \\ &= \sum_{\tilde{\mathbf{A}}_1, b_1, i'_1, \tilde{\mathbf{I}}_1} \sum_{m_1, m_2, m_3, m_4} \mathbb{U}_{m_1}^{\tilde{\mathbf{I}}_1} \bar{\mathbb{U}}_{\tilde{\mathbf{A}}_1}^{m_4} \bar{\mathbb{U}}_{\tilde{\mathbf{I}}_1}^{m_2} \mathbb{U}_{m_3}^{\tilde{\mathbf{A}}_1} t_{m_4 b_1}^{i'_1 m_1} \hat{a}_{i'_1 m_2}^{m_3 b_1} \\ &= \sum_{b_1, m_3, i'_1, m_2} \left( \sum_{\tilde{\mathbf{A}}_1, \tilde{\mathbf{I}}_1, m_1, m_4} \mathbb{U}_{m_1}^{\tilde{\mathbf{I}}_1} \bar{\mathbb{U}}_{\tilde{\mathbf{I}}_1}^{m_2} \bar{\mathbb{U}}_{\tilde{\mathbf{A}}_1}^{m_4} \mathbb{U}_{m_3}^{\tilde{\mathbf{A}}_1} t_{m_4 b_1}^{i'_1 m_1} \right) \hat{a}_{i'_1 m_2}^{m_3 b_1} \end{aligned} \quad (3.53)$$

$$\neq \hat{T}_\alpha, \left( \hat{T}_\alpha = \sum_{\mathbf{A}_1, b_1, i'_1, \mathbf{I}_1} t_{\mathbf{A}_1, b_1}^{i'_1 \mathbf{I}_1} \hat{a}_{i'_1 \mathbf{I}_1}^{\mathbf{A}_1 b_1} \right). \quad (3.54)$$

$\tilde{T}_\alpha \neq \hat{T}_\alpha$  because  $m_3$  and  $m_2$  in  $\hat{a}_{i'_1 m_2}^{m_3 b_1}$  run over the whole active orbital space, while  $\mathbf{A}_1$  and  $\mathbf{I}_1$  in  $\hat{a}_{i'_1 \mathbf{I}_1}^{\mathbf{A}_1 b_1}$  are restricted; thus certain excitations in  $\tilde{T}_\alpha$  are not present in  $\hat{T}_\alpha$ .

Therefore,  $\hat{T}_\alpha$  is not invariant. The above arguments can be applied to other classes of excitation operators. Hence  $\hat{T}^{\text{ext}}$  is not invariant, and we conclude the lack of invariance of the wavefunction and the energy.

The linear excitation manifold of CASCC is the same as that of MRCI at the same level; for example, CASCCSD has the same linear excitation manifold as does MRCISD. Thus the projection manifold does not create a problem for orbital invariance in the active space. In this sense, the problem comes from the nonlinear ansatz. However, this understanding is possibly misleading because, if we compare SRCC to SRCI, the nonlinear parameterization form in SRCC does not affect the invariance property. The essential problem comes from singling out one particular determinant in the multi-determinantal reference function to further divide active orbitals into two disjoint sets, thus narrowing the invariance space. The foregoing rather technical discussion



is just a reflection of the problem. In the JM-ansatz based methods, every reference determinant has its corresponding excitation operator, whose amplitudes implicitly depend on the particular reference determinant through the residual equations, instead of depending only on the whole reference function (as in internally contracted methods). In some sense, there are multiple *vacua* and the orbitals in each excitation operator are divided into two disjoint sets. This complicated division even precludes a restricted invariance space.

Following the arguments about CASCC, we now illustrate the potential difficulty in analyzing the invariance property using the tensor technique. The difficulty lies in establishing the tensor character of the amplitudes. When we argue about the lack of invariance in the active orbital space, we purposely assume that  $\hat{T}^{\text{int}}$  is fixed from the previous CASSCF calculation such that we can write the wavefunction in a product form:

$$|\psi\rangle = e^{\hat{T}^{\text{ext}}} |\psi_{\text{CASSCF}}\rangle. \quad (3.55)$$

Since  $|\psi_{\text{CASSCF}}\rangle$  is invariant,  $e^{\hat{T}^{\text{ext}}}$ , and hence also  $\hat{T}^{\text{ext}}$ , must be invariant to make the wavefunction  $|\psi\rangle$  invariant (this is the initial *assumption* and the starting point of our arguments). Then we can establish the tensor character of the  $\hat{T}^{\text{ext}}$ -amplitudes. Finally, a contradiction is reached, and we conclude the lack of invariance. Without the assumption that  $\hat{T}^{\text{int}}$  is fixed from the previous CASSCF calculation, we cannot separate  $|\psi\rangle$  into an invariant part ( $|\psi_{\text{CASSCF}}\rangle$ ) and another part whose invariance property is unclear, as in Eq. (3.55). It is then unclear how to proceed to determine the tensor properties of the amplitudes, and it would be awkward to prove (if still possible mathematically) the lack of invariance for CASCC.

An another example to illustrate the difficulty, we write the MRCI wavefunction ansatz by linearizing the CASCC ansatz:

$$|\psi_{\text{MRCI}}\rangle = (1 + \hat{T}^{\text{ext}} + \hat{T}^{\text{ext}})|0\rangle, \quad (3.56)$$

since the linear excitation manifold of CASCC is the same as MRCI at the same level. In this expansion, any operator in  $\hat{T}^{\text{ext}} + \hat{T}^{\text{ext}}$  may be written as  $t(p_1, p_2, \dots, p_f; q_1, q_2, \dots, q_f) \hat{a}_{q_1 q_2 \dots q_f}^{p_1 p_2 \dots p_f}$ ,

not as  $t_{p_1 p_2 \dots p_f}^{q_1 q_2 \dots q_f} \hat{a}_{q_1 q_2 \dots q_f}^{p_1 p_2 \dots p_f}$ , because the tensor character of  $t(p_1, p_2, \dots, p_f; q_1, q_2, \dots, q_f)$  is not yet known, while the form  $t_{p_1 p_2 \dots p_f}^{q_1 q_2 \dots q_f}$  would imply it is a tensor covariant of rank  $f$  and contravariant of rank  $f$ . In this ansatz, since  $|0\rangle$  is not invariant with respect to orbital rotations in the active space, the initial assumption of the invariance of the wavefunction  $|\psi_{\text{MRCI}}\rangle$  does not lead to the conclusion that  $\hat{T}^{\text{ext}} + \hat{T}^{\text{ext}}$  must be invariant. Therefore we cannot proceed to determine the tensor character of the amplitudes, and we can not easily demonstrate the invariance for MRCI. We emphasize that we are not led to the wrong conclusion that MRCI is not invariant; it is just that we cannot prove it straightforwardly. The point of the foregoing discussions is that it can be tricky to establish the tensor character of the amplitudes, and caution is needed to apply the tensor technique. To prove that a method is invariant, as the first step we try various possibilities for expressing the amplitudes in tensor forms until we find one which renders the invariance of the wavefunction explicit.

### 3.4 MRCC: JM-ansatz based methods

In this section, we focus on the JM-ansatz based methods. From the analysis below, we will see that there are serious difficulties in making JM-ansatz based methods orbital invariant with respect to active space rotation. It will be clear by the end of this section that these methods are not affected by rotations in core orbital space or rotations in inactive virtual orbital space.

#### 3.4.1 Residual equation

Let us first make a ‘coarse’ analysis, neglecting the potential orbital invariance problem with excitation operators and the wavefunction. We will, following the same arguments as before, focus on the tensor structure of residuals indicated by the ket and bra states. For complete-model-space (CMS)-based methods, the wavefunction from the JM ansatz assumes the form:

$$|\psi\rangle = \sum_{\mu} e^{\hat{T}\mu} |\mu\rangle C_{\mu}, \quad (3.57)$$

where  $|\mu\rangle$  is a determinant in the active space. For the majority of the JM-ansatz based methods, we can abstract the residual equation to the following form:

$$\langle l^{(\mu)} | \hat{Z} | \mu \rangle = 0, \quad (3.58)$$

where  $|l^{(\mu)}\rangle$  is a determinant excited from  $|\mu\rangle$ , and

$$\hat{Z} = \begin{cases} e^{-\hat{T}_\mu} \hat{H} e^{\hat{T}_\mu} - \sum_\nu e^{-\hat{T}_\mu} e^{\hat{T}_\nu} |\nu\rangle \langle \nu| e^{-\hat{T}_\mu} \hat{H} e^{\hat{T}_\mu} & \text{(HSCC)[55, 57, 58]} \\ \hat{H} e^{\hat{T}_\mu} - E e^{\hat{T}_\mu} & \text{(BWCC)[61, 135, 153, 134]} \\ e^{-\hat{T}_\mu} \hat{H} e^{\hat{T}_\mu} C_\mu - \sum_\nu \langle \mu | e^{-\hat{T}_\nu} \hat{H} e^{\hat{T}_\nu} | \nu \rangle C_\nu e^{-\hat{T}_\mu} e^{\hat{T}_\nu} & \text{(Mk-MRCC)[63, 65, 66, 136, 68, 69, 70].} \end{cases}$$

(The closely related MRexpT [71, 130, 72] method is not discussed here, because it cannot easily be cast into the above form. The discussion in next subsection, however, also applies to MRexpT.)

Let us assume that  $\hat{Z}$  is invariant (for all the methods except Mk-MRCC, all indices in  $\hat{Z}$  are summation indices, and  $\hat{Z}$  is *formally* invariant; in other words, we first neglect the problem with  $\hat{Z}$  and focus on the residual equations). Then the tensor character of the residual is determined by  $\langle l^{(\mu)} |$  and  $|\mu\rangle$ . As an example, we look at these methods truncated at the level of singles and doubles and examine the system of 4 active orbitals ( $\phi_{m_1}, \phi_{m_2}, \phi_{m_3}, \phi_{m_4}$ ), 2 core electrons, 2 active electrons, and

$$|\mu\rangle = |\phi_{i'_1} \phi_{i'_2} \phi_{m_1} \phi_{m_2}\rangle, \quad (3.59)$$

$$\langle l^{(\mu)} | = \langle \phi_{b_1} \phi_{b_2} \phi_{m_1} \phi_{m_2} |. \quad (3.60)$$

$\langle l^{(\mu)} |$  is a doubly excited determinant from core orbitals to virtual orbitals. Then the residual is

$$\begin{aligned} \mathbb{R} &= \langle l^{(\mu)} | \hat{Z} | \mu \rangle = \langle \phi_{b_1} \phi_{b_2} \phi_{m_1} \phi_{m_2} | \hat{Z} | \phi_{i'_1} \phi_{i'_2} \phi_{m_1} \phi_{m_2} \rangle \\ &= \langle | \hat{a}_{b_1 b_2 m_1 m_2} \hat{Z} \hat{a}^{i'_1 i'_2 m_1 m_2} | \rangle \\ &= \mathbb{R}_{b_1 b_2 m_1 m_2}^{i'_1 i'_2 m_1 m_2}. \end{aligned} \quad (3.61)$$

Notice that the repeated indices here are not summation indices, so there is no tensor contraction.

Upon an orbital rotation in active space, the residual becomes

$$\mathbb{R}_{b_1 b_2 \tilde{m}_1 \tilde{m}_2}^{i_1' i_2' \tilde{m}_1 \tilde{m}_2} = \sum_{m_\alpha, m_\beta, m_\gamma, m_\rho} \mathbb{U}_{m_\alpha}^{\tilde{m}_1} \mathbb{U}_{m_\beta}^{\tilde{m}_2} \bar{\mathbb{U}}_{\tilde{m}_1}^{m_\gamma} \bar{\mathbb{U}}_{\tilde{m}_2}^{m_\rho} \mathbb{R}_{b_1 b_2 m_\gamma m_\rho}^{i_1' i_2' m_\alpha m_\beta}. \quad (3.62)$$

Now in the rotated orbital basis, the residual does not vanish. For example,  $\mathbb{R}_{b_1 b_2 \tilde{m}_1 \tilde{m}_2}^{i_1' i_2' \tilde{m}_1 \tilde{m}_2}$  has a contribution from

$$\begin{aligned} \mathbb{R}_{b_1 b_2 m_1 m_2}^{i_1' i_2' m_3 m_4} &= \langle \phi_{b_1} \phi_{b_2} \phi_{m_1} \phi_{m_2} | \hat{Z} | \phi_{i_1'} \phi_{i_2'} \phi_{m_3} \phi_{m_4} \rangle. \\ & \quad (\text{set } m_\alpha = m_3, m_\beta = m_4, m_\gamma = m_1, m_\rho = m_2 \text{ in Eq(3.62)}) \end{aligned} \quad (3.63)$$

This is a quadruple excitation with respect to  $|\phi_{i_1'} \phi_{i_2'} \phi_{m_3} \phi_{m_4}\rangle$ , and the residual is non-zero. This observation can be extended to general active spaces.

### 3.4.2 Wavefunction and Energy

From the discussion of residual equations, it is clear that the methods under discussion are not orbital invariant. However, we will see that neither the wavefunction nor the energy would be invariant, *even if the residual equations would be satisfied upon orbital rotations* for the methods under study. Let us first look at the wavefunction:

$$|\psi\rangle = \sum_{\mu} e^{\hat{T}_\mu} |\mu\rangle C_\mu. \quad (3.64)$$

Without going into details, we see that the invariance of the wavefunction would be limited by that of the excitation operator  $\hat{T}_\mu$ , even if we could assume that  $|\mu\rangle C_\mu$  did not affect the invariance property, which itself is not a valid assumption. In  $\hat{T}_\mu$ , the summation of active indices is done separately for active orbitals contained in  $|\mu\rangle$  and for the other active orbitals. This limits the ‘invariance’ of  $\hat{T}_\mu$  to orbital rotations in the two subspaces, as in CASCC. However, the situation is even worse, because every  $\hat{T}_\mu$ , corresponding to each  $|\mu\rangle$ , has its own ‘invariance’ space, and

the ‘invariance’ spaces for different  $\hat{T}_\mu$ ’s differ and at the same time also overlap. Thus the total wavefunction cannot be invariant in the whole active space. Even a more restricted invariance in subspaces of the active space does not seem possible, because it is hard to divide the active orbital space into a few disjoint sets of orbitals associated with every  $|\mu\rangle$ .

Let us go one step further. Even if we lift the restrictions on the range of every active summation index in every  $\hat{T}_\mu$ , the invariance problem with the wavefunction still exists, as long as we retain the implicit dependence of the  $\hat{T}$ -amplitudes on  $|\mu\rangle$  (otherwise the method becomes internally contracted). If the active summation index runs over the whole active orbital space,  $\hat{T}_\mu$ ’s appear ‘formally’ to be orbital invariant with respect to active orbital space rotation (certainly the redundancy problem in this case will be more severe, but we suppose that it is possible to design certain sufficiency conditions to solve the redundancy problem). However, the ‘formal’ invariance contradicts the dependence of  $\hat{T}_\mu$  on  $|\mu\rangle$ . To see this, let us look at the example introduced before: a system of 2 core electrons, 2 active electrons, and 4 active orbitals.

$$|\psi\rangle = \sum_{\mu} e^{\hat{T}_\mu} |\mu\rangle C_\mu = \sum_{m_1, m_2} e^{\hat{T}(|i'_1 i'_2 m_1 m_2\rangle)} \hat{a}^{i'_1 i'_2 m_1 m_2} |C_{i'_1 i'_2 m_1 m_2}\rangle. \quad (3.65)$$

$\hat{T}(|i'_1 i'_2 m_1 m_2\rangle)$  manifests the dependence of  $\hat{T}_\mu$ -amplitudes on  $|\mu\rangle = |i'_1 i'_2 m_1 m_2\rangle$ . Since  $|\mu\rangle$  is determined by the active orbitals in it  $\phi_{m_1}$  and  $\phi_{m_2}$ , the dependence of  $\hat{T}_\mu$ -amplitudes on  $|\mu\rangle$  implies the dependence on  $\phi_{m_1}$  and  $\phi_{m_2}$ , in an abstract way. More precisely,  $\hat{T}_\mu$  has a certain dependence on the combination of  $\phi_{m_1}$  and  $\phi_{m_2}$  which specifies the active space determinant  $|i'_1 i'_2 m_1 m_2\rangle$ . This dependence on a special subset of the active indices certainly contradicts the ‘invariance’ of  $\hat{T}_\mu$  in the whole active space. Therefore, we see that summations of indices do *not automatically* imply orbital invariance.

If the dependence does not exist,  $\hat{T}_\mu = \hat{T}_\nu, \forall \mu, \nu$ ,  $\hat{T}_\mu$ ’s can be pulled out, the ansatz changes and becomes internally contracted [76, 154, 63, 64, 79, 80, 155, 156]:

$$|\psi\rangle = e^{\hat{T}} \sum_{m_1, m_2} \hat{a}^{i'_1 i'_2 m_1 m_2} |C_{i'_1 i'_2 m_1 m_2}\rangle = e^{\hat{T}} |\psi_{\text{active}}\rangle. \quad (3.66)$$

Then we can readily show that this approach is orbital invariant, provided that the active sum-

mation indices in  $\hat{T}$  run over the whole active space and that the residual equation is modified correspondingly, for example:

$$\langle \psi_{\text{active}} | \hat{T}_{\lambda}^+ e^{-\hat{T}} \hat{H} e^{\hat{T}} | \psi_{\text{active}} \rangle = 0. \quad (3.67)$$

As another example, see Ref. [64].

Finally let us look at the energy in JM-ansatz based methods:

$$E = \langle \psi_{\text{active}} | \hat{H} | \psi \rangle, \quad (3.68)$$

which can be derived from the usual definition equation:

$$\langle \mu | \hat{H} | \psi \rangle = EC_{\mu}, \forall \mu \quad (3.69)$$

by multiplying both sides by  $C_{\mu}$  and summing over all  $\mu$ 's. Since both  $\hat{H}$  and  $\langle \psi_{\text{active}} |$  are invariant, the invariance of  $E$  requires the invariance of the wavefunction  $|\psi\rangle$ . Thus, the problem with the wavefunction shows up here again.

The redundancy problem inherent in the JM ansatz forces *ad hoc* definitions of residual equations. The ansatz itself conflicts with the orbital invariance property, which leads to the orbital invariance problem in residual equations. From the discussions, the problem is the use of multiple *vacua* and the dependence of the excitation operator amplitudes on the associated reference determinant. This issue seems unlikely to be solved without modifying the ansatz. For example, even if  $\hat{T}_{\mu}$ 's covered a much larger manifold, the problem with the wavefunction and energy would remain. Internal contraction provides one possible solution, upon proper definitions of residual equations.

For all the discussions in this section, we assumed that  $\hat{Z}$  is orbital invariant. At this point, we can see that this is not really the case. Indeed, the tensor character of the residual equation is even more troublesome. Since we have already drawn a rather strong conclusion from the analysis of the wavefunction, we will not go back to analyze the residual equation.

### 3.5 Conclusion

Tensor theory has been applied to examine the invariance properties of various *ab initio* methods upon orbital rotations. By utilizing the tensor properties of second-quantized operators, we can write determinants in tensor notation. Another noticeable technique employed here has been rewriting antisymmetric tensors in contracted forms to expose the essential tensor properties. To examine the orbital invariance issue, we have proposed a simple self-consistency-checking algorithm.

Using this algorithm, we demonstrate that HF, single reference CI and CC methods are all invariant with respect to rotations within occupied and unoccupied orbital spaces. The CASSCF and MRCI methods are invariant with respect to rotations in three spaces: core orbital space, active orbital space and inactive virtual orbital space. The particular versions of CASCC and CCSDt methods which are discussed in this chapter are invariant with respect to rotations in the four spaces: core orbitals, active-occupied orbitals, active-virtual orbitals, and inactive virtual orbitals. The JM-ansatz based methods are not invariant with respect to rotations in the active space, although they are invariant with respect to rotations in core orbital space and inactive virtual orbital space. The problem is revealed first by analyzing the residual equations and then by analyzing the wavefunction. The lack of invariance is inherent in the ansatz, and there does not seem to be an easy solution without modifying the ansatz. Loosely speaking, the essential deficiency is the use of multiple *vacua* and associated cluster operators whose amplitudes implicitly depend on the corresponding reference determinant. Internal contraction provides one candidate solution.

We have demonstrated theoretically the lack of orbital invariance for some methods. To what extent the results from these methods are affected by the problem is a separate issue which needs to be tested numerically.

This completes our discussion of the orbital invariance property. Starting with next chapter, we will focus on the method on which we have been working: the State Specific Equation of Motion Coupled Cluster (SS-EOMCC) method. From the discussion of the current chapter, we can easily see that SS-EOMCC is orbital invariant.

## Chapter 4

# State Specific Equation of Motion Coupled Cluster Method

### 4.1 General framework

The State Specific Equation of Motion Coupled Cluster (SS-EOMCC) method follows the first-transformation-then-diagonalization route. As in EOMCC, the final state energies are obtained from diagonalizing a transformed Hamiltonian  $\hat{H} = e^{-\hat{T}} \hat{H} e^{\hat{T}}$  over a suitable manifold of electronic states. The definition of the operator  $\hat{T}$  is in principle arbitrary, as the eigenvalues of  $\hat{H}$ , (when diagonalized over the complete Hilbert space), do not change under a similarity transformation. To define the cluster operator, we are therefore guided by convenience and the practical requirement that diagonalization of  $\hat{H}$  over a truncated manifold yields satisfactory results. Two issues require definitions: the parameterization of the cluster operator  $\hat{T}$  or the excitation operators included in  $\hat{T}$ , and the specification of a set of equations for the t-amplitudes. In SS-EOMCC, we proceed as follows. Initially we parameterize the wavefunction in the following way (in order to obtain t-amplitude equations):

$$|\Psi\rangle = e^{\hat{T}}|R\rangle, \tag{4.1}$$



where  $|R\rangle$  is the reference function obtained in some way, usually from a complete-active-space self-consistent-field (CASSCF) calculation. The definition of the cluster operator is analogous to the single reference case:

$$\hat{T} = \sum_{\lambda} t_{\lambda} \hat{\Omega}_{\lambda} = \hat{T}_1 + \hat{T}_2 = \sum_{i,a} t_a^i \hat{E}_i^a + \frac{1}{2} \sum_{i,j,a,b} t_{ab}^{ij} \hat{E}_{ij}^{ab}, \quad (4.2)$$

where  $\hat{\Omega}_{\lambda}$  stands for any excitation operator present in  $\hat{T}$ . Only single and double excitations are included to capture the major dynamical correlation. In the above definition, i/j denotes a hole orbital and a/b denotes a particle orbital. We take *both core orbitals and all active orbitals as hole orbitals*, and the others as particle orbitals. Equivalently, any orbital (fully or partially) occupied in the reference function is taken as a hole orbital. If we define as the physical vacuum the determinant  $|0\rangle$ , in which all hole orbitals are doubly occupied, that is,

$$|0\rangle = \prod_i \hat{a}_i^{\uparrow} \hat{a}_i^{\downarrow} | \rangle, \quad (4.3)$$

the structure of the cluster operator in SS-EOMCC is the same as that in single reference CCSD. In  $\hat{T}$ , since the active orbital creation operators are missing, not all two-body excitations out of the active space are included, for example, core-active and semi-internal excitations are omitted. Both types of excitations are included in the final diagonalization.

The  $\hat{E}$  operators are spin-free:

$$\hat{E}_i^a = \sum_{\sigma=\alpha,\beta} \hat{a}_{i\sigma}^{a\sigma}, \quad (4.4)$$

$$\hat{E}_{ij}^{ab} = \sum_{\substack{\sigma=\alpha,\beta \\ \rho=\alpha,\beta}} \hat{a}_{i\sigma}^{a\sigma} \hat{a}_{j\rho}^{b\rho}. \quad (4.5)$$

Since the spin-free operators are spin-singlet operators [1], the wavefunction is spin-adapted provided that  $|R\rangle$  is a spin eigenfunction.

The t-amplitude equations are defined as:

$$\langle R | \hat{\Omega}_\lambda^\dagger e^{-\hat{T}} \hat{H} e^{\hat{T}} | R \rangle = \langle R | \hat{\Omega}_\lambda^\dagger \hat{H} | R \rangle = 0, \forall \hat{\Omega}_\lambda. \quad (4.6)$$

The transformed Hamiltonian  $\hat{H}$  is obtained once these equations are solved. Then  $\hat{H}$  is diagonalized over the multireference configuration-interaction singles (MRCIS) space in an uncontracted fashion to yield the final wavefunction and energy. The MRCIS space consists of all determinants in the reference space and all determinants which can be reached by a single excitation of any reference determinant. The final diagonalization takes care of differential orbital relaxation, semi-internal excitations and non-dynamical correlation effects. If we denote the eigenfunction of  $\hat{H}$  from the diagonalization in MRCIS space as  $|C\rangle$ , the final wavefunction has the form

$$|\Psi\rangle = e^{\hat{T}}|C\rangle.$$

Hence the ansatz has relaxed singles (core-active and semi-internal excitations) from  $|C\rangle$  and contracted singles and doubles from cluster operators. However, one problem still remains: the core-active double excitations are missing from both  $\hat{T}$  and the final diagonalization. As a temporary fix to this problem, we do not allow core orbitals, and all hole orbitals are taken as active, which makes the method more expensive. A more economical way would be to include the missing excitations in the cluster operator in a contracted fashion, but this introduces the complication that components of the cluster operator do not commute. This problem will be addressed in future work.

Important features of the method are:

- The ansatz is internally contracted [76, 79, 81, 80, 82], which makes the parameterization rather compact. The wavefunction is qualitatively correct and rigorously spin-adapted. The method is state-specific. It is applicable to both ground and excited states. The energy is invariant with respect to orbital rotations in core, active and virtual subspaces. In the first step, we obtain  $|R\rangle$  from a CASSCF calculation, so  $|R\rangle = |\psi_{\text{CASSCF}}\rangle$  is orbital invariant.

For the residual equation, using the double excitation amplitude equation as an example,

$$\mathbb{R}_{ab}^{ij} = \langle R | \hat{E}_{ab}^{ij} e^{-\hat{T}} \hat{H} e^{\hat{T}} | R \rangle = \langle R | \hat{E}_{ab}^{ij} \hat{\tilde{H}} | R \rangle. \quad (4.7)$$

If we assume the tensor structure of t-amplitudes, this is clearly a tensor equation, if we follow arguments similar to those used for CID (see Chapter 3). That is, the residual remains zero upon orbital rotation. The last step is the diagonalization of the invariant quantity  $\hat{\tilde{H}}$  in the MRCIS space. Following the proof for MRCISD, it follows that the energy is invariant. Hence, the SS-EOMCC method is orbital invariant.

- SS-EOMCC is not size-extensive, but it is core-extensive [127], and relatedly size-intensive [128, 129]. That is, if a molecule separates into one single-reference fragment and one multireference fragment, the SS-EOMCC method will be size-consistent, provided that the orbitals in the CAS space can be localized. To save space, we do not give a detailed proof, but simply notice that a separable solution exists in such a situation,

$$|\Psi_{AB}\rangle = (e^{\hat{T}_A} \hat{C}_A) (e^{\hat{T}_B} \hat{C}_B)|\rangle,$$

where A is the single-reference fragment and all operators are second-quantized operators, to avoid explicit antisymmetrization.  $\hat{C}_A|\rangle$  gives the one determinant reference for fragment A, and  $\hat{C}_B|\rangle$  gives the reference function for fragment B, which comes from the diagonalization of  $\hat{\tilde{H}}_B = e^{-\hat{T}_B} \hat{H} e^{\hat{T}_B}$  in the MRCIS space. The proof is straightforward, following the techniques presented in Ref. [127].

- The spin-flip idea developed by Krylov [125, 126, 157, 158] is quite natural in the current EOMCC framework. For example, we can calculate  $\hat{T}$  amplitudes based on a triplet state calculation and use them to construct the transformed Hamiltonian and do diagonalization to extract other states. In the SS-EOMCC framework all states are spin-adapted (or spin-pure), including the states obtained from a spin-flip calculation.
- A Brueckner orbital scheme [159, 160, 161, 162, 163] can be implemented. We can rotate

orbitals using the  $\hat{T}_1$  operator and solve for T-amplitudes self-consistently, until finally  $\hat{T}_1 = 0$ . Since we usually interpret in the fashion that  $\hat{T}_2$  takes care of dynamical correlation effects and  $\hat{T}_1$  take into account orbital relaxation effects, we may regard Brueckner orbitals as orbitals optimized in the presence of dynamical correlation, in contrast to, say, CASSCF orbitals, which are optimized in the absence of dynamical correlation effects.

The computational cost of SS-EOMCC consists of two parts: evaluation of residuals and diagonalization of  $\hat{H}$  in the MRCIS space. The cost of the first part scales as  $v^4 o^2$  (there are three terms with the cost of  $v^4 o^2$  in the residual equation, where  $v$  is the number of virtual orbitals and  $o$  the number of hole orbitals), similar to single reference CCSD. This scaling is due to the specific approximation we made in the residual equation: approximating many-particle density matrices by one- and two-particle cumulants (see next subsection for detailed discussions of density matrices). For the diagonalization of  $\hat{H}$ , to reduce computational expense we may include only up to two-body terms from  $\hat{H}$ , which will make the cost the same as that of diagonalizing the bare Hamiltonian  $\hat{H}$  in the same space (the exact diagonalization needs up to three-body components of  $\hat{H}$ , because up to singles are included in the diagonalization space, and the cluster operator only includes pure hole-to-virtual excitations). In Ref. [164], it has been shown that this additional approximation yields small errors when the cluster amplitudes are small, at least for the cases studied. For large active spaces, the MRCIS diagonalization dominates the computational cost and the double excitation effect is included in the cluster operator instead of in the final diagonalization, so we essentially get the (internally contracted) double excitation effect for free. In contrast, for internally contracted MRCI, in the diagonalization, the contracted doubles interact directly with the uncontracted singles, and this step dominates the computational expense (more expensive than evaluating singles-singles interactions). Thus with proper implementation, the SS-EOMCC method is potentially much cheaper than the internally contracted MRCI method.

## 4.2 Appearance of density matrices

To illustrate the appearance of density matrices (DM's) in residual equations, we take the doubles equations as an example and use spin orbital normal order theory with respect to the true vacuum  $| \rangle$  for clarity:

$$\langle R | \hat{a}_{ab}^{ij} \hat{H} | R \rangle = 0, \quad (4.8)$$

where  $\hat{a}$  stands for the normal order operator with respect to the true vacuum  $| \rangle$ :

$$\hat{a}_{\dots rs}^{\dots pq} = \dots \hat{a}_p^+ \hat{a}_q^+ \hat{a}_s \hat{a}_r \dots. \quad (4.9)$$

Corresponding to this normal order theory, there is a generalized Wick theorem which tells how to expand the product of two normal order operators into a series of normal order operators by carrying out contractions (the contractions are simply Kronecker deltas). Utilizing the theorem, we expand  $\hat{a}_{ab}^{ij} \hat{H}$ :

$$\hat{a}_{ab}^{ij} \hat{H} = \hat{a}_{ab}^{ij} e^{-\hat{T}} \hat{H} e^{\hat{T}} = z_0 + z_r^s \hat{a}_s^r + \frac{1}{2} z_{uv}^{wt} \hat{a}_{wt}^{uv} + \dots, \quad (4.10)$$

$$\langle R | \hat{a}_{ab}^{ij} \hat{H} | R \rangle = z_0 + z_r^s \langle R | \hat{a}_s^r | R \rangle + \frac{1}{2} z_{uv}^{wt} \langle R | \hat{a}_{wt}^{uv} | R \rangle + \dots \quad (4.11)$$

$$= z_0 + z_r^s \gamma_s^r + \frac{1}{2} z_{wt}^{uv} \gamma_{wt}^{uv} + \dots \quad (4.12)$$

$$= 0. \quad (4.13)$$

The amplitudes  $z$  depend on the external labels and DM's are defined as the expectation values of normal order operators:

$$\gamma_q^p = \langle R | \hat{a}_q^p | R \rangle, \quad (4.14)$$

$$\gamma_{qs}^{pr} = \langle R | \hat{a}_{qs}^{pr} | R \rangle, \quad (4.15)$$

$$\dots \quad (4.16)$$

Thus, DM's appear in residual equations. Besides the Hamiltonian matrix elements and  $t$ -amplitudes, DM's are the only information needed. Thus the normal order theory allows us to express residual equations in a compact way, in terms of DM's.

For the SS-EOMCC method, due to the special structure of the cluster operator, *up to* four-particle DM's appear in residual equations. Since  $|R\rangle$  has contributions from only hole orbitals,  $\gamma = 0$ , if it has particle indices. Thus, for the normal order expansion of  $\hat{a}_{ab}^{ij} \hat{H}$ , we only need to consider terms whose operators do not contain any particle index. Therefore, all particle indices in  $\hat{a}_{ab}^{ij} \hat{H}$  must be contracted.  $\hat{T}$  has only particle creation operators, which must be contracted by particle annihilation operators in  $\hat{a}_{ab}^{ij}$  and  $\hat{H}$ . Since  $\hat{H}$  contains at most two particle annihilation operators,  $\hat{a}_{ab}^{ij}$  and  $\hat{H}$  can contract at most four particle creation operators. Then it follows that at most quadratic  $\hat{T}_2$  will contribute to residual equations, because cubic and higher powers of  $\hat{T}_2$  have more than four particle creation operators.

$$\hat{H} = e^{-\hat{T}} \hat{H} e^{\hat{T}} = e^{-\hat{T}_2} (e^{-\hat{T}_1} \hat{H} e^{\hat{T}_1}) e^{\hat{T}_2} \quad (4.17)$$

$$= e^{-\hat{T}_2} \hat{H}_s e^{\hat{T}_2} \quad (4.18)$$

$$= \hat{H}_s + [\hat{H}_s, \hat{T}_2] + \frac{1}{2} [[\hat{H}_s, \hat{T}_2], \hat{T}_2] + \dots \quad (4.19)$$

$$\text{and} \quad (4.20)$$

$$\langle R | \hat{a}_{ab}^{ij} \hat{H} | R \rangle = \langle R | \hat{a}_{ab}^{ij} \left( \hat{H}_s + [\hat{H}_s, \hat{T}_2] + \frac{1}{2} [[\hat{H}_s, \hat{T}_2], \hat{T}_2] \right) | R \rangle, \quad (4.21)$$

where we have defined

$$\hat{H}_s = e^{-\hat{T}_1} \hat{H} e^{\hat{T}_1}. \quad (4.22)$$

If we denote the particle rank of an operator  $\hat{A}$  by  $\mathcal{N}(\hat{A})$ , then  $\mathcal{N}(\hat{H}_s) \leq 2$ ,  $\mathcal{N}([\hat{H}_s, \hat{T}_2]) \leq 3$ , and  $\mathcal{N}(\frac{1}{2} [[\hat{H}_s, \hat{T}_2], \hat{T}_2]) \leq 4$ . If we assume that all particle indices in  $\hat{a}_{ab}^{ij}$  are contracted to indices in  $\hat{H}$ , then  $\mathcal{N}(\hat{a}_{ab}^{ij} \hat{H}_s) \leq 2$ ,  $\mathcal{N}(\hat{a}_{ab}^{ij} [\hat{H}_s, \hat{T}_2]) \leq 3$ , and  $\mathcal{N}(\hat{a}_{ab}^{ij} \frac{1}{2} [[\hat{H}_s, \hat{T}_2], \hat{T}_2]) \leq 4$ . Therefore, the particle ranks of terms, which will contribute to  $\langle R | \hat{a}_{ab}^{ij} \hat{H} | R \rangle$ , do not exceed four. It follows that there are up to four-particle DM's in residual equations.

The many-particle DM's are expensive to compute, and their inclusion in the residual equation would also be expensive. We approximate the three- and four-particle DM's by expanding them in terms of cumulants [83, 84, 85, 86, 87, 88, 89, 90, 91]. Any contributions containing three- or four-particle cumulants are discarded. In addition, quadratic two-particle cumulants are not included either. This particular approximation scheme can be viewed as a natural approach from the perspective of a novel normal order theory ( $\gamma$ -normal order), the details of which are presented in Chapter 5.

For biradical-like systems (treated by the SS-EOMCC[+2] approach), we need not approximate residual equations, and up to two-particle DM's are sufficient. Let us see why. With  $|0\rangle$  as the vacuum (see Eq. (4.3)), all determinants in  $|R\rangle$  are two-hole states:

$$|R\rangle = \sum_{ij} C_{ij} \hat{a}_i \hat{a}_j |0\rangle. \quad (4.23)$$

If we use particle-hole formalism based normal order theory with  $|0\rangle$  as the vacuum and write every quantity in  $\hat{a}_{ab}^{ij} \hat{H}$  in this normal order, we can expand  $\hat{a}_{ab}^{ij} \hat{H}$  accordingly. With this normal order (denoted by ‘ $\sim$ ’ and ‘ $\{ \}$ ’), the normal order operators are defined as:

$$\tilde{a}_{i_2}^{i_1} = \{\hat{a}_{i_2}^{i_1}\} = -\hat{a}_{i_2} \hat{a}_{i_1}^+, \quad (4.24)$$

$$\tilde{a}_{i_3 i_4}^{i_1 i_2} = \{\hat{a}_{i_3 i_4}^{i_1 i_2}\} = \hat{a}_{i_4} \hat{a}_{i_3} \hat{a}_{i_1}^+ \hat{a}_{i_2}^+, \quad (4.25)$$

$$\dots \quad (4.26)$$

The above arguments about particle ranks also hold here, so we have up to four-particle DM's. However, in this case, the hole-type DM's are expectation values of  $\tilde{a}$ 's. We term them as  $\xi$ :

$$\xi_{i_2}^{i_1} = \langle R | \tilde{a}_{i_2}^{i_1} | R \rangle, \quad (4.27)$$

$$\xi_{i_3 i_4}^{i_1 i_2} = \langle R | \tilde{a}_{i_3 i_4}^{i_1 i_2} | R \rangle, \quad (4.28)$$

$$\dots \quad (4.29)$$

In particular, three- and four-particle  $\xi$ 's vanish. For example:

$$\xi_{i_4 i_5 i_6}^{i_1 i_2 i_3} = \langle R | \tilde{a}_{i_4 i_5 i_6}^{i_1 i_2 i_3} | R \rangle = \langle R | \hat{a}_{i_6} \hat{a}_{i_5} \hat{a}_{i_4} \hat{a}_{i_1}^+ \hat{a}_{i_2}^+ \hat{a}_{i_3}^+ | R \rangle = 0, \quad (4.30)$$

because all determinants in  $|R\rangle$  are two-hole states, and  $\hat{a}_{i_1}^+ \hat{a}_{i_2}^+ \hat{a}_{i_3}^+ | R \rangle = 0$ . Hence, only  $\xi_1$  and  $\xi_2$  are needed and they are expressed in terms of  $\gamma_1$  and  $\gamma_2$ . Thus we have argued that up to two-particle DM's are sufficient to evaluate residuals for biradical-like systems. In practice, we use the above strategy to evaluate residuals for this type of systems, such as the single-bond breaking processes of  $F_2$ .

### 4.3 Convergence Scheme

In this subsection three issues will be discussed that are important in the context of converging the cluster amplitudes in the internally contracted SS-EOMCC equations. The first issue concerns the amplitude updating scheme and the solution of the typically nearly-singular non-linear equations. The second issue concerns the definition of orbital energies and a diagonal zeroth-order Hamiltonian that defines the denominator updates and the first-order perturbative corrections. The last issue addresses a perturbative correction that attempts to provide reasonable estimates for amplitudes that are discarded from the CC equations, which is applied to provide smoothed potential energy surfaces. In the result section we will provide some examples that illustrate the effectiveness of the approach.

#### 4.3.1 Solving the near-singular non-linear equations

The cluster equations read

$$\mathbb{R}_\rho = \langle R | \hat{\Omega}_\rho^+ e^{-\hat{T}} \hat{H} e^{\hat{T}} | R \rangle = 0. \quad (4.31)$$



If we assume a current guess  $\hat{T}$  for the amplitudes, the correction  $\Delta$  to the t-amplitudes is obtained from the following update equation:

$$\langle R|\hat{\Omega}_\rho^+ e^{-(\hat{T}+\hat{\Delta})} \hat{H} e^{\hat{T}+\hat{\Delta}}|R\rangle \approx \langle R|\hat{\Omega}_\rho^+ e^{-\hat{T}} \hat{H} e^{\hat{T}}|R\rangle + \langle R|\hat{\Omega}_\rho^+ [\hat{H}_0, \hat{\Delta}]|R\rangle \quad (4.32)$$

$$= \mathbb{R}_\rho + \langle R|\hat{\Omega}_\rho^+ [\hat{H}_0, \hat{\Delta}]|R\rangle, \quad (4.33)$$

where  $\hat{\Delta} = \sum_{i,j,a,b} \Delta_{ij}^{ab} \hat{E}_{ij}^{ab}$ . The zeroth-order Hamiltonian is assumed to have the simple form  $\hat{H}_0 = \sum_p \epsilon_p \{\hat{a}_p^\dagger \hat{a}_p\}$  (to be discussed later), and the commutator  $[\hat{H}_0, \hat{\Delta}] = \hat{X} = \sum_{i,j,a,b} X_{ij}^{ab} \hat{E}_{ij}^{ab}$  is then easily evaluated. Hence, if  $X$  is known the solution of the amplitudes  $\Delta$  reduces to a conventional denominator update

$$\Delta_i^a = \frac{X_i^a}{\epsilon_a - \epsilon_i}; \quad \Delta_{ij}^{ab} = \frac{X_{ij}^{ab}}{\epsilon_a + \epsilon_b - \epsilon_i - \epsilon_j}. \quad (4.34)$$

Solving for the amplitudes of the operator  $X$  requires the solution of a set of potentially ill-conditioned linear equations. Let us consider the doubles part of the equations explicitly (the singles equations are treated similarly).

$$\sum_{k,l} \langle R|\hat{E}_{ab}^{ij} \hat{E}_{kl}^{ab}|R\rangle X_{kl}^{ab} = \sum_{k,l} S_{ij,kl} X_{kl}^{ab} = -\mathbb{R}_{ij}^{ab}. \quad (4.35)$$

These equations are diagonal in the virtual orbitals because the reference state has zero occupation for these orbitals. The metric matrix  $S$  can be nearly singular, and a regularized inverse of this matrix is determined by diagonalization:

$$S_{ij,kl} = \sum_{\lambda} U_{ij,\lambda} \lambda U_{kl,\lambda}; \quad S_{ij,kl}^{-1} = \sum_{\lambda > \eta} U_{ij,\lambda} \lambda^{-1} U_{kl,\lambda}. \quad (4.36)$$

In the sum over  $\lambda$ , only those vectors are included whose eigenvalues  $\lambda$  exceed a threshold value  $\eta$ . Together with the regularized inverse, we also define a projector on the regular subspace

$$P_{kl}^{ij} = \sum_{\lambda > \eta} U_{ij,\lambda} U_{kl,\lambda}. \quad (4.37)$$

In addition, for future reference we define a projector on a nearly singular subspace

$$Q_{kl}^{ij} = \sum_{\delta < \lambda < \eta} U_{ij,\lambda} U_{kl,\lambda}. \quad (4.38)$$

In practice the threshold  $\eta$  is taken to be fairly large, on the order of  $10^{-2}$ , while the lower threshold  $\delta$  can be fairly small, on the order of  $10^{-4}$ . (For all calculations shown in this chapter, the value  $\eta = 0.01$  is used, unless specified otherwise) The reason for the relatively large value of the threshold is that amplitudes corresponding to small eigenvalues can easily grow large, and they cause trouble due to the non-linearity of the CC equations. This is quite different from an internally contracted MRCI calculation, where one also discards amplitudes corresponding to small eigenvalues of the metric matrix, but larger amplitudes do less harm as they make only a small contribution to the final wave function. Typical thresholds for MRCI would be similar to our threshold  $\delta$  that defines the truly singular subspace. The metric matrices and the regularized inverse as well as the projectors are calculated once, and the diagonalization spaces involved are small in general, as they only involve occupied orbitals. With the metric matrix defined as above, the t-amplitudes correction, projected on the regular subspace, are obtained as

$$\Delta_{ij}^{ab} = \sum_{k,l} P_{kl}^{ij} \left( \sum_{m,n} \frac{S^{-1mn} \mathbb{R}_{mn}^{ab}}{\epsilon_a + \epsilon_b - \epsilon_k - \epsilon_l} \right). \quad (4.39)$$

The DIIS convergence accelerator [165] is used to improve convergence of the denominator update, and we ensure that after a DIIS extrapolation the t-amplitudes still only have components along the regular subspace, using the projector operator.

### 4.3.2 Orbital energies in the zeroth order Hamiltonian

The choice of orbital energies is critical, and desirable criteria for the zeroth-order Hamiltonian include:

1. Smooth convergence of the CC equations and the MRCIS diagonalization step.
2. Replacing the full CC amplitudes by their perturbative analogs from first-order perturbation

theory results in minor changes in final state energies.

The latter criterion is quite demanding, and a less stringent requirement is that excitation energies obtained by diagonalizing the transformed Hamiltonian over the MRCIS space are only marginally affected by a substitution of CC by PT amplitudes, at least for simple problems.

The virtual orbital energies present no problem, and we simply use the Fock matrix corresponding to the one-particle density matrix of the reference state, and diagonalize this operator over the virtual space. Since all of the excitations involve annihilation of an occupied orbital and promotion of the electron into a virtual orbital, it is important that all occupied orbital energies be substantially lower (negative) than the lowest virtual orbital energy (positive). This condition would typically not be satisfied if we used the Fock matrix of the reference state and diagonalize over the active space. While it is fine to diagonalize this Fock operator over the core space of doubly occupied orbitals, active orbitals that are weakly occupied (essentially virtual orbitals), may attain large (positive) orbital energies, and this can destroy convergence behavior. Moreover, this behavior is also not physical in the sense of requirement 2. To solve this problem we use orbitals and orbital energies from the the extended Koopmans' theorem [166].

A set of active orbitals is obtained by solving a generalized eigenvalue problem

$$KC = DC\varepsilon, C^+DC = \mathbf{1}, \quad (4.40)$$

where

$$K_{ij} = \langle R|\hat{a}_i^+[\hat{H}, \hat{a}_j]|R\rangle, D_{ij} = \langle R|\hat{a}_i^+\hat{a}_j|R\rangle. \quad (4.41)$$

These orbital energies are interpreted as the variationally optimum ionization potentials that can be obtained from the basis states  $\hat{a}_j|R\rangle$ . This ionization potential interpretation is consistent with the promotion of an electron from orbital  $j$  to a virtual orbital  $a$  in the non-interacting limit where the excitation energy reduces to the sum of an ionization potential plus an electron affinity. Since the orbitals obtained from the EKT procedure are not orthogonal, after diagonalization the orbitals are orthogonalized using Löwdin's  $S^{-1/2}$  orthogonalization procedure [167], while

the orbital energies remain the EKT values. The above definition of orbital energies provides a smooth convergence of the CC and MRCIS equations, and it defines first-order t-amplitudes that can be used effectively in the singular perturbation step (see next subsection). The first-order t-amplitudes are obtained by solving the first order residual equation:

$$\langle R | \hat{E}_{ab}^{ij} (\hat{H} + [\hat{H}_0, \hat{T}^{(1)}]) | R \rangle = 0. \quad (4.42)$$

If we use the first-order t-amplitudes instead of those from solving the complete residual equation, we call the method SS-EOMPT. The effectiveness of constructing the zeroth order Hamiltonian using the EKT orbital energies is also reflected in the fact that excitation energies from first order SS-EOMPT are in fair agreement with SS-EOMCC. We illustrate this using the example of vertical excitation energies of ozone.

For comparison, we carry out two sets of calculations using SS-EOMCC[+2] and SS-EOMPT[+2], and the results are listed in Table 4.1 ('+2' indicates that we include one more orbital,  $2b_1$ , to construct the vacuum). In this table we list the vertical excitation energies for the lowest excitations from  $1^1A_1$  to both singlet and triplet states in each symmetry block:  $A_1, B_1, B_2$  and  $A_2$ . The results from EOM-CCSDT-3 [168] are also included. In addition, we present results from state-averaged SS-EOMCC calculations (here the cluster amplitudes are solved by using the average one- and two-particle density matrices and using an equal weighting of the ground and all eight excited states considered). For all these calculations, we use CASSCF orbitals and the PBS basis set [169]. For state specific calculations, the difference for the vertical excitation energies between SS-EOMCC and SS-EOMPT is at most 0.07 eV. For state-averaged calculations, the difference is even smaller, around 0.01 eV. In contrast, the absolute energies from SS-EOMCC and SS-EOMPT calculations can differ as much as 6.7 eV. Therefore from SS-EOMCC to SS-EOMPT, the energy for each state is shifted by approximately the same amount. We also notice a significant difference for the vertical excitation energy from  $1^1A_1$  to  $2^1A_1$  between SS-EOMCC (or SS-EOMPT) and EOM-CCSDT-3. This transition is dominated by double excitations:  $6a_1^2 \rightarrow 2b_1^2$  and  $4b_2^2 \rightarrow 2b_1^2$ . Thus, the accuracy of EOM-CCSDT-3 is suspicious, because probably up to quadruples are needed to get satisfactory results for double excitations. In comparison, the SS-EOMCC method treats

both single and multiple valence excitations in a balanced way, so that very likely the excitation energy from EOM-CCSDT-3 for this particular transition is too high, and this speculation is supported by the the CR-EOMCCSD(T) study of the adiabatic excitation energies of ozone by Kowalski, Piecuch and co-workers [22, 170].

Table 4.1: The excitation energies of the first four singlet and triplet states of ozone in the PBS basis set [169]. The total energies are in  $E_h$  and others are in eV. (the superscript ‘ex’ means ‘excitation energy’. The subscript ‘EOM’ refers to EOM-CCSDT-3 [168]. ‘ $\Delta$ ’ stands for  $E_{CC}^{\text{ex}} - E_{PT}^{\text{ex}}$ )

state specific						
state	$E_{CC}$	$E_{PT}$	$E_{CC}^{\text{ex}}$	$E_{PT}^{\text{ex}}$	$E_{EOM}^{\text{ex}}$	$\Delta$
$1^1A_1$	-225.0329	-225.0100				
$2^1A_1$	-224.8643	-224.8410	4.59	4.60	5.95	-0.01
$1^1B_1$	-224.9498	-224.9253	2.26	2.30	2.29	-0.04
$1^1B_2$	-224.8322	-224.8119	5.46	5.39	5.21	0.07
$1^1A_2$	-224.9530	-224.9282	2.17	2.23	2.23	-0.05
$1^3A_1$	-224.7342	-224.7119	8.13	8.11	7.90	0.02
$1^3B_1$	-224.9655	-224.9410	1.83	1.88	1.77	-0.05
$1^3B_2$	-224.9668	-224.9429	1.80	1.83	1.61	-0.03
$1^3A_2$	-224.9618	-224.9373	1.93	1.98	1.91	-0.04
state-averaged						
state	$E_{CC}$	$E_{PT}$	$E_{CC}^{\text{ex}}$	$E_{PT}^{\text{ex}}$	$E_{EOM}^{\text{ex}}$	$\Delta$
$1^1A_1$	-225.0346	-225.0099				
$2^1A_1$	-224.8718	-224.8474	4.43	4.42	5.95	0.01
$1^1B_1$	-224.9527	-224.9283	2.23	2.22	2.29	0.01
$1^1B_2$	-224.8371	-224.8125	5.37	5.37	5.21	0.00
$1^1A_2$	-224.9557	-224.9313	2.15	2.14	2.23	0.01
$1^3A_1$	-224.7386	-224.7140	8.05	8.05	7.90	0.00
$1^3B_1$	-224.9681	-224.9441	1.81	1.79	1.77	0.01
$1^3B_2$	-224.9700	-224.9455	1.76	1.75	1.61	0.01
$1^3A_2$	-224.9637	-224.9395	1.93	1.92	1.91	0.01

### 4.3.3 Singular perturbative correction

Since a fairly large threshold is used and a substantial number of t-amplitudes might be discarded, this can cause troubles in obtaining smooth potential energy surfaces, as a different number of amplitudes are retained at different geometries. The result is that SS-EOMCC potential energy surfaces generally are not smooth. For a similar reason, SS-EOMCC might not yield balanced energy differences between two critical points on a potential energy surface (for example, transition

state energy) if different numbers of t-amplitudes are discarded at different geometries. To partly correct for this behavior, we make a perturbative estimate of the amplitudes discarded from the CC equations. To this end, we solve the following set of equations:

$$\sum_{k,l} Q_{kl}^{ij} \langle R | \hat{E}_{ab}^{kl} (\hat{H} + [\hat{H}_0, \hat{T}^{(1)}]) | R \rangle = 0, \quad (4.43)$$

$$(\mathbf{1} - Q)_{kl}^{ij} t_{ab}^{(1)kl} = 0, \quad (4.44)$$

where  $Q$  is the projector in the nearly singular subspace (Eq (4.38)). This near-singular perturbative correction is solved at the initial stage of the CC iteration, and the overall t-amplitudes are defined as the sum of the regular  $t_P$  and near-singular  $t_Q$  components:

$$t_{ij}^{ab} = t_{Pij}^{ab} + t_{Qij}^{ab} = \sum_{k,l} P_{ij}^{kl} t_{Pkl}^{ab} + \sum_{k,l} Q_{ij}^{kl} t_{Qkl}^{(1)ab}. \quad (4.45)$$

These mixed t-amplitudes enter the transformed Hamiltonian which is used both in the solution of the equations for the regular t-amplitudes, and in the final MRCIS diagonalization step (only the correction for double excitation amplitudes is implemented). The inclusion of the singular perturbative correction does smoothen the potential energy surfaces, but there is a remaining discontinuity as we switch equations between the regular and nearly-singular amplitudes.

A possibly more attractive alternative would be to define a single equation

$$\sum_{k,l} Q_{kl}^{ij} \langle R | \hat{E}_{ab}^{kl} (\hat{H} + [\hat{H}_0, \hat{T}^{(1)}]) | R \rangle + \sum_{k,l} P_{kl}^{ij} \langle R | \hat{E}_{ab}^{kl} e^{-\hat{T}} \hat{H} e^{\hat{T}} | R \rangle = 0, \quad (4.46)$$

and to use a smooth switching function to define the P and Q operators which would satisfy the condition that their sum projects on the complete non-singular space (following recent work by Subotnik and Head-Gordon for local correlation approaches [171].) This fully smooth strategy has not been followed yet, as we first wish to examine the effect of the use of different equations on the results. As we will see, current results are already fairly smooth, in comparison to not using the correction (as shown by the example of  $N_2$  ground state energies in next section).

In the next chapter, we discuss normal order theory in a wide context, and we are not confined

to the particular normal order used in our approach. Instead, we first focus on the multireference normal order theory developed by Mukherjee and Kutzelnigg, which is a beautiful generalization of the traditional particle-hole formalism based normal order theory. Then we can demonstrate the normal order, used in SS-EOMCC to approximate the residual, and exhibit its relations to other normal orders.

## Chapter 5

# Normal order and generalized Wick theorem

In the case of the true vacuum state  $| \rangle$ , a normal order is an order of the creation or annihilation operators  $\cdots \hat{a}_p^+ \cdots \hat{a}_q \cdots$  in which the annihilation operators are to the right of the creation operators. For example,  $\hat{a}_q^p, \hat{a}_{rs}^{pq}, \cdots$  are in normal order if the operators are defined as follows:

$$\hat{a}_q^p \equiv \hat{a}_p^+ \hat{a}_q, \quad (5.1)$$

$$\hat{a}_{rs}^{pq} \equiv \hat{a}_p^+ \hat{a}_q^+ \hat{a}_s \hat{a}_r, \quad (5.2)$$

$$\cdots, \quad (5.3)$$

$$\hat{a}_{q \cdots s}^{p \cdots r} \equiv \hat{a}_p^+ \cdots \hat{a}_r^+ \hat{a}_s \cdots \hat{a}_q. \quad (5.4)$$

Let us call this normal order  $v$ -normal order ( $v$  means *true vacuum*). If we define particle-number-conserving operators as those which have the same number of creation operators and annihilation operators, all  $\hat{a}$  defined above are particle-number-conserving operators. This class of operators is the most important case in practice, and we will only be concerned with this particular class in this work. If we call the true vacuum  $| \rangle$  the reference state in this case, then the expectation



value of any v-normal order operator vanishes:  $\langle |\hat{a}_q^{p\cdots} \rangle = 0, \forall \hat{a}$ . For v-normal order, we have a corresponding series of rules which tells how to express a product of any two v-normal order operators  $\hat{a}_q^{p\cdots}$  and  $\hat{a}_s^{r\cdots}$  in terms of a set of normal order terms (a normal order term is a normal order operator with a certain coefficient). These rules are called the generalized Wick theorem (GWT).[172] In this special case of v-normal order, let us call them v-GWT.

The definition of normal order can be extended. In general we can define operators in other normal orders (directly or indirectly) in terms of v-normal order operators. When defining new normal order operators (denoted by  $\tilde{a}$ ) in terms of  $\hat{a}$ 's, we often require that for  $\tilde{a}$  of any particle rank, the maximum particle rank of  $\hat{a}$ 's in the definition is the same as that of  $\tilde{a}$ . Thus, given an operator

$$\hat{Z} = z_0 + z_p^q \hat{a}_q^p + z_{pr}^{qs} \hat{a}_{qs}^{pr} + \cdots, \quad (5.5)$$

we can rewrite it in a new normal order:

$$\hat{Z} = z'_0 + z'_p{}^q \tilde{a}_q^p + z'_{pr}{}^{qs} \tilde{a}_{qs}^{pr} + \cdots. \quad (5.6)$$

The relation between the coefficients  $z$  and the coefficients  $z'$  depends on the definition of the particular normal order.

In single reference coupled cluster theory, the reference function  $|R\rangle$  is one determinant, usually the Hartree-Fock determinant  $|\psi_{\text{HF}}\rangle$ . In the particle-hole formalism, the orbitals occupied in the reference determinant are called *hole* orbitals, and those unoccupied are called *particle* orbitals. With respect to  $|R\rangle$ , if any hole creation operator  $\hat{a}_i^+$  or any particle annihilation operator  $\hat{a}_b$  acts on  $|R\rangle$ , it annihilates  $|R\rangle$ :

$$\hat{a}_i^+ |R\rangle = 0, \forall i, \quad (5.7)$$

$$\hat{a}_b |R\rangle = 0, \forall b, \quad (5.8)$$

where  $i$  is a hole orbital index and  $b$  is a particle orbital index. Therefore it is justified to call hole

creation and particle annihilation operators *quasi-annihilation* operators, and other operators (hole annihilation and particle creation operators) *quasi-creation* operators. We can define a normal order of operators  $\cdots \hat{a}_p^+ \cdots \hat{a}_q \cdots$  such that all quasi-annihilation operators are to the right of quasi-creation operators. If we denote the operator in this normal order as  $\tilde{a}_q^{p\cdots}$ , then it can be verified that  $\langle \tilde{a}_q^{p\cdots} \rangle = 0, \forall \tilde{a}$ . Let us call this normal order *h-normal order*, and the corresponding GWT (denoted as *h-GWT*) gives the rules for how to expand the product of two *h-normal order* operators into a series of *h-normal order* terms.

In multireference cases, where  $|R\rangle$  is a multi-determinantal function, it is not obvious how to define a normal order of physical significance. A cumulant [83, 84, 85, 86, 87, 88, 89, 90, 91] based normal order theory [63, 77, 78, 64, 87, 173, 174, 175, 176, 177] was proposed by Mukherjee and Kutzelnigg, which is a generalization of *h-GWT* to multi-determinantal reference functions. In this theory, the expectation value of any normal order operator vanishes, and cumulants (denoted by  $\lambda$ ) appear naturally as contractions in the theory. For simplicity, let us call this normal order  $\lambda$ -normal order. The definition was outlined in Ref. [78], but the rules regarding how to expand the product of two  $\lambda$ -normal order operators, that is, generalized Wick theorem (GWT), were neither given explicitly nor proven. Here we give an algebraic proof for the GWT (denoted as  $\lambda$ -GWT), and this formal proof is based purely on the normal order definition.

Normal order theory is important to us for the following reasons:

- It helps to derive working equations, as briefly explained in Section 6.1. In principle, commutator relations suffice for this purpose, but using them would be far more cumbersome. Normal order theory in general facilitates deriving details of equations.
- It enables us to define approximations more easily, as will be clear at the end of this chapter.
- It allows us to define a normal order exponential ansatz  $\{e^{\hat{T}}\}$ , which is not used in SS-EOMCC, but is used in the internally contracted MRCC method, as detailed in Chapter 9.

Let us first define reduced density matrices for later use, denoted by  $\gamma$ 's:

$$\gamma_q^p \equiv \langle R | \hat{a}_q^p | R \rangle, \quad (5.9)$$

$$\gamma_{qs}^{pr} \equiv \langle R | \hat{a}_{qs}^{pr} | R \rangle, \quad (5.10)$$

$$\dots, \quad (5.11)$$

$$\gamma_{q\dots s}^{p\dots r} \equiv \langle R | \hat{a}_{q\dots s}^{p\dots r} | R \rangle. \quad (5.12)$$

Cumulants, denoted by  $\lambda$ 's, are defined recursively in terms of  $\gamma$ , by using the antisymmetrization operator  $\hat{\mathbb{A}}$ :

$$\gamma_q^p \equiv \lambda_q^p, \quad (5.13)$$

$$\gamma_{qs}^{pr} \equiv \lambda_{qs}^{pr} + \lambda_q^p \lambda_s^r - \lambda_s^p \lambda_q^r = \lambda_{qs}^{pr} + \hat{\mathbb{A}}(\lambda_q^p \lambda_s^r), \quad (5.14)$$

$$\begin{aligned} \gamma_{qsu}^{prt} &\equiv \lambda_{qsu}^{prt} + (\lambda_q^p \lambda_s^r \lambda_u^t - \lambda_q^p \lambda_s^t \lambda_u^r + \lambda_q^r \lambda_s^t \lambda_u^p - \lambda_q^r \lambda_s^p \lambda_u^t + \lambda_q^t \lambda_s^p \lambda_u^r - \lambda_q^t \lambda_s^r \lambda_u^p) + \\ &\quad (\lambda_q^p \lambda_s^r \lambda_u^t - \lambda_s^p \lambda_q^r \lambda_u^t + \lambda_u^p \lambda_s^r \lambda_q^t + \lambda_s^r \lambda_q^p \lambda_u^t - \lambda_q^r \lambda_s^p \lambda_u^t - \lambda_u^p \lambda_q^r \lambda_s^t + \lambda_u^t \lambda_q^p \lambda_s^r - \lambda_q^t \lambda_u^p \lambda_s^r - \lambda_s^t \lambda_q^p \lambda_u^r) \\ &= \lambda_{qsu}^{prt} + \hat{\mathbb{A}}(\lambda_q^p \lambda_s^r \lambda_u^t) + \hat{\mathbb{A}}(\lambda_q^p \lambda_s^r \lambda_u^t) \\ &= \lambda_{qsu}^{prt} + \hat{\mathbb{A}}(\lambda_q^p \lambda_s^r \lambda_u^t + \lambda_q^p \lambda_s^r \lambda_u^t). \end{aligned} \quad (5.15)$$

(the antisymmetrization operator  $\hat{\mathbb{A}}$  is defined in Section II). The antisymmetry of  $\lambda$  is explicit from the definition. All the quantities (including the operators in the following arguments) are antisymmetric with respect to a transposition of any two of the upper indices or any two of the lower indices.

## 5.1 Antisymmetrization operator

In this section, we define an antisymmetrization operator  $\hat{\mathbb{A}}$ . Given a quantity  $f(\dots, p, \dots, q, \dots)$ , where  $p, q, \dots$  are the indices of  $f$ , we require  $\hat{\mathbb{A}}$  such that

1.  $\hat{\mathbb{A}}f(\dots, p, \dots, q, \dots)$  is antisymmetric with respect to the transposition of any two indices, that is:  $\hat{\mathbb{A}}f(\dots, p, \dots, q, \dots) = -\hat{\mathbb{A}}f(\dots, q, \dots, p, \dots), \forall p, q$ .

2. In addition,  $\hat{\mathbb{A}}f = f$  if  $f$  itself is already antisymmetric without the action of  $\hat{\mathbb{A}}$ .

To fulfill the requirement (1), we define  $\hat{\mathbb{A}}$  such that

$$\begin{aligned}
& \hat{\mathbb{A}}f(r_1, r_2, \dots, r_n) \\
\equiv & \sum_{\substack{u_1 u_2 \dots u_n \in \text{all possible} \\ \text{permutations of the sequence } r_1 r_2 \dots r_n}} (-1)^{\mathcal{P}_{r_1 r_2 \dots r_n}^{u_1 u_2 \dots u_n}} \hat{\mathbb{P}}_{r_1 r_2 \dots r_n}^{u_1 u_2 \dots u_n} f(r_1, r_2, \dots, r_n) \\
= & \sum_{\substack{u_1 u_2 \dots u_n \in \text{all possible} \\ \text{permutations of the sequence } r_1 r_2 \dots r_n}} (-1)^{\mathcal{P}_{r_1 r_2 \dots r_n}^{u_1 u_2 \dots u_n}} f(u_1, u_2, \dots, u_n). \tag{5.16}
\end{aligned}$$

In this definition, the sequence  $u_1 u_2 \dots u_n$  is a permutation of the index sequence of  $r_1 r_2 \dots r_n$ ,  $\hat{\mathbb{P}}$  is the permutation operator such that  $\hat{\mathbb{P}}_{r_1 r_2 \dots r_n}^{u_1 u_2 \dots u_n} f(r_1, r_2, \dots, r_n) = f(u_1, u_2, \dots, u_n)$ , and  $\mathcal{P}_{r_1 r_2 \dots r_n}^{u_1 u_2 \dots u_n}$  is the number of transpositions needed to permute  $u_1 u_2 \dots u_n$  to  $r_1 r_2 \dots r_n$ . Thus  $(-1)^{\mathcal{P}_{r_1 r_2 \dots r_n}^{u_1 u_2 \dots u_n}}$  is  $+1$  if the parity of  $\mathcal{P}_{r_1 r_2 \dots r_n}^{u_1 u_2 \dots u_n}$  is even, and  $-1$  if the parity of  $\mathcal{P}_{r_1 r_2 \dots r_n}^{u_1 u_2 \dots u_n}$  is odd.

For example,

$$\begin{aligned}
\hat{\mathbb{A}}f(p, q) &= \sum_{\text{the sequence } xy \in \{pq, qp\}} (-1)^{\mathcal{P}_{pq}^{xy}} f(x, y) \\
&= (-1)^{\mathcal{P}_{pq}^{pq}} f(pq) + (-1)^{\mathcal{P}_{pq}^{qp}} f(q, p) \\
&= (-1)^0 f(p, q) + (-1)^1 f(q, p) \\
&= f(p, q) - f(q, p). \tag{5.17}
\end{aligned}$$

If  $f$  is already antisymmetric with respect to index transpositions in a few groups of indices in  $f$ , for example,  $\{a_1, \dots, a_m\}, \{b_1, \dots, b_n\}$ , in order to satisfy the requirement (2), we extend the definition of  $\hat{\mathbb{A}}$  such that:

$$\begin{aligned}
\hat{\mathbb{A}}f(r_1, r_2, \dots, r_n) &\equiv \frac{1}{m!n!} \sum_{\substack{u_1 u_2 \dots u_n \in \\ \text{permutations of } r_1 r_2 \dots r_n}} (-1)^{\mathcal{P}_{r_1 r_2 \dots r_n}^{u_1 u_2 \dots u_n}} f(u_1, u_2, \dots, u_n) \\
&= \frac{1}{\mathcal{F}_{\text{ind-sym}}} \sum_{\substack{u_1 u_2 \dots u_n \in \\ \text{permutations of } r_1 r_2 \dots r_n}} (-1)^{\mathcal{P}_{r_1 r_2 \dots r_n}^{u_1 u_2 \dots u_n}} f(u_1, u_2, \dots, u_n), \tag{5.18}
\end{aligned}$$

where  $\mathcal{F}_{\text{ind-sym}} = m!n!$ , is the symmetry factor due to the antisymmetry of some indices in  $f$ . For example, if  $g(p, q)$  is antisymmetric, that is,  $g(p, q) = -g(q, p)$ , then

$$\begin{aligned}\hat{\mathbb{A}}g(p, q) &= \frac{1}{2!} \sum_{\text{the sequence } xy \in \{pq, qp\}} (-1)^{\mathcal{P}_{pq}^{xy}} g(x, y) \\ &= \frac{1}{2!} (g(p, q) - g(q, p)) \\ &= g(p, q).\end{aligned}\tag{5.19}$$

Therefore, this symmetry factor eliminates duplicate terms.

All the quantities to be used in this chapter have both upper indices and lower indices. To antisymmetrize those quantities such that they are antisymmetric with respect to transpositions of upper indices and transpositions of lower indices, we extend the definition of  $\hat{\mathbb{A}}$ :

$$\begin{aligned}\hat{\mathbb{A}}f_{s_1 s_2 \dots s_n}^{r_1 r_2 \dots r_n} &\equiv \frac{1}{\mathcal{F}_{\text{ind-sym}}} \sum_{\substack{u_1 u_2 \dots u_n \in \\ \text{permutations of } r_1 r_2 \dots r_n}} (-1)^{\mathcal{P}_{r_1 r_2 \dots r_n}^{u_1 u_2 \dots u_n}} \hat{\mathbb{P}}_{r_1 r_2 \dots r_n}^{u_1 u_2 \dots u_n} \left( \right. \\ &\quad \left. \sum_{\substack{v_1 v_2 \dots v_n \in \\ \text{permutations of } s_1 s_2 \dots s_n}} (-1)^{\mathcal{P}_{s_1 s_2 \dots s_n}^{v_1 v_2 \dots v_n}} \hat{\mathbb{P}}_{s_1 s_2 \dots s_n}^{v_1 v_2 \dots v_n} f_{s_1 s_2 \dots s_n}^{r_1 r_2 \dots r_n} \right) \\ &= \frac{1}{\mathcal{F}_{\text{ind-sym}}} \sum_{\substack{u_1 u_2 \dots u_n \in \\ \text{permutations of } r_1 r_2 \dots r_n}} \sum_{\substack{v_1 v_2 \dots v_n \in \\ \text{permutations of } s_1 s_2 \dots s_n}} \\ &\quad (-1)^{\mathcal{P}_{r_1 r_2 \dots r_n}^{u_1 u_2 \dots u_n} + \mathcal{P}_{s_1 s_2 \dots s_n}^{v_1 v_2 \dots v_n}} f_{v_1 v_2 \dots v_n}^{u_1 u_2 \dots u_n}.\end{aligned}\tag{5.20}$$

That is, we antisymmetrize the upper indices and the lower indices sequentially.

Clearly,  $(-1)^{\mathcal{P}_{r_1 r_2 \dots r_n}^{u_1 u_2 \dots u_n} + \mathcal{P}_{s_1 s_2 \dots s_n}^{v_1 v_2 \dots v_n}}$  is determined by the parity of the permutation, which operation permutes  $f_{v_1 v_2 \dots v_n}^{u_1 u_2 \dots u_n}$  to  $f_{s_1 s_2 \dots s_n}^{r_1 r_2 \dots r_n}$ . It can be shown that this parity is the same as that of the permutation, which brings indices  $f_{v_1 v_2 \dots v_n}^{u_1 u_2 \dots u_n}$  into a form having the same index pairing order as in  $f_{s_1 s_2 \dots s_n}^{r_1 r_2 \dots r_n}$ , that is, the lower index corresponding to  $s_1$  is  $r_1$ , the lower index corresponding to  $s_2$  is  $r_2$ ,  $\dots$ . Thus, to determine the parity, it is not necessary to carry out the complete permutation from  $f_{v_1 v_2 \dots v_n}^{u_1 u_2 \dots u_n}$  to  $f_{s_1 s_2 \dots s_n}^{r_1 r_2 \dots r_n}$ ; instead, we can stop permuting once the permuted form have the same index pairing order as in the original form. From now on, we will use the latter parity for  $(-1)^{\mathcal{P}_{r_1 r_2 \dots r_n}^{u_1 u_2 \dots u_n} + \mathcal{P}_{s_1 s_2 \dots s_n}^{v_1 v_2 \dots v_n}}$ , because the sign rule with this parity is applicable to all the

cases in this chapter.

When antisymmetrizing product terms, for example,  $\hat{\mathbb{A}}(B_q^p C_s^r)$ , we treat  $B_q^p C_s^r$  as a compound quantity  $X$ , whose upper indices are the collection of the upper indices from all the component quantities of the product, and similarly for lower indices. Thus  $X_{qs}^{pr} = B_q^p C_s^r$ , and  $\hat{\mathbb{A}}$  acts on the product  $B_q^p C_s^r$  in the same way as it does on a single quantity:

$$\begin{aligned} \hat{\mathbb{A}}(B_q^p C_s^r) = \hat{\mathbb{A}}X_{qs}^{pr} &= X_{qs}^{pr} - X_{sq}^{pr} + X_{sq}^{rp} - X_{qs}^{rp} \\ &= B_q^p C_s^r - B_s^p C_q^r + B_s^r C_q^p - B_q^r C_s^p. \end{aligned} \quad (5.21)$$

In general, if the product term is  $B_{q_1 \dots q_n}^{p_1 \dots p_m} C_{s_1 \dots s_k}^{r_1 \dots r_l} \dots$ , then  $\hat{\mathbb{A}}$  acts on the product in the same way as it does on a compound quantity. By extending the definition of  $\hat{\mathbb{A}}$  in this way, for every product term  $Y$ ,  $\hat{\mathbb{A}}Y$  is antisymmetric with respect to a transposition of any two upper indices or of any two lower indices, where the indices may or may not come from the same component quantity of the product.

In case the same type of quantities appear in the product, for example,  $B = C$ , a straightforward application of the antisymmetrization operator  $\hat{\mathbb{A}}$  leads to:

$$\begin{aligned} \hat{\mathbb{A}}(B_q^p C_s^r) = \hat{\mathbb{A}}(B_q^p B_s^r) &= B_q^p B_s^r - B_s^p B_q^r + B_p^r C_s^q - B_p^r B_s^q \\ &= 2(B_q^p B_s^r - B_s^p B_q^r). \end{aligned} \quad (5.22)$$

To eliminate duplicate terms, we need to take into account this *type* of symmetry. (Quantities of the same *type* must have the same number of indices. For example,  $B_q^p$  and  $B_s^r$  are of the same type, but  $B_q^p$  and  $B_{sv}^{ru}$  are of different types.) Suppose that in a product term, there are  $m$  quantities of a certain type,  $n$  quantities of another type, etc., then we can define a symmetry factor  $\mathcal{F}_{\text{group-sym}} = m!n!\dots$ . Then the overall symmetry factor is changed to

$$\mathcal{F}_{\text{sym}} = \mathcal{F}_{\text{ind-sym}} \times \mathcal{F}_{\text{group-sym}}. \quad (5.23)$$

Therefore, the final form of the definition of  $\hat{\mathbb{A}}$  is:

$$\hat{\mathbb{A}}f_{s_1 s_2 \dots s_n}^{r_1 r_2 \dots r_n} \equiv \frac{1}{\mathcal{F}_{\text{sym}}} \sum_{\substack{u_1 u_2 \dots u_n \in \\ \text{permutations of } r_1 r_2 \dots r_n}} \sum_{\substack{v_1 v_2 \dots v_n \in \\ \text{permutations of } s_1 s_2 \dots s_n}} (-1)^{\mathcal{P}_{r_1 r_2 \dots r_n}^{u_1 u_2 \dots u_n} + \mathcal{P}_{s_1 s_2 \dots s_n}^{v_1 v_2 \dots v_n}} f_{v_1 v_2 \dots v_n}^{u_1 u_2 \dots u_n}. \quad (5.24)$$

The effect of the symmetry factor  $\mathcal{F}_{\text{sym}}$  is to eliminate duplicate terms such that after merging equivalent terms (after that every term is unique), every permuted form appears with a coefficient unity (the sign is determined by the sign rule). Here *equivalent terms* refers to those terms which differ from each other only by the coefficients.  $B_q^r C_s^p$  and  $C_s^r B_q^p$  are equivalent, and  $D_{qs}^{pr} E_{uw}^{tv}$  and  $E_{wu}^{tv} D_{qs}^{rp}$  are also equivalent if  $D$  and  $E$  are antisymmetric quantities. In other words, we may state the definition of the antisymmetrization operator  $\hat{\mathbb{A}}$  as follows:

When  $\hat{\mathbb{A}}$  acts on a quantity  $f$ , such that  $\hat{\mathbb{A}}f$  is antisymmetric with respect to a transposition of any two indices between the upper indices or between the lower indices, it generates all forms by permuting the upper indices and permuting the lower indices in all possible ways. Every unique permuted form appears with a coefficient unity. The sign for any permuted form is determined by the parity of the permutation, which brings the indices of the permuted form into the original *index pairing order*.

## 5.2 $\lambda$ -normal order

The  $\lambda$ -normal order operators, such as  $\tilde{a}_q^p, \tilde{a}_{qs}^{pr}, \tilde{a}_{qsu}^{prt}, \dots$ , are defined recursively:

$$\hat{a}_q^p \equiv \tilde{a}_q^p + \lambda_q^p, \quad (5.25)$$

$$\hat{a}_{qs}^{pr} \equiv \tilde{a}_{qs}^{pr} + \hat{\mathbb{A}}(\lambda_q^p \tilde{a}_s^r) + \hat{\mathbb{A}}(\lambda_q^p \lambda_s^r + \lambda_{qs}^{pr}) = \tilde{a}_{qs}^{pr} + \hat{\mathbb{A}}(\lambda_q^p \tilde{a}_s^r + \lambda_q^p \lambda_s^r + \lambda_{qs}^{pr}), \quad (5.26)$$

$$\hat{a}_{qsu}^{prt} \equiv \tilde{a}_{qsu}^{prt} + \hat{\mathbb{A}}(\lambda_q^p \tilde{a}_{su}^{rt} + \lambda_q^p \lambda_s^r \tilde{a}_u^t + \lambda_{qs}^{pr} \tilde{a}_u^t + \lambda_q^p \lambda_s^r \lambda_u^t + \lambda_q^p \lambda_{su}^{rt} + \lambda_{qsu}^{prt}), \quad (5.27)$$

$$\dots, \quad (5.28)$$

(the above definition is equivalent to the one given in Ref. [78]). Clearly, the operators  $\tilde{a}_q^p$ ,  $\tilde{a}_{q_s}^{p_r}$ , etc. are uniquely defined if  $\lambda_q^p$ ,  $\lambda_{q_s}^{p_r}$ , etc. are specified. We may call  $\lambda_q^p$ ,  $\lambda_{q_s}^{p_r}$ , etc. cumulants, but we prefer to term them *contractions* for consistent terminology.

In the above definition, a contraction is a quantity obtained in the following way: if we take  $m$  upper indices  $\{p_1, p_2, \dots, p_m\}$ , take  $m$  lower indices  $\{q_1, q_2, \dots, q_m\}$  and associate them with a quantity  $\lambda$ , then we get a contraction  $\lambda_{q_1 q_2 \dots q_m}^{p_1 p_2 \dots p_m}$ . If  $m = 1$ , we call this contraction a one-one contraction; otherwise  $m > 1$ , and we call it an m-m contraction, or simply a multiple contraction. Later in this chapter we will meet contractions for a product  $A_{s_1 s_2 \dots}^{r_1 r_2 \dots} \times B_{y_1 y_2 \dots}^{x_1 x_2 \dots}$ . In this case, contractions are obtained similarly: in a contraction  $\lambda_{v_1 v_2 \dots}^{u_1 u_2 \dots}$ , the upper indices  $\{u_1, u_2, \dots\}$  may come from  $A$  or from  $B$  or from both, and the same is true for the lower indices  $\{v_1, v_2, \dots\}$ . If all the indices of a contraction come purely from  $A$  or purely from  $B$ , we call this contraction an *internal-contraction*; otherwise we call it a *cross-contraction*. In the above definition (5.25-5.28), there is no constraint on the contractions, as long as any index appears only once in each term.

*Formally*, the chain of definitions can be taken as the expansion of  $\hat{a}$  in terms of  $\lambda$ -normal order  $\tilde{a}$ , and can be stated as:

- In the expansions, all possible contractions are allowed.
- Every contraction contributes a  $\lambda$ .
- In each normal order term, the uncontracted indices appear in the normal order operator.
- Every unique term has a coefficient of unity. The sign rule is the same as in the definition of  $\lambda$ 's: the sign of each term is determined by the parity of the permutation which brings the indices of the term into the original index pairing order.

To illustrate, let us look at  $\hat{a}_{qsuwyk}^{prtvxz}$ . If there are a few one-one contractions p-s, r-q, t-w and x-k, we get the coefficient  $\lambda_s^p \lambda_q^r \lambda_w^t \lambda_k^x$ . The uncontracted upper indices  $v$  and  $z$  and the uncontracted lower indices  $u$  and  $y$  go to the normal order operator  $\tilde{a}_{uy}^{vz}$ . Thus we get a term  $\lambda_s^p \lambda_q^r \lambda_w^t \lambda_k^x \tilde{a}_{uy}^{vz}$ . Compared with the original order  $\hat{a}_{qsuwyk}^{prtvxz}$ , an odd number of transpositions are needed to reproduce the original pairing order, so the sign is negative and the final form from these four contractions is  $-\lambda_s^p \lambda_q^r \lambda_w^t \lambda_k^x \tilde{a}_{uy}^{vz}$ .



Although we have defined  $\lambda$ 's as cumulants, the definition of normal order is certainly not confined to this particular case. Indeed, we have the freedom of defining  $\lambda$ 's, and every definition of  $\lambda$ 's corresponds to a definition of normal order. In the following proof, we do not refer to the explicit definition of  $\lambda$ 's. Instead, the *only assumption of the proof is that the  $\lambda$ 's in the definitions are antisymmetric*, which can be trivially satisfied by a proper definition. Thus, the  $\lambda$ -normal order theory can be made more general by allowing the extra freedom of defining  $\lambda$ . If  $\lambda$ 's are identified with cumulants, the expectation value of any  $\lambda$ -normal order operator vanishes. (Henceforth, GWT and contraction rules and expansion rules will be used interchangeably.)

### 5.3 Generalized Wick Theorem

Suppose that the  $\lambda$ 's are defined in a way such that the antisymmetry property is enforced. Given any two normal order operators  $\tilde{a}^\sigma$  and  $\tilde{a}^\rho$ ,

$$\tilde{a}^\sigma = \tilde{a}_{q_1 q_2 \dots q_m}^{p_1 p_2 \dots p_m}, \quad (5.29)$$

$$\tilde{a}^\rho = \tilde{a}_{y_1 y_2 \dots y_n}^{x_1 x_2 \dots x_n}, \quad (5.30)$$

the GWT gives the result of expanding the product

$$\tilde{a}^\sigma \times \tilde{a}^\rho = \tilde{a}_{q_1 q_2 \dots q_m}^{p_1 p_2 \dots p_m} \times \tilde{a}_{y_1 y_2 \dots y_n}^{x_1 x_2 \dots x_n} \quad (5.31)$$

into a series of terms, the operator being in  $\lambda$ -normal order in each term. For easy reference, let us denote the upper indices of  $\tilde{a}^\sigma$  as LU (left up), the lower indices of  $\tilde{a}^\sigma$  as LL (left low), the upper indices of  $\tilde{a}^\rho$  as RU (right up) and the lower indices of  $\tilde{a}^\rho$  as RL (right low).

Now we can state the GWT (to be proved) corresponding to  $\lambda$ -normal order:

- Any possible contractions are allowed except internal-contractions (internal-contractions are those whose indices come purely from  $\tilde{a}^\sigma$  or  $\tilde{a}^\rho$ ).
- Each multiple contraction contributes a  $\lambda$ , with the only exception of one-one RU-LL con-

tractions: any one-one contraction  $p$ - $q$  between an RU index ( $p$ ) and an LL index ( $q$ ) contributes a  $\xi_q^p$  ( $\xi_q^p = \lambda_q^p + \Theta_q^p = \lambda_q^p - \delta_q^p$ ,  $\Theta_q^p \equiv -\delta_q^p$ ,  $\xi_q^p = -\eta_q^p$ ,  $\eta_q^p$  being the *one hole density matrix*; we use  $\xi$ , instead of  $\eta$ , to make the sign rule the same as in the  $\lambda$ -normal order definition, in order to have a universal sign rule).

- In each normal order term from the product expansion, the uncontracted indices appear in the operator.
- Every unique term in the expansion has a coefficient of unity. The sign rule is also the same as in the normal order definition: the sign of every term is determined by the parity of the permutation of bringing the indices of the term into the original index pairing order.

For example, according to GWT, if we expand the product  $\tilde{a}_q^p \times \tilde{a}_s^r$ , we get:

$$\tilde{a}_q^p \times \tilde{a}_s^r = \tilde{a}_{qs}^{pr} - \lambda_s^p \times \tilde{a}_q^r - \xi_q^r \tilde{a}_s^p - \lambda_s^p \xi_q^r + \lambda_{qs}^{pr}. \quad (5.32)$$

If we compare the result of expanding  $\hat{a}^{\sigma+\rho}$  in terms of  $\lambda$ -normal order operators (according to the definition (5.25) - (5.28)) to the result of expanding the product of two  $\lambda$ -normal order operators  $\tilde{a}^\sigma \times \tilde{a}^\rho$  according to GWT, we notice that there are only two differences:

1. In the product expansion, there is no internal-contraction. Only cross-contractions are allowed.
2. Any one-one contraction  $p$ - $q$  between an RU index ( $p$ ) and an LL index ( $q$ ) becomes  $\xi_q^p$ , instead of  $\lambda_q^p$ .

## 5.4 Proof

Now let us proceed to prove the contraction rules for the product of a general  $m$ -body normal order operator  $\tilde{a}^\sigma$  and an  $n$ -body normal order operator  $\tilde{a}^\rho$ , or simply  $(m, n)$ . Suppose  $m+n = \Omega$ .

$$\tilde{a}^\sigma = \tilde{a}_{q_1 q_2 \dots q_m}^{p_1 p_2 \dots p_m} \left( = \hat{a}_{q_1 q_2 \dots q_m}^{p_1 p_2 \dots p_m} - (\tilde{a}_{q_1 q_2 \dots q_m}^{p_1 p_2 \dots p_m})_{d.c.} = \hat{a}^\sigma - \tilde{a}_{d.c.}^\sigma \right), \quad (5.33)$$

$$\tilde{a}^\rho = \tilde{a}_{y_1 y_2 \dots y_n}^{x_1 x_2 \dots x_n} \left( = \hat{a}_{y_1 y_2 \dots y_n}^{x_1 x_2 \dots x_n} - (\tilde{a}_{y_1 y_2 \dots y_n}^{x_1 x_2 \dots x_n})_{d.c.} = \hat{a}^\rho - \tilde{a}_{d.c.}^\rho \right). \quad (5.34)$$

For convenience, let us define a notation:

$$(\tilde{a}_q^p)_{d.c.} \equiv \hat{a}_q^p - \tilde{a}_q^p = \lambda_q^p, \quad (5.35)$$

$$(\tilde{a}_{qs}^{pr})_{d.c.} \equiv \hat{a}_{qs}^{pr} - \tilde{a}_{qs}^{pr} = \hat{\mathbb{A}}(\lambda_q^p \tilde{a}_s^r + \lambda_q^r \tilde{a}_s^p + \lambda_{qs}^{pr}), \quad (5.36)$$

$$\begin{aligned} (\tilde{a}_{qsu}^{prt})_{d.c.} &\equiv \hat{a}_{qsu}^{prt} - \tilde{a}_{qsu}^{prt} \\ &= \hat{\mathbb{A}}(\lambda_q^p \tilde{a}_{su}^{rt} + \lambda_q^r \tilde{a}_s^t + \lambda_{qs}^{pr} \tilde{a}_u^t + \lambda_q^p \lambda_s^r \lambda_u^t + \lambda_q^r \lambda_s^p \lambda_u^t + \lambda_{qsu}^{prt}), \end{aligned} \quad (5.37)$$

$$(\tilde{a}_{q\dots}^{p\dots})_{d.c.} \equiv \hat{a}_{q\dots}^{p\dots} - \tilde{a}_{q\dots}^{p\dots}, \quad (5.38)$$

(*d.c.* means *disconnected*, for example, all contributions to  $(\tilde{a}_{qsu}^{prt})_{d.c.}$  appear disconnected except  $\lambda_{qsu}^{prt}$ ). We interpret  $\tilde{a}_{d.c.}$  as  $\tilde{a}$  with internal-contractions.

We first notice that  $\lambda$ -GWT holds for a special case, one of the operator is a constant:  $(n, 0)$ , or  $(0, n)$ . In this case, since one of the operators has a particle rank of zero, no cross-contraction is possible, thus the product expansion only gives one term with no contraction, according to  $\lambda$ -GWT:

$$c \times \tilde{a}_{q_1 q_2 \dots q_m}^{p_1 p_2 \dots p_m} = c \cdot \tilde{a}_{q_1 q_2 \dots q_m}^{p_1 p_2 \dots p_m}. \quad (5.39)$$

This is certainly what the product should be in normal order form. We first state this particular case because it does show up in the following general proof, although implicitly.

Now let us start to prove  $\lambda$ -GWT in general, *by induction*. For  $\Omega = 1$ , there are only two possibilities:  $(0, 1)$ , or  $(1, 0)$ .  $\lambda$ -GWT trivially holds for both, according to the previous paragraph.

For  $\Omega = 2$ , the only nontrivial case is:  $(1, 1)$ . Let us demonstrate explicitly that  $\lambda$ -GWT holds for this case:

$$\begin{aligned}
\tilde{a}_q^p \times \tilde{a}_s^r &= (\hat{a}_q^p - \lambda_q^p) \times (\hat{a}_s^r - \lambda_s^r) \\
&= \hat{a}_q^p \hat{a}_s^r - \lambda_q^p \hat{a}_s^r - \lambda_s^r \hat{a}_q^p + \lambda_q^p \lambda_s^r \\
&= \hat{a}_{qs}^{pr} + \delta_q^r \hat{a}_s^p - \lambda_q^p (\tilde{a}_s^r + \lambda_s^r) - \lambda_s^r (\tilde{a}_q^p + \lambda_q^p) + \lambda_q^p \lambda_s^r \\
&= (\tilde{a}_{qs}^{pr} + \lambda_q^p \tilde{a}_s^r + \lambda_s^r \tilde{a}_q^p - \lambda_s^p \tilde{a}_q^r - \lambda_q^r \tilde{a}_s^p + \lambda_q^p \lambda_s^r - \lambda_s^p \lambda_q^r + \lambda_{qs}^{pr}) + \\
&\quad \delta_q^r (\tilde{a}_s^p + \lambda_s^p) - \lambda_q^p (\tilde{a}_s^r + \lambda_s^r) - \lambda_s^r (\tilde{a}_q^p + \lambda_q^p) + \lambda_q^p \lambda_s^r \\
&= \tilde{a}_{qs}^{pr} - \lambda_s^p \tilde{a}_q^r - \xi_q^r \tilde{a}_s^p - \lambda_s^p \xi_q^r + \lambda_{qs}^{pr}.
\end{aligned} \tag{5.40}$$

Now assume that we have proved that the contraction rules hold for the case  $(M, N)$ , for all  $M$  and  $N$  such that  $M + N < m + n = \Omega$ .

$$\begin{aligned}
\tilde{a}^\sigma \times \tilde{a}^\rho &= \tilde{a}_{q_1 q_2 \dots q_m}^{p_1 p_2 \dots p_m} \times \tilde{a}_{y_1 y_2 \dots y_n}^{x_1 x_2 \dots x_n} \\
&= (\hat{a}^\sigma - \tilde{a}_{d.c.}^\sigma) \times (\hat{a}^\rho - \tilde{a}_{d.c.}^\rho) \\
&= \hat{a}^\sigma \times \hat{a}^\rho - (\tilde{a}_{d.c.}^\sigma \times \hat{a}^\rho + \hat{a}^\sigma \times \tilde{a}_{d.c.}^\rho - \tilde{a}_{d.c.}^\sigma \times \tilde{a}_{d.c.}^\rho) \\
&= T_1 - (T_2 + T_3 - T_4),
\end{aligned} \tag{5.41}$$

$$T_1 = \hat{a}^\sigma \times \hat{a}^\rho, \tag{5.42}$$

$$T_2 = \tilde{a}_{d.c.}^\sigma \times \hat{a}^\rho, \tag{5.43}$$

$$T_3 = \hat{a}^\sigma \times \tilde{a}_{d.c.}^\rho, \tag{5.44}$$

$$T_4 = \tilde{a}_{d.c.}^\sigma \times \tilde{a}_{d.c.}^\rho, \tag{5.45}$$

$$\begin{aligned}
T_2 + T_3 - T_4 &= \tilde{a}_{d.c.}^\sigma \times \hat{a}^\rho + \hat{a}^\sigma \times \tilde{a}_{d.c.}^\rho - \tilde{a}_{d.c.}^\sigma \times \tilde{a}_{d.c.}^\rho \\
&= \tilde{a}_{d.c.}^\sigma \times (\hat{a}^\rho + \tilde{a}_{d.c.}^\rho) + (\tilde{a}^\sigma + \tilde{a}_{d.c.}^\sigma) \times \tilde{a}_{d.c.}^\rho - \tilde{a}_{d.c.}^\sigma \times \tilde{a}_{d.c.}^\rho \\
&= \tilde{a}_{d.c.}^\sigma \times \tilde{a}^\rho + \tilde{a}^\sigma \times \tilde{a}_{d.c.}^\rho + \tilde{a}_{d.c.}^\sigma \times \tilde{a}_{d.c.}^\rho.
\end{aligned} \tag{5.46}$$

### 5.4.1 $T_2 + T_3 - T_4$

Each term in  $T_2 + T_3 - T_4$  is a product of a term of particle rank  $M$  and a term of particle rank  $N$ . Since there is at least one internal-contraction in the product term, either the particle rank of the operator in the first term decreases, or the particle rank of the operator in the second term decreases, or both. Thus, the requirement that  $M + N < m + n$  is satisfied. From recursion, the contraction rules for all product terms in  $T_2 + T_3 - T_4$  are known.

From  $\lambda$ -GWT, when  $T_2 + T_3 - T_4$  are expanded, only cross-contractions take place; that is, no *extra* internal-contractions other than the ones already present in  $\tilde{a}_{d.c.}^\sigma$  and  $\tilde{a}_{d.c.}^\rho$  appear from the expansion. Therefore, upon expansion terms from  $T_2$  and  $T_3$  and  $T_4$  are characterized by the types of internal-contractions in them, and all terms from the expansion of the three products are unique:

- The internal-contractions in every term of  $T_2$  are purely from  $\hat{a}^\sigma$ .
- The internal-contractions in every term of  $T_3$  are purely from  $\hat{a}^\rho$ .
- Every term of  $T_4$  has internal-contractions both from  $\hat{a}^\sigma$  and from  $\hat{a}^\rho$ . Therefore  $T_2$ ,  $T_3$  and  $T_4$  form three distinct classes, and there is no overlap between them.
- In each of the three classes, every term is unique.

On carrying out all the contractions for  $T_2 + T_3 - T_4$ , we get terms of normal order operators whose coefficients contains all possible (including zero) contractions between the upper indices LU + RU and the lower indices LL + RL. Hence,  $T_2 + T_3 - T_4$  is the complete set of normal order terms, with the only constraint that every term contains at least one internal-contraction (in Fig. 5.1, the three diagrams corresponds to the three terms in Eq. (5.46), the *bridges* correspond to cross-contractions, and the straight lines connecting two heavy dots stand for internal-contractions in  $\tilde{a}^\sigma$  and/or  $\tilde{a}^\rho$ ). Since finally there should be no internal-contraction surviving in the expansion of  $\tilde{a}^\sigma \times \tilde{a}^\rho$  if the GWT is valid in general, all (normal order) terms in  $T_2 + T_3 - T_4$  shall be canceled out by terms from  $T_1$ , and only terms containing purely cross-contractions survive (every  $\lambda$  or  $\xi$  contains indices from both  $\sigma$  and  $\rho$ ) (the lower part of Fig. 5.1).

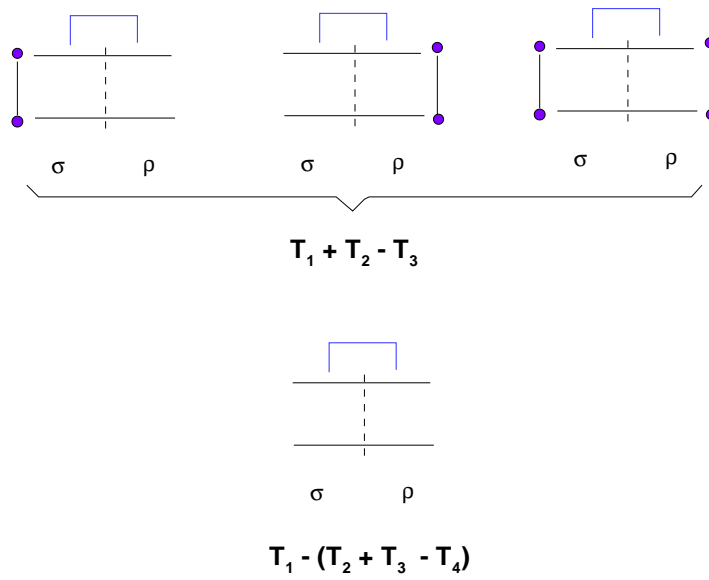


Figure 5.1: Illustrative diagrams

### 5.4.2 $T_1$

Now let us focus on  $T_1$ . Applying the GWT with respect to the true vacuum, we get

$$\begin{aligned}
T_1 &= \hat{a}^\sigma \times \hat{a}^\rho \\
&= \hat{a}_{q_1 q_2 \dots q_m}^{p_1 p_2 \dots p_m} \times \hat{a}_{y_1 y_2 \dots y_n}^{x_1 x_2 \dots x_n} \\
&= \hat{a}_{q_1 q_2 \dots q_m}^{p_1 p_2 \dots p_m} |_{y_1 y_2 \dots y_n}^{x_1 x_2 \dots x_n} + \left( \sum_{\substack{x_\alpha \in \text{RU} \\ q_\beta \in \text{LL}}} \delta_{q_\beta}^{x_\alpha} \hat{a}_{q_1 \dots q_{\beta-1} y_\alpha q_{\beta+1} \dots q_m}^{p_1 \dots p_{\beta-1} p_\beta p_{\beta+1} \dots p_m} |_{y_1 \dots y_{\alpha-1} y_{\alpha+1} \dots y_n}^{x_1 \dots x_{\alpha-1} x_{\alpha+1} \dots x_n} + \text{nonum}(\text{br47}) \right. \\
&\quad \sum_{\substack{(x_\alpha, x_\theta) \in \text{RU}, \alpha \neq \theta \\ (q_\beta, q_\epsilon) \in \text{LL}, \beta \neq \epsilon}} \delta_{q_\beta}^{x_\alpha} \delta_{q_\epsilon}^{x_\theta} \hat{a}_{q_1 q_{\beta-1} y_\alpha q_{\beta+1} \dots q_{\epsilon-1} y_\theta q_{\epsilon+1} \dots q_m}^{p_1 p_{\beta-1} p_\beta p_{\beta+1} \dots p_{\epsilon-1} p_\epsilon p_{\epsilon+1} \dots p_m} |_{y_1 \dots y_{\alpha-1} y_{\alpha+1} \dots y_{\theta-1} y_{\theta+1} \dots y_n}^{x_1 \dots x_{\alpha-1} x_{\alpha+1} \dots x_{\theta-1} x_{\theta+1} \dots x_n} + \\
&\quad \left. \dots \text{ ( terms containing more than two } \delta' \text{ s )} \right) \\
&= T_{1a} + T_{1b}, \tag{5.48}
\end{aligned}$$

$$T_{1a} = \hat{a}_{q_1 q_2 \dots q_m}^{p_1 p_2 \dots p_m} |_{y_1 y_2 \dots y_n}^{x_1 x_2 \dots x_n} = \hat{a}^{\sigma+\rho}. \tag{5.49}$$

(For clarity, the ‘|’ separates indices of  $\hat{a}^\sigma$  from indices of  $\hat{a}^\rho$ .) The contraction rules with respect to the true vacuum are:

- There can only be contractions between RU indices and LL indices.
- There are no multiple contractions, and any one-one contraction contributes a  $\delta$ .
- If the uncontracted indices in the operators are lined up according to the contractions, there is no sign change.

It is interesting to see that the sign rule can be recast in the following form:

If we replace  $\delta_q^p$  by  $\Theta_q^p$  ( $\Theta_q^p = -\delta_q^p$ ), then the overall sign for every term is determined by the parity of the permutations needed to bring the indices of the term into the original index pairing order.

Thus,

$$\begin{aligned}
T_1 = & \hat{a}^{\sigma+\rho} + \left( \sum_{\substack{x_\alpha \in \text{RU} \\ q_\beta \in \text{LL}}} -\Theta_{q_\beta}^{x_\alpha} \hat{a}_{q_1 \dots q_{\beta-1} y_\alpha q_{\beta+1} \dots p_m}^{p_1 \dots p_{\beta-1} p_\beta p_{\beta+1} \dots p_m} | x_1 \dots x_{\alpha-1} x_{\alpha+1} \dots x_n + \right. \\
& \sum_{\substack{(x_\alpha, x_\theta) \in \text{RU}, \alpha \neq \theta \\ (q_\beta, q_\epsilon) \in \text{LL}, \beta \neq \epsilon}} \Theta_{q_\beta}^{x_\alpha} \Theta_{q_\epsilon}^{x_\theta} \hat{a}_{q_1 q_{\beta-1} y_\alpha q_{\beta+1} \dots q_{\epsilon-1} y_\theta q_{\epsilon+1} \dots q_m}^{p_1 p_{\beta-1} p_\beta p_{\beta+1} \dots p_{\epsilon-1} p_\epsilon p_{\epsilon+1} \dots p_m} | x_1 \dots x_{\alpha-1} x_{\alpha+1} \dots x_{\theta-1} x_{\theta+1} \dots x_n \\
& \left. + \dots \text{ ( terms containing more than two } \delta' \text{ s) } \right). \tag{5.50}
\end{aligned}$$

With the introduction of  $\Theta_q^p$ , we do not have to deal with different sign rules. Instead, the sign rule is universal and consistent with the one already in use.

Now let us focus on  $T_{1a}$ . According to the definitions of (5.25)-(5.28), if we expand  $\hat{a}^{\sigma+\rho}$ , we get terms with all possible internal- or/and cross-contractions. As in  $T_2 + T_3 - T_4$ , all internal-contractions contribute  $\lambda$ 's, and all multiple cross-contractions contribute  $\lambda$ 's. The difference, however, is that according to the normal order definition, in  $T_{1a}$ , every one-one cross-contraction between a RU index and a LL index contributes a  $\lambda$ , instead of  $\xi$  (as in  $T_2 + T_3 - T_4$ ).

Suppose we *replace all one-body  $\lambda$ 's in  $T_{1a}$ , which come from one-one RU-LL cross-contractions, by  $\xi$ 's*; then we can classify the normal order terms in  $T_{1a}$  into two classes: terms containing internal-contraction (from  $\sigma$  or/and  $\rho$ ) and terms without internal-contractions. The first class of terms will cancel out terms from  $T_2 + T_3 - T_4$ , since the sign rule is the same, and both are the complete set of those normal order terms in which every term contains at least one internal-contraction. The second class of terms is exactly what we expect from the expansion of the product  $\tilde{a}^\sigma \times \tilde{a}^\rho$  according to GWT in the case of  $(m, n)$  (the lower part of Fig. 5.1). Thus, if we can show that *the effect of adding  $T_{1b}$  to  $T_{1a}$  is simply changing every  $\lambda$  from a one-one RU-LL cross-contraction to  $\xi = \lambda + \Theta$* , the GWT in the case of  $(m, n)$  is proved, and therefore the GWT is proved in general from recursion.



### 5.4.3 $T_{1a} + T_{1b}$

Let us proceed to prove the above hypothesis. When we refer to  $T_{1a}$  or  $T_{1b}$ , we mean their expansions in terms of normal order terms. The difference between  $T_{1a}$  and  $T_{1b}$  is that each term in  $T_{1b}$  contains at least one  $\Theta$ , which is a one-one RU-LL contraction. Since other types of contractions are the same and the sign rule is the same, we can just focus on the one-one RU-LL cross-contractions. We can classify all normal order terms into classes according to the number of one-one RU-LL cross-contractions. For terms in a particular class, we can group terms according to the pairing or correspondence of the one-one RU-LL contractions. For terms with the same number and the same pairing of one-one RU-LL cross-contractions, we can further classify them according to the numbers and index pairing of the other types of contractions (one-one RL-LU cross-contractions and multiple contractions).

Now we will consider a general case: the terms in  $T_{1a} + T_{1b}$  with  $s$  one-one RU-LL (corresponding) cross-contractions between the RU indices  $\{x_{i_1}, x_{i_2}, \dots, x_{i_s}\}$  and the LL indices  $\{q_{j_1}, q_{j_2}, \dots, q_{j_s}\}$ , multiple contractions being same (if existent). That is, the pairing of the one-one RU-LL contraction indices is  $[x_{i_1}, q_{j_1}], [x_{i_2}, q_{j_2}], \dots, [x_{i_s}, q_{j_s}]$ . If we prove that the above hypothesis holds for this general case, we have proved the hypothesis.

Since the sign rule is the same for both  $T_{1a}$  and  $T_{1b}$ , all terms in this case have the same sign. Therefore we can focus on the one-one RU-LL contractions without worrying about the sign.  $T_{1a}$  will contribute a term with the coefficient  $\lambda_{q_{j_1}}^{x_{i_1}} \lambda_{q_{j_2}}^{x_{i_2}} \dots \lambda_{q_{j_s}}^{x_{i_s}}$ , those terms in  $T_{1b}$  which contain one  $\Theta$  will contribute  $\binom{s}{1}$  terms, such as  $\Theta_{q_{j_1}}^{x_{i_1}} \lambda_{q_{j_2}}^{x_{i_2}} \dots \lambda_{q_{j_s}}^{x_{i_s}}$ ,  $\Theta_{q_{j_2}}^{x_{i_2}} \lambda_{q_{j_1}}^{x_{i_1}} \dots \lambda_{q_{j_s}}^{x_{i_s}}$ , etc. Similarly, those terms in  $T_{1b}$  which contain two  $\delta$ 's will contribute  $\binom{s}{2}$  terms, such as  $\Theta_{q_{j_1}}^{x_{i_1}} \Theta_{q_{j_2}}^{x_{i_2}} \lambda_{q_{j_3}}^{x_{i_3}} \dots \lambda_{q_{j_s}}^{x_{i_s}}$ ,  $\Theta_{q_{j_1}}^{x_{i_1}} \Theta_{q_{j_3}}^{x_{i_3}} \lambda_{q_{j_2}}^{x_{i_2}} \dots \lambda_{q_{j_s}}^{x_{i_s}}$ , etc. Similarly for terms containing more  $\Theta$ 's. In total, from  $T_{1b}$ , we will get

$$\binom{s}{1} + \binom{s}{2} + \binom{s}{3} + \dots + \binom{s}{s} = 2^s - 1 \quad (5.51)$$

terms. Together with the term  $\lambda_{q_{j_1}}^{x_{i_1}} \lambda_{q_{j_2}}^{x_{i_2}} \dots \lambda_{q_{j_s}}^{x_{i_s}}$  from  $T_{1a}$ , we get in total  $2^s$  terms with  $s$  one-one contractions,  $2^s$  being just the number of terms we need to replace the  $\lambda_{q_{j_1}}^{x_{i_1}} \lambda_{q_{j_2}}^{x_{i_2}} \dots \lambda_{q_{j_s}}^{x_{i_s}}$  by

$(\lambda_{q_{j_1}}^{x_{i_1}} + \Theta_{q_{j_1}}^{x_{i_1}})(\lambda_{q_{j_2}}^{x_{i_2}} + \Theta_{q_{j_2}}^{x_{i_2}}) \cdots (\lambda_{q_{j_s}}^{x_{i_s}} + \Theta_{q_{j_s}}^{x_{i_s}}) = \xi_{q_{j_1}}^{x_{i_1}} \xi_{q_{j_2}}^{x_{i_2}} \cdots \xi_{q_{j_s}}^{x_{i_s}}$ . In the  $2^s$  terms, each term is unique (only appears once in the expansion), and its origin can be traced back by counting the number of  $\Theta$ 's. Now we have all needed terms, all terms are unique (no double counting), all terms are counted (no term missing), the number of terms is correct, and the signs are correct. We have therefore proved that for this general case of  $\mathbf{s}$  one-one (corresponding) cross-contractions, adding  $T_{1b}$  to  $T_{1a}$  simply changes every  $\lambda$  coming from a LU-RL cross-contraction to  $\xi = \lambda + \Theta$ . Thus the GWT in the case of  $(m, n)$  is proved, and GWT is proved in general from recursion.

## 5.5 Extension

The proof is purely formal, with the only assumption that  $\lambda$ 's are antisymmetric. Hence, the validity of the proof is more general than the original GWT. If  $\lambda$ 's are defined as cumulants related to reduced density matrices (as in Eq. (5.13)-(5.15)), the expectation value of any  $\lambda$ -normal order operator vanishes:  $\langle R|\tilde{a}^\sigma|R\rangle = 0, \forall \sigma$ . If  $\lambda$ 's are defined in other ways, this property does not hold in general, but the proof still holds, and thus the GWT still holds.

In addition, we notice another interesting generalization due to the generality of the proof. If we truncate the particle rank of  $\lambda$ 's to a certain level  $K$  in the recursive definition of normal order operators, the whole proof still holds. Thus the GWT holds, with the only modification that only up to  $K$ -body  $\lambda$ 's (contractions) are allowed when expanding the product of two normal order operators. This truncation can be regarded as a family of different normal order theories. Due to the truncation, the property,  $\langle R|\tilde{a}|R\rangle = 0$ , does not hold in general. Instead, it only holds for those normal order operators of rank lower than or equal to  $K$  if  $\lambda$ 's are defined as cumulants (as in Eq. (5.13)-(5.15)).

## 5.6 $\gamma$ -normal order

For  $K = 1$ ,

$$\hat{a}_q^p = \tilde{a}_q^p + \gamma_q^p, \quad (5.52)$$

$$\hat{a}_{qs}^{pr} = \tilde{a}_{qs}^{pr} + \gamma_q^p \tilde{a}_s^r + \gamma_s^r \tilde{a}_q^p - \gamma_s^p \tilde{a}_q^r - \gamma_q^r \tilde{a}_s^p + \gamma_q^p \gamma_s^r - \gamma_s^p \gamma_q^r \quad (5.53)$$

$$= \tilde{a}_{qs}^{pr} + \hat{\mathbb{A}}(\gamma_q^p \tilde{a}_s^r) + \hat{\mathbb{A}}(\gamma_s^r \tilde{a}_q^p), \quad (5.54)$$

$$\hat{a}_{qsu}^{prt} = \tilde{a}_{qsu}^{prt} + \hat{\mathbb{A}}(\gamma_q^p \tilde{a}_{su}^{rt}) + \hat{\mathbb{A}}(\gamma_s^r \tilde{a}_u^t) + \hat{\mathbb{A}}(\gamma_q^p \gamma_s^r \tilde{a}_u^t), \quad (5.55)$$

$$\dots \quad (5.56)$$

In the discussion of  $\lambda$ -normal order, we use  $\lambda$  to denote contractions for consistency. Here only one-particle contractions appear, and we use  $\gamma$  instead of  $\lambda$  to denote them. The reason is that we will define  $\gamma$  as the one-particle reduced density matrix,  $\gamma_q^p = \langle R | \hat{a}_q^p | R \rangle$ ; therefore, using  $\gamma$  is consistent with the notation introduced at the beginning of the chapter. Let us call this normal order  $\gamma$ -normal order (we emphasize that only one-body contractions are present in  $\gamma$ -normal order). The corresponding expansion rules,  $\gamma$ -GWT, should already be clear from the discussion. According to Sec. 5.5, even the one-body contractions can be defined freely, and  $\gamma$  is not restricted to be the one-particle reduced density matrix. In that case  $\langle R | \tilde{a}_q^p | R \rangle$  does not vanish, in contrast to Eq. (5.60) where the contraction is defined as the one-particle reduced density matrix.

In single reference case, the contraction  $\gamma_q^p = \langle R | \hat{a}_q^p | R \rangle = \delta_q^p$  if both  $p$  and  $q$  are hole indices, and zero otherwise, so  $\gamma$ -normal order reduces to  $h$ -normal order, the particle-hole formalism based normal order. Therefore  $\gamma$ -normal order can be regarded as a generalization of single reference  $h$ -normal order.

If we define  $\gamma$ -normal order density matrix (DM) as the expectation values of the  $\gamma$ -normal

order operators:

$$\zeta_q^p \equiv \langle R | \tilde{a}_q^p | R \rangle, \quad (5.57)$$

$$\zeta_{qs}^{pr} \equiv \langle R | \tilde{a}_{qs}^{pr} | R \rangle, \quad (5.58)$$

$$\dots, \quad (5.59)$$

it is not hard to verify that:

$$\zeta_q^p = 0, \quad (5.60)$$

$$\zeta_{qs}^{pr} = \lambda_{qs}^{pr}, \quad (5.61)$$

$$\zeta_{qsu}^{prt} = \lambda_{qsu}^{prt}, \quad (5.62)$$

$$\zeta_{qsuw}^{prtv} = \lambda_{qsuw}^{prtv} + \hat{\mathbb{A}}(\lambda_{qs}^{pr} \lambda_{uw}^{tv}), \quad (5.63)$$

$$\dots, \quad (5.64)$$

if we take  $\lambda$ 's as cumulants, as defined in in Eq. (5.13)-(5.15). It can be shown that all indices in  $\zeta$  must be active in order for  $\zeta$  not to vanish, which is a nice property shared by cumulants. [78]

$\gamma$ -normal order is used in the SS-EOMCC method. We rewrite every quantity in the residual equation in  $\gamma$ -normal order and carry out the expansions for  $\hat{T}_\lambda^+ \hat{H}$ . Similar arguments, as in Chapter 4, tell that there will be up to 4-particle ( $\gamma$ -normal order) DM's, so we can keep up to

4-particle normal order terms in the expansion of  $\hat{T}_\lambda^+ \hat{H}$ :

$$\hat{T}_\lambda^+ \hat{H} = c_0 + c_1 \times \tilde{a}_1 + c_2 \times \tilde{a}_2 + c_3 \times \tilde{a}_3 + c_4 \times \tilde{a}_4 + \dots, \quad (5.65)$$

$$\begin{aligned} \langle R | \hat{T}_\lambda^+ \hat{H} | R \rangle &= \langle R | c_0 + c_1 \times \tilde{a}_1 + c_2 \times \tilde{a}_2 + c_3 \times \tilde{a}_3 + c_4 \times \tilde{a}_4 | R \rangle \\ &= c_0 + c_1 \langle R | \tilde{a}_1 | R \rangle + c_2 \langle R | \tilde{a}_2 | R \rangle + c_3 \langle R | \tilde{a}_3 | R \rangle + c_4 \langle R | \tilde{a}_4 | R \rangle \\ &= c_0 + c_1 \zeta_1 + c_2 \zeta_2 + c_3 \zeta_3 + c_4 \zeta_4 \\ &= c_0 + c_2 \zeta_2 + c_3 \zeta_3 + c_4 \zeta_4 \\ &\approx c_0 + c_2 \zeta_2 \\ &= c_0 + c_2 \lambda_2, \end{aligned} \quad (5.66)$$

where  $c_1, c_2, \dots$  are coefficients. The equation is written in a general way and we simply denote the rank of the operators and DM's by the subscripts without showing the indices explicitly. We discard terms containing  $\zeta_3$  and  $\zeta_4$ , to approximate the residual. In other words, we discard terms containing three- or four-particle or quadratic two-particle cumulants. This is an approximation made to simplify the theory.

All the contractions are  $\gamma_q^p = \langle R | \hat{a}_p^\dagger \hat{a}_q | R \rangle$ . If the reference function  $|R\rangle$  is an eigenfunction of  $\hat{S}_z$ , as in our method,  $p$  and  $q$  must have the same spin projection for non-vanishing  $\gamma_q^p$ :

$$\gamma_{q_\alpha}^{p_\beta} = \gamma_{q_\beta}^{p_\alpha} = 0. \quad (5.67)$$

Furthermore, if  $|R\rangle$  is an eigenfunction of  $\hat{S}^2$  with  $S = 0$  or an  $|S, M_S\rangle$  state with  $M_S = 0$ ,  $\gamma_{q_\alpha}^{p_\alpha} = \gamma_{q_\beta}^{p_\beta} = \frac{1}{2} \sum_\sigma \gamma_{q_\sigma}^{p_\sigma} = \frac{1}{2} \Gamma_q^p$ , where  $\Gamma_q^p$  is the one-particle spatial density matrix. Therefore the contractions for two spatial indices  $p$  and  $q$  of various spin projections are

$$\gamma_{q_\alpha}^{p_\beta} = \gamma_{q_\beta}^{p_\alpha} = 0, \quad (5.68)$$

$$\gamma_{q_\alpha}^{p_\alpha} = \gamma_{q_\beta}^{p_\beta} = \frac{1}{2} \sum_\sigma \gamma_{q_\sigma}^{p_\sigma} = \frac{1}{2} \Gamma_q^p. \quad (5.69)$$

So we need not worry about the explicit spin projections of  $\gamma_q^p$ , as long as  $p$  and  $q$  have the same

spin projection.

With these results, the spin-free form of the  $\gamma$ -normal order theory is a trivial extension of the spin-orbital form. It turns out that the normal order operator in spin-free form is simply the spin summation of spin-orbital normal order operators:

$$\tilde{E}_{qs\dots}^{pr\dots} = \sum_{\sigma,\rho} \tilde{a}_{q\sigma}^{p\sigma} \tilde{a}_{s\rho}^{r\rho} \dots, \quad (5.70)$$

and the contractions  $\gamma_q^p$  are replaced by  $\frac{1}{2}\Gamma_q^p$ 's. In addition, it can be verified that the *spin-free*  $\gamma$ -normal order operator  $\tilde{E}_{qs\dots}^{pr\dots}$  can be expressed as a linear combination of spin-free v-normal order operators ( $\hat{E}$ ), which are spin singlet operators.[1] Therefore, the *spin-free*  $\gamma$ -normal order operators are also spin singlet operators, and  $\zeta_{qs}^{pr} = \langle R | \tilde{E}_{qs}^{pr} | R \rangle$  can be expressed in terms of the spatial density matrices ( $\Gamma$ ). Now, in the residual equation both  $\hat{T}$  and  $\hat{H}$  can be written in spin-free  $\gamma$ -normal order; hence, all the quantities in the expansion  $\hat{T}_\lambda^+ \hat{H}$  are spin-free and the residual equation is spin-free. Explicit spin projection quantities do not show up in the formulation and the method.

Now we examine the non-singlet case ( $S \neq 0$ ). From the above discussions, we observe that the key element in  $\gamma$ -normal order to achieve a spin-free formulation is the property:

$$\gamma_{q\alpha}^{p\alpha} = \gamma_{q\beta}^{p\beta}. \quad (5.71)$$

This equality does not hold in general for non-singlet states. Now let us see how we can develop a spin-free formulation for these states such that the equality (5.71) holds. (To be rigorous, the equality  $\gamma_{q\alpha}^{p\beta} = \gamma_{q\beta}^{p\alpha} = 0$  is also required to hold. In the following discussions we will not consider this equality explicitly because it holds for any reference function which is a spin eigenfunction  $|S, M_S\rangle$ , and this is always the case in our theory).

Suppose the residual equation for a particular method can be written as:

$$\langle R | \hat{T}_\lambda^+ (\hat{H} - E) e^{\hat{T}} | R \rangle = 0. \quad (5.72)$$

To simplify the notation, we further define  $\hat{J} = \hat{T}_\lambda^+(\hat{H} - E)e^{\hat{T}}$ . Since both  $\hat{H}$  and  $\hat{T}$  contain only v-normal order spin-free operators ( $\hat{E}$ ), which are spin singlet operators,  $\hat{J}$  is also a spin singlet operator. Therefore

$$[\hat{J}, \hat{S}^+] = 0, \quad (5.73)$$

$$[\hat{J}, \hat{S}^-] = 0. \quad (5.74)$$

In SS-EOMCC,  $|R\rangle$  comes from a CASSCF calculation and is a spin eigenfunction:  $|R\rangle = |S, M_S\rangle$ , where  $M_S$  is the spin projection eigenvalue. The above equation therefore can be written as:

$$\langle S, M_S | \hat{J} | S, M_S \rangle = 0. \quad (5.75)$$

Following Ref. [178], with the use of spin ladder operators  $\hat{S}^+$  and  $\hat{S}^-$ , it is straightforward to show that if the residual equation holds for a particular spin multiplet state,

$$\langle S, M_S | \hat{J} | S, M_S \rangle = 0, \quad (5.76)$$

then it holds for all spin multiplet states:

$$\langle S, M'_S | \hat{J} | S, M'_S \rangle = 0, \quad \forall M'_S. \quad (5.77)$$

Therefore,

$$\frac{1}{2S+1} \sum_{M_S=-S}^S \langle S, M_S | \hat{J} | S, M_S \rangle = 0, \quad (5.78)$$

(the factor  $\frac{1}{2S+1}$  is added for convenience, as will be clear later). Therefore we can use the above equation as the residual equation for non-singlet states. With this residual equation, the

contraction  $\gamma$  will be defined correspondingly:

$$\gamma_y^x = \frac{1}{2S+1} \sum_{M_S=-S}^S \langle S, M_S | \hat{a}_y^x | S, M_S \rangle. \quad (5.79)$$

The nice thing about this definition is that Eq. (5.71) is satisfied:

$$\gamma_{q_\alpha}^{p_\alpha} = \gamma_{q_\beta}^{p_\beta}, \quad (5.80)$$

$$\gamma_{q_\alpha}^{p_\beta} = \gamma_{q_\beta}^{p_\alpha} = 0, \quad (5.81)$$

due to the average over all multiplet states. Therefore a *spin-free  $\gamma$ -normal order formulation is achieved*, as for singlet states.

In addition, as has been discussed, in this spin-free formulation, we can simply replace the contraction  $\gamma_{q_\alpha}^{p_\alpha}$  or  $\gamma_{q_\beta}^{p_\beta}$  by the spatial density matrix  $\frac{1}{2}\Gamma_q^p$ , where:

$$\Gamma_q^p = \frac{1}{2S+1} \sum_{M_S=-S}^S \langle S, M_S | (\hat{a}_{q_\alpha}^{p_\alpha} + \hat{a}_{q_\beta}^{p_\beta}) | S, M_S \rangle \quad (5.82)$$

$$= \frac{1}{2S+1} \sum_{M_S=-S}^S \langle S, M_S | \hat{E}_q^p | S, M_S \rangle. \quad (5.83)$$

Using spin ladder operators, we can show that the spatial density matrix is independent of the spin multiplet states:

$$\langle S, M_S | \hat{E}_q^p | S, M_S \rangle = \langle S, M'_S | \hat{E}_q^p | S, M'_S \rangle, \forall M'_S, \quad (5.84)$$

and likewise for the spatial density matrices of higher ranks. Therefore

$$\Gamma_q^p = \frac{1}{2S+1} (2S+1) \langle S, M_S | \hat{E}_q^p | S, M_S \rangle = \langle S, M_S | \hat{E}_q^p | S, M_S \rangle, \quad (5.85)$$

and we can use any spin multiplet state to calculate the spatial density matrix  $\Gamma_q^p$ , instead of averaging over all states.



This ends our discussion of normal order theory, and the approximation in the residual equation in SS-EOMCC should be clear now. In next chapter, we look at how the method is implemented.

## Chapter 6

# Automatic program generator

The process of manipulating second quantized operators to derive working equations for various many-electron theories and translating these equations into efficient computer programs is extremely tedious and prone to error as the complexity of the theory increases. Hence, computer-aided implementation is indispensable for that purpose. From the automatic derivation of perturbation theory [179, 180] to the development of the Tensor Contraction Engine [181, 182], there has been much effort [183, 184, 111, 112, 185, 186, 15, 16, 17, 187, 188, 189, 190, 191, 155, 192, 193, 194, 195, 196, 197, 181, 198, 199, 200] devoted to automatic implementation (see Ref. [201] for a nice review and references therein).

This chapter describes our endeavor to tackle this problem. An automatic program generator (APG) is written to derive equations (SRCC or MRCC) and generate Fortran codes. The primary goal is to use the symbolic manipulation program to implement MRCC methods. The APG program, written in Python [202], is completely based on normal order theory; in other words, on the generalized Wick theorem (GWT) [172, 77, 78]. Due to the extensive use of the *class* data type, great flexibility is achieved and the capability of the program can be enhanced readily. Section 6.1 briefly explains conceptually how to obtain equations from GWT. Section 6.2 presents details of how the GWT is implemented. Section 6.3 tells how to generate Fortran codes from derived equations.

## 6.1 Obtain Equations from Normal Order Theory

Let us start with a typical parameterization:

$$|\Psi\rangle = \hat{\Omega}|R\rangle = e^{\hat{S}}|R\rangle, \quad (6.1)$$

where  $|R\rangle$  is either a single determinant or multi-determinantal reference function,  $\hat{\Omega}$  is the wave operator and  $\hat{S}$  is the cluster operator. The defining equations are usually obtained from projection:

$$\langle R|\hat{S}_\lambda^+ e^{-\hat{S}} \hat{H} e^{\hat{S}}|R\rangle = 0, \quad (6.2)$$

where  $\hat{S}_\lambda$  denotes any excitation operator present in  $\hat{S}$ . Let us write this equation in a general form:

$$\langle R|\hat{\alpha}|R\rangle = 0, \quad (6.3)$$

where  $\hat{\alpha}$  is usually a composite operator. Suppose a certain normal order is defined and that the corresponding contraction rules between two normal order operators are derived. Then, upon expansion we can write  $\alpha$  as

$$\hat{\alpha} = z_0 + z_p^q \hat{\tau}_q^p + \frac{1}{2} z_{pq}^{rs} \hat{\tau}_{rs}^{pq} + \dots, \quad (6.4)$$

and the equation is obtained:

$$\langle R|\hat{\alpha}|R\rangle = z_0 + z_p^q \langle R|\hat{\tau}_q^p|R\rangle + \frac{1}{2} z_{pq}^{rs} \langle R|\hat{\tau}_{rs}^{pq}|R\rangle + \dots \quad (6.5)$$

$$= z_0 + z_p^q D_q^p + \frac{1}{2} z_{pq}^{rs} D_{rs}^{pq} + \dots \quad (6.6)$$

$$= 0, \quad (6.7)$$

where  $\hat{\tau}_s^r = \{\hat{a}_r^+ \hat{a}_s\}$  ( $\{\}$  denotes a certain normal order), and  $D_s^r$  is the expectation value of the normal order operator  $\hat{\tau}_s^r$  with respect to the reference function.

Although the program works in both spin orbital and spatial orbital forms, our interest lies in spin-adapted MRCC theory. To achieve spin-adaptation, spin free operators are used:

$$\hat{E}_q^p = \hat{\tau}_{q\alpha}^{p\alpha} + \hat{\tau}_{q\beta}^{p\beta} \quad (6.8)$$

$$\hat{E}_{rs}^{pq} = \hat{\tau}_{r\alpha s\alpha}^{p\alpha q\alpha} + \hat{\tau}_{r\alpha s\beta}^{p\alpha q\beta} + \hat{\tau}_{r\beta s\alpha}^{p\beta q\alpha} + \hat{\tau}_{r\beta s\beta}^{p\beta q\beta}. \quad (6.9)$$

Provided that the reference function is a spin eigenfunction and the excitation operators are defined in terms of the  $\hat{E}$ 's, the wavefunction is spin-adapted because  $\hat{E}$ 's are spin singlet operators [1] and commute with  $\hat{S}_z$  and  $\hat{S}^2$ . (Henceforth all the orbital indices refer to spatial orbitals unless stated otherwise.)

## 6.2 Equation Derivation

From the discussion in Section I, clearly the most basic manipulation for equation derivation is to expand the binary product of any two operators  $\hat{A} \times \hat{B}$  according to GWT. For an expression involving products of more than two normal order operators, we can evaluate the products sequentially. The sequential expansion idea is general enough to obtain tensor equations for usual coupled cluster theories. Let us first see how to represent every term in the APG program.

### 6.2.1 Term representation: hierarchical *class* structure

Here is one example of a term:

$$\frac{1}{2} t_{p_1 p_2}^{h_1 h_2} f_{h_3}^{h_4} \hat{E}_{h_1 h_2}^{p_1 p_2} \hat{E}_{h_4}^{h_3}. \quad (6.10)$$

We define a class **Term**, to represent this type of quantity. From the example, every term mainly has two attributes: **Coefficient** (here,  $\frac{1}{2} t_{p_1 p_2}^{h_1 h_2} f_{h_3}^{h_4}$ ) and **Operators** (here,  $\hat{E}_{h_1 h_2}^{p_1 p_2} \hat{E}_{h_4}^{h_3}$ ).

Following the chain of definitions, we have a hierarchical contraction for a term:

- **Operators** is a list of **Operator**'s (here,  $\hat{E}_{h_1 h_2}^{p_1 p_2}$  and  $\hat{E}_{h_4}^{h_3}$ ).
- The class **Operator** has two attributes: 'upperIndices' and 'lowerIndices', which in turn are lists of indices (for  $\hat{E}_{h_1 h_2}^{p_1 p_2}$ ,  $[p_1, p_2]$  is the 'upperIndices' and  $[h_1, h_2]$  is the 'lowerIndices').

- The class **Index** mainly has two attributes: ‘type’, ‘num’. For the index ‘p1’, ‘type’ = ‘p’ (particle), and ‘num’ = ‘1’.
- The class **Coefficient** has two attributes: ‘const’ and ‘matElement’. For  $\frac{1}{2}t_{p_1 p_2}^{h_1 h_2} f_{h_3}^{h_4}$ , ‘const’ =  $\frac{1}{2}$ , ‘matElement’ =  $[t_{p_1 p_2}^{h_1 h_2}, f_{h_3}^{h_4}]$ . ‘matElement’ is a list of **MatElement**.
- The class **MatElement** mainly has three attributes: ‘name’, ‘matUpperIndices’ and ‘matLowerIndices’. For  $t_{p_1 p_2}^{h_1 h_2}$ , ‘name’ = ‘t’, ‘matUpperIndices’ =  $[h_1, h_2]$ , and ‘matLowerIndices’ =  $[p_1, p_2]$ . The ‘matUpperIndices’ and ‘matLowerIndices’ are lists of indices.

In our program, more *attributes* are attached to some classes, but the basic structure is as shown above.

### 6.2.2 Generalized Wick Theorem

We first explain the implementation of  $h$ -GWT, that is, the GWT corresponding to the particle-hole formalism based normal order. Once the data structure is established, the implementation of  $h$ -GWT involves finding all possible contractions and replacing the contractions by Kronecker delta’s (provided that the coefficient is modified properly depending on the contraction type). One example of an  $h$ -GWT contraction is shown below:

$$\begin{aligned}
& \frac{1}{2}v_{h_1h_2}^{p_1p_2}\hat{E}_{p_1p_2}^{h_1h_2} \times \frac{1}{2}t_{p_3p_4}^{h_3h_4}\hat{E}_{h_3h_4}^{p_3p_4} \\
= & 0.25v_{h_1h_2}^{p_1p_2}t_{p_3p_4}^{h_3h_4}\hat{E}_{p_1p_2h_3h_4}^{h_1h_2p_3p_4} + 0.25v_{h_1h_2}^{p_3p_2}t_{p_3p_4}^{h_3h_4}\hat{E}_{h_3p_2h_4}^{h_1h_2p_4} + 0.25v_{h_1h_2}^{p_4p_2}t_{p_3p_4}^{h_3h_4}\hat{E}_{h_4p_2h_3}^{h_1h_2p_3} + (\text{term 1-3}) \\
& 0.25v_{h_1h_2}^{p_1p_3}t_{p_3p_4}^{h_3h_4}\hat{E}_{p_1h_3h_4}^{h_1h_2p_4} + 0.25v_{h_1h_2}^{p_1p_4}t_{p_3p_4}^{h_3h_4}\hat{E}_{p_1h_4h_3}^{h_1h_2p_3} - 0.25v_{h_3h_2}^{p_1p_2}t_{p_3p_4}^{h_3h_4}\hat{E}_{p_1p_2h_4}^{p_3h_2p_4} \quad (\text{term 4-6}) \\
& -0.25v_{h_4h_2}^{p_1p_2}t_{p_3p_4}^{h_3h_4}\hat{E}_{p_1p_2h_3}^{p_4h_2p_3} - 0.25v_{h_1h_3}^{p_1p_2}t_{p_3p_4}^{h_3h_4}\hat{E}_{p_1p_2h_4}^{h_1p_3p_4} - 0.25v_{h_1h_4}^{p_1p_2}t_{p_3p_4}^{h_3h_4}\hat{E}_{p_1p_2h_3}^{h_1p_4p_3} + (\text{term 7-9}) \\
& 0.25v_{h_1h_2}^{p_3p_4}t_{p_3p_4}^{h_3h_4}\hat{E}_{h_3h_4}^{h_1h_2} + 0.25v_{h_1h_2}^{p_4p_3}t_{p_3p_4}^{h_3h_4}\hat{E}_{h_4h_3}^{h_1h_2} + 0.5v_{h_3h_2}^{p_3p_2}t_{p_3p_4}^{h_3h_4}\hat{E}_{p_2h_4}^{h_2p_4} \quad (\text{term 10-12}) \\
& -0.25v_{h_4h_2}^{p_3p_2}t_{p_3p_4}^{h_3h_4}\hat{E}_{p_2h_3}^{h_2p_4} - 0.25v_{h_1h_3}^{p_3p_2}t_{p_3p_4}^{h_3h_4}\hat{E}_{p_2h_4}^{h_1p_4} - 0.25v_{h_1h_4}^{p_3p_2}t_{p_3p_4}^{h_3h_4}\hat{E}_{h_3p_2}^{h_1p_4} \quad (\text{term 13-15}) \\
& -0.25v_{h_3h_2}^{p_4p_2}t_{p_3p_4}^{h_3h_4}\hat{E}_{p_2h_4}^{h_2p_3} + 0.5v_{h_4h_2}^{p_4p_2}t_{p_3p_4}^{h_3h_4}\hat{E}_{p_2h_3}^{h_2p_3} - 0.25v_{h_1h_3}^{p_4p_2}t_{p_3p_4}^{h_3h_4}\hat{E}_{h_4p_2}^{h_1p_3} \quad (\text{term 16-18}) \\
& -0.25v_{h_1h_4}^{p_4p_2}t_{p_3p_4}^{h_3h_4}\hat{E}_{p_2h_3}^{h_1p_3} - 0.25v_{h_3h_2}^{p_1p_3}t_{p_3p_4}^{h_3h_4}\hat{E}_{p_1h_4}^{h_2p_4} - 0.25v_{h_4h_2}^{p_1p_3}t_{p_3p_4}^{h_3h_4}\hat{E}_{p_1h_3}^{p_4h_2} + (\text{term 19-21}) \\
& 0.5v_{h_1h_3}^{p_1p_3}t_{p_3p_4}^{h_3h_4}\hat{E}_{p_1h_4}^{h_1p_4} - 0.25v_{h_1h_4}^{p_1p_3}t_{p_3p_4}^{h_3h_4}\hat{E}_{p_1h_3}^{h_1p_4} - 0.25v_{h_3h_2}^{p_1p_4}t_{p_3p_4}^{h_3h_4}\hat{E}_{p_1h_4}^{p_3h_2} \quad (\text{term 22-24}) \\
& -0.25v_{h_4h_2}^{p_1p_4}t_{p_3p_4}^{h_3h_4}\hat{E}_{p_1h_3}^{h_2p_3} - 0.25v_{h_1h_3}^{p_1p_4}t_{p_3p_4}^{h_3h_4}\hat{E}_{p_1h_4}^{h_1p_3} + 0.5v_{h_1h_4}^{p_1p_4}t_{p_3p_4}^{h_3h_4}\hat{E}_{p_1h_3}^{h_1p_3} + (\text{term 25-27}) \\
& 0.25v_{h_3h_4}^{p_1p_2}t_{p_3p_4}^{h_3h_4}\hat{E}_{p_1p_2}^{p_3p_4} + 0.25v_{h_4h_3}^{p_1p_2}t_{p_3p_4}^{h_3h_4}\hat{E}_{p_1p_2}^{p_4p_3} - 0.5v_{h_3h_4}^{p_3p_2}t_{p_3p_4}^{h_3h_4}\hat{E}_{p_2}^{p_4} + (\text{term 28-30}) \\
& 0.25v_{h_4h_3}^{p_3p_2}t_{p_3p_4}^{h_3h_4}\hat{E}_{p_2}^{p_4} + 0.25v_{h_3h_4}^{p_4p_2}t_{p_3p_4}^{h_3h_4}\hat{E}_{p_2}^{p_3} - 0.5v_{h_4h_3}^{p_4p_2}t_{p_3p_4}^{h_3h_4}\hat{E}_{p_2}^{p_3} + (\text{term 31-33}) \\
& 0.25v_{h_3h_4}^{p_1p_3}t_{p_3p_4}^{h_3h_4}\hat{E}_{p_1}^{p_4} - 0.5v_{h_4h_3}^{p_1p_3}t_{p_3p_4}^{h_3h_4}\hat{E}_{p_1}^{p_4} - 0.5v_{h_3h_4}^{p_1p_4}t_{p_3p_4}^{h_3h_4}\hat{E}_{p_1}^{p_3} + (\text{term 34-36}) \\
& 0.25v_{h_4h_3}^{p_1p_4}t_{p_3p_4}^{h_3h_4}\hat{E}_{p_1}^{p_3} + 0.5v_{h_3h_2}^{p_3p_4}t_{p_3p_4}^{h_3h_4}\hat{E}_{h_4}^{h_2} - 0.25v_{h_4h_2}^{p_3p_4}t_{p_3p_4}^{h_3h_4}\hat{E}_{h_3}^{h_2} \quad (\text{term 37-39}) \\
& -0.25v_{h_1h_3}^{p_3p_4}t_{p_3p_4}^{h_3h_4}\hat{E}_{h_4}^{h_1} + 0.5v_{h_1h_4}^{p_3p_4}t_{p_3p_4}^{h_3h_4}\hat{E}_{h_3}^{h_1} - 0.25v_{h_3h_2}^{p_4p_3}t_{p_3p_4}^{h_3h_4}\hat{E}_{h_4}^{h_2} + (\text{term 40-42}) \\
& 0.5v_{h_4h_2}^{p_4p_3}t_{p_3p_4}^{h_3h_4}\hat{E}_{h_3}^{h_2} + 0.5v_{h_1h_3}^{p_4p_3}t_{p_3p_4}^{h_3h_4}\hat{E}_{h_4}^{h_1} - 0.25v_{h_1h_4}^{p_4p_3}t_{p_3p_4}^{h_3h_4}\hat{E}_{h_3}^{h_1} + (\text{term 43-45}) \\
& v_{h_3h_4}^{p_3p_4}t_{p_3p_4}^{h_3h_4} - 0.5v_{h_4h_3}^{p_3p_4}t_{p_3p_4}^{h_3h_4} - 0.5v_{h_3h_4}^{p_4p_3}t_{p_3p_4}^{h_3h_4} + v_{h_4h_3}^{p_4p_3}t_{p_3p_4}^{h_3h_4}. \quad (\text{term 46-50}) \tag{6.11}
\end{aligned}$$

We illustrate the contraction rules with this example. We denote the four positions of indices in the two operators (in this case  $\hat{E}_{p_1p_2}^{h_1h_2}$  and  $\hat{E}_{h_3h_4}^{p_3p_4}$ ) as LU (LU = ‘left up’, the position of  $h_1$  and  $h_2$  in  $\hat{E}_{p_1p_2}^{h_1h_2}$ ), LL (LL = ‘left low’, the position of  $p_1$  and  $p_2$  in  $\hat{E}_{p_1p_2}^{h_1h_2}$ ), RU (RU = ‘right up’, the position of  $p_3$  and  $p_4$  in  $\hat{E}_{h_3h_4}^{p_3p_4}$ ) and RL (RL = ‘right low’, the position of  $h_3$  and  $h_4$  in  $\hat{E}_{h_3h_4}^{p_3p_4}$ ). In  $h$ -GWT, contractions only take place between a hole-creation operator/particle-annihilation operator on the left and a hole-annihilation/particle-creation operator on the right, respectively,

in this case between a hole operator in LU (quasi-annihilation operator) and a hole operator in RL (quasi-creation operator), or between a particle operator in LL (quasi-annihilation operator) and a particle operator in RU (quasi-creation operator). By examining the number of each type of index in each position, we can determine the maximum number of contractions, in this case 4. Therefore there can be 0, 1, 2, 3 or 4 contractions. We examine the possibilities sequentially. For the case of  $n$ -contractions, if there is a contraction between an operator in LU and one in RL, the contraction contributes a Kronecker delta  $\delta$  and a coefficient  $(-1)$ , and then the corresponding uncontracted operators in LL and RU are aligned. The sixth term is an example ('h1' and 'h3' are contracted). For a particle-particle contraction between LL and RU, the rule is similar, but the sign of the coefficient does not change, as seen from the second term. In the case of more than one contraction, the coefficient is further multiplied by  $(-2)$  if the contractions form a loop, as seen from the twelfth term. The factor of 2 accounts for the fact that spin can be either  $\alpha$  or  $\beta$  and is a result of using a spin-free formulation. The  $\delta$ 's are not explicitly present in the expression because they are absorbed into the equation by equating contracted indices.

To incorporate  $\lambda$ -GWT into the program, we allow multiple contractions between two normal order operators, and the number of contractions increases rapidly. The possible contraction patterns are more complicated. To expand the product of two  $\lambda$ -normal order operators, say,

$$\tilde{a}_{rs}^{pq} \times \tilde{a}_{vw}^{tu},$$

(all indices refer to spin orbitals here), the following procedure, according to  $\lambda$ -GWT, is adopted:

- Firstly, the maximum contractions are determined, in this case 4.
- Corresponding to a fixed number of total contractions (in this case, the number can be 0, 1, 2, 3, or 4), all possible contraction patterns are determined. For example, if the number is

3, the possible patterns are

$$\left\{ \begin{array}{l} \text{three 1-1 contractions} \\ \text{one 1-1 contraction and one 2-2 contraction} \\ \text{one 3-3 contraction} \end{array} \right.$$

- Corresponding to each contraction pattern, all possible contraction ‘configurations’, defined by the specification of which index (indices) is contracted to which index (indices), are determined.
- For each contraction configuration, every LU-RL contraction is replaced by a  $\lambda$ , every 1-1 LL-RU contraction is replaced by a  $\eta = \delta - \lambda$ , every multiple LL-RU contraction is replaced by a  $\lambda$ .
- The sign rule is stated in the previous chapter.



Thus

$$\begin{aligned}
& \tilde{a}_{rs}^{pq} \times \tilde{a}_{vw}^{tu} \\
= & \tilde{a}_{rsvw}^{pqtu} - \lambda_v^p \tilde{a}_{srw}^{qtu} - \lambda_w^p \tilde{a}_{svr}^{qtu} - \lambda_v^q \tilde{a}_{rsw}^{ptu} - \lambda_w^q \tilde{a}_{rvs}^{ptu} + \eta_r^t \tilde{a}_{vsw}^{pqu} + \eta_s^t \tilde{a}_{rvw}^{pqu} + \\
& \eta_r^u \tilde{a}_{vsw}^{pqt} + \eta_s^u \tilde{a}_{rvw}^{pqt} - \lambda_{vs}^{tu} \tilde{a}_{rw}^{pq} - \lambda_{sw}^{tu} \tilde{a}_{rv}^{pq} + \eta_r^t \eta_s^u \tilde{a}_{vw}^{pq} + \eta_s^t \eta_r^u \tilde{a}_{vw}^{pq} + \lambda_{rs}^{tu} \tilde{a}_{vw}^{pq} \\
& - \lambda_{vr}^{tu} \tilde{a}_{ws}^{pq} - \lambda_{rw}^{tu} \tilde{a}_{vs}^{pq} - \lambda_{wv}^{qt} \tilde{a}_{rs}^{pu} + \lambda_v^q \eta_s^t \tilde{a}_{rw}^{pu} + \lambda_{sv}^{qt} \tilde{a}_{rw}^{pu} - \lambda_w^q \eta_s^t \tilde{a}_{rv}^{pu} - \lambda_{sw}^{qt} \tilde{a}_{rv}^{pu} \\
& - \lambda_{sr}^{qt} \tilde{a}_{vw}^{pu} - \lambda_v^q \eta_r^t \tilde{a}_{sw}^{pu} - \lambda_{rv}^{qt} \tilde{a}_{sw}^{pu} - \lambda_w^q \eta_r^t \tilde{a}_{vs}^{pu} + \lambda_{rw}^{qt} \tilde{a}_{sv}^{pu} - \lambda_{vw}^{qu} \tilde{a}_{rs}^{pt} - \lambda_v^q \eta_s^u \tilde{a}_{rv}^{pt} \\
& - \lambda_{sv}^{qu} \tilde{a}_{rw}^{pt} + \lambda_w^q \eta_s^u \tilde{a}_{rv}^{pt} + \lambda_{sw}^{qu} \tilde{a}_{rv}^{pt} - \lambda_{sr}^{qu} \tilde{a}_{vw}^{pt} - \lambda_v^q \eta_r^u \tilde{a}_{ws}^{pt} + \lambda_{rv}^{qu} \tilde{a}_{sw}^{pt} - \lambda_w^q \eta_r^u \tilde{a}_{sv}^{pt} \\
& - \lambda_{vw}^{qu} \tilde{a}_{sv}^{pt} + \lambda_v^p \lambda_w^q \tilde{a}_{rs}^{tu} + \lambda_w^p \lambda_v^q \tilde{a}_{sr}^{tu} + \lambda_{vw}^{pq} \tilde{a}_{rs}^{tu} - \lambda_{vs}^{pq} \tilde{a}_{rw}^{tu} - \lambda_{ws}^{pq} \tilde{a}_{vr}^{tu} - \lambda_{rv}^{pq} \tilde{a}_{sw}^{tu} \\
& - \lambda_{rw}^{pq} \tilde{a}_{vs}^{tu} - \lambda_{wv}^{pt} \tilde{a}_{sr}^{qu} - \lambda_v^p \eta_s^t \tilde{a}_{rw}^{qu} - \lambda_{sv}^{pt} \tilde{a}_{rw}^{qu} - \lambda_w^p \eta_s^t \tilde{a}_{vr}^{qu} + \lambda_{sw}^{pt} \tilde{a}_{rv}^{qu} - \lambda_{rs}^{pt} \tilde{a}_{vw}^{qu} + \\
& \lambda_v^p \eta_r^t \tilde{a}_{sw}^{qu} + \lambda_{rv}^{pt} \tilde{a}_{sw}^{qu} - \lambda_w^p \eta_r^t \tilde{a}_{sv}^{qu} - \lambda_{rv}^{pt} \tilde{a}_{sv}^{qu} - \lambda_{vw}^{pu} \tilde{a}_{sr}^{qt} - \lambda_v^p \eta_s^u \tilde{a}_{wr}^{qt} + \lambda_{sv}^{pu} \tilde{a}_{rw}^{qt} \\
& - \lambda_{sv}^{pu} \eta_s^u \tilde{a}_{rv}^{qt} - \lambda_{sw}^{pu} \tilde{a}_{rv}^{qt} - \lambda_{rs}^{pu} \tilde{a}_{wv}^{qt} - \lambda_v^p \eta_r^u \tilde{a}_{sw}^{qt} - \lambda_{rv}^{pu} \tilde{a}_{sw}^{qt} + \lambda_w^p \eta_r^u \tilde{a}_{sv}^{qt} + \lambda_{rw}^{pu} \tilde{a}_{sv}^{qt} \\
& - \lambda_v^q \lambda_{sw}^{tu} \tilde{a}_r^p - \lambda_w^q \lambda_{vs}^{tu} \tilde{a}_r^p + \eta_s^t \lambda_{vw}^{qu} \tilde{a}_r^p + \eta_s^u \lambda_{vw}^{qt} \tilde{a}_r^p + \lambda_{svw}^{qtu} \tilde{a}_r^p + \lambda_v^q \lambda_{rw}^{tu} \tilde{a}_s^p + \lambda_w^q \lambda_{vr}^{tu} \tilde{a}_s^p \\
& - \eta_r^t \lambda_{vw}^{qu} \tilde{a}_s^p - \eta_r^u \lambda_{vw}^{qt} \tilde{a}_s^p - \lambda_{rvw}^{qtu} \tilde{a}_s^p - \lambda_v^q \eta_r^t \eta_s^u \tilde{a}_w^p + \lambda_v^q \eta_s^t \eta_r^u \tilde{a}_w^p - \lambda_v^q \lambda_{rs}^{tu} \tilde{a}_w^p - \eta_r^t \lambda_{sv}^{qu} \tilde{a}_w^p + \\
& \eta_s^t \lambda_{rv}^{qu} \tilde{a}_w^p + \eta_r^u \lambda_{sv}^{qt} \tilde{a}_w^p - \eta_s^u \lambda_{rv}^{qt} \tilde{a}_w^p - \lambda_{svr}^{qtu} \tilde{a}_w^p + \lambda_w^q \eta_r^t \eta_s^u \tilde{a}_v^p - \lambda_w^q \eta_s^t \eta_r^u \tilde{a}_v^p + \lambda_w^q \lambda_{rs}^{tu} \tilde{a}_v^p + \\
& \eta_r^t \lambda_{sw}^{qu} \tilde{a}_v^p - \eta_s^t \lambda_{rw}^{qu} \tilde{a}_v^p - \eta_r^u \lambda_{sw}^{qt} \tilde{a}_v^p + \eta_s^u \lambda_{rw}^{qt} \tilde{a}_v^p - \lambda_{srw}^{qtu} \tilde{a}_v^p + \lambda_v^p \lambda_{sw}^{tu} \tilde{a}_r^q + \lambda_w^p \lambda_{vs}^{tu} \tilde{a}_r^q
\end{aligned}$$

$$\begin{aligned}
& -\eta_s^t \lambda_{vw}^{pu} \tilde{a}_r^q - \eta_s^u \lambda_{vw}^{pt} \tilde{a}_r^q - \lambda_{svw}^{ptu} \tilde{a}_r^q - \lambda_v^p \lambda_{rw}^{tu} \tilde{a}_s^q - \lambda_w^p \lambda_{vr}^{tu} \tilde{a}_s^q + \eta_r^t \lambda_{vw}^{pu} \tilde{a}_s^q + \eta_r^u \lambda_{vw}^{pt} \tilde{a}_s^q + \\
& \lambda_{rvw}^{ptu} \tilde{a}_s^q + \lambda_v^p \eta_r^t \eta_s^u \tilde{a}_w^q - \lambda_v^p \eta_s^t \eta_r^u \tilde{a}_w^q + \lambda_v^p \lambda_{rs}^{tu} \tilde{a}_w^q + \eta_r^t \lambda_{sv}^{pu} \tilde{a}_w^q - \eta_s^t \lambda_{rv}^{pu} \tilde{a}_w^q - \eta_r^u \lambda_{sv}^{pt} \tilde{a}_w^q + \\
& \eta_s^u \lambda_{rv}^{pt} \tilde{a}_w^q - \lambda_{rvs}^{ptu} \tilde{a}_w^q - \lambda_w^p \eta_r^t \eta_s^u \tilde{a}_v^q + \lambda_w^p \eta_s^t \eta_r^u \tilde{a}_v^q - \lambda_w^p \lambda_{rs}^{tu} \tilde{a}_v^q - \eta_r^t \lambda_{sw}^{pu} \tilde{a}_v^q + \eta_s^t \lambda_{rv}^{pu} \tilde{a}_v^q + \\
& \eta_r^u \lambda_{sw}^{pt} \tilde{a}_v^q - \eta_s^u \lambda_{rv}^{pt} \tilde{a}_v^q - \lambda_{rsw}^{ptu} \tilde{a}_v^q + \lambda_v^p \lambda_w^q \eta_s^t \tilde{a}_r^u - \lambda_w^p \lambda_v^q \eta_s^t \tilde{a}_r^u + \lambda_v^p \lambda_{sw}^{qt} \tilde{a}_r^u - \lambda_w^p \lambda_{sv}^{qt} \tilde{a}_r^u \\
& - \lambda_v^q \lambda_{sw}^{pt} \tilde{a}_r^u + \lambda_w^q \lambda_{sv}^{pt} \tilde{a}_r^u + \eta_s^t \lambda_{vw}^{pq} \tilde{a}_r^u - \lambda_{wsv}^{pqt} \tilde{a}_r^u - \lambda_v^p \lambda_w^q \eta_r^t \tilde{a}_s^u + \lambda_w^p \lambda_v^q \eta_r^t \tilde{a}_s^u - \lambda_v^p \lambda_{rw}^{qt} \tilde{a}_s^u + \\
& \lambda_w^p \lambda_{rv}^{qt} \tilde{a}_s^u + \lambda_v^q \lambda_{rw}^{pt} \tilde{a}_s^u - \lambda_w^q \lambda_{rv}^{pt} \tilde{a}_s^u - \eta_r^t \lambda_{vw}^{pq} \tilde{a}_s^u - \lambda_{rvw}^{pqt} \tilde{a}_s^u - \lambda_v^p \lambda_{st}^{qt} \tilde{a}_w^u - \lambda_v^q \lambda_{rs}^{pt} \tilde{a}_w^u + \\
& \eta_r^t \lambda_{vs}^{pq} \tilde{a}_w^u + \eta_s^t \lambda_{rv}^{pq} \tilde{a}_w^u + \lambda_{rsv}^{pqt} \tilde{a}_w^u + \lambda_w^p \lambda_{sr}^{qt} \tilde{a}_v^u + \lambda_w^q \lambda_{rs}^{pt} \tilde{a}_v^u - \eta_r^t \lambda_{ws}^{pq} \tilde{a}_v^u - \eta_s^t \lambda_{rv}^{pq} \tilde{a}_v^u \\
& - \lambda_{rsv}^{pqt} \tilde{a}_v^u - \lambda_v^p \lambda_w^q \eta_s^u \tilde{a}_r^t + \lambda_w^p \lambda_v^q \eta_s^u \tilde{a}_r^t - \lambda_v^p \lambda_{sw}^{qu} \tilde{a}_r^t + \lambda_w^p \lambda_{sv}^{qu} \tilde{a}_r^t + \lambda_v^q \lambda_{sw}^{qu} \tilde{a}_r^t - \lambda_w^q \lambda_{sv}^{qu} \tilde{a}_r^t \\
& - \eta_s^u \lambda_{vw}^{pq} \tilde{a}_r^t - \lambda_{vsw}^{pqu} \tilde{a}_r^t + \lambda_v^p \lambda_w^q \eta_r^u \tilde{a}_s^t - \lambda_w^p \lambda_v^q \eta_r^u \tilde{a}_s^t + \lambda_v^p \lambda_{rw}^{qu} \tilde{a}_s^t - \lambda_w^p \lambda_{rv}^{qu} \tilde{a}_s^t - \lambda_v^q \lambda_{rw}^{qu} \tilde{a}_s^t + \\
& \lambda_w^q \lambda_{rv}^{qu} \tilde{a}_s^t + \eta_r^u \lambda_{vw}^{pq} \tilde{a}_s^t - \lambda_{rvw}^{pqu} \tilde{a}_s^t + \lambda_v^p \lambda_{sr}^{qu} \tilde{a}_w^t + \lambda_w^q \lambda_{rs}^{qu} \tilde{a}_w^t - \eta_r^u \lambda_{vs}^{pq} \tilde{a}_w^t - \eta_s^u \lambda_{rv}^{pq} \tilde{a}_w^t \\
& - \lambda_{rvs}^{pqu} \tilde{a}_w^t - \lambda_w^p \lambda_{sr}^{qu} \tilde{a}_v^t - \lambda_w^q \lambda_{rs}^{qu} \tilde{a}_v^t + \eta_r^u \lambda_{vw}^{pq} \tilde{a}_v^t + \eta_s^u \lambda_{rv}^{pq} \tilde{a}_v^t + \lambda_{rsw}^{pqu} \tilde{a}_v^t + \lambda_v^p \lambda_w^q \eta_r^t \eta_s^u \\
& - \lambda_w^p \lambda_v^q \eta_s^t \eta_r^u - \lambda_w^p \lambda_v^q \eta_r^t \eta_s^u + \lambda_w^p \lambda_v^q \eta_s^t \eta_r^u + \lambda_v^p \lambda_w^q \lambda_{rs}^{tu} - \lambda_w^p \lambda_v^q \lambda_{rs}^{tu} + \lambda_v^p \eta_r^t \lambda_{sw}^{qu} - \lambda_v^q \eta_s^t \lambda_{rw}^{qu} \\
& - \lambda_w^p \eta_r^t \lambda_{sv}^{qu} + \lambda_w^p \eta_s^t \lambda_{rv}^{qu} - \lambda_v^p \eta_r^u \lambda_{sw}^{qt} + \lambda_v^p \eta_s^u \lambda_{rw}^{qt} + \lambda_w^p \eta_r^u \lambda_{sv}^{qt} - \lambda_w^p \eta_s^u \lambda_{rv}^{qt} - \lambda_v^q \eta_r^t \lambda_{sw}^{pu} + \\
& \lambda_v^q \eta_s^t \lambda_{rv}^{pu} + \lambda_w^q \eta_r^t \lambda_{sv}^{pu} - \lambda_w^q \eta_s^t \lambda_{rv}^{pu} + \lambda_v^q \eta_r^u \lambda_{sw}^{pt} - \lambda_v^q \eta_s^u \lambda_{rw}^{pt} - \lambda_w^q \eta_r^u \lambda_{sv}^{pt} + \lambda_w^q \eta_s^u \lambda_{rv}^{pt} + \\
& \eta_r^t \eta_s^u \lambda_{vw}^{pq} - \eta_s^t \eta_r^u \lambda_{vw}^{pq} - \lambda_v^p \lambda_{srw}^{qtu} - \lambda_w^p \lambda_{svr}^{qtu} - \lambda_v^q \lambda_{rsw}^{ptu} - \lambda_w^q \lambda_{rvs}^{ptu} + \eta_r^t \lambda_{vsw}^{pqu} + \\
& \eta_s^t \lambda_{rvw}^{pqu} + \eta_r^u \lambda_{wsv}^{pqt} + \eta_s^u \lambda_{rvw}^{pqt} + \lambda_{vw}^{pq} \lambda_{rs}^{tu} - \lambda_{vs}^{pq} \lambda_{rw}^{tu} - \lambda_{ws}^{pq} \lambda_{vr}^{tu} - \lambda_{rv}^{pq} \lambda_{sw}^{tu} \\
& - \lambda_{rw}^{pq} \lambda_{vs}^{tu} - \lambda_{wv}^{pt} \lambda_{sr}^{qu} - \lambda_{sv}^{pt} \lambda_{rw}^{qu} + \lambda_{sw}^{pt} \lambda_{rv}^{qu} - \lambda_{rs}^{pt} \lambda_{vw}^{qu} + \lambda_{rv}^{pt} \lambda_{sw}^{qu} - \lambda_{rw}^{pt} \lambda_{sv}^{qu} \\
& - \lambda_{vw}^{pu} \lambda_{sr}^{qt} + \lambda_{sv}^{pu} \lambda_{rw}^{qt} - \lambda_{sw}^{pu} \lambda_{rv}^{qt} - \lambda_{rs}^{pu} \lambda_{vw}^{qt} - \lambda_{rv}^{pu} \lambda_{sw}^{qt} + \lambda_{rw}^{pu} \lambda_{sv}^{qt} + \lambda_{rsvw}^{pqt}. \tag{6.12}
\end{aligned}$$

### 6.2.3 Canonicalization

Upon expansion, generally there will be many terms generated which are equivalent. The canonicalization procedure reduces equivalent terms to a unique form and merges them. The canonicalization algorithm in spin free form is somewhat simpler than in spin orbital form. We illustrate the algorithm using the example of Eq. 6.11,  $\frac{1}{2} v_{h_1 h_2}^{p_1 p_2} \hat{E}_{p_1 p_2}^{h_1 h_2} \times \frac{1}{2} t_{p_3 p_4}^{h_3 h_4} \hat{E}_{h_3 h_4}^{p_3 p_4}$ , and the algorithm in spin orbital form is straightforward to obtain by suitable extensions.

The same term can appear in different forms. All equivalent forms can be obtained from each other by permutations (the allowed permutations in spin-free cases include the order of the matrix elements and the order of the index pairs in each matrix element). Suppose all permuted forms are generated for a term  $\mathfrak{A}$ . What is needed to canonicalize a term is to define a criterion to select a unique one from them. There are many ways to define the criteria. For example, the following rules work:

- A preferred order of matrix elements of different names is defined, for example, “  $f/v \rightarrow t_1 \rightarrow t_2 \rightarrow t_3 \rightarrow \gamma > \eta \dots$  ”.  $f/v$  stands for the one/two particle Hamiltonian matrix element,  $t_1/t_2/t_3$  stands for the  $\hat{T}_1/\hat{T}_2/\hat{T}_3$  amplitude. The permutation forms which do not conform to this criterion are discarded.
- For surviving terms, we compare each index correspondingly according to the criteria given below. The comparison is done term by term, and those less favored forms are discarded. That is, during the comparison of form X to form Y, we compare every index at the same position in A and B. Once a difference is located according to the criterion, the less favored term (X or Y) is discarded. Suppose X is discarded; we then compare Y with next form in the same way. The following criteria are employed: (a) indices of explicit particle or hole type are preferred to those of general type, (b) particle indices are preferred to hole ones, (c) uncontracted (i.e., external) indices are preferred to contracted (i.e., summation or dummy) ones, As we follow the procedure, we check one by one the matrix elements one by one whose indices from already-checked matrix elements form gradually-growing libraries  $\mathbb{X}$  and  $\mathbb{Y}$  for X and Y, respectively. Thus a specific order of indices is developed for both X and Y, respectively. For the contracted index  $x$  in  $\mathbb{X}$  and  $y$  in  $\mathbb{Y}$  in comparison, the one which is contracted to an index already in the library is preferred. If both  $x$  and  $y$  satisfy this condition (suppose  $x$  is contracted to  $\bar{x}$ ,  $y$  is contracted to  $\bar{y}$ ), we compare the position of  $\bar{x}$  and  $\bar{y}$  in their corresponding libraries  $\mathbb{X}$  and  $\mathbb{Y}$ . If  $\bar{x}$  appears in  $\mathbb{X}$  earlier than  $\bar{y}$  in  $\mathbb{Y}$ , then X is preferred, and Y is discarded.
- The above criteria can be extended when necessary. For example, when some indices are

active, the selection criteria can be incremented by requiring that active indices are preferred to the other indices.

In principle, we can first generate all permuted forms and then select one according to the above criteria. In practice, however, for efficiency consideration we can proceed sequentially. For example, we first permute the order of the matrix elements in a term without permuting index pairs. Then we select the forms conforming to criterion A. In the next step we permute the index pairs of the terms (survived from last selection), and then select the forms conforming to the rules which are stated above.

For one term, if we finally get more than one form after this selection, we take any one of them. The last step of canonicalization is reducing the *numbers* of indices. For example, we have two terms  $\frac{1}{2}v_{h_1 h_2}^{p_1 p_3} \hat{E}_{p_1 p_3}^{h_1 h_2}$  and  $\frac{1}{2}v_{h_1 h_3}^{p_1 p_4} \hat{E}_{p_1 p_4}^{h_1 h_3}$ . The program can not recognize that they are equivalent at this moment. After ‘number’ reduction, both are converted to the same form  $\frac{1}{2}v_{h_1 h_2}^{p_1 p_2} \hat{E}_{p_1 p_2}^{h_1 h_2}$ . The reduction is done through a mapping process. Given a term, from the first to the last matrix element, from upper to lower indices, from left to right indices, the first particle index is mapped to  $p_1$ , the second particle index is mapped to  $p_2$ , etc. After this mapping process, the original indices are replaced by the mapped ones. This is the procedure of canonicalization implemented in our program. From the brief discussion of the algorithm in Ref. [181], it appears that ours is rather similar to Hirata’s algorithm. An alternative canonicalization algorithm which is applicable to connected terms in which there is no quantity of particle rank larger than two (which is the most frequent situation in coupled cluster theory) is briefly discussed in Ref. [200].

The canonicalization procedure simplifies the expression (6.11) greatly:

$$\begin{aligned}
& \frac{1}{2} v_{h_1 h_2}^{p_1 p_2} \hat{E}_{p_1 p_2}^{h_1 h_2} \times \frac{1}{2} t_{p_3 p_4}^{h_3 h_4} \hat{E}_{h_3 h_4}^{p_3 p_4} \\
= & 0.25 v_{h_1 h_2}^{p_1 p_2} t_{p_3 p_4}^{h_3 h_4} \hat{E}_{p_1 p_2 h_3 h_4}^{h_1 h_2 p_3 p_4} + v_{h_1 h_2}^{p_1 p_2} t_{p_3 p_1}^{h_3 h_4} \hat{E}_{h_4 p_2 h_3}^{h_1 h_2 p_3} - v_{h_1 h_2}^{p_1 p_2} t_{p_3 p_4}^{h_3 h_1} \hat{E}_{p_1 p_2 h_3}^{p_4 h_2 p_3} + \\
& 0.5 v_{h_1 h_2}^{p_1 p_2} t_{p_1 p_2}^{h_3 h_4} \hat{E}_{h_3 h_4}^{h_1 h_2} + 2.0 v_{h_1 h_2}^{p_1 p_2} t_{p_3 p_1}^{h_3 h_1} \hat{E}_{p_2 h_3}^{h_2 p_3} - v_{h_1 h_2}^{p_1 p_2} t_{p_1 p_3}^{h_3 h_1} \hat{E}_{p_2 h_3}^{h_2 p_3} \\
& - v_{h_1 h_2}^{p_1 p_2} t_{p_3 p_2}^{h_3 h_1} \hat{E}_{p_1 h_3}^{h_2 p_3} - v_{h_1 h_2}^{p_1 p_2} t_{p_2 p_3}^{h_3 h_1} \hat{E}_{h_3 p_1}^{h_2 p_3} + 0.5 v_{h_1 h_2}^{p_1 p_2} t_{p_3 p_4}^{h_1 h_2} \hat{E}_{p_1 p_2}^{p_3 p_4} \\
& - 2.0 v_{h_1 h_2}^{p_1 p_2} t_{p_3 p_2}^{h_1 h_2} \hat{E}_{p_1}^{p_3} + v_{h_1 h_2}^{p_1 p_2} t_{p_3 p_1}^{h_1 h_2} \hat{E}_{p_2}^{p_3} + 2.0 v_{h_1 h_2}^{p_1 p_2} t_{p_2 p_1}^{h_3 h_1} \hat{E}_{h_3}^{h_2} \\
& - v_{h_1 h_2}^{p_1 p_2} t_{p_1 p_2}^{h_3 h_1} \hat{E}_{h_3}^{h_2} + 2.0 v_{h_1 h_2}^{p_1 p_2} t_{p_1 p_2}^{h_1 h_2} - v_{h_1 h_2}^{p_1 p_2} t_{p_2 p_1}^{h_1 h_2}.
\end{aligned} \tag{6.13}$$

## 6.3 Generating Fortran Codes

Once residual equations are obtained, the structure of each term in the equations is parsed, a factorization of the residual expression is performed, primarily for efficiency consideration. The proper subroutines are invoked thereafter to evaluate residuals.

### 6.3.1 Factorization

Suppose we have the residual expression:

$$\begin{aligned}
R_{h_1 h_2}^{p_1 p_2} &= \alpha + \beta + \dots \\
&= ABCD + EF + \dots
\end{aligned} \tag{6.14}$$

To add the product of  $ABCD$  to  $R_{h_1 h_2}^{p_1 p_2}$ , if we carry out the multiplications sequentially, there are 24 different orders to calculate  $ABCD$ : A-B-C-D (from right to left, first multiply C by D together, then multiply the product by B, then by A), A-B-D-C, A-C-B-D,  $\dots$ . Different orders often results in different computational costs. We first find the most efficient order by comparing the costs of all permutations. This is a local optimization procedure (strength reduction).

Now we illustrate the factorization algorithm implemented in our code (though not yet tested)

with one simple example:

$$\begin{aligned}
 R &= A_1 + \\
 &\quad A_2 \times B_2 + \\
 &\quad A_3 \times B_3 \times C_3 + \\
 &\quad A_4 \times B_4 \times C_4.
 \end{aligned} \tag{6.15}$$

Suppose that for each term, the multiplication order is already determined (as indicated from its form, from right to left). We first examine the terms which have the most components, in this case, the third and the fourth terms which have 3 components. We check if  $A_3 = A_4$  and  $B_3 = B_4$ . If that is true, a factorization is possible:

$$R = \dots + A_3 \times B_3 \times (C_3 + C_4). \tag{6.16}$$

In this case, we can define an intermediate:  $I_x = C_3 + C_4$  and get

$$\begin{aligned}
 R &= A_1 + \\
 &\quad A_2 \times B_2 + \\
 &\quad A_3 \times B_3 \times I_x
 \end{aligned} \tag{6.17}$$

$$\begin{aligned}
 &= A_1 + \\
 &\quad A_2 \times B_2 + \\
 &\quad A_3 \times I_y,
 \end{aligned} \tag{6.18}$$

upon defining  $I_y = B_3 \times I_x$ . Now we check whether  $A_2 = A_3$ . If that is true, another factorization is possible. In general, we first classify terms by the number of components (for notational simplicity, let us call the number the ‘rank’ of the term), and carry out factorizations following the order of decreasing rank. For terms of the same rank, we compare all the components except the rightmost one. For this comparison, we simply compare element by element. If any two

terms have the same components except the rightmost one, a factorization is found. In the example above, if  $A_4 = B_3$  and  $A_3 = B_4$ , a factorization is possible in principle, but this requires comparisons of permutations. In general, this comparison is rather expensive if done fully.

Clearly, this factorization algorithm is far from optimal, and further optimization is possible. We did not pursue further improvements, because our first goal is to get a reasonable working code to test our theory. Very high efficiency will be of high priority to us when our method is robust and satisfactory. Here we list a few potential issues which may be considered in future to develop better factorization algorithms:

- The type of factorization  $A \times B \times C + A \times D \times C = A \times (B + D) \times C$  is not considered in the current algorithm.
- It is hard to recognize common factors among terms of different types, for example,  $(B + C)$  in

$$A \times (B + C) \times D + E \times (B + C) \times F.$$

- By identifying common factors which occur many times in the equation and storing them during the computation process, the number of floating point operations can be reduced, whereas more disk space is required. The space-time tradeoff is an important issue to consider.
- A satisfactory algorithm should consider more sophisticated factorizations. For example, instead of multiplying ABCD as follows,

$$\begin{aligned} I_1 &= C \times D, \\ I_2 &= B \times I_1, \\ ABCD = I_3 &= A \times I_2, \end{aligned} \tag{6.19}$$

other ways should be examined:

$$\begin{aligned}
 I_1 &= C \times D, \\
 I_2 &= A \times B, \\
 ABCD &= I_2 \times I_1.
 \end{aligned} \tag{6.20}$$

The final costs may differ greatly. For example, to compute

$$A_{wx}^{rz} \times B_{vy}^{wx} \times C_{su}^{vt} \times D_{tr}^{qs},$$

the first route leads to a cost  $\propto N^7$ :

$$\begin{aligned}
 I_{1qv}^{ur} &= C_{su}^{vt} \times D_{tr}^{qs}, \\
 I_{2xqw}^{yur} &= B_{vy}^{wx} \times I_{1qv}^{ur}, \\
 ABCD = (I_{3zq}^{yu}) &= A_{wx}^{rz} \times I_{2xqw}^{yur}.
 \end{aligned} \tag{6.21}$$

In comparison, the second route leads to a cost  $\propto N^6$ :

$$\begin{aligned}
 I_{1qv}^{ur} &= C_{su}^{vt} \times D_{tr}^{qs}, \\
 I_{2rz}^{vy} &= A_{wx}^{rz} \times B_{vy}^{wx}, \\
 ABCD = (I_{3zq}^{yu}) &= I_{2rz}^{vy} \times I_{1qv}^{ur}.
 \end{aligned} \tag{6.22}$$

The difference is clear from the illustration Fig. 6.1.

Suppose that we have developed factorization algorithms of different levels of sophistication. Usually it is not practical to carry out a complete search to find the optimum factorization of the whole equation. In other words, global optimization is often not attainable. Presumably only a small portion of the terms are of leading costs and determine the overall cost scaling of the whole residual evaluation, so they should be the focus of the factorization step. Therefore, it



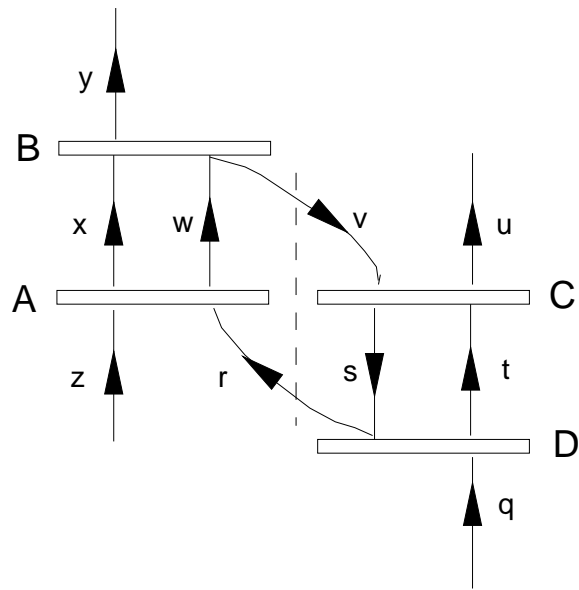


Figure 6.1:  $A^{rz} \times B^{wx} \times C^{vt} \times D^{qs}$  contraction pattern

appears more practical to apply different factorization algorithms to different groups of terms. To illustrate, we outline one plausible schematic procedure which may be implemented in future:

1. Group terms into classes according to their individual computational cost scaling, based on strength reduction.
2. Apply the most sophisticated factorization algorithm implemented to terms of leading costs, and less time-demanding algorithms to the other terms. In principle, we can set up a few levels of algorithms if necessary.
3. If the costs for the leading terms are reduced substantially upon factorization, and some other terms dominate the overall cost, we can repeat step (2).

In general, it is a complicated problem to find a good factorization algorithm; this issue has been discussed in the literature[203].

### 6.3.2 Multiplication and addition subroutines

After factorization, the real input to the code generation module is the intermediates. Here is an example. For the product ABCD, suppose the most efficient order is A-B-C-D.  $C \times D$  generates one intermediate quantity, say  $I_1$ :

$$\begin{aligned}
 I_1 &= C \times D, \\
 I_2 &= B \times I_1, \\
 I_3 &= A \times I_2, \\
 R_{h_1 h_2}^{p_1 p_2} &+ = I_3.
 \end{aligned}
 \tag{6.23}$$

The intermediates themselves are products of other quantities, and are represented by a class which allows internal structures. This class has an attribute which has the value ‘P’ or ‘S’, where ‘P’ means the intermediate is a product of two quantities, and ‘S’ means it is the sum of two quantities. This class also has an attribute to store the constituent quantities of the product or summation.

In this case, the code generation module receives  $I_3$  as the input, parses its structure and decides that it is the product of  $A$  and  $I_2$ , which itself is an intermediate. By tracing the internal structures, the module finally gets to  $I_1$ , and find that it is a product of two quantities, which are not intermediates, e.g.,  $t_{p_1 p_2}^{i_3 i_4}$  and  $v_{i_3 i_4}^{i_1 i_2}$ . Then it starts to call multiplication and addition subroutines to execute  $I_1 = C \times D$ . Once  $I_1$  is obtained,  $I_2, I_3, R_{h_1 h_2}^{p_1 p_2}$  will be calculated sequentially. In other words, the module deciphers the intermediate  $I_3$  and traces its internal structure to the lowest level, then starts to call subroutines to execute the operations sequentially, following the trace.

All intermediate quantities and primitive quantities such as  $t_{p_1 p_2}^{i_3 i_4}$  and  $v_{i_3 i_4}^{i_1 i_2}$  are represented as *lists*. A list is an integer which tells where the quantities are stored. It is pre-determined how the quantities represented by a list are stored, with symmetry being taken into account to reduce the required space. Besides, every list has its associated particle-hole type, which tells the particle-hole type of the indices in the quantity represented by the list. For example,  $t_{p_1 p_2}^{i_3 i_4}$  is represented by a list named *ltaaii* and the particle-hole type of the list is 'aaii'. When the particle-hole type is passed to the subroutine as an argument, it may contain information specifying how to select a particular subclass of its corresponding quantity. This is illustrated later in this section. For brevity, we will henceforth use interchangeably a *list* and the quantity it represents.

A series of highly efficient general-purpose addition and multiplication subroutines are written. Every subroutine can realize a particular operation depending on the number of indices in every quantity involved and the number of contracted indices. For example, to execute the operation

$$R_{p_1 p_2}^{i_1 i_2} + = 0.5 \times v_{i_3 i_4}^{i_1 i_2} \times t_{p_1 p_2}^{i_3 i_4}, \quad (6.24)$$

we need to call the subroutine *diagram444*. In general, to implement  $C = a \times C + b \times A \times B$ , where  $a$  and  $b$  are coefficients ( $C+ = b \times A \times B$  is a special case of  $a = 1$ ), we call the subroutine *diagramXYZ*, where  $X$  refers to the number of indices in  $A$ ,  $Y$  refers to the number of indices in  $B$ , and  $Z$  refers to the number of indices in  $C$ . To complete the call, the program needs to decipher the expression (6.24):

- determine which lists the quantities correspond to:  $v_{i_3 i_4}^{i_1 i_2} \leftrightarrow lviiii, t_{p_1 p_2}^{i_3 i_4} \leftrightarrow ltaaii, R_{p_1 p_2}^{i_1 i_2} \leftrightarrow lraaii$ . The correspondence is determined by the definition which is implemented in the program.
- determine how to permute the orders of indices of lists  $lviiii$ ,  $ltaaii$  and  $lraaii$ . *Diagram* subroutines are implemented in such a way that it requires a particular ordering, for example, the last two indices of list  $A$  and the first two indices of list  $B$  are the contracted indices, and the uncontracted indices in  $A$  and  $B$  are in the same order as in  $C$ :

$$C(p, q, r, s) = b \times A(p, q, x, y) \times B(x, y, r, s). \quad (6.25)$$

Since how  $A$ ,  $B$  and  $C$  are stored is pre-defined and may not conform to the requirement, the orders of the indices in them need to be changed. The program permutes the orders of indices in  $A$ ,  $B$  and  $C$  until the required ordering is achieved. By permuting indices, the *diagram* procedures can use effective BLAS matrix multiplication subroutines.

- determine the particle-hole types of the lists after permutation (if there is no reordering, the particle-hole types are the same as initially defined). Adding particle-hole types to the arguments of *diagram*, instead of inferring it from the definition of the lists and their indices orders, makes the call more explicit. More importantly, the particle-hole types may be used to specify to *shrink* lists. Here is an example. Suppose in a subroutine the order of the list  $ltaaii$  is not changed, that is ‘aaii’. If instead of  $v_{i_3 i_4}^{i_1 i_2} \times t_{p_1 p_2}^{i_3 i_4}$  the multiplication is  $v_{i_3 m_1}^{i_1 i_2} \times t_{p_1 p_2}^{i_3 m_1}$  ( $m_1$  is an active-hole index), the list corresponding to  $t_{p_1 p_2}^{i_3 m_1}$  is still  $ltaaii$ , but its particle-hole list in the subroutine is ‘aaim’ instead of ‘aaii’. The program will then only select the portion of  $ltaaii$  in which the fourth index is an active-hole index and use them in the multiplication. The automatic *shrinking* enhances the flexibility of the *diagram* subroutines. The particle-hole list in the subroutine for  $lviiii$  will be changed correspondingly.
- determine the multiplication coefficients  $a$  and  $b$ .

Once the program deciphers the expression and extracts all the information needed for the ar-

guments, the call can be completed. In APG, the multiplication and addition subroutines are represented by two *classes*, and *attributes* are assigned to these classes to represent the arguments. For example, for the class which represents multiplication subroutines, there are attributes to determine which specific multiplication subroutine to be called, attributes to pass the multiplication coefficient, attributes to determine how to reorder the indices in the multiplication component quantities, etc.

Now we show a piece of the Fortran code generated, which corresponds to the operation

$$R_{p_1 p_2}^{i_1 i_2} = 0.5 \times v_{i_3 i_4}^{i_1 i_2} \times t_{p_1 p_2}^{i_3 i_4}. \quad (6.26)$$

```

!      R[ a1 a2, i1 i2 ] =      v[ i3 i4, i1 i2 ]      t[ a1 a2, i3 i4 ]
!      R[ a1 a2, i1 i2 ] =      v[ i1 i2, i3 i4 ]      t[ a1 a2, i3 i4 ]
! lraaii[ i1 i2, a1 a2 ] =      lviiii[ i1 i2, i3 i4 ]  ltaaii[ i3 i4, a1 a2 ]
!      [ 3 4, 1 2 ] = 'N' [ 1 2, 3 4 ] 'N' [ 3 4, 1 2 ]

      call diagram444(lviiii, 'iiii', '1234', 'N',
$          ltaaii, 'iaaa', '3412', 'N', 0.5d0,
$          lraaii, 'iaaa',
$          '3412', 1.0d0 , scr, mxcor)

```

The first four lines are comments generated by the program (coefficients neglected in the comment lines). The first line is the same as the actual input expression (6.26) (except the factor of 0.5 which can be printed out if desirable); the second line writes the indices in the orders as they are stored, which are pre-defined; the third line gives the indices in the orders which conform to the requirement of the *diagram444* subroutine; the fourth line prints out explicitly the permutations, which can be understood by comparing the second to the third comment line. ‘N’ means ‘no transposition’, and is related to the ‘N’ and ‘T’ arguments in BLAS DGEMM calls. The next

four lines are the actual call of the subroutine *diagram444*.

The above is the basic mechanism how Fortran codes are generated. In the above example, what *appears* to the end user is: the term  $A \times B \times C \times D$  is the ‘feed-in’, the program finds the optimal order from permutations, calls one multiplication subroutine to multiply  $C \times D$  and store the result in  $I_1, \dots$ , and finally call one addition subroutine to add  $I_3$  to  $R_{h_1 h_2}^{p_1 p_2}$ .

### 6.3.3 Minimize the number of intermediates

Now we study how to minimize the number of intermediates to save disk space. For the product A-B-C-D, as shown in Eq. (6.23), three intermediates are created (if desired, the last two operations can be incorporated into one,  $R_{h_1 h_2}^{p_1 p_2} + = A \times I_2$ , then only two intermediates are created). For an equation containing many terms, many intermediates are created. Some effort is made to maximize the reuse of intermediates. For example, after the second step, the intermediate  $I_1$  is free and ready for reuse. The same is true for  $I_2$  after the third step. We achieve this by monitoring the states (‘free’ or ‘busy’) of all intermediates all the time and reuse them whenever they are free. In this way, we maximize the use of intermediates such that we need at most two intermediates for each type (the ‘type’ is characterized by the number of particle and hole indices).

## 6.4 Conclusion

The automatic program generator (APG) program is written in Python, which includes two modules: equation derivation and Fortran code generation. The first module is based on the generalized Wick theorem (GWT). Various versions of GWT are implemented:  $h$ -GWT,  $\gamma$ -GWT and  $\lambda$ -GWT. In the second module, partial optimization to minimize computational cost is implemented. The equation derivation module is presented in great detail. Usually the derivation of an explicit residual equation is the first step of the implementation, so this module is of general use and independent of the second module. The second module, Fortran code generation, is based on a series of general-purpose multiplication and addition subroutines which are embedded in the ACESII quantum chemistry program [204].

So far, the APG code can derive various coupled cluster (spin-adapted or spin-orbital) equations, call subroutines to realize additions and multiplications automatically, output equations in Latex form, etc. Extensive use of classes makes the program rather flexible, and its functions can be extended readily. We are currently pursuing the development of some internally contracted multireference coupled cluster methods with the aid of the APG program.

This ends our discussion of the method: theory and implementation. In next chapter we presents benchmark results.

## Chapter 7

# Benchmark results

Prior applications of SS-EOMCC focused on biradical-like systems or singly bonded species, in which only one extra orbital is needed to construct the active space. The method at this level is termed as SS-EOMCC[+2], where ‘[+2]’ signifies that *formally* two extra electrons are needed to construct the closed-shell vacuum state. SS-EOMCC[+2] has been applied to study the ground and excited states of O<sub>2</sub> and F<sub>2</sub> [155], the dissociation of LiF [205], and organic biradicals [164] such as the automerization barrier of cyclobutadiene, singlet-triplet gaps of trimethylmethylene, and the activation and reaction energies of the Bergman reaction. Now the applicability of the method is extended to systems with general active spaces.<sup>1</sup>

In Section 7.1, the method is applied to the triplet  $^3\Sigma_u^-$  state of F<sub>2</sub> to examine its behavior for single reference systems. In section 7.2, tests are done on H<sub>2</sub>O, CO and N<sub>2</sub>. In section 7.3, the effect of a perturbative correction which attempts to alleviate the redundancy issue, is illustrated.

All the studies in this section use the CASSCF orbitals, and the orbitals which define the active space include all core and valence orbitals. For F<sub>2</sub>, the active space is (18 e, 10 o). For H<sub>2</sub>O, the active space is (10 e, 7 o). For N<sub>2</sub> and CO, the active space is (14 e, 10 o). All single reference computations are done with the ACES II quantum chemistry package [204] and CASPT2/MR-AQCC/MRCI results are obtained using the MOLPRO package [206].

<sup>1</sup>Contents of this chapter and Chapter 3 are being published in J. Chem. Phys. (in press)



## 7.1 Triplet state of $F_2$

The triplet  ${}^3\Sigma_u^-$  state of  $F_2$  molecule is a single reference system over the whole bond distance range, and is used to test the performance of the SS-EOMCC method in single reference cases. For this system, unrestricted CCSD(T) should give highly accurate results, and we compare the results from unrestricted CCSD and SS-EOMCC with it. The numerical results are included in supporting information and the comparison is plotted in Fig. 7.1. UCCSD exhibits a fairly large absolute error (up to  $12.3 mE_h$ ) and non-parallelity error (NPE) (ca.  $4.9 mE_h$ ). SS-EOMCC has smaller absolute error values (up to  $4.6 mE_h$ ). More importantly, the NPE is significantly reduced (ca.  $0.3 mE_h$ ). Naively we might expect similar accuracy from CCSD and SS-EOMCC, as in both cases the cluster operator only includes single and double excitations from a single reference determinant (in SS-EOMCC, the determinant is  $|0\rangle$ ). We attribute the superiority of SS-EOMCC over CCSD to the partial inclusion of triple excitations. For example (see Fig. 7.2), the determinant on the left is the dominant determinant in  $|R\rangle$ , and the determinant on the right, which is included in the MRCIS space, is triply excited with respect to the reference determinant. On the other hand, compared with CCSD(T), the inclusion of triple excitations is incomplete. Hence, for single reference systems, we would expect the order of the accuracy to be:

$$\text{CCSD} < \text{SS-EOMCC} < \text{CCSD(T)}.$$

## 7.2 General active spaces: $N_2$ , $H_2O$ and $CO$

Now we look at multi-bond breaking processes. All computations are done with both cc-pVDZ and cc-pVTZ basis sets [207]. The  $C_{2v}$  symmetry group is used for all three molecules. For  $H_2O$ , both O-H bonds are broken symmetrically, while the bond angle is kept at  $109.57^\circ$ . The comparisons are with MRCI+Q [145, 146, 148] (the benchmark calculations in Ref. [80] demonstrates the high accuracy of MRCI+Q, but whether it remains so for large basis sets is uncertain). The MRCI method in MOLPRO is internally contracted. In addition, we investigated these molecules with

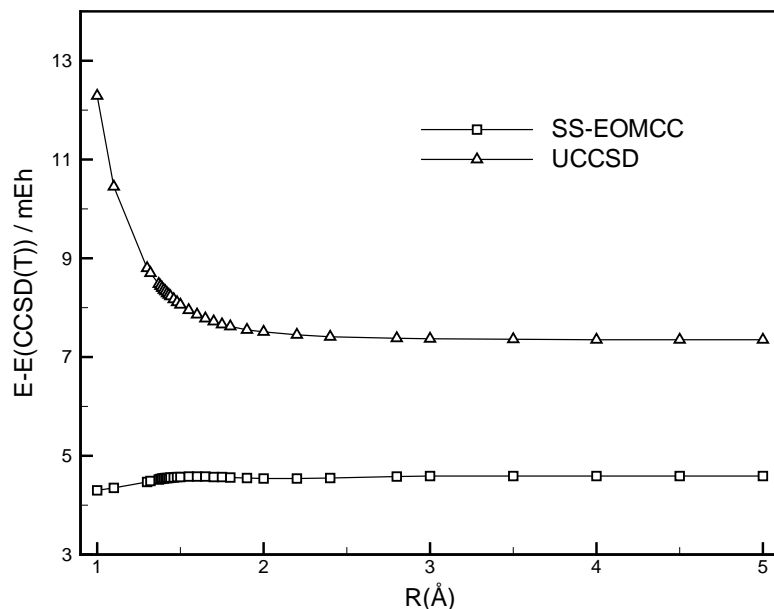


Figure 7.1: Energy difference from CCSD(T) for  $F_2$   $^3\Sigma_u^-$  state. SS-EOMCC computations use an active space of (18 e, 10 o).

the CASPT2 [208, 209] and MR-AQCC [210, 211] methods. To investigate the effect of three-body terms in the transformed Hamiltonian, we also list results where these terms are included when diagonalizing the transformed Hamiltonian.

The errors of different methods compared with MRCI+Q are plotted in Fig. 7.3-7.8 (all the numbers can be found in supplementary information). The mean absolute errors (MAE's) and NPE's are tabulated in Table 7.1, and, plotted in Fig. 7.9 and 7.10.

For  $N_2$  in the cc-pVDZ basis set, MR-AQCC has the smallest NPE and MAE. The error curve of CASPT2 has a large fluctuation. The inferiority of CASPT2 to the other methods is probably because the perturbative treatment of dynamical correlation is not sufficient. MRCI has errors ranging from 7.7 to 10.9  $mE_h$ . Clearly the a posteriori quadruple correction in MRCI+Q is important. The absolute errors for SS-EOMCC, ranging from 5.0 to 8.2  $mE_h$ , are lower than for MRCI, but the NPE is similar to MRCI. The MAE decreases by 2  $mE_h$  and the NPE decreases by 0.9  $mE_h$ , when three-body terms are included for SS-EOMCC. In the cc-pVTZ basis set, MR-AQCC has its MAE increased by 1.3  $mE_h$ , but the NPE does not change. CASPT2 becomes

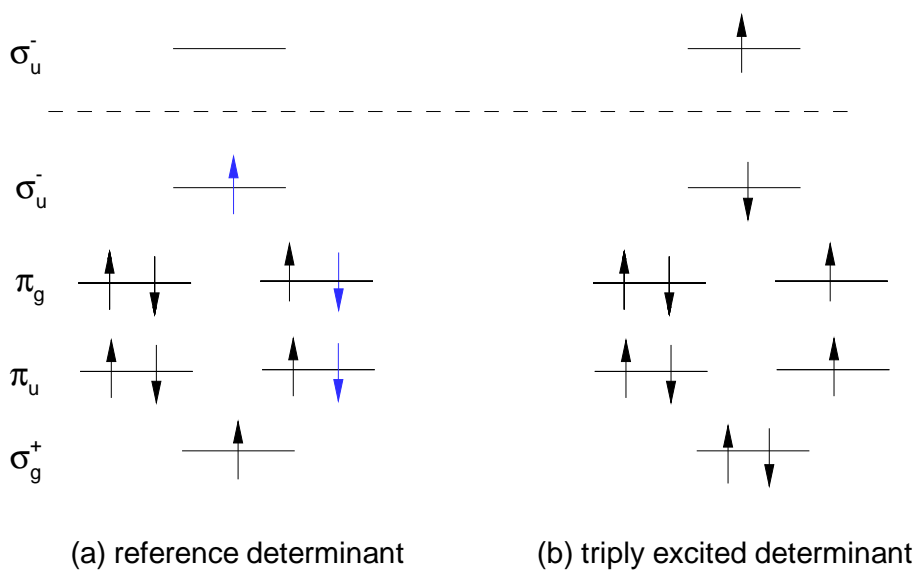


Figure 7.2: ]  
 Illustration of certain triple excitations present in SS-EOMCC[+2].

even less stable, with an NPE of  $11.9 mE_h$ . MRCI has its MAE increased by  $6.2 mE_h$ , but NPE only increased by  $0.4 mE_h$ . For SS-EOMCC, both MAE and NPE exhibit a minor change. When three-body terms are included, the MAE decreases by  $1.6 mE_h$  and the NPE decreases by  $0.3 mE_h$ , compared with when three-body terms are neglected.

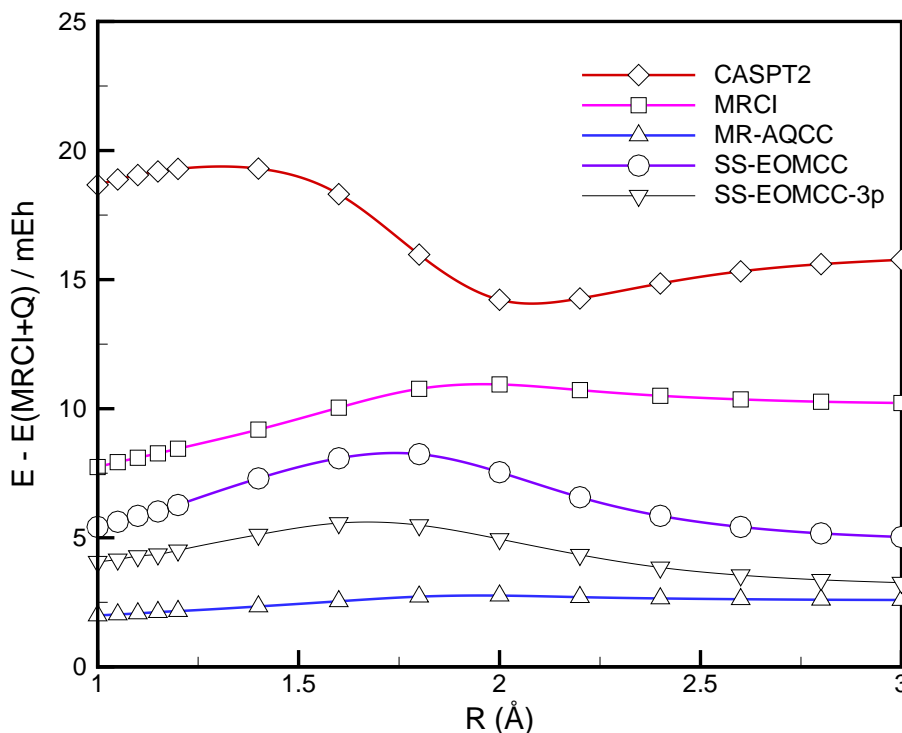


Figure 7.3: Comparison with MRCI+Q for  $N_2$  ground state in the cc-pVDZ basis set. The active space is (14 e, 10 o) (SS-EOMCC-3p means that three-body terms are included when diagonalizing the transformed Hamiltonian, refer to Section II).

For CO in the cc-pVDZ basis set, MR-AQCC is again the most stable, and the large fluctuation for CASPT2 is again observed. SS-EOMCC has a MAE smaller than MRCI by  $2.0 mE_h$  and a NPE smaller by  $0.7 mE_h$ . Including three-body terms decreases the MAE and NPE by  $1.8 mE_h$  and  $1.4 mE_h$ , respectively. In the cc-pVTZ basis set, MR-AQCC has its MAE increased by 1.4

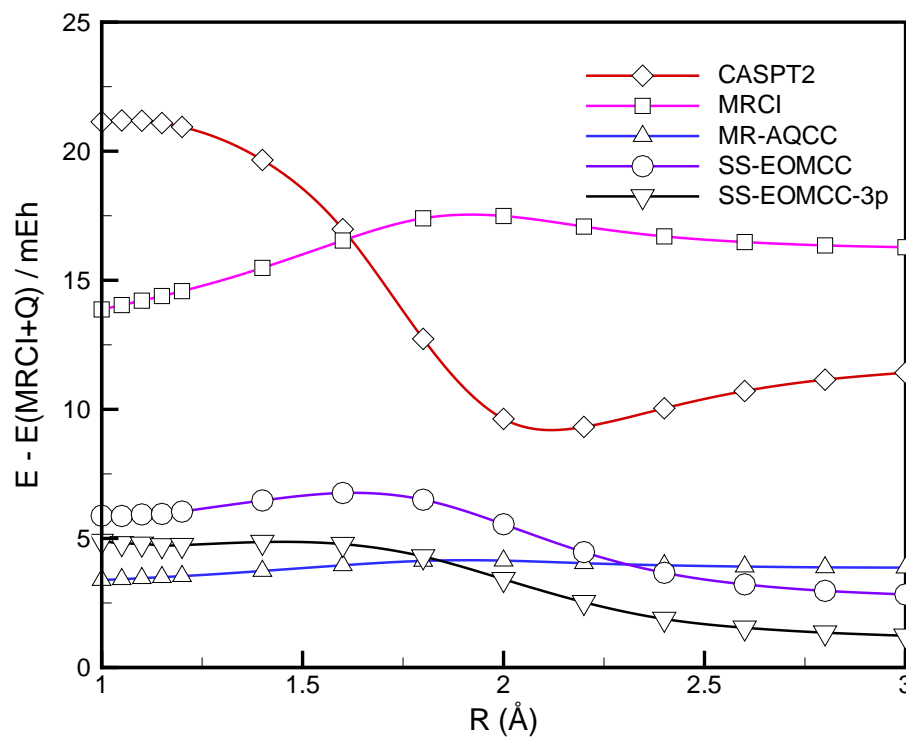


Figure 7.4: Comparison with MRCI+Q for  $\text{N}_2$  ground state in the cc-pVTZ basis set. The active space is (14 e, 10 o) (SS-EOMCC-3p means that three-body terms are included when diagonalizing the transformed Hamiltonian).

$mE_h$  (the changes are roughly the same for all three systems studied in this subsection) and NPE unaffected. For CASPT2, the NPE increases by  $6 mE_h$ . In comparison, it only increases by  $1.0 mE_h$  for MRCI. Interestingly, the SS-EOMCC error curve becomes flatter than in the cc-pVDZ basis set, and the NPE decreases by  $0.8 mE_h$ . When three-body terms are included, the MAE decreases by  $1.2 mE_h$  while the NPE increases by  $1.1 mE_h$ , compared with when three-body terms are neglected.

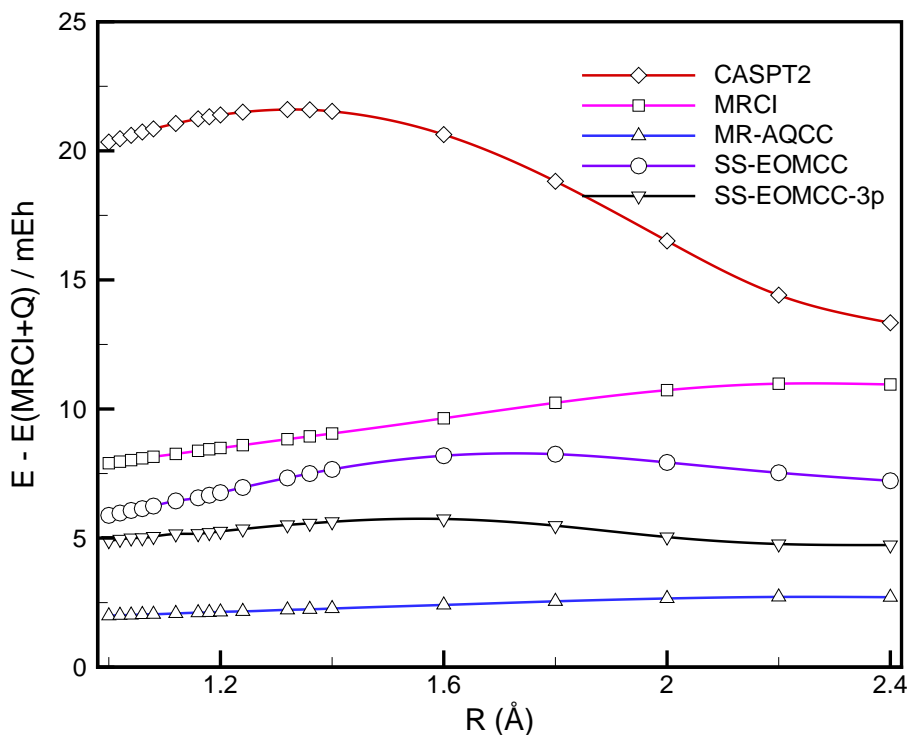


Figure 7.5: Comparison with MRCI+Q for CO ground state in the cc-pVDZ basis set. The active space is (14 e, 10 o) (SS-EOMCC-3p means that three-body terms are included when diagonalizing the transformed Hamiltonian).

For  $H_2O$  in the cc-pVDZ basis set, MR-AQCC and SS-EOMCC behave similarly. The MAE and NPE decrease by  $1.0 mE_h$  and  $0.3 mE_h$ , respectively, when three-body terms are included.

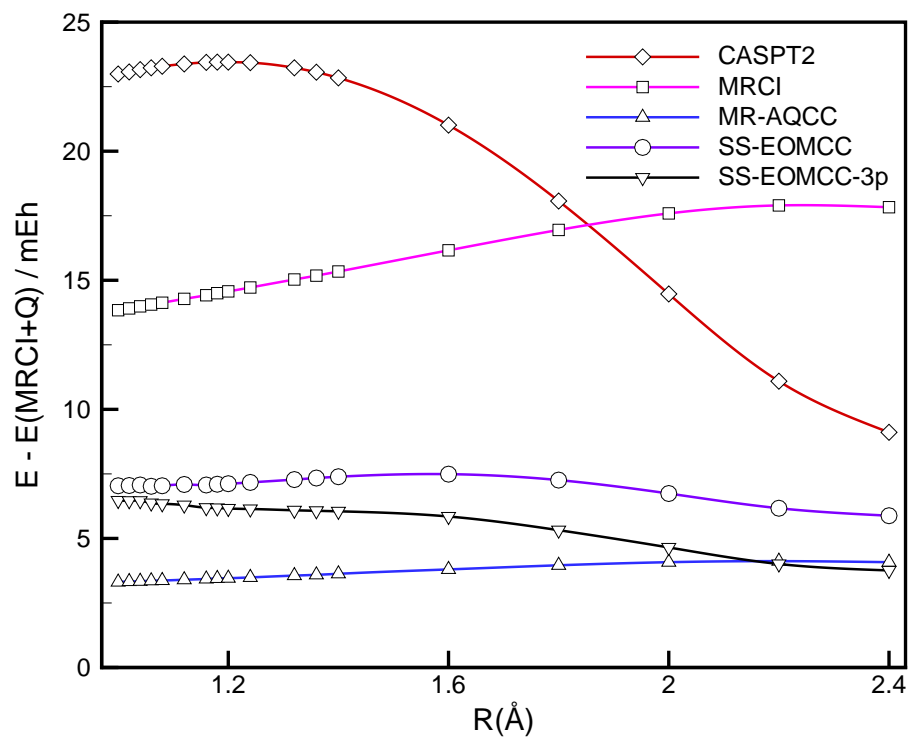


Figure 7.6: Comparison with MRCI+Q for CO ground state in the cc-pVTZ basis set. The active space is (14 e, 10 o) (SS-EOMCC-3p means that three-body terms are included when diagonalizing the transformed Hamiltonian).

CASPT2 has the largest MAE and NPE among all methods. MRCI error curve lies in between, with an NPE of  $2.4 mE_h$ . In the cc-pVTZ basis set, the NPE's for CASPT2, MRCI and SS-EOMCC increases by about  $2 mE_h$ , while only  $0.7 mE_h$  for MR-AQCC. In terms of MAE, only MRCI is affected largely, MAE increasing by  $3.6 mE_h$ . For SS-EOMCC, including three-body terms decreases the MAE by  $0.6 mE_h$  while increases the NPE by  $0.2 mE_h$ , in comparison to when three-body terms are neglected.

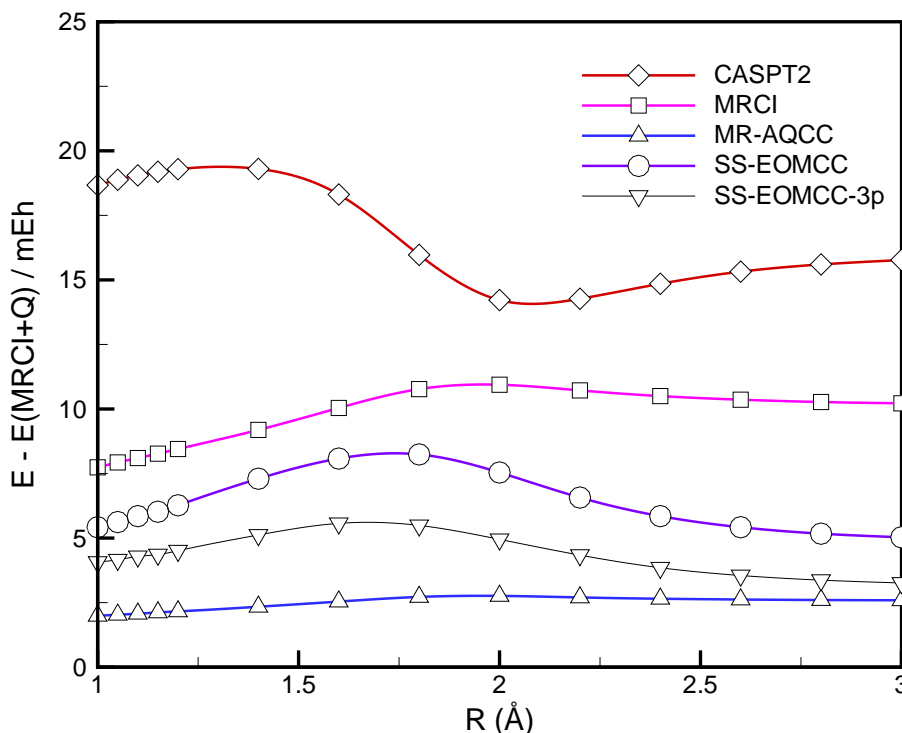


Figure 7.7: Comparison with MRCI+Q for  $H_2O$  ground state in the cc-pVDZ basis set. The active space is  $(10e, 7o)$ ,  $\angle HOH = 109.57^\circ$  and O-H bonds are stretched symmetrically (SS-EOMCC-3p means that three-body terms are included when diagonalizing the transformed Hamiltonian).

Overall, MR-AQCC gives the best results in average, measured in terms of MAE, with respect to the MRCI+Q approach. CASPT2 gives the largest MAE for all systems studied. The MAE's



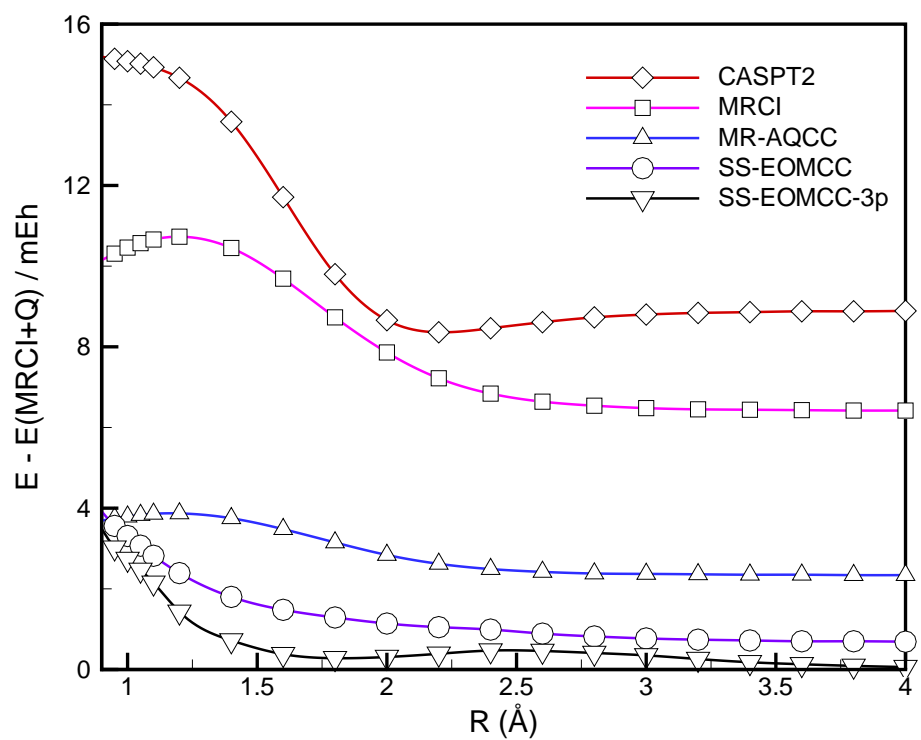


Figure 7.8: Comparison with MRCI+Q for  $\text{H}_2\text{O}$  ground state in the cc-pVTZ basis set. The active space is  $(10e, 7o)$ ,  $\angle\text{HOH} = 109.57^\circ$  and O-H bonds are stretched symmetrically (SS-EOMCC-3p means that three-body terms are included when diagonalizing the transformed Hamiltonian).

for MRCI are clearly larger than for SS-EOMCC. The relatively large MAE of MRCI is due to the size-extensivity problem, which is less severe for SS-EOMCC, as this method is core-extensive. The dependence of MAE on the basis set is most severe for MRCI.

For NPE, MR-AQCC again performs the best and CASPT2 the worst. CASPT2 also exhibits a dependence on the basis set. MRCI and SS-EOMCC lie between MR-AQCC and CASPT2 and behave similarly. For all the systems studied, their NPE's are in the range of 1-4  $mE_h$ .

For SS-EOMCC, when three-body terms are included MAE always decreases while no clear pattern is observed for the change of NPE, which may decrease or increase depending on the system studied. For the three systems investigated here, the change of NPE is within 1.4  $mE_h$ .

Table 7.1: MAE's and NPE's for different methods in  $mE_h$ . For CO and N<sub>2</sub>, the active space is (14e, 10o). For H<sub>2</sub>O, the active space is (10e, 7o),  $\angle\text{HOH} = 109.57^\circ$  and O-H bonds are stretched symmetrically (SS-EOMCC-3p means that three-body terms are included when diagonalizing the transformed Hamiltonian).

	CASPT2	MRCI	SS-EOMCC	SS-EOMCC-3p	MR-AQCC
MAE					
N <sub>2</sub> (cc-pVDZ)	17.05	9.54	6.31	4.35	2.42
N <sub>2</sub> (cc-pVTZ)	15.51	15.78	5.15	3.56	3.78
H <sub>2</sub> O(cc-pVDZ)	10.36	4.64	1.56	0.60	1.72
H <sub>2</sub> O(cc-pVTZ)	11.05	8.27	1.64	0.99	3.00
CO(cc-pVDZ)	19.89	8.98	6.96	5.20	2.25
CO(cc-pVTZ)	20.88	15.24	7.02	5.83	3.60
NPE					
N <sub>2</sub> (cc-pVDZ)	5.08	3.20	3.21	2.31	0.77
N <sub>2</sub> (cc-pVTZ)	11.87	3.62	3.93	3.67	0.75
H <sub>2</sub> O(cc-pVDZ)	4.88	2.44	1.12	0.86	0.89
H <sub>2</sub> O(cc-pVTZ)	6.82	4.31	3.23	3.43	1.53
CO(cc-pVDZ)	8.26	3.08	2.37	1.01	0.72
CO(cc-pVTZ)	14.35	4.06	1.61	2.71	0.80

### 7.3 Effect of a perturbative correction

The linear dependence of the states  $\{\hat{\Omega}_\lambda|R\rangle, \forall\lambda\}$ , which is reflected in the singularity of the metric matrix (Eq. (4.36)), leads to the redundancy issue. Thus there are not enough residual equations for t-amplitudes. To solve this problem, one way is to only solve the residual equations in the

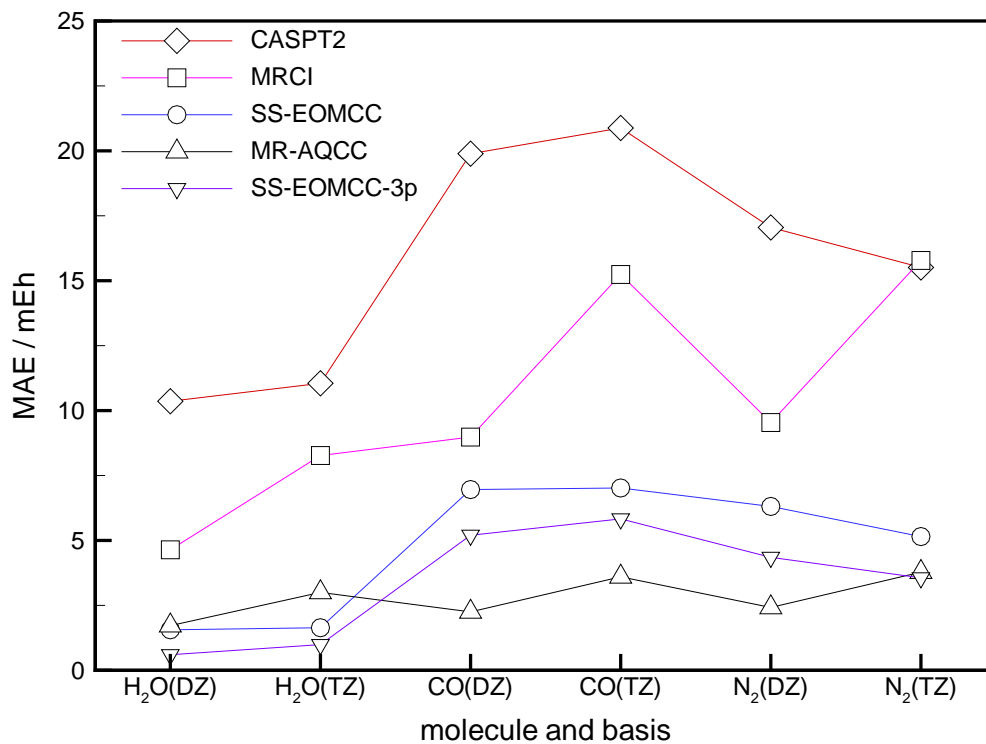


Figure 7.9: MAE's of different methods for different systems ('DZ' stands for 'cc-pVDZ', 'TZ' stands for 'cc-pVTZ'). For CO and N<sub>2</sub>, the active space is (14e, 10o). For H<sub>2</sub>O, the active space is (10e, 7o),  $\angle\text{HOH} = 109.57^\circ$  and O-H bonds are stretched symmetrically (SS-EOMCC-3p means that three-body terms are included when diagonalizing the transformed Hamiltonian).

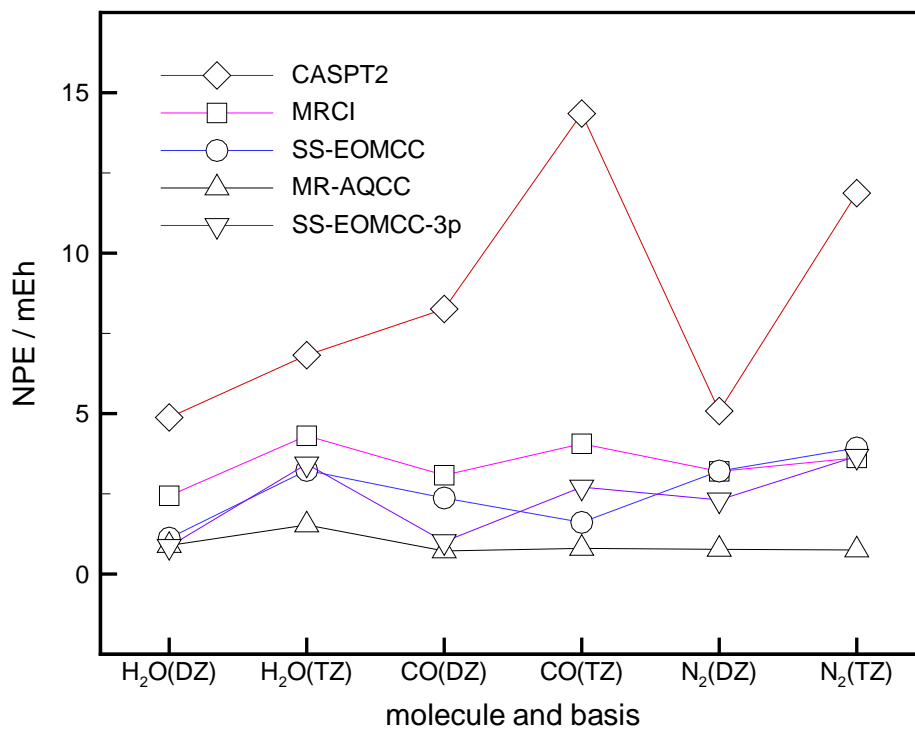


Figure 7.10: NPE's of different methods for different systems ('DZ' stands for 'cc-pVDZ', 'TZ' stands for 'cc-pVTZ'). For CO and N<sub>2</sub>, the active space is (14e, 10o). For H<sub>2</sub>O, the active space is (10e, 7o),  $\angle\text{HOH} = 109.57^\circ$  and O-H bonds are stretched symmetrically (SS-EOMCC-3p means that three-body terms are included when diagonalizing the transformed Hamiltonian).

non-redundant subspace defined by the projector  $P$  (Eq. (4.37)) and simply discard the redundant equations:

$$\sum_{k,l} P_{kl}^{ij} \langle R | \hat{E}_{ab}^{kl} e^{-\hat{T}} \hat{H} e^{\hat{T}} | R \rangle = 0, \quad (7.1)$$

$$(\mathbf{1} - P)_{kl}^{ij} t_{ab}^{kl} = 0. \quad (7.2)$$

An alternative is to add a perturbative correction in the nearly singular subspace, which has been discussed in a prior section. Here we examine the effect of a perturbative correction, using the example of ground state energies of  $N_2$  in the cc-pVDZ basis set with different thresholds.

We compare the energies obtained with and without the perturbative correction using large thresholds  $\eta = 0.1$  and  $\eta = 0.05$ , to results obtained with  $\eta = 0.01$  and including the perturbative correction. The results are plotted in Fig. 7.11-7.12. It is clear from the figure that the number of discarded t2-amplitudes is the largest at short bond distances, when  $|R\rangle$  is dominated by very few determinants. This phenomenon is also observed for other molecules. Since the number may vary significantly at different geometries, it is nontrivial to find a universal threshold which works well for all geometries. If  $\eta$  is too low, the convergence issue appears because some residual equations are ill defined. If  $\eta$  is too high, many t-amplitudes are discarded and the quality of the results is compromised. From Fig. 7.11, as  $\eta$  decreases from 0.1 to 0.05, the number of discarded amplitudes decreases at certain geometries. Once we decrease  $\eta$  to the standard value 0.01, the number further decreases substantially. To be precise, the number refers to the discarded hole orbital pairs ‘ij’ in  $\hat{E}_{ij}^{ab}$  (since it is determined by the discarded eigenvalues of the metric matrix  $S_{kl}^{ij}$ ), so the number of actually discarded t2-amplitudes should be multiplied by the number of virtual orbital pairs. The percentages of discarded amplitudes may be roughly estimated by dividing the discarded amplitudes by the total number of hole orbital pairs (in this case, there are ten hole orbitals, and thus one hundred hole orbital pairs). Therefore, from Fig. 7.11, at short bond distances as much as 50% of t2-amplitudes can be discarded, while at large bond distances around 12% of t2-amplitudes are discarded.

Clearly, switching off the perturbative correction and using a high threshold  $\eta = 0.1$  gives

the worst result: significant deviation and large fluctuation. Once we switch on the perturbative correction while maintaining the same  $\eta$ , we obtain great improvements. Similar things happen for  $\eta = 0.05$ . We also see that as  $\eta$  decreases by 0.1 to 0.05, the improvement from the perturbative correction is less prominent, which is as expected. At certain geometries, the curves for  $\eta = 0.1$  and  $\eta = 0.05$  overlap, because in those cases the same number of amplitudes are discarded. It is also clear from the figures that the most significant improvement when switching  $\eta$  from 0.1 to 0.05 (with or without the perturbative correction), happens at those geometries for which the change in  $\eta$  leads to a substantial decrease of the number of discarded t-amplitudes.

In practice, we have to choose a reasonable  $\eta$  to achieve both high accuracy and to avoid the convergence issue. For all the calculations in this chapter, we adopt  $\eta = 0.01$  and always switch on the perturbative correction.

## 7.4 Conclusions

We have presented a generalization of the Equation of Motion Coupled Cluster method to a state-specific multireference variant that is suitable for use with arbitrary active spaces. The methodology has a number of attractive features, but there are also a number of less desirable aspects. We will summarize these features here, and put our findings in a broader perspective.

As is common to all multireference approaches, the SS-EOMCC approach is built upon a qualitatively correct wave function, and the inclusion of the remaining electron correlation effects is a minor correction to the wave function, although the effect on the energy is certainly significant from a chemical perspective. The parameterization of the cluster operator in SS-EOMCC is such that the final wavefunction is spin-adapted, the results are invariant to rotations of the orbitals within the core, active and virtual subspaces, while the number of cluster amplitudes is the same as in a closed-shell calculation, in which all partially occupied orbitals in the reference state would be fully occupied. The amplitude equations for the t-amplitudes are connected, such that the only problem with extensivity can arise from the final diagonalization step. The amplitude equations only require the spatial one- and two-body density matrices corresponding to the reference state

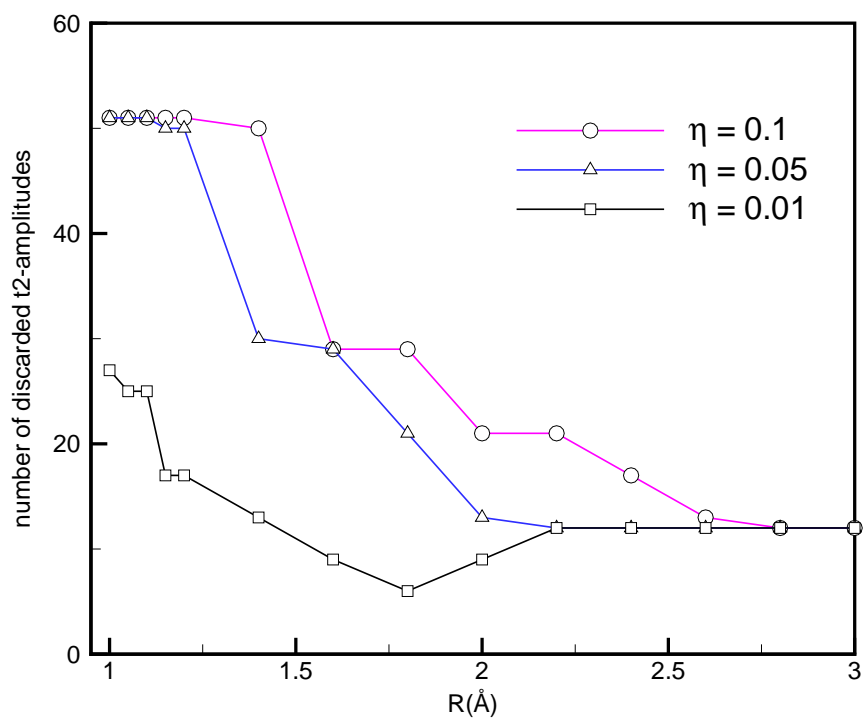


Figure 7.11: Test of the effect of perturbative correction for  $N_2$  in the cc-pVDZ basis set: discarded t2-amplitudes for different thresholds.

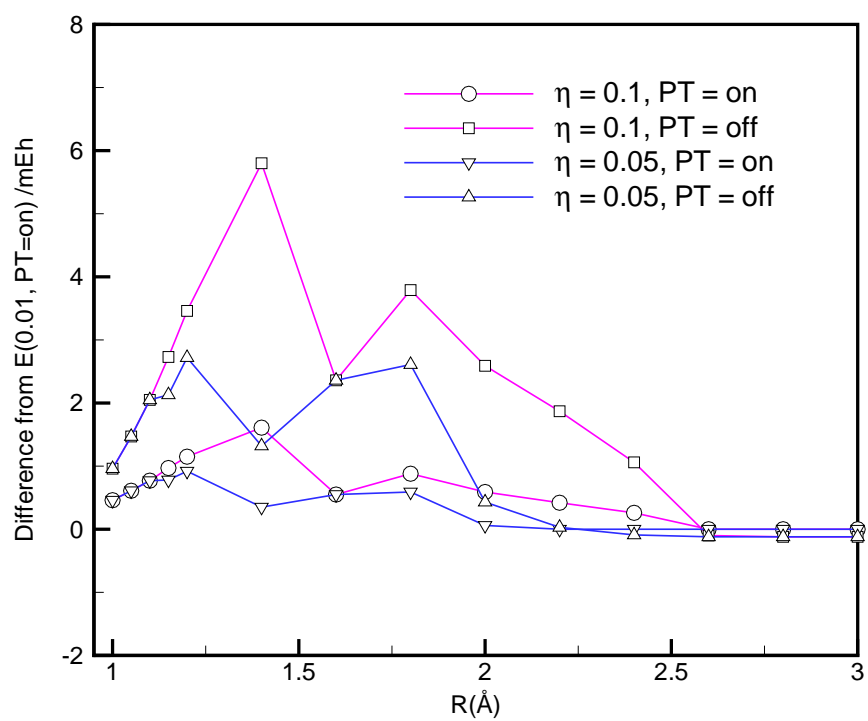


Figure 7.12: Test of the effect of perturbative correction for  $N_2$  in the cc-pVDZ basis set: deviations for different thresholds. ('PT' stands for 'perturbative correction').



(and Hamiltonian integrals of course), and the computational cost per iteration of the cluster amplitude equations is approximately three times the cost of a single reference closed-shell CCSD calculation. As in closed-shell CC theory, the amplitude equations are quadratic in  $\hat{T}_2$  and quartic in  $\hat{T}_1$ . The method can be used in both a state-selective mode, in which both the orbitals and cluster amplitudes are optimized precisely for the state of interest, or the method can be used in a state-averaged fashion, by using the density matrices from a state-averaged CASSCF calculation, for example. The approach is conceptually straightforward, and the potential exactness of the approach is guaranteed if no truncation would be made in the final diagonalization step. In this sense, the definition of the equations for the cluster amplitudes is arbitrary. Using the amplitude equations as presented here, the SS-EOM-CCSD approach is exact for two-electron systems provided Brueckner orbitals are used such that the singles amplitudes are zero, while still satisfying the singles residual equations.

Besides these considerable strong points of the approach, there are a number of drawbacks. While the cost of solving the cluster amplitudes is minor in the context of MRCC approaches, the final diagonalization over the MRCIS space is relatively expensive, in particular when three-body contributions from the transformed Hamiltonian are included. It is clear that the MRCIS step presents the bottleneck in the calculation, and this prevents the application of the method to systems that require large active spaces. In the present incarnation of the method, all doubly occupied orbitals also have to be included in the final diagonalization, but this we view as primarily a technical problem that will be addressed in the future. In common with other internally contracted exponential parameterizations, there is a severe issue with near-linear dependencies. In the calculations presented here, we discard perhaps up to 20% of the cluster amplitudes, even with the quite low threshold of 0.01 for the selection criterion we denoted as  $\eta$ . The number of discarded amplitudes depends on the character of the reference wavefunction and typically more amplitudes are discarded in the near single reference regime. This problem can partly be alleviated by providing a perturbative treatment for discarded amplitudes, as we have done in the standard applications in this chapter. From the test cases considered, this seems to work fairly well, but it is not unlikely that some of the non-parallelity errors we observed are due to this not

particularly elegant feature.

There are other aspects to the SS-EOMCC approach which are not entirely clear at present. The effect of using the cumulant approximation to the three and four-particle density matrices is unknown. To establish whether the effect from this approximation contributes significantly to the error one would need to compare to results in which the full three- and four-body density matrices are used in the amplitude equations. In addition, there is no coupling in the SS-EOMCC amplitude equations between the semi-internal excitations and the internally contracted double excitations. This is quite different from internally contracted MRCI, and also different from other internally contracted exponential parameterizations. While we have argued that the cluster amplitudes are to some extent arbitrary, they are undoubtedly critical to the accuracy of the approach when the final diagonalization is over the MRCIS space only, as is the case in practice. In practice, it would be desirable if accurate results could be obtained without including a connected triples correction. It is not clear (or perhaps doubtful) if this can be accomplished, in particular in cases when one needs to balance the results between single-reference and multireference types of situations. The present results indicate that an important fraction of correlation effects which can be associated with connected triple excitations are included in the MRCIS step. This is exemplified by calculations on the single reference case of the  ${}^3\Sigma_u^-$  state of the fluorine molecule, and it is also indicated by the relatively minor MAE and NPE errors for the other molecules, in particular when viewed from the perspective that the cluster amplitudes include singles and doubles only.

The SS-EOMCC approach can in principle be applied to a broad class of problems, and its application by users is expected to be about as difficult as the CASSCF calculation of the reference state. In particular, it is anticipated that the selection of the active space is comparable to the selection of a CASSCF active space, and this is a different problem from selecting an active space for a MRCI+Q, MR-AQCC or CASPT2 calculation, which often requires a larger active space than needed from the perspective of a qualitatively correct description of the wavefunction. For example, in MRCI the size of the active space may have to be increased to reduce size-extensivity effects or to include 'connected triple' effects, while in CASPT2 the active space might need to

be enlarged to account for deficiencies of the perturbative treatment. In SS-EOMCC and other exponential multireference approaches, the hope is that the powerful cluster ansatz will allow the use of a minimal active space that solely provides a qualitatively correct wavefunction.

In the benchmark calculations in this chapter, the methodology is applied to potential energy surfaces of relatively small molecules. When comparing to MRCI+Q calculations, the non-parallelity errors range between about 1 and 4  $mE_h$ , which is comparable to other exponential multireference approaches such as canonical transformation [79, 80], block correlated CC [92, 93] and the anti-Hermitian contracted Schrödinger equation methodology [81, 82]. However, these results are not as accurate as MR-AQCC [210, 211] or the MRexpT approaches [71, 72], or as internally contracted MRCI+Q itself [145, 146, 148, 80]. While we used these type of problems to benchmark the approach, the target application for the SS-EOMCC approach is not so much a potential energy surface of spectroscopic utility. Target problems for SS-EOMCC we have in mind are, for example, the calculation of energy differences between critical points on a potential energy surface such as activation barriers or isomerization energies for systems that require a multiconfigurational treatment, or the energetics or geometry of the lowest point on a conical intersection in a photochemical reaction. These kinds of target systems are similar to systems that are currently the focus of CASPT2 calculations, and in this respect the SS-EOMCC approach and other exponential multireference approaches likely represent a significant improvement in accuracy, as can be gauged from the NPE for CASPT2 for the problems considered here, which are considerably larger than for SS-EOMCC and strongly dependent on the basis set.

Considering the pros and cons of the SS-EOMCC approach, we think that further improvements are needed. Finding a better solution to the redundancy or near singularity problem is high on our list, while in the future we will also explore parameterizations in which semi-external excitations are treated in an internally contracted fashion, to avoid the MRCIS bottleneck in the calculations. It is likely that such modifications will build on the current design principles underlying the SS-EOMCC approach: diagonalization of a spin-free transformed Hamiltonian, a cumulant approximation for higher rank density matrices, EKT-based orbital denominators, and a suitable definition of the concept of normal order.

## Chapter 8

# Ligated $\text{Cu}_2\text{O}_2$ models

Many metalloenzymes have been characterized which contain one, two or more copper atoms which activate molecular oxygen to oxidize organic substrates [212, 213, 214, 215, 216, 217, 218, 219, 220, 221, 222, 223, 224, 225, 226, 227]. Hence, much interest has been attracted to molecules containing  $\text{Cu}_2\text{O}_2$  during the last decade [228, 229, 230, 231, 232, 233, 234]. For example, Tyrosinase [212, 215, 216, 218] is an enzyme whose active site incorporates a  $\text{Cu}_2\text{O}_2$  core. Spectroscopic and X-ray structure studies have characterized several motifs for the binding of molecular  $\text{O}_2$  to two supported Cu(I) atoms (Fig. 8.1) [222, 235]. With the coordination of different ligands, the competition between local bond strength and steric effect leads to different motifs adopted for different ligated compounds. Besides, the thermodynamically stable product could differ from the kinetically stable one. This further complicates the situation.

Studying model compounds containing a  $\text{Cu}_2\text{O}_2$  core can help to understand mechanisms of how more complicated molecules with the same core participate in fundamental processes. In general, however, it is not an easy task to theoretically study these transition metal compounds. To study reaction paths, a balanced treatment of (possibly rapidly) varying dynamical and nondynamical electron correlation effects has to be maintained. Systems with significant nondynamical correlation effects (multireference systems) have proven to be hard to deal with. Despite the widespread use of the DFT method for studying transition metal compounds, its applicability is

not well established and cases where it fails are not unusual. CR-CC [21, 22, 23, 236] has been successfully applied to many systems [237, 238, 239, 240, 24, 241, 242, 243, 244], but being essentially a single reference method, it is not transparent to what extent it can be used for multireference systems. Multireference Configuration Interaction (MRCI), Multireference Perturbation Theory (MRPT, especially CASPT2 [208, 209]) are well established *ab initio* methods. However, the linear ansatz of MRCI limits its ability to account for dynamical correlation effects (which leads to the size-consistency/extensivity error). Although CASPT2 has been applied to many transition metal compounds successfully, the selection of active space can be a subtle issue, and requires expertise. In addition, the convergence behavior of perturbation theory w.r.t. the perturbation order is generally unclear. Multireference Coupled Cluster (MRCC) [47, 55, 245, 38, 39] methods have been in development for many years, but at the same time they have been haunted by problems such as the intruder state problem and conflict between redundancy and flexibility.

Comparisons have been done before between completely renormalized coupled cluster (CR-CC), CASPT2 and DFT methods. DFT (whether pure or hybrid functional) results were irregular and no systematic behavior was observed, which illuminates its deficiency, at least in treating these systems. CASPT2 (and MSCASPT2) suffered from the convergence difficulty. A large active space of size up to (16,14) have been employed in CASPT2 calculations, but no convergence in relative energies was achieved with increasing active space size, and no systematic agreement with CR-CC was achieved. The complicated interaction between static and dynamical correlation seems to be the reason for the poor performance of CASPT2 (to be more specific, we had better talk about the interaction in the context of a particular set of orbitals). In contrast, in the SS-EOMCC[+2] theory, only a small reference space is used; that is, only one extra spatial orbital is added compared to the closed shell. The hypothesis is that the  $\hat{T}_2$  amplitudes will be small, while the additional relaxation of the reference state coefficients is presumably not so important. A big difference from CASPT2 is the use of Brueckner orbitals [159, 160, 161, 162, 163] in our theory. Brueckner orbitals are optimized in the presence of dynamical correlation, in contrast to, say, CASSCF orbitals.

In this work, the results for compound **0** and **1** are presented (Fig. 8.2) and compared with

those from previous work by Cramer and co-workers [233] (systems with more ligands are still computationally demanding for our current code). In addition to  $^1A_g$  state,  $^1B_g$  and  $^3B_g$  states are also computed, and the spin-flip idea is tested. Finally, conclusions are briefly given. <sup>1</sup>

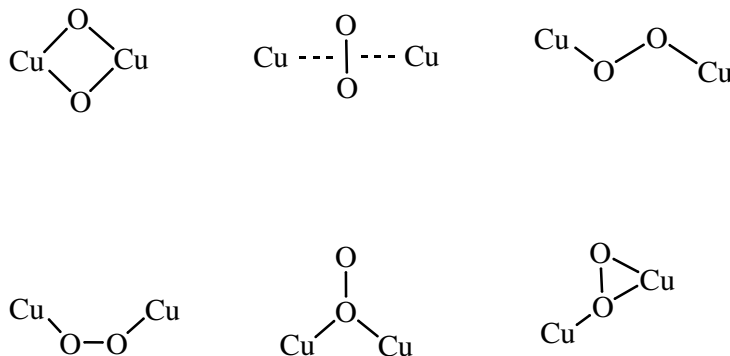
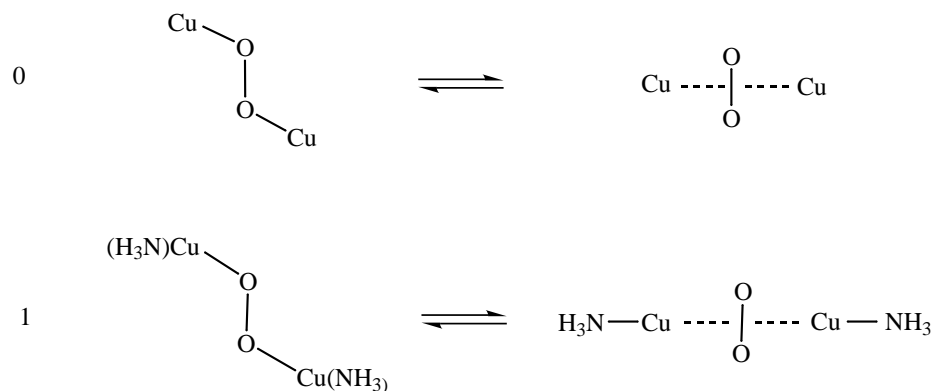
Figure 8.1: Binding motifs for  $\text{Cu}_2\text{O}_2$ .

Figure 8.2: Model compounds

## 8.1 Computational Details

Following Cramer and co-workers [233], the Stuttgart 10-electron pseudopotential and associated basis functions (ECP10MWB) [246, 247] are used for Cu atoms (the difference from the parameters

<sup>1</sup>Contents of this chapter were published in *Int. J. Quant. Chem.* **108**, 2097 (2008).

listed on the website is that: (a) in the pseudopotential, angular momentum up to f is used, (b) in the basis set, [12s12p9d] is contracted to [6s6p4d]). For light atoms, the Roos augmented triple zeta ANO basis set [248, 249] is used. A [8s4p|2s1p] contraction is used for H and a [14s9p4d|4s3p2d] contraction is used for N and O. As in the paper of Cramer and co-workers [233], this basis set was named ‘BS1’.

In all the calculations, Brueckner orbitals are used (except those using B-CI orbitals for comparison). N and O 1s orbitals and Cu orbitals up to 3p are kept frozen.

The geometries are taken from the paper of Cramer and co-workers [233]. To be clear, they are briefly restated below. The geometries of system **0** and **1** (including all intermediate geometries) belong to the  $C_{2h}$  point group. Intermediate geometries along linear isomerization paths are generated for **0** and **1** according to

$$q_i(F) = q_i(0) + \frac{F}{100} [q_i(100) - q_i(0)] \quad (8.1)$$

where  $q_i$  is a given atomic Cartesian coordinate and F is the fraction of progress along the isomerization coordinate so that 0 and 100 define the  $\mu$ -1:2 and  $\mu$ - $\eta^2$ : $\eta^2$  peroxo geometries, respectively (the less clear nomenclature ( $\mu$ - $\eta^1$ : $\eta^1$ ) was used in the original paper [233], but  $\mu$ -1:2 is more specific and has been used in later work [234]). Reference to a particular structure along an isomerization coordinate will henceforth be made by adding F as a subscript the structure cardinal, for example,  $\mathbf{1}_{20}$  refers to the structure 20% converted from  $\mathbf{1}_0$  to  $\mathbf{1}_{100}$ .

## 8.2 ${}^1A_g$ states of $\text{Cu}_2\text{O}_2^{2+}$ (**0**) and $\{(\text{H}_3\text{N})\text{Cu}\}_2\text{O}_2^{2+}$ (**1**).

The  ${}^1A_g$  state energies for structures of **0** as a function of F are presented in Table 8.1 and the relative energies in Table 8.2. Fig. 8.3 graphs the relative energy vs isomerization coordinates predicted by different theories. Note that SS-EOMCC[+2] gives results very close to those from CR-CC(2,3)+Q. In contrast, DFT curves have different shapes for different functionals and CASPT2 is comparatively far above CR-CC curve (underestimate the stability of  $\mu$ -1:2 and MSCASPT overestimates). But all theories predict that  $\mu(1:2)$  is more stable than  $\mu$ - $\eta^2$ : $\eta^2$ .

The  $^1A_g$  state energies for structures of **1** as a function of F are presented in Table 8.3 and the relative energies in Table 8.4. Fig. 8.4 graphs the relative energy vs isomerization coordinates predicted by different theories. SS-EOMCC[+2] gives results relatively close to those from CR-CC(2,3)+Q. In contrast, DFT predicts reverse relative stability and CASPT2 does not achieve converged results.

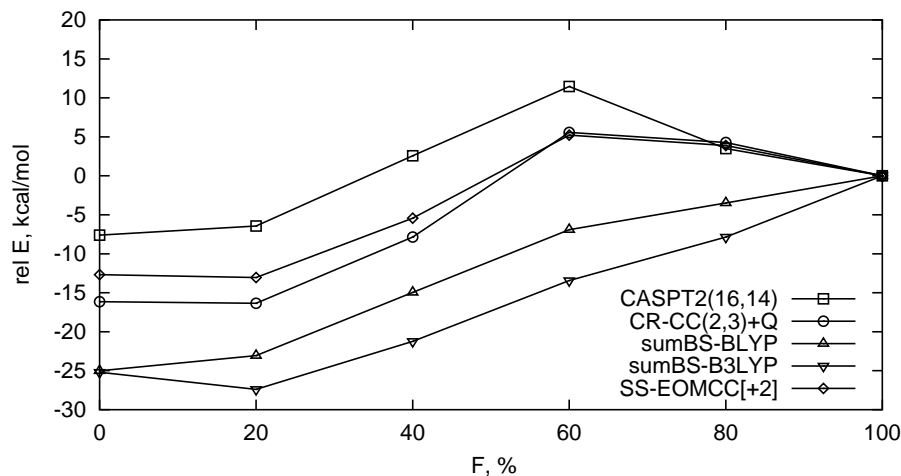


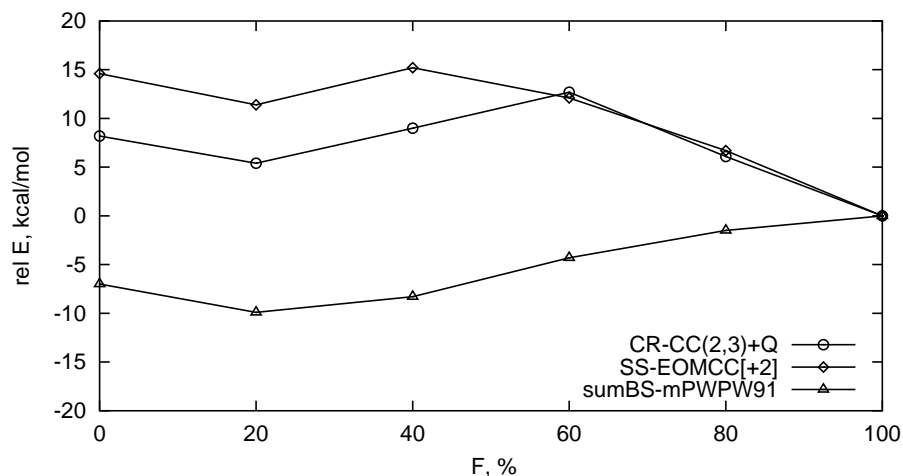
Figure 8.3:  $^1A_g$  state relative energy vs F for **0** at selected levels of theory (legend inset).

Table 8.1: Absolute energy (Hartree) of  $\mathbf{0}_F$  structures with BS1

F		0	20	40	60	80	100
CR-CC(2, 3)+Q	$^1A_g$	-542.16894	-542.16927	-542.15572	-542.13434	-542.13641	-542.14321
SS-EOMCC[+2]	$^1A_g$	-542.12661	-542.12720	-542.11506	-542.09807	-542.10021	-542.10641
mrSF-EOMCC[+2]	$^1A_g$	-542.12576	-542.12700	-542.11431	-542.09766	-542.09793	-542.10954
SS-EOMCC[+2](B-CI)	$^1A_g$	-542.14146	-542.14213	-542.13029	-542.10931	-542.10785	-542.10932
SS-EOMCC[+2]	$^3B_g$	-542.14954	-542.15348	-542.14454	-542.13294	-542.12305	-542.10745
SS-EOMCC[+2]	$^1B_g$	-542.12180	-542.12411	-542.11547	-542.10619	-542.10158	-542.09094
mrSF-EOMCC[+2]	$^1B_g$	-542.12137	-542.12313	-542.11447	-542.10578	-542.10164	-542.09322
CASPT2(16, 14)	$^1A_g$	-542.40875	-542.40688	-542.39254	-542.37837	-542.39108	-542.39664
MSCASPT2(16, 14)	$^1A_g$	-542.43252	-542.42741	-542.41094	-542.39047	-542.39674	-542.39670
SumBS-BLYP	$^1A_g$	-544.25169	-544.24859	-544.23566	-544.22283	-544.21738	-544.21183
SumBS-B3LYP	$^1A_g$	-544.31860	-544.32209	-544.31227	-544.29986	-544.29095	-544.27844
SumBS-TPSS	$^1A_g$	-544.20265	-544.20137	-544.19021	-544.17973	-544.17621	-544.17232

DFT and CR-CC data are from [233].



Figure 8.4:  $^1A_g$  state relative energy vs F for **1** at select levels of theory (legend inset).Table 8.2:  $^1A_g$  state relative energy ( $\text{kcal}\cdot\text{mol}^{-1}$ ) of  $\mathbf{0}_F$  structures with BS1

F	0	20	40	60	80	100
CR-CC(2, 3)+Q	-16.1	-16.4	-7.8	5.6	4.3	0.0
SS-EOMCC[+2]	-12.7	-13.0	-5.4	5.2	3.9	0.0
mrSF-EOMCC[+2]	-10.2	-11.0	-3.0	7.5	27.0	0.0
SS-EOMCC[+2](B-CI)	-20.2	-20.6	-13.2	0.01	0.9	0.0
CASPT2(16, 14)	-7.69	-6.4	2.6	11.5	3.5	0.0
MSCASPT2(16, 14)	-22.5	-19.3	-8.9	3.9	-0.0	0.0
sumBS-BLYP	-25.0	-23.1	-15.0	-6.9	-3.5	0.0
sumBS-B3LYP	-25.2	-27.4	-21.2	-13.4	-7.8	0.0
sumBS-TPSS	-19.0	-18.2	-11.2	-4.6	-2.4	0.0

DFT and CR-CC data are from [233].

Table 8.3: Absolute energy (Hartree) of  $\mathbf{1}_F$  structures with BS1

F		0	20	40	60	80	100
CR-CC(2, 3)+Q	$^1A_g$	-655.26877	-655.27321	-655.26739	-655.26154	-655.27203	-655.28178
SS-EOMCC[+2]	$^1A_g$	-655.20731	-655.21248	-655.20631	-655.21126	-655.21992	-655.23057
mrSF-EOMCC[+2]	$^1A_g$	-655.20507	-655.21068	-655.20675	-655.20801	-655.21930	-655.23408
SS-EOMCC[+2]	$^3B_g$	-655.22331	-655.23005	-655.23099	-655.22739	-655.22237	-655.21537
SS-EOMCC[+2]	$^1B_g$	-655.20798	-655.21676	-655.21835	-655.21489	-655.20981	-655.20459
mrSF-EOMCC[+2]	$^1B_g$	-655.20510	-655.21561	-655.21796	-655.21465	-655.21003	-655.20515
sumBS-BLYP	$^1A_g$	-657.60831	-657.61162	-657.60773	-657.60024	-657.59473	-657.59109
sumBS-B3LYP	$^1A_g$	-657.71802	-657.72257	-657.72018	-657.71384	-657.70826	-657.70433
sumBS-mPWPW91	$^1A_g$	-657.89622	-657.90084	-657.89821	-657.89187	-657.88738	-657.88501
sumBS-TPSS	$^1A_g$	-657.60969	-657.61430	-657.61220	-657.60684	-657.60375	-657.60297

DFT and CR-CC data are from [233].

Table 8.4:  ${}^1A_g$  state relative energy ( $\text{kcal}\cdot\text{mol}^{-1}$ ) of  $\mathbf{1}_F$  structures with BS1

F	0	20	40	60	80	100
CR-CC(2, 3)+Q	8.2	5.4	9.0	12.7	6.1	0.0
SS-EOMCC[+2]	14.6	11.4	15.2	12.1	6.7	0.0
mrSF-EOMCC[+2]	18.2	14.7	17.1	16.4	9.3	0.0
sumBS-BLYP	-10.8	-12.9	-10.4	-5.7	-2.3	0.0
sumBS-B3LYP	-8.6	-11.4	-10.0	-6.0	-2.5	0.0
sumBS-mPWPW91	-7.0	-9.9	-8.3	-4.3	-1.5	0.0
sumBS-TPSS	-4.2	-7.1	-5.8	-2.4	-0.5	0.0

DFT and CR-CC data are from [233].

### 8.3 Effect of Brueckner orbitals.

In the wave operator,  $e^{\hat{T}_2}$  takes into account dynamical correlation effects and  $e^{\hat{T}_1}$  takes into account orbital relaxation effects. At the end of the Brueckner rotation,  $\hat{T}_1 = 0$ . Due to the presence of  $\hat{T}_2$ , the dynamical correlation is felt by the orbital rotation. In this sense, Brueckner orbitals are optimized in the presence of dynamical correlation. To test the effect of Brueckner orbitals, we optimize orbitals in a different way: switch off dynamical correlation ( $\hat{T}_2 = 0$ ) and rotate orbitals until  $\hat{T}_1 = 0$ . Orbitals optimized this ways are termed B-CI orbitals [205]. Then we use these orbitals to carry out SS-EOMCC[+2] calculations. In other words, with the definition of the vacuum described in this chapter, the B-CI orbital optimization works precisely as follows: diagonalize  $H$  in 2-hole plus 3-hole-1-particle sector of the Fock space to obtain  $\hat{C}|0\rangle$ , take the 2-hole component of  $\hat{C}|0\rangle$  as  $|R\rangle$  and substitute into  $\hat{T}_1$  amplitude equations and then use  $\hat{T}_1$  amplitudes to rotate orbitals. The procedure is carried out self-consistently until finally  $t_a^i = 0$ . Dynamical correlation is not present in this optimization process. The results are presented in Table 8.1 and Fig. 8.5 and denoted by SS-EOMCC[+2] (B-CI) [205].

From Fig. 8.5, with every set of data calibrated to  $F = 100$ , Brueckner orbital calculations outperform B-CI orbital ones, especially for  $F = 80$  and  $F = 60$ , based on comparison with CR-CC results. On the other hand, results from the B-CI orbitals are still reasonable. Notice that in obtaining the B-CI orbitals the diagonalization is done over the MRCIS space, and this distinguishes this set of orbitals from the CASSCF orbitals. Relative to the CAS space (here more precisely, the 2-hole sector of Fock space), the inclusion of the extra singles space passes more

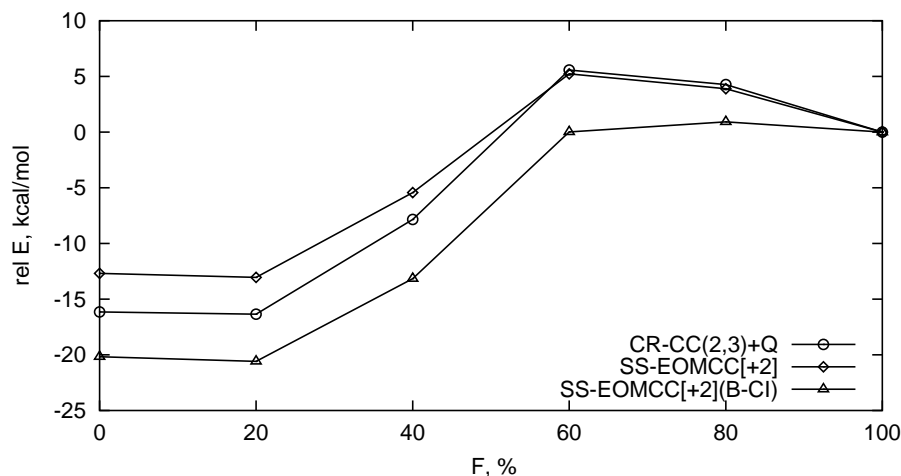


Figure 8.5:  ${}^1A_g$  state relative energy vs F for  $\mathbf{0}$  from SS-EOMCC[+2] calculated with Brueckner orbitals and CAS orbitals, respectively (legend inset).

information to the orbital optimization process and reinforces the state-specificity. In the study of the LiF molecule [205], the CASSCF orbital optimization was plagued with the root-flipping problem while the B-CI orbital optimization did not experience the convergence problem. As is pointed out in Ref. [205], it is likely that the B-CI states (the states obtained when B-CI orbital optimization is finished and they contain contributions from singles space) are not very different from the CASSCF states (no singles space contribution), and they might even serve as a starting point to optimize the true CASSCF states, if so desired. The B-CI procedure might be of value in other procedures that require a CASSCF solution without resorting to a state-averaged procedure.

## 8.4 Convergence of EOMCC[+2] w.r.t. reference space

The question concerning the quality of the data from EOMCC[+2] is how well these calculations converge with respect to the reference space. A convincing answer could be obtained if we do the same type of calculations using a larger reference space (EOMCC[+n],  $n > 2$ ). An indirect way is examining the  $t$  amplitudes. As in single reference coupled cluster calculations, say CCSD, if all  $t_2$  amplitudes are small, the calculation is very likely converged w.r.t. excitation level. For

our MRCC method, the hope is that the reference space is able to cover static correlation effects and the exponential operator takes care of dynamic correlation (and therefore  $t$ -amplitudes are small). Thus, if the final  $t$ -amplitudes are small, we can reasonably believe that the calculation is converged w.r.t. the reference space. That is what we observed in our calculations (whether for  $\mathbf{0}$  or  $\mathbf{1}$ , only a few excitation amplitudes are over 0.02, and they are all smaller than 0.03).

## 8.5 Neighboring states

Previous studies focused on the  $^1A_g$  state of model compounds with various ligands. There is, however, no good reason to exclude the possibility of ground states of different spin or spatial symmetries. Even if the ground state is indeed a  $^1A_g$  state, examining neighboring states (if there are closely-lying states) will no doubt help to gain insight into the complexity of the systems under study.

SS-EOMCC is a general theory and states of different spatial or spin symmetries can be computed without difficulty. In Table 8.1,  $^1B_g$  and  $^3B_g$  state energies for  $\mathbf{0}$  are presented and graphed in Fig. 8.6.  $^1B_g$  and  $^3B_g$  state energies for  $\mathbf{1}$  are included in Table 8.3 and graphed in Fig. 8.7 (all the compounds studied here belong to the  $C_{2h}$  point group).

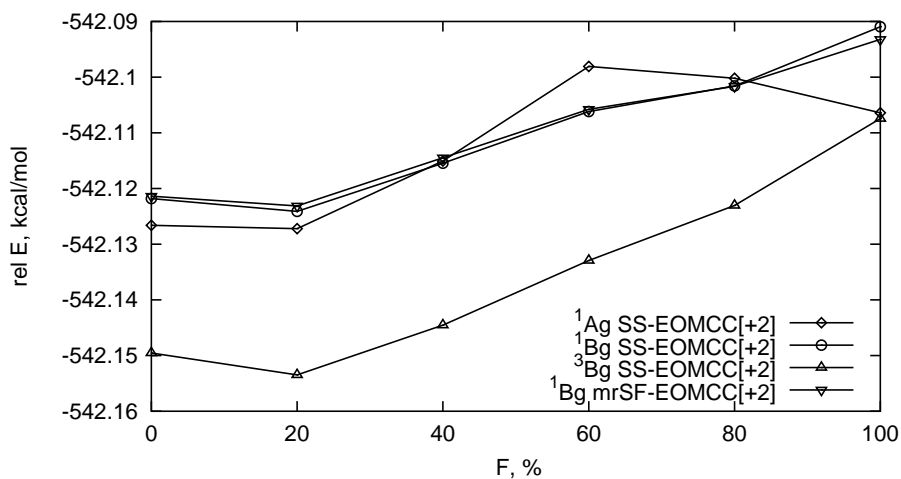
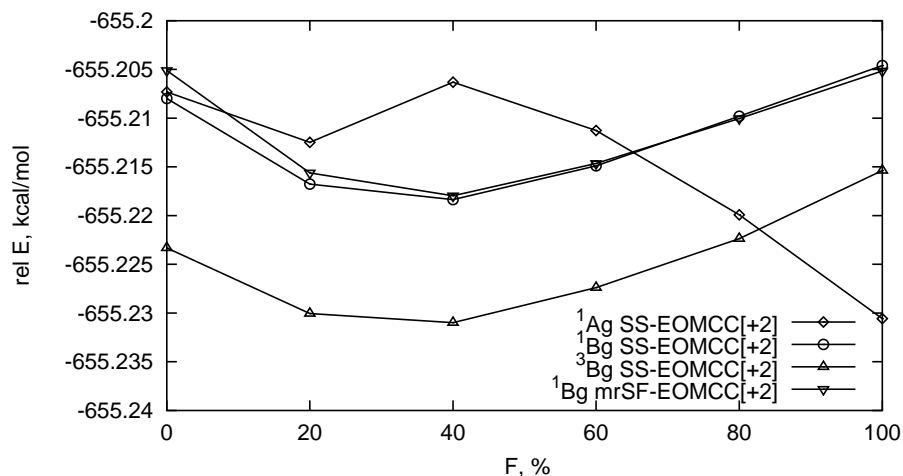


Figure 8.6: Absolute energy vs F for different states of  $\mathbf{0}$ .

Figure 8.7: Absolute energy vs F for different states of **1**.

Although **0** and **1** are structurally simple compared to large model compounds with more ligands or compounds which actually function in biochemical processes, the calculations on them already reveal the complexity of the real world. For **0**, the SS-EOMCC[+2] calculation shows that the triplet state ( $^3B_g$ ) is more stable than the  $^1A_g$  state (nearly degenerate for  $\mathbf{0}_{100}$ ), though for both states  $\mathbf{0}_0$  is more stable than  $\mathbf{0}_{100}$ . Suppose somehow only singlet states can be accessed, the close lying  $^1B_g$  state would still complicate the situation. From Fig. 8.6, at some intermediate geometries it is lower in energy than the  $^1A_g$  state, while at the initial and final geometries it is higher than the  $^1A_g$  state. Besides, the  $^1B_g$  calculations also suggest that  $\mathbf{0}_0$  is more stable than  $\mathbf{0}_{100}$ .

For **1**, SS-EOMCC[+2] calculations show that the  $^3B_g$  state is more stable than the  $^1A_g$  state except at  $\mathbf{1}_{100}$ . As far as singlet states are concerned, the  $^1B_g$  state is lower in energy than  $^1A_g$  for  $\mathbf{1}_{20}$ ,  $\mathbf{1}_{40}$  and  $\mathbf{1}_{60}$ , higher in energy for  $\mathbf{1}_{80}$  and  $\mathbf{1}_{100}$ , and nearly degenerate for  $\mathbf{1}_0$ .

For both **0** and **1**, since the  $^1B_g$  and  $^1A_g$  states are so close, further studies would be desirable to investigate the potential energy surfaces for lower symmetry where both states have the same symmetry.

Since the triplet states are supposed to be reasonably single-determinantal, DFT and single reference coupled cluster method may work well in that situation. The comparison between

DFT [233], Brueckner Coupled Cluster Doubles (BCCD), Brueckner Coupled Cluster Doubles with noniterative triples correction (BCCD(T)) and SS-EOMCC[+2] for  ${}^3B_g$  states of **0** and **1** is done. The single reference coupled cluster calculations are done using the Gaussian 03 quantum chemistry program [250] and the Brueckner orbitals are used to provide a better comparison with our multireference Brueckner orbital calculations. The results are shown in Table 8.5 and graphed in Fig. 8.8 and 8.9 (for clarity, only B3LYP and TPSS functional result is graphed). From the graphs, the difference between BCCD and BCCD(T) is noticeable. All functionals, BCCD, BCCD(T) and SS-EOMCC[+2] predict that  $F = 0$  is more stable than  $F = 100$  for both **0** and **1**, but for different functionals [233], the relative stability spans a range of about  $6 \text{ kcal} \cdot \text{mol}^{-1}$ . In addition, the shapes of the curves are functional-dependent. For **0**, the SS-EOMCC[+2] curve agrees with B3LYP and BCCD(T) very well (maximal difference less than  $1.1 \text{ kcal} \cdot \text{mol}^{-1}$ ). For **1**, DFT methods predict a higher stability of  $\mathbf{1}_0$  relative to  $\mathbf{1}_{100}$  than SS-EOMCC[+2], BCCD and BCCD(T). SS-EOMCC[+2] curve again agrees with BCCD(T) very well, compared with DFT results. The discrepancy between BCCD and BCCD(T) and the close agreement between SS-EOMCC[+2] and BCCD(T) seem to indicate that the triplet state of **1** has a multi-configuration character.

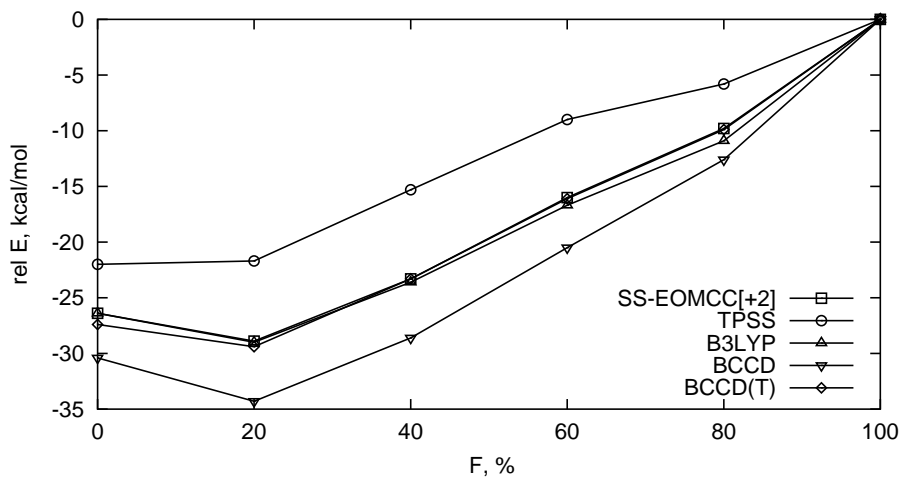
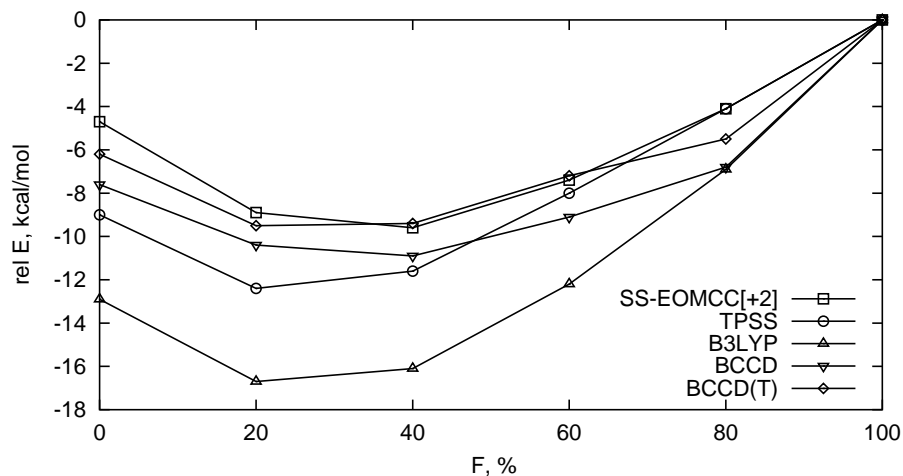


Figure 8.8: Relative energy vs F for  ${}^3B_g$  state of **0**.

Figure 8.9: Relative energy vs F for  ${}^3B_g$  state of **1**.Table 8.5:  ${}^3B_g$  state relative energy (Hartree) of  $\mathbf{0}_F$  and  $\mathbf{1}_F$  structures with BS1

F	molecule	0	20	40	60	80	100
SS-EOMCC[+2]	<b>0</b>	-26.4	-28.9	-23.3	-16.0	-9.8	0.0
BCCD	<b>0</b>	-30.4	-34.3	-28.6	-20.5	-12.6	0.0
BCCD(T)	<b>0</b>	-27.4	-29.4	-23.3	-16.1	-9.9	0.0
bs-BLYP	<b>0</b>	-27.5	-26.0	-18.6	-11.1	-6.7	0.0
bs-B3LYP	<b>0</b>	-26.4	-29.0	-23.6	-16.7	-10.9	0.0
bs-mPWPW91	<b>0</b>	-24.8	-24.7	-18.2	-11.2	-7.0	0.0
bs-mPW1PW91	<b>0</b>	-24.7	-29.3	-24.8	-18.2	-12.1	0.0
bs-MPW1K	<b>0</b>	-26.7	-34.3	-30.6	-23.3	-15.3	0.0
bs-TPSS	<b>0</b>	-22.0	-21.7	-15.3	-9.0	-5.8	0.0
bs-TPSSh	<b>0</b>	-22.0	-23.7	-18.2	-12.1	-8.1	0.0
SS-EOMCC[+2]	<b>1</b>	-4.7	-8.9	-9.6	-7.4	-4.1	0.0
BCCD	<b>1</b>	-7.6	-10.4	-10.9	-9.1	-6.8	0.0
BCCD(T)	<b>1</b>	-6.2	-9.5	-9.4	-7.2	-5.5	0.0
bs-BLYP	<b>1</b>	-15.0	-17.5	-15.7	-11.1	-5.8	0.0
bs-B3LYP	<b>1</b>	-12.9	-16.7	-16.1	-12.2	-6.9	0.0
bs-mPWPW91	<b>1</b>	-11.2	-14.5	-13.5	-9.5	-5.0	0.0
bs-mPW1PW91	<b>1</b>	-10.0	-14.5	-14.5	-11.3	-6.5	0.0
bs-MPW1K	<b>1</b>	-8.8	-13.8	-14.6	-11.9	-7.1	0.0
bs-TPSS	<b>1</b>	-9.0	-12.4	-11.6	-8.0	-4.1	0.0
bs-TPSSh	<b>1</b>	-8.9	-12.8	-12.4	-9.1	-5.0	0.0

DFT data are from [233].

## 8.6 mrSF-EOMCC.

One feature of the SS-EOMCC method is that it is state-specific, but we can modify it to make a multireference spin-flip EOMCC method (mrSF-EOMCC). However, our mrSF-EOMCC is rigorously spin-adapted because the excitation operator, the Hamiltonian and the transformed Hamiltonian are all singlet operators.

For **0**, the  $^1B_g$  state is closely related to the  $^3B_g$  state from symmetry consideration. To test the spin-flip idea,  $\hat{T}$  amplitudes from  $^3B_g$  state calculations are used to calculate the  $^1B_g$  state. Results are presented in Table 8.1 and Fig. 8.6 (where they are identified as mrSF-EOMCC[+2]). These two  $B_g$  states are expected to have similar dynamical correlation effects, which is confirmed by the close agreement between the two sets of calculations for  $^1B_g$  state (Fig. 8.6). This also partially justifies the quality of the calculations.  $^3B_g \rightarrow ^1A_g$  spin-flip calculation also gives reasonable results (see Tables 8.1 and 8.2).

For **1**, reasonable agreement is achieved for both  $^3B_g \rightarrow ^1B_g$  and  $^3B_g \rightarrow ^1A_g$  spin-flip calculations (see Tables 8.3-8.4 and Fig. 8.7).

## 8.7 Conclusions

The relative energetics of  $\mu$ -1:2 (trans end-on) and  $\mu$ - $\eta^2$ : $\eta^2$  (side-on) peroxo isomers of  $\text{Cu}_2\text{O}_2$  fragments supported by 0 and 2 ammonia ligands are computed with the newly developed State Specific Equation of Motion Coupled Cluster (SS-EOMCC) method. A small reference space is used (SS-EOMCC[+2]) and reasonable agreement is achieved between SS-EOMCC and CR-CC results. Calculations on states other than  $^1A_g$  states reveals a complication of this class of systems. In addition to the multireference character of the systems, close lying states (near degeneracy) and state-crossing pose a great challenge to quantum chemistry methods.

The spin-flip idea can be included in the framework of the SS-EOMCC method naturally, and it is rigorously spin-adapted due to the use of spin free operators and a complete reference space. Brueckner orbitals can be regarded as orbitals optimized in the presence of dynamical correlation. The results presented here indicate the superiority of Brueckner orbitals over B-



CI orbitals, which are close to CASSCF orbitals. On the other hand, the B-CI procedure may be helpful to converge CASSCF calculations. However, in other test calculations, we did not observe a universal overperformance of Brueckner orbitals over CASSCF orbitals, so it is not completely clear yet what type of orbitals are the best. It is possible that Brueckner orbitals are advantageous when calculating transition metals compounds, which are probably more sensitive to orbital choices.

## Chapter 9

# Beyond SS-EOMCC: more cost-effective solutions

The SS-EOMCC method involves the diagonalization of the transformed Hamiltonian  $\hat{H}$  in the MRCIS space. This step is potentially very expensive, even if we approximate  $\hat{H}$  by its one- and two-body components. If the dimension of the active space is  $M$ , the number of hole orbitals is  $o$ , and the number of virtual orbitals is  $v$ , then the dimension of the MRCIS space is roughly  $o \times v \times M$ . To reduce the computational cost, it is desirable to have a method, in which the final diagonalization is confined to the active space only.

The purpose of diagonalizing  $\hat{H}$  in the MRCIS space instead of in the active space is to take into account the differential orbital relaxation effects and semi-internal excitations. These effects are missing in  $\hat{T}$ . In contrast to the expensive diagonalization, a more economic way is to include in the cluster operator a semi-internal operator  $\hat{T}_{\text{semi-int}}$  to partially include these effects. By including  $\hat{T}_{\text{semi-int}}$ , we can confine the diagonalization within the active space, hopefully without losing much accuracy. This idea is the topic of this chapter, and work in this direction is in progress.

The other problem with SS-EOMCC is that core orbitals need to be included the diagonalization space, due to the lack of the core-active excitation operator in  $\hat{T}$ . In future we would like to

address this issue too.

## 9.1 Internally contracted multireference coupled cluster method (ic-MRCC): ansatz

As the first step of our endeavor to develop an MRCC method, in SS-EOMCC, the semi-internal and core-active excitations are excluded from  $\hat{T}$  to avoid complicated algebra and achieve a clean formulation. In SS-EOMCC,  $\hat{T}_1$  and  $\hat{T}_2$  commute and the transformed Hamiltonian  $\hat{\hat{H}} = e^{-\hat{T}} \hat{H} e^{\hat{T}}$  terminates automatically after the fourth order in the Baker-Campbell-Hausdorff expansion. In comparison, if  $\hat{T}_{\text{semi-int}}$  is included in  $\hat{T}$ ,  $\hat{\hat{H}}$  may not terminate after a finite expansion due to the contractions between the  $\hat{T}_{\text{semi-int}}$  and  $\hat{T}_1 + \hat{T}_2$ . Therefore, the corresponding residual equation becomes more complicated.

To avoid the complication, we propose to use the normal order exponential ansatz:

$$|\Psi\rangle = \{e^{\hat{S}}\}|R\rangle, \quad (9.1)$$

where we use  $\hat{S}$  instead of  $\hat{T}$  to distinguish it from the cluster operator in SS-EOMCC. Compared to  $e^{\hat{S}}$ , the contractions between  $\hat{S}$  operators are eliminated in the normal order exponential  $\{e^{\hat{S}}\}$ . Currently, the only semi-internal excitation operator included is  $\hat{E}_{ij}^{am}$ , where  $a$  is a virtual orbital index,  $m$  is an active orbital index,  $i$  and  $j$  are two occupied/hole orbital indices, active or core. Therefore, we may write the cluster operator as:

$$\hat{S} = \sum_{i,a} t_a^i \hat{E}_i^a + \frac{1}{2} \sum_{i,j,a,b} t_{ab}^{ij} \hat{E}_{ij}^{ab} + \sum_{i,j,a,m} s_{am}^{ij} \hat{E}_{ij}^{am}. \quad (9.2)$$

In the implementation we have used both  $h$ -normal order and  $\gamma$ -normal order. Since  $h$ -normal order can be viewed as a special case of  $\gamma$ -normal order, here we only discuss  $\gamma$ -normal order in the formal development. All the equations corresponding to  $h$ -normal order can be obtained by replacing the spatial density matrix  $\Gamma_j^i$  by  $2\delta_j^i$ .

We rewrite the cluster operator in  $\gamma$ -normal order:

$$\hat{S} = \sum_{i,a} t_a^i \hat{E}_i^a + \frac{1}{2} \sum_{i,j,a,b} t_{ab}^{ij} \hat{E}_{ij}^{ab} + \sum_{i,j,a,m} s_{am}^{ij} \hat{E}_{ij}^{am} \quad (9.3)$$

$$= \sum_{i,a} t_a^i \tilde{E}_i^a + \frac{1}{2} \sum_{i,j,a,b} t_{ab}^{ij} \tilde{E}_{ij}^{ab} + \sum_{i,j,a,m} s_{am}^{ij} (\tilde{E}_{ij}^{am} + \Gamma_j^m E_i^a - \frac{1}{2} \Gamma_i^m E_j^a) \quad (9.4)$$

$$= \sum_{i,a} (t_a^i + \sum_{m,j} (s_{am}^{ij} - \frac{1}{2} s_{am}^{ji}) \Gamma_j^m) \tilde{E}_i^a + \frac{1}{2} \sum_{i,j,a,b} t_{ab}^{ij} \tilde{E}_{ij}^{ab} + \sum_{i,j,a,m} s_{am}^{ij} \tilde{E}_{ij}^{am}, \quad (9.5)$$

because

$$\hat{E}_i^a = \tilde{E}_i^a, \quad (9.6)$$

$$\hat{E}_{ij}^{ab} = \tilde{E}_{ij}^{ab}, \quad (9.7)$$

$$\hat{E}_{ij}^{am} = \tilde{E}_{ij}^{am} + \Gamma_j^m \tilde{E}_i^a - \frac{1}{2} \Gamma_i^m \tilde{E}_j^a. \quad (9.8)$$

Therefore, instead of parameterizing  $\hat{S}$  as in Eq. 9.2, we can parameterize it in  $\gamma$ -normal order:

$$\hat{S} = \sum_{i,a} t_a^i \tilde{E}_i^a + \frac{1}{2} \sum_{i,j,a,b} t_{ab}^{ij} \tilde{E}_{ij}^{ab} + \sum_{i,j,a,m} s_{am}^{ij} \tilde{E}_{ij}^{am}. \quad (9.9)$$

(9.2) and (9.9) just correspond to a definition of coefficients. We prefer to use (9.9), because  $\gamma$ -normal order facilitates a natural way to approximate the residual equation, as shown in Eq. (5.65) - (5.66).

Therefore, the ansatz for the wavefunction in our ic-MRCC method is:

$$|\Psi\rangle = \{e^{\hat{S}}\}|R\rangle, \quad (9.10)$$

$$\hat{S} = \sum_{i,a} t_a^i \tilde{E}_i^a + \frac{1}{2} \sum_{i,j,a,b} t_{ab}^{ij} \tilde{E}_{ij}^{ab} + \sum_{i,j,a,m} s_{am}^{ij} \tilde{E}_{ij}^{am}. \quad (9.11)$$

## 9.2 ic-MRCC: residual equation

Substituting the above ansatz in the Schrödinger equation gives:

$$\hat{H}\{e^{\hat{S}}\}|R\rangle = E\{e^{\hat{S}}\}|R\rangle, \quad (9.12)$$

$$\{e^{\hat{S}}\}^{-1}\hat{H}\{e^{\hat{S}}\}|R\rangle = E|R\rangle, \quad (9.13)$$

$$\langle R|\hat{\tau}_\lambda^+\{e^{\hat{S}}\}^{-1}\hat{H}\{e^{\hat{S}}\}|R\rangle = E\langle R|\hat{\tau}_\lambda^+|R\rangle = 0, \quad (9.14)$$

where  $\hat{\tau}_\lambda \in \{\tilde{E}_i^a, \tilde{E}_{ij}^{ab}, \tilde{E}_{ij}^{am}, \forall i, j, a, m\}$ . If we define

$$\hat{G} = \{e^{\hat{S}}\}^{-1}\hat{H}\{e^{\hat{S}}\}, \quad (9.15)$$

the above equations become:

$$\hat{G}|R\rangle = E|R\rangle, \quad (9.16)$$

$$\langle R|\hat{\tau}_\lambda^+\hat{G}|R\rangle = 0. \quad (9.17)$$

Therefore, if we can solve for  $\hat{G}$ , then we can diagonalize it in the multireference space (including all hole orbitals) and get the energy  $E$ .

Now let us see how to obtain the residual equation. As shown in Eq. (5.65)-(5.66), if we know  $\hat{G}$  in  $\gamma$ -normal order, we can expand  $\hat{\tau}_\lambda^+\hat{G}$ :

$$\hat{\tau}_\lambda^+\hat{G} = c_0 + c_1 \times \tilde{a}_1 + c_2 \times \tilde{a}_2 + c_3 \times \tilde{a}_3 + \dots, \quad (9.18)$$

$$\langle R|\hat{\tau}_\lambda^+\hat{G}|R\rangle = \langle R|c_0 + c_1 \times \tilde{a}_1 + c_2 \times \tilde{a}_2 + c_3 \times \tilde{a}_3 + \dots|R\rangle \quad (9.19)$$

$$= c_0 + c_1\langle R|\tilde{a}_1|R\rangle + c_2\langle R|\tilde{a}_2|R\rangle + c_3\langle R|\tilde{a}_3|R\rangle + \dots \quad (9.20)$$

$$= c_0 + c_1\zeta_1 + c_2\zeta_2 + c_3\zeta_3 + \dots \quad (9.21)$$

$$= c_0 + c_2\zeta_2 + c_3\zeta_3 + \dots \quad (9.22)$$

By truncating the terms in  $\hat{T}_\lambda^+\hat{G}$  at some level, we obtain an approximation to the residual

equation.

Now let us see how to evaluate  $\hat{G}$ . Following the arguments in Ref. [51], we get the following expression for  $\hat{G}$ :

$$\hat{G} = (\hat{H}\{e^{\hat{S}}\})_c - ((\{e^{\hat{S}}\} - 1)\hat{G})_c. \quad (9.23)$$

This expression suggest a backward substitution procedure to obtain the components of  $\hat{G}$  step by step, as demonstrated in Ref. [51]. We approximate  $\hat{G}$  by its one- and two-body components. In addition, when evaluating  $((\{e^{\hat{S}}\} - 1)\hat{G})_c$ , for simplicity we only use  $\hat{G}_{hole}$ , where  $\hat{G}_{hole}$  includes up to two-body components of  $\hat{G}$  with only hole labels:

$$\hat{G}_{hole} = g_0 + g_j^i \tilde{E}_i^j + \frac{1}{2} g_{ij}^{kl} \tilde{E}_{kl}^{ij}. \quad (9.24)$$

Therefore,

$$\hat{G} \approx (\hat{H}\{e^{\hat{S}}\})_c - ((\{e^{\hat{S}}\} - 1)\hat{G}_{hole})_c. \quad (9.25)$$

Now let us see how to evaluate  $\hat{G}_{hole}$ . The normal order expansion of  $((\{e^{\hat{S}}\} - 1)\hat{G})_c$  must contain at least one particle creation operator, since every operator in  $\hat{S}$  contains at least one particle creation operator, which cannot be contracted to any operator index from a term on its right. Therefore  $((\{e^{\hat{S}}\} - 1)\hat{G})_c$  will not contribute to the components of  $\hat{G}_{hole}$ , and thus we can determine  $g_0, g_j^i$  and  $g_{ij}^{kl}$  from the expansion of  $(\hat{H}\{e^{\hat{S}}\})_c$ . That is, if we expand  $(\hat{H}\{e^{\hat{S}}\})_c$  as

$$(\hat{H}\{e^{\hat{S}}\})_c = \mu_0 + \mu_j^i \tilde{E}_i^j + \frac{1}{2} \mu_{ij}^{kl} \tilde{E}_{kl}^{ij} + \dots, \quad (9.26)$$

we can identify  $g$  with  $\mu$ :

$$g_0 = \mu_0, g_j^i = \mu_j^i, g_{ij}^{kl} = \mu_{ij}^{kl}. \quad (9.27)$$

It follows that all ingredients required to calculate  $\hat{G}_{hole}$  and the residual equation (9.22) can be readily obtained using the APG.

### 9.3 ic-MRCC: $h$ -normal order

Our first attempt is to develop an ic-MRCC method based on  $h$ -normal order, which is a natural extension of the SS-EOMCC method. For biradical-like systems (as discussed in Section 4.2), if we choose  $|0\rangle$  as the vacuum, only up to two-body density matrices are needed for the residual equation. As explained in Section 4.1,  $|0\rangle$  stands for the determinant with all core and active orbitals occupied.

To solve for the semi-internal  $s$ -amplitudes, the three-body metric matrix  $\langle R | (\hat{E}_{ij}^{am})^+ \hat{E}_{kl}^{an} | R \rangle$  is needed, which can be evaluated from one- and two-body density matrices. This matrix is typically nearly singular, and we discuss  $s$ -amplitudes by analogy with the discussion in Chapter 4. Test calculations show that the  $s$ -amplitudes tend to be somewhat large, and that there are serious convergence issues. As for accuracy, the smoothness of potential energy surfaces is not very satisfactory. As we want to make the transition to general active spaces eventually, we proceed to the next level and will discuss a way to avoid convergence problems, to some extent.

### 9.4 ic-MRCC: $\gamma$ -normal order

To avoid large  $s$ -amplitudes and also extend the applicability of ic-MRCC to general active spaces, we also explore the  $\gamma$ -normal order based ic-MRCC method and the idea of renormalization.

In the expression

$$\hat{T}_\lambda^+ \hat{G} = c_0 + c_1 \times \tilde{a}_1 + c_2 \times \tilde{a}_2 + c_3 \times \tilde{a}_3 + \dots, \quad (9.28)$$

the constant term  $c_0$  stands for the fully contracted terms of  $\hat{T}_\lambda^+ \hat{G}$ . That is

$$c_0 = (\hat{T}_\lambda^+ \hat{G})_{f.c.} \quad (9.29)$$

$$= \left( \hat{T}_\lambda^+ \left( (\hat{H}\{e^{\hat{S}}\})_c - ((\{e^{\hat{S}}\} - 1)\hat{G})_c \right) \right)_{f.c.} \quad (9.30)$$

$$= \left( \hat{T}_\lambda^+ (\hat{H}\{e^{\hat{S}}\})_c \right)_{f.c.} - \left( \hat{T}_\lambda^+ ((\{e^{\hat{S}}\} - 1)\hat{G})_c \right)_{f.c.}. \quad (9.31)$$

The first term,  $\left(\hat{T}_\lambda^+(\hat{H}\{e^{\hat{S}}\})_c\right)_{f.c.}$ , is presumably the dominant contribution, because it contains the bare Hamiltonian term  $\left(\hat{T}_\lambda^+(\hat{H})_c\right)_{f.c.}$ , while the second term contains at least t/s-amplitude  $\left(\hat{T}_\lambda^+(\hat{S}\hat{G})_c\right)_{f.c.}$  and t/s-amplitudes are usually small. Let us focus on the first term. In this term, since  $\{e^{\hat{S}}\}$  sits on the right, every hole index in  $\hat{T}_1$  and  $\hat{T}_2$ , which appear as an annihilation operator, must be contracted to a creation index on the left, thus contributing a  $\gamma$ . Therefore, every  $t_a^i$  is accompanied by a  $\gamma_i^k$ , and every  $t_{ab}^{ij}$  is accompanied by a product  $\gamma_i^k\gamma_j^l$ . Similarly, we find that every  $s_{am}^{ij}$  is accompanied by a product  $\gamma_i^k\gamma_j^l\eta_m^n$ , where the one hole density matrix  $\eta_m^n = \delta_m^n - \gamma_m^n$ . Therefore it is possible to define renormalized amplitudes

$$\tilde{t}_a^i = t_a^k\gamma_k^i, \quad (9.32)$$

$$\tilde{t}_{ab}^{ij} = t_{ab}^{kl}\gamma_k^i\gamma_l^j, \quad (9.33)$$

$$\tilde{s}_{am}^{ij} = s_{am}^{kl}\gamma_k^i\gamma_l^j\eta_m^n, \quad (9.34)$$

and rewrite  $\left(\hat{T}_\lambda^+(\hat{H}\{e^{\hat{S}}\})_c\right)_{f.c.}$  fully in terms of  $\tilde{t}$  and  $\tilde{s}$ .

The motivation for renormalized amplitudes can be understood from the example  $\tilde{t}_{ab}^{ij}$ . For simplicity, let us assume using natural orbitals such that the density matrix  $\gamma$  is diagonal for hole orbitals:  $\gamma_j^i = \gamma_i^i\delta_j^i$ , where  $\gamma_i^i$  is the occupation number of the orbital  $i$ . The singularity problem discussed in Chapter 4 comes from the weakly occupied orbitals, and leads to numerical instability. The t-amplitudes will grow rapidly after a few iterations if no threshold is set. For those weakly occupied orbitals, say  $i$  and  $j$ , the corresponding orbital occupation numbers are very small:  $\gamma_i^i \approx 0$  and  $\gamma_j^j \approx 0$ . Therefore  $\tilde{t}_{ab}^{ij}$  is *damped* if one or both orbitals  $i$  and  $j$  are very weakly occupied. Similarly for  $\tilde{s}_{am}^{ij}$ . In  $\tilde{s}_{am}^{ij}$  ( $\tilde{s}_{am}^{ij} = \tilde{s}_{an}^{kl}\tilde{\gamma}_k^i\tilde{\gamma}_l^j\eta_m^n$ ),  $\eta_m^n = \delta_m^n(1 - \gamma_m^m)$ , which is small for a strongly occupied orbital  $m$ . Thus  $\tilde{s}_{am}^{ij}$  is damped for excitations from weakly occupied orbitals to a strongly occupied active orbital. The damping effect is desirable and the numerical instability can be alleviated.

If  $\left(\hat{T}_\lambda^+(\{e^{\hat{S}}\}-1)\hat{G}\right)_{f.c.}$  and non-fully-contracted terms ( $c_1 \times \tilde{a}_1 + c_2 \times \tilde{a}_2 + \dots$ ) are included in  $\hat{T}_\lambda^+\hat{G}$ , the above observation breaks down. The hole indices in  $\hat{T}_1$  and  $\hat{T}_2$  may be contracted



to form  $\eta$ 's or they may be left uncontracted to go to  $\zeta$ 's when evaluating  $\langle R|\hat{T}_\lambda^+\hat{G}|R\rangle$ . However, in this case it is still possible to rewrite the residual equation in terms of  $\tilde{t}/\tilde{s}$  by introducing the inverse density matrix  $\bar{\gamma} = \gamma^{-1}$  and the inverse hole density matrix  $\bar{\eta} = \eta^{-1}$ :

$$t_a^i = t_a^k \delta_k^i = t_a^k (\gamma_k^l \bar{\gamma}_l^i) = \tilde{t}_a^l \bar{\gamma}_l^i, \quad (9.35)$$

$$t_{ab}^{ij} = t_{ab}^{i_1 i_2} \delta_{i_1}^i \delta_{i_2}^j = t_{ab}^{i_1 i_2} \gamma_{i_1}^k \bar{\gamma}_i^k \gamma_{i_2}^l \bar{\gamma}_l^j = (t_{ab}^{i_1 i_2} \gamma_{i_1}^k \gamma_{i_2}^l) \bar{\gamma}_k^i \bar{\gamma}_l^j = \tilde{t}_{ab}^{kl} \bar{\gamma}_k^i \bar{\gamma}_l^j, \quad (9.36)$$

$$\begin{aligned} s_{am}^{ij} &= s_{am_1}^{i_1 i_2} \delta_{i_1}^i \delta_{i_2}^j \delta_m^{m_1} = s_{am_1}^{i_1 i_2} \gamma_{i_1}^k \bar{\gamma}_i^k \gamma_{i_2}^l \bar{\gamma}_l^j \eta_n^{m_1} \bar{\eta}_m^n \\ &= (s_{am_1}^{i_1 i_2} \gamma_{i_1}^k \gamma_{i_2}^l \eta_n^{m_1}) \bar{\gamma}_k^i \bar{\gamma}_l^j \bar{\eta}_m^n = \tilde{s}_{an}^{kl} \bar{\gamma}_k^i \bar{\gamma}_l^j \bar{\eta}_m^n. \end{aligned} \quad (9.37)$$

However,  $\bar{\gamma}_j^i$  is ill-behaved for weakly occupied orbitals, and  $\bar{\eta}_n^m$  is ill-behaved for strongly occupied active orbitals. Large inverse density/hole-density matrices are associated with small  $\zeta$  matrix elements, but contributions from the products of inverse matrices such as  $\bar{\gamma}_j^i \times \bar{\gamma}_l^k \times \bar{\gamma}_y^x \times \bar{\eta}_n^m$  can be expected to be problematic even if  $\zeta$  is small. Approximations are needed to avoid numerical instability associated with them, and the advantage of using renormalized amplitudes is compromised to some extent. Numerical experimentation is needed to determine the effect of using renormalized amplitudes, and to find a satisfactory solution to remaining problems.

We first tested including only fully contracted terms  $c_0$ . As anticipated, the renormalized amplitudes are stable and we did not encounter convergence problems. The metric matrix  $\langle R|(\tilde{E}_{ij}^{am})^+ \tilde{E}_{kl}^{an}|R\rangle_{f.c.}$  is a unit matrix. Fig. 9.1 plots the error curve for the  $^1\Sigma^+$  state of the HF molecule in the 6-31G\*\* basis set, with the active space of (2 e, 2 o) (the  $3\sigma$  and  $4\sigma$  orbitals chosen as the active orbitals). While the accuracy at large bond distances is reasonable, it deteriorates strongly at small bond distances, where the  $4\sigma$  orbital is almost unoccupied and we need to compromise in the use of  $\gamma^{-1}$ .

Fig. 9.2 plots the error curve for the singlet ground state of the  $N_2$  molecule in the cc-pVDZ basis set, with the active space (6 e, 6 o), compared with MRCI+Q results. In this case, the accuracy in the intermediate region is compromised, where cumulants (such as  $\zeta_2$ ) are not small. Therefore, if we only keep fully contracted terms, a large number of terms containing cumulants is discarded, which leads to loss of accuracy. Hence, it seems necessary to include the non-fully-

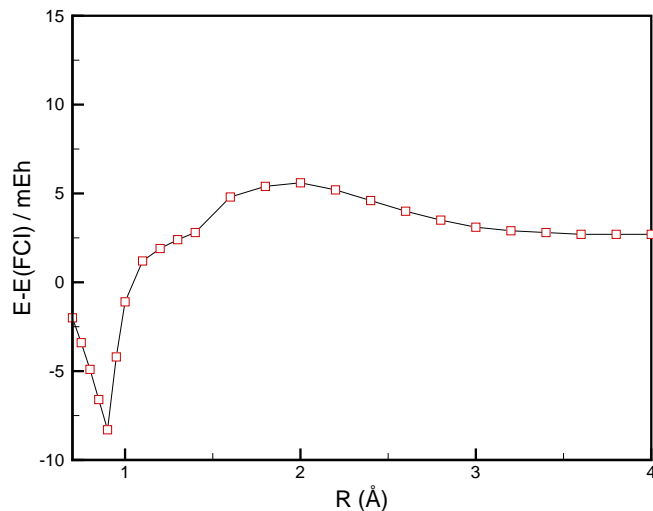


Figure 9.1: Comparison with FCI for HF  $^1\Sigma^+$  state in the 6-31G\*\* basis set.

contracted terms.

Once we include the non-fully-contracted terms, the computational cost increases greatly. In addition, the convergence problem resurfaces again, partly due to the inclusion of the inverse matrices  $\bar{\gamma}_j^i$  and  $\bar{\eta}_n^m$ .

## 9.5 Final remarks

We have not been fortunate in developing a satisfactory internally contracted MRCC method. Important issues which still need to be addressed include: the near singularity issue, better schemes to approximate residual equations and more powerful convergence algorithms, none of which is trivial. The varying single reference and multireference features of the wavefunctions in different situations stand in the way of designing a universal ansatz which works for all cases. The APG has been very powerful in generating equations and subroutines. Unfortunately, we do not yet have a similar generator for good ideas.

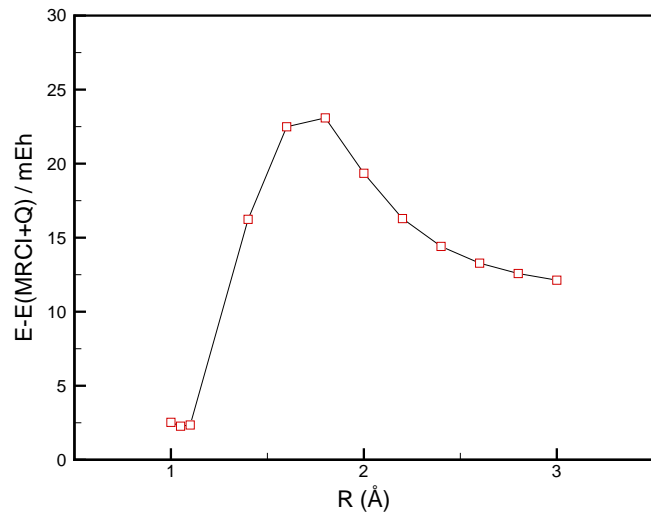


Figure 9.2: Comparison with MRCI+Q for the  $\text{N}_2$  ground state in the cc-pVDZ basis set.

# APPENDICES

## Appendix A

# Supporting information

Table A.1: Comparison with UCCSD(T) for  $F_2$   ${}^3\Sigma_u^-$  state in the cc-pVTZ basis set. The UCCSD(T) energies are in  $E_h$  and other values ( $mE_h$ ) are energy differences vs UCCSD(T). SS-EOMCC computations use an active space of (18 e, 10 o).

R ( $\text{\AA}$ )	UCCSD(T)	UCCSD	SS-EOMCC
1.00	-198.12348	12.29	4.30
1.10	-198.50142	10.45	4.35
1.30	-198.93540	8.80	4.47
1.32	-198.96206	8.70	4.49
1.37	-199.01963	8.48	4.52
1.38	-199.02975	8.44	4.53
1.39	-199.03946	8.40	4.54
1.40	-199.04876	8.36	4.54
1.41	-199.05768	8.33	4.55
1.42	-199.06623	8.29	4.55
1.43	-199.07442	8.26	4.55
1.44	-199.08227	8.23	4.56
1.46	-199.09702	8.17	4.56
1.48	-199.11057	8.11	4.57
1.50	-199.12302	8.06	4.57
1.55	-199.14990	7.95	4.58
1.60	-199.17167	7.86	4.58
1.65	-199.18929	7.78	4.58
1.70	-199.20356	7.72	4.57
1.75	-199.21512	7.66	4.57
1.80	-199.22449	7.62	4.56
1.90	-199.23825	7.55	4.55
2.00	-199.24730	7.51	4.54
2.20	-199.25712	7.45	4.54
2.40	-199.26127	7.41	4.55
2.80	-199.26374	7.38	4.58
3.00	-199.26405	7.37	4.59
3.50	-199.26426	7.36	4.59
4.00	-199.26431	7.35	4.59
4.50	-199.26434	7.35	4.59
5.00	-199.26436	7.35	4.59

Table A.2: Comparison with MRCI+Q for the  $N_2^1\Sigma_g$  state in the cc-pVDZ basis set with the active space (14 e, 10 o). MRCI+Q energies are in  $E_h$  and others are differences from MRCI+Q in  $mE_h$  (SS-EOMCC-3p means that three-body terms are included when diagonalizing the transformed Hamiltonian, refer to Section II).

R ( $\text{\AA}$ )	MRCI+Q	CASPT2	MRCI	AQCC	SS-EOMCC	SS-EOMCC-3p
1.00	-109.23292	18.67	7.74	1.99	5.42	4.07
1.05	-109.26793	18.88	7.93	2.03	5.62	4.16
1.10	-109.28174	19.05	8.10	2.07	5.85	4.29
1.15	-109.28062	19.19	8.27	2.12	6.02	4.36
1.20	-109.26926	19.29	8.45	2.16	6.27	4.51
1.40	-109.17899	19.30	9.19	2.34	7.30	5.12
1.60	-109.08520	18.31	10.04	2.54	8.08	5.57
1.80	-109.02051	15.97	10.77	2.72	8.24	5.49
2.00	-108.98674	14.22	10.94	2.76	7.54	4.95
2.20	-108.97275	14.27	10.72	2.70	6.57	4.34
2.40	-108.96741	14.85	10.50	2.65	5.85	3.85
2.60	-108.96518	15.32	10.36	2.62	5.42	3.55
2.80	-108.96408	15.60	10.27	2.60	5.17	3.37
3.00	-108.96345	15.77	10.22	2.59	5.03	3.26

Table A.3: Comparison with MRCI+Q for the  $N_2^1\Sigma_g$  state in the cc-pVTZ basis set with the active space (14 e, 10 o). MRCI+Q energies are in  $E_h$  and others are differences from MRCI+Q in  $mE_h$  (SS-EOMCC-3p means that three-body terms are included when diagonalizing the transformed Hamiltonian).

R ( $\text{\AA}$ )	MRCI+Q	CASPT2	MRCI	AQCC	SS-EOMCC	SS-EOMCC-3p
1.00	-109.36534	21.14	13.87	3.39	5.88	4.90
1.05	-109.39237	21.19	14.04	3.42	5.87	4.81
1.10	-109.40029	21.18	14.21	3.46	5.93	4.79
1.15	-109.39485	21.09	14.39	3.50	5.95	4.73
1.20	-109.38030	20.94	14.58	3.54	6.04	4.74
1.40	-109.28346	19.66	15.48	3.74	6.47	4.86
1.60	-109.18622	16.98	16.54	3.96	6.76	4.78
1.80	-109.11745	12.73	17.40	4.13	6.50	4.30
2.00	-109.07945	9.63	17.49	4.14	5.55	3.42
2.20	-109.06258	9.32	17.08	4.04	4.47	2.53
2.40	-109.05584	10.04	16.70	3.96	3.67	1.88
2.60	-109.05305	10.71	16.48	3.91	3.22	1.54
2.80	-109.05176	11.15	16.35	3.88	2.97	1.35
3.00	-109.05106	11.42	16.28	3.87	2.83	1.23



Table A.4: Comparison with MRCI+Q for the  $\text{H}_2\text{O}^1A_1$  state in the cc-pVDZ basis set with the active space (1o e, 7 o).  $\angle\text{HOH} = 109.57^\circ$  and O-H bonds are stretched symmetrically. MRCI+Q energies are in  $E_h$  and others are differences from MRCI+Q in  $mE_h$  (SS-EOMCC-3p means that three-body terms are included when diagonalizing the transformed Hamiltonian).

R ( $\text{\AA}$ )	MRCI+Q	CASPT2	MRCI	AQCC	SS-EOMCC	SS-EOMCC-3p
0.90	-76.23442	13.31	5.93	2.20	2.00	1.12
0.95	-76.24279	13.31	6.00	2.22	1.87	0.83
1.00	-76.24056	13.27	6.04	2.23	1.86	0.71
1.05	-76.23097	13.21	6.06	2.24	1.88	0.60
1.10	-76.21645	13.11	6.07	2.24	1.91	0.47
1.20	-76.17918	12.80	6.01	2.22	2.00	0.26
1.40	-76.09740	11.72	5.67	2.09	2.12	0.31
1.60	-76.02778	10.29	5.15	1.90	2.13	0.52
1.80	-75.97771	9.08	4.64	1.71	2.02	0.69
2.00	-75.94606	8.48	4.23	1.57	1.82	0.79
2.20	-75.92849	8.43	3.96	1.47	1.59	0.82
2.40	-75.91970	8.60	3.81	1.41	1.41	0.81
2.60	-75.91546	8.77	3.73	1.38	1.25	0.75
2.80	-75.91337	8.88	3.68	1.37	1.15	0.69
3.00	-75.91229	8.94	3.66	1.36	1.09	0.61
3.20	-75.91172	8.98	3.65	1.35	1.06	0.52
3.40	-75.91140	9.00	3.64	1.35	1.03	0.44
3.60	-75.91123	9.01	3.63	1.35	1.02	0.38
3.80	-75.91112	9.01	3.63	1.35	1.01	0.34
4.00	-75.91106	9.02	3.63	1.35	1.01	0.32

Table A.5: Comparison with MRCI+Q for the  $\text{H}_2\text{O}^1A_1$  state in the cc-pVTZ basis set with the active space (1o e, 7 o).  $\angle\text{HOH} = 109.57^\circ$  and O-H bonds are stretched symmetrically. MRCI+Q energies are in  $E_h$  and others are differences from MRCI+Q in  $mE_h$  (SS-EOMCC-3p means that three-body terms are included when diagonalizing the transformed Hamiltonian).

R ( $\text{\AA}$ )	MRCI+Q	CASPT2	MRCI	AQCC	SS-EOMCC	SS-EOMCC-3p
0.90	-76.33757	15.19	10.15	3.69	3.92	3.49
0.95	-76.34428	15.14	10.31	3.75	3.56	3.02
1.00	-76.34073	15.08	10.46	3.79	3.31	2.74
1.05	-76.33003	15.02	10.57	3.83	3.07	2.47
1.10	-76.31447	14.93	10.66	3.86	2.82	2.15
1.20	-76.27514	14.67	10.73	3.87	2.39	1.43
1.40	-76.18914	13.58	10.45	3.75	1.80	0.72
1.60	-76.11510	11.71	9.69	3.48	1.48	0.38
1.80	-76.06061	9.80	8.73	3.15	1.29	0.28
2.00	-76.02521	8.66	7.86	2.84	1.14	0.31
2.20	-76.00502	8.36	7.22	2.62	1.05	0.39
2.40	-75.99464	8.46	6.84	2.49	0.99	0.47
2.60	-75.98955	8.61	6.64	2.42	0.89	0.46
2.80	-75.98706	8.73	6.54	2.38	0.82	0.41
3.00	-75.98583	8.80	6.48	2.37	0.77	0.35
3.20	-75.98520	8.84	6.45	2.36	0.74	0.26
3.40	-75.98486	8.86	6.44	2.35	0.72	0.18
3.60	-75.98467	8.88	6.43	2.35	0.70	0.13
3.80	-75.98457	8.88	6.42	2.34	0.70	0.09
4.00	-75.98450	8.89	6.42	2.34	0.69	0.06

Table A.6: Comparison with MRCI+Q for the  $\text{CO}^1A_1$  state in the cc-pVDZ basis set with the active space (14 e, 10 o). MRCI+Q energies are in  $E_h$  and others are differences from MRCI+Q in  $mE_h$  (SS-EOMCC-3p means that three-body terms are included when diagonalizing the transformed Hamiltonian).

R ( $\text{\AA}$ )	MRCI+Q	CASPT2	MRCI	AQCC	SS-EOMCC	SS-EOMCC-3p
1.00	-112.99683	20.34	7.90	1.99	5.88	4.90
1.02	-113.01561	20.47	7.96	2.01	5.97	4.95
1.04	-113.03045	20.60	8.02	2.02	6.07	5.00
1.06	-113.04184	20.73	8.09	2.04	6.14	5.01
1.08	-113.05019	20.85	8.15	2.05	6.24	5.06
1.12	-113.05926	21.06	8.26	2.08	6.44	5.16
1.16	-113.06020	21.24	8.38	2.11	6.56	5.17
1.18	-113.05827	21.32	8.44	2.12	6.66	5.21
1.20	-113.05502	21.39	8.49	2.14	6.76	5.26
1.24	-113.04529	21.50	8.60	2.16	6.96	5.35
1.32	-113.01694	21.60	8.83	2.22	7.33	5.51
1.36	-113.00009	21.59	8.94	2.24	7.50	5.57
1.40	-112.98232	21.53	9.05	2.27	7.66	5.63
1.60	-112.89310	20.63	9.64	2.41	8.19	5.74
1.80	-112.81898	18.82	10.24	2.55	8.25	5.48
2.00	-112.76479	16.51	10.73	2.66	7.93	5.04
2.20	-112.72840	14.41	10.98	2.72	7.53	4.77
2.40	-112.70583	13.34	10.95	2.71	7.22	4.73

Table A.7: Comparison with MRCI+Q for the  $\text{CO}^1A_1$  state in the cc-pVTZ basis set with the active space (14 e, 10 o). MRCI+Q energies are in  $E_h$  and others are differences from MRCI+Q in  $mE_h$  (SS-EOMCC-3p means that three-body terms are included when diagonalizing the transformed Hamiltonian).

R ( $\text{\AA}$ )	MRCI+Q	CASPT2	MRCI	AQCC	SS-EOMCC	SS-EOMCC-3p
1.00	-113.12704	22.99	13.84	3.31	7.04	6.47
1.02	-113.14382	23.07	13.91	3.33	7.05	6.46
1.04	-113.15686	23.16	13.99	3.34	7.07	6.46
1.06	-113.16663	23.23	14.06	3.36	7.02	6.37
1.08	-113.17352	23.29	14.13	3.37	7.04	6.34
1.12	-113.18009	23.38	14.28	3.40	7.09	6.29
1.16	-113.17898	23.44	14.42	3.43	7.07	6.19
1.18	-113.17617	23.45	14.50	3.45	7.10	6.18
1.20	-113.17213	23.45	14.57	3.46	7.12	6.16
1.24	-113.16104	23.43	14.72	3.49	7.17	6.14
1.32	-113.13065	23.23	15.03	3.56	7.28	6.09
1.36	-113.11303	23.06	15.18	3.59	7.34	6.07
1.40	-113.09461	22.84	15.34	3.63	7.39	6.05
1.60	-113.00292	21.01	16.16	3.80	7.49	5.85
1.80	-112.92635	18.07	16.95	3.96	7.26	5.32
2.00	-112.86969	14.47	17.59	4.08	6.74	4.65
2.20	-112.83107	11.09	17.90	4.12	6.17	4.01
2.40	-112.80676	9.11	17.83	4.08	5.88	3.76

# Bibliography

- [1] T. Helgaker, P. Jørgensen, and J. Olsen, *Molecular Electronic-Structure Theory* (Wiley, Chichester, 2000).
- [2] F. Coester, Nucl. Phys. **7**, 421 (1958).
- [3] F. Coester and H. Kümmel, Nucl. Phys. **17**, 477 (1960).
- [4] J. Čížek, J. Chem. Phys. **45**, 4256 (1966).
- [5] J. Paldus, J. Čížek, and I. Shavitt, Phys. Rev. A **5**, 50 (1972).
- [6] G. D. Purvis and R. J. Bartlett, J. Chem. Phys. **76**, 1910 (1982).
- [7] Y. S. Lee, S. A. Kucharski, and R. J. Bartlett, J. Chem. Phys. **81**, 5906 (1984).
- [8] G. E. Scuseria and H. F. Schaefer, Chem. Phys. Lett. **152**, 382 (1988).
- [9] J. D. Watts and R. J. Bartlett, J. Chem. Phys. **93**, 6104 (1990).
- [10] K. Raghavachari, G. W. Trucks, J. A. Pople, and M. Head-Gordon, Chem. Phys. Lett. **157**, 479 (1989).
- [11] G. E. Scuseria and T. J. Lee, J. Chem. Phys. **93**, 5851 (1990).
- [12] G. E. Scuseria, Chem. Phys. Lett. **176**, 27 (1991).
- [13] S. A. Kucharski and R. J. Bartlett, J. Chem. Phys. **97**, 4282 (1992).

- [14] J. M. Cullen and M. C. Zerner, *J. Chem. Phys.* **77**, 4088 (1982).
- [15] S. Hirata and R. J. Bartlett, *Chem. Phys. Lett.* **321**, 216 (2000).
- [16] M. Kállay and P. Surján, *J. Chem. Phys.* **113**, 1359 (2000).
- [17] J. Olsen, *J. Chem. Phys.* **113**, 7140 (2000).
- [18] O. Hino, T. Kinoshita, G. K.-L. Garnet, and R. J. Bartlett, *J. Chem. Phys.* **124**, 114311 (2006).
- [19] J. Paldus and J. Planelles, *Theor. Chim. Acta* **89**, 13 (1994).
- [20] X. Li and J. Paldus, *J. Chem. Phys.* **107**, 6257 (1997).
- [21] K. Kowalski and P. Piecuch, *J. Chem. Phys.* **113**, 18 (2000).
- [22] K. Kowalski and P. Piecuch, *J. Chem. Phys.* **120**, 1715 (2003).
- [23] K. Kowalski and P. Piecuch, *J. Chem. Phys.* **122**, 074107 (2005).
- [24] P. Piecuch, M. Wloch, J. R. Gour, and A. Kinal, *Chem. Phys. Lett.* **418**, 467 (2006).
- [25] N. Oliphant and L. Adamowicz, *J. Chem. Phys.* **94**, 1229 (1991).
- [26] P. Piecuch, N. Oliphant, and L. Adamowicz, *J. Chem. Phys.* **99**, 1875 (1993).
- [27] P. Piecuch, S. A. Kucharski, and R. J. Bartlett, *J. Chem. Phys.* **110**, 6103 (1999).
- [28] J. Arponen, *Ann. Phys.* **151**, 311 (1983).
- [29] R. J. Bartlett and J. Noga, *Chem. Phys. Lett.* **150**, 29 (1988).
- [30] R. J. Bartlett, S. A. Kucharski, and J. Noga, *Chem. Phys. Lett.* **155**, 133 (1989).
- [31] R.F. Bishop, J.S. Arponen, E. Pajanne. *Aspects of Many- Body Effects in Molecules and Extended Systems*, Vol. 50, Lecture Notes in Chemistry, D. Mukherjee (Ed.), p. 79, Springer, Berlin (1989).

- [32] R.J. Bartlett, S.A. Kucharski, J. Noga, J.D. Watts, G.W. Trucks. *Many-Body Methods in Quantum Chemistry*, Vol. 52, Lecture Notes in Chemistry, U. Kaldor (Ed.), p. 124, Springer, Berlin (1989).
- [33] P. G. Szalay, M. Nooijen, and R. J. Bartlett, *J. Chem. Phys.* **103**, 281 (1995).
- [34] P. Piecuch and R. J. Bartlett, *Adv. Quantum Chem.* **34**, 295 (1999).
- [35] T. V. Voorhis and M. Head-Gordon, *Chem. Phys. Lett.* **330**, 585 (2000).
- [36] P.-D. Fan, K. Kowalski, and P. Piecuch, *Mol. Phys.* **103**, 2191 (2005).
- [37] I. Lindgren and J. Morrison, *Atomic many-body theory* (Springer, Berlin, 1982).
- [38] D. Mukherjee and S. Pal, *Adv. Quantum Chem.* **20**, 291 (1989).
- [39] J. Paldus and X. Li, *Adv. Chem. Phys.* **110**, 1 (1999).
- [40] D. Mukherjee, R. K. Moitra, and A. Mukhopadhyay, *Mol. Phys.* **33**, 955 (1977).
- [41] I. Lindgren, *Int. J. Quant. Chem.: Symp.* **12**, 33 (1978).
- [42] A. Mukhopadhyay, R. K. Moitra, and D. Mukherjee, *J. Phys. B* **12**, 1 (1979).
- [43] L. Z. Stolarczyk and H. J. Monkhorst, *Phys. Rev. A* **32**, 725 (1985).
- [44] I. Lindgren and D. Mukherjee, *Phys. Rep.* **151**, 93 (1987).
- [45] S. Pal, M. Rittby, R. J. Bartlett, D. Sinha, and D. Mukherjee, *Chem. Phys. Lett.* **137**, 273 (1987).
- [46] S. Pal, M. Rittby, R. J. Bartlett, D. Sinha, and D. Mukherjee, *J. Chem. Phys.* **88**, 4357 (1988).
- [47] B. Jeziorski and J. Paldus, *J. Chem. Phys.* **90**, 2714 (1989).
- [48] C. M. L. Rittby and R. J. Bartlett, *Theor. Chim. Acta* **80**, 469 (1991).
- [49] J. F. Stanton, R. J. Bartlett, and C. M. L. Rittby, *J. Chem. Phys.* **97**, 5560 (1992).

- [50] K. Jankowski, J. Paldus, I. Grabowski, and K. Kowalski, *J. Chem. Phys.* **97**, 7600 (1992).
- [51] M. Nooijen, *J. Chem. Phys.* **104**, 2638 (1996).
- [52] M. Nooijen and R. J. Bartlett, *J. Chem. Phys.* **107**, 6812 (1997).
- [53] D. Jana and D. Mukherjee, *J. Chem. Phys.* **122**, 234101 (2005).
- [54] D. Datta and D. Mukherjee, *Int. J. Quant. Chem.* **108**, 2211 (2008).
- [55] B. Jeziorski and H. J. Monkhorst, *Phys. Rev. A* **24**, 1668 (1981).
- [56] S. A. Kucharski, A. Balková, P. G. Szalay, and R. J. Bartlett, *J. Chem. Phys.* **97**, 4289 (1992).
- [57] J. Paldus, P. Piecuch, L. Pylypow, and B. Jeziorski, *Phys. Rev. A* **47**, 2738 (1993).
- [58] P. Piecuch and J. Paldus, *Phys. Rev. A* **49**, 3479 (1994).
- [59] L. Kong, *Int. J. Quant. Chem.* **109**, 441 (2009).
- [60] I. Hubač,.
- [61] J. Mášik and I. Hubač, in *Quantum Systems in Chemistry and Physics: Trends in Methods and Applications*, edited by R. McWeeny, J. Maruani, Y. G. Smeyers, and S. Wilson (Kluwer Academic, Dordrecht, 1997), pp. 283-308.
- [62] J. Pittner, O. Demel, P. Čársky, and I. Hubač, *Int. J. Quant. Chem.* **90**, 1031 (2002).
- [63] D. Mukherjee, in *Recent Progress in Many-body Theories, Volume 4*, Edited by E. Schachinger, R. Mitter and H. Stormann (Plenum, New York, 1995), Vol. 10.
- [64] U. S. Mahapatra, B. Datta, B. Bandyopadhyay, and D. Mukherjee, *Adv. Quantum Chem.* **30**, 163 (1998).
- [65] U. S. Mahapatra, B. Datta, and D. Mukherjee, *Mol. Phys.* **94**, 157 (1998).
- [66] U. S. Mahapatra, B. Datta, and D. Mukherjee, *J. Chem. Phys.* **110**, 6171 (1999).



- [67] D. Pahari, S. Chattopadhyay, S. Das, and D. Mukherjee, *Chem. Phys. Lett.* **381**, 223 (2003).
- [68] S. Das, N. Bera, S. Ghosh, and D. Mukherjee, *J. Mol. Structure (Theochem)* **771**, 79 (2006).
- [69] F. A. Evangelista, W. D. Allen, and H. F. Schaefer, *J. Chem. Phys.* **125**, 154113 (2006).
- [70] F. A. Evangelista, W. D. Allen, and H. F. Schaefer, *J. Chem. Phys.* **127**, 024102 (2007).
- [71] M. Hanrath, *J. Chem. Phys.* **123**, 084102 (2005).
- [72] M. Hanrath, *J. Chem. Phys.* **128**, 154118 (2008).
- [73] Orbital Invariance Issue in Multireference Methods, L. Kong, submitted (2009).
- [74] A. Banerjee and J. Simons, *Int. J. Quant. Chem.* **19**, 207 (1981).
- [75] A. Banerjee and J. Simons, *J. Chem. Phys.* **76**, 4548 (1982).
- [76] M. R. Hoffmann and J. Simons, *J. Chem. Phys.* **88**, 993 (1988).
- [77] D. Mukherjee, *Chem. Phys. Lett.* **274**, 561 (1997).
- [78] W. Kutzelnigg and D. Mukherjee, *J. Chem. Phys.* **107**, 432 (1997).
- [79] T. Yanai and G. K.-L. Chan, *J. Chem. Phys.* **124**, 194106 (2006).
- [80] T. Yanai and G. K.-L. Chan, *J. Chem. Phys.* **127**, 104107 (2007).
- [81] D. A. Mazziotti, *Phys. Rev. Lett.* **97**, 143002 (2006).
- [82] D. A. Mazziotti, *Phys. Rev. A* **75**, 022505 (2007).
- [83] C. Valdemoro, *Phys. Rev. A* **45**, 4462 (1992).
- [84] H. Nakatsuji and K. Yasuda, *Phys. Rev. Lett.* **76**, 1039 (1996).
- [85] K. Yasuda and H. Nakatsuji, *Phys. Rev. A* **56**, 2648 (1997).
- [86] D. Mazziotti, *Phys. Rev. A* **57**, 4219 (1998).
- [87] W. Kutzelnigg and D. Mukherjee, *J. Chem. Phys.* **110**, 2800 (1999).

- [88] D. Mazziotti, *Chem. Phys. Lett.* **326**, 212 (2000).
- [89] F. E. Harris, *Int. J. Quant. Chem.* **90**, 105 (2002).
- [90] M. Nooijen, M. Wladyslawski, and A. Hazra, *J. Chem. Phys.* **118**, 4832 (2003).
- [91] J. Herbert, *Int. J. Quant. Chem.* **107**, 703 (2007).
- [92] T. Fang and S. H. Li, *J. Chem. Phys.* **127**, 204108 (2007).
- [93] T. Fang, J. Shen, and S. H. Li, *J. Chem. Phys.* **128**, 224107 (2008).
- [94] S. R. White, *Phys. Rev. Lett.* **69**, 2863 (1992).
- [95] S. R. White, *Phys. Rev. B* **48**, 10345 (1993).
- [96] G. K.-L. Chan and M. Head-Gordon, *J. Chem. Phys.* **116**, 4462 (2002).
- [97] D. Zgid and M. Nooijen, *J. Chem. Phys.* **128**, 014107 (2008).
- [98] D. Zgid and M. Nooijen, *J. Chem. Phys.* **128**, 144115 (2008).
- [99] D. Zgid and M. Nooijen, *J. Chem. Phys.* **128**, 144116 (2008).
- [100] D. J. Rowe, *Rev. Mod. Phys.* **40**, 153 (1968).
- [101] K. Emrich, *Nucl. Phys. A* **351**, 379 (1981).
- [102] J. Geertsen, M. Rittby, and R. J. Bartlett, *Chem. Phys. Lett.* **164**, 57 (1989).
- [103] J. F. Stanton and R. J. Bartlett, *J. Chem. Phys.* **98**, 7029 (1993).
- [104] D. Sinha, S. Mukhopadhyay, and D. Mukherjee, *Chem. Phys. Lett.* **129**, 369 (1986).
- [105] A. I. Krylov, *Ann. Rev. Phys. Chem.* **59**, 433 (2008).
- [106] H. J. Monkhorst, *Int. J. Quant. Chem.: Symp.* **11**, 421 (1977).
- [107] D. Mukherjee and P. K. Mukherjee, *Chem. Phys.* **39**, 325 (1979).
- [108] E. Dalgaard and H. J. Monkhorst, *Phys. Rev. A* **28**, 1217 (1983).

- [109] H. Sekino and R. J. Bartlett, *Int. J. Quant. Chem.: Symp.* **18**, 255 (1984).
- [110] H. Koch and P. Jorgensen, *J. Chem. Phys.* **93**, 3333 (1990).
- [111] A. E. Kondo, P. Piecuch, and J. Paldus, *J. Chem. Phys.* **104**, 8566 (1996).
- [112] P. Piecuch and J. Paldus, *J. Math. Chem.* **21**, 51 (1997).
- [113] S. Chattopadhyay, U. S. Mahapatra, and D. Mukherjee, *J. Chem. Phys.* **112**, 7939 (2000).
- [114] H. Nakatsuji and K. Hirao, *J. Chem. Phys.* **68**, 2053 (1977).
- [115] H. Nakatsuji, *Chem. Phys. Lett.* **59**, 362 (1978).
- [116] H. Nakatsuji, *Chem. Phys. Lett.* **67**, 329 (1979).
- [117] M. Nooijen and J. Snijders, *Int. J. Quant. Chem.: Symp.* **26**, 55 (1992).
- [118] M. Nooijen and J. Snijders, *Int. J. Quant. Chem.* **48**, 15 (1993).
- [119] M. Nooijen and J. Snijders, *J. Chem. Phys.* **102**, 1681 (1995).
- [120] M. Nooijen and R. J. Bartlett, *J. Chem. Phys.* **102**, 3629 (1995).
- [121] M. Nooijen and R. J. Bartlett, *J. Chem. Phys.* **102**, 6735 (1995).
- [122] J. F. Stanton and J. Gauss, *J. Chem. Phys.* **101**, 8938 (1994).
- [123] M. Wladyslawski and M. Nooijen, *ACS Symp. Ser.* **828**, 65 (2002).
- [124] K. W. Sattelmeyer, H. F. Schaefer, and J. F. Stanton, *Chem. Phys. Lett.* **378**, 42 (2003).
- [125] A. I. Krylov, *Chem. Phys. Lett.* **338**, 375 (2001).
- [126] A. I. Krylov, *Acc. Chem. Res.* **39**, 83 (2006).
- [127] M. Nooijen, K. R. Shamasundar, and D. Mukherjee, *Mol. Phys.* **103**, 2277 (2005).
- [128] H. Koch, H. J. A. Jensen, P. Jørgensen, and T. Helgaker, *J. Chem. Phys.* **93**, 3345 (1990).
- [129] L. Meissner and R. J. Bartlett, *J. Chem. Phys.* **102**, 7490 (1995).

- [130] M. Hanrath, Chem. Phys. Lett. **420**, 426 (2006).
- [131] This possibility was suggested to the author by Francesco A. Evangelista, Center for Computational Chemistry, the University of Georgia.
- [132] J. Pittner, J. Chem. Phys. **118**, 10876 (2003).
- [133] J. Pittner, J. Smydke, P. Čársky, and I. Hubač, J. Mol. Structure (Theochem) **547**, 239 (2001).
- [134] I. Hubač and S. Wilson, J. Phys. B **33**, 365 (2000).
- [135] J. Mášik and I. Hubač, Adv. Quantum Chem. **31**, 75 (1999).
- [136] S. Chattopadhyay, U. S. Mahapatra, and D. Mukherjee, J. Chem. Phys. **111**, 3820 (1999).
- [137] F. A. Evangelista, A. C. Simmonett, W. D. Allen, H. F. Schaefer, and J. Gauss, J. Chem. Phys. **128**, 124104 (2008).
- [138] W. Meyer, Int. J. Quant. Chem.: Symp. **5**, 341 (1971).
- [139] W. Meyer, J. Chem. Phys. **58**, 1017 (1972).
- [140] R. Ahlrichs, H. Lischka, V. Staemmler, and W. Kutzelnigg, J. Chem. Phys. **62**, 1225 (1975).
- [141] J. P. Daudey, J. L. Heully, and J. P. Malrieu, J. Chem. Phys. **99**, 1240 (1993).
- [142] M. Nooijen and R. J. L. Roy, J. Mol. Structure (Theochem) **768**, 25 (2006).
- [143] I. S. Sokolnikoff, *Tensor Analysis: Theory and Applications to Geometry and Mechanics of Continua* (Wiley, New York, 1967).
- [144] M. Head-Gordon, P. E. Maslen, and C. A. White, J. Chem. Phys. **108**, 616 (1998).
- [145] H.-J. Werner and E.-A. Reinsch, J. Chem. Phys. **76**, 3144 (1982).
- [146] H.-J. Werner, J. Chem. Phys. **89**, 5803 (1988).
- [147] R. J. Gdanitz and R. Ahlrichs, Chem. Phys. Lett. **143**, 413 (1988).

- [148] P. J. Knowles and H.-J. Werner, *Chem. Phys. Lett.* **145**, 514 (1988).
- [149] P. Piecuch and L. Adamowicz, *J. Chem. Phys.* **100**, 5792 (1994).
- [150] A. Szabo and N. S. Ostlund, *Modern Quantum Chemistry: Introduction to Advanced Electronic Structure Theory* (McGraw-Hill, New York, 1989).
- [151] Section 40, I. S. Sokolnikoff, *Tensor Analysis: Theory and Applications to Geometry and Mechanics of Continua* (Wiley, New York, 1967).
- [152] P. Piecuch and L. Adamowicz, *Chem. Phys. Lett.* **221**, 121 (1994).
- [153] I. Hubač, J. Pittner, and P. Čársky, *J. Chem. Phys.* **112**, 8779 (2000).
- [154] M. R. Hoffmann and J. Simons, *Chem. Phys. Lett.* **142**, 451 (1987).
- [155] M. Nooijen, *Int. J. Mol. Sci.* **3**, 656 (2002).
- [156] L. Kong and M. Nooijen, *Int. J. Quant. Chem.* **108**, 2097 (2008).
- [157] A. I. Krylov, *Chem. Phys. Lett.* **350**, 522 (2001).
- [158] L. V. Slipchenko and A. I. Krylov, *J. Chem. Phys.* **117**, 4694 (2002).
- [159] K. Jankowski, K. Rubinić, and P. Sterna, *Chem. Phys. Lett.* **277**, 275 (1997).
- [160] K. Jankowski, K. Rubinić, and P. Sterna, *Mol. Phys.* **94**, 29 (1998).
- [161] K. Jankowski, L. Meissner, and K. Rubinić, *J. Mol. Structure (Theochem)* **547**, 55 (2001).
- [162] K. Jankowski and K. Rubinić, *Mol. Phys.* **100**, 1741 (2002).
- [163] K. Jankowski, K. Nowakowski, and J. Wasilewski, *Chem. Phys. Lett.* **389**, 393 (2004).
- [164] O. Demel, K. R. Shamasundar, L. Kong, and M. Nooijen, *J. Phys. Chem. A* **112**, 11895 (2008).
- [165] P. Pulay, *Chem. Phys. Lett.* **73**, 393 (1980).
- [166] D. W. Smith and O. W. Day, *J. Chem. Phys.* **62**, 113 (1975).

- [167] P.-O. Löwdin, *J. Chem. Phys.* **18**, 365 (1950).
- [168] J. D. Watts and R. J. Bartlett, *Spectrochimica Acta Part A* **55**, 495 (1999).
- [169] A. J. Sadlej, *Coll. Czech. Chem. Commun* **53**, 1995 (1988).
- [170] P. Piecuch, K. Kowalski, I. S. O. Pimienta, P.-D. Fan, M. Lodriguito, M. J. McGuire, S. A. Kucharski, T. Kuś, and M. Musiał, *Theor. Chim. Acta* **112**, 349 (2004).
- [171] J. E. Subotnik, A. Sodt, and M. Head-Gordon, *J. Chem. Phys.* **125**, 074116 (2006).
- [172] G. C. Wick, *Phys. Rev.* **80**, 268 (1950).
- [173] D. Mukherjee, *Chem. Phys. Lett.* **317**, 567 (2000).
- [174] D. Mukherjee and W. Kutzelnigg, *J. Chem. Phys.* **114**, 2047 (2001).
- [175] W. Kutzelnigg and D. Mukherjee, *J. Chem. Phys.* **116**, 4787 (2002).
- [176] W. Kutzelnigg and D. Mukherjee, *J. Chem. Phys.* **120**, 7340 (2004).
- [177] W. Kutzelnigg and D. Mukherjee, *J. Chem. Phys.* **120**, 7350 (2004).
- [178] M. Nooijen and R. J. Bartlett, *J. Chem. Phys.* **104**, 2652 (1996).
- [179] H. C. Wong and J. Paldus, *Comp. Phys. Commun.* **6**, 1 (1973).
- [180] H. C. Wong and J. Paldus, *Comp. Phys. Commun.* **6**, 9 (1973).
- [181] S. Hirata, *J. Phys. Chem. A* **107**, 9887 (2003).
- [182] A. A. Auer, G. Baumgartner, D. E. Bernholdt, A. Bibireata, V. Choppella, D. Cociorva, X. Y. Gao, R. Harrison, S. Krishnamoorthy, S. Krishnan, C. C. Lam, Q. D. Lu, *et al.*, *Mol. Phys.* **104**, 211 (2006).
- [183] C. E. Dykstra and P. G. Jasien, *Chem. Phys. Lett.* **109**, 388 (1984).
- [184] C. E. Dykstra, *J. Chem. Phys.* **82**, 4120 (1985).

- [185] P. J. Knowles, K. Somasundram, N. C. Handy, and K. Hirao, *Chem. Phys. Lett.* **113**, 8 (1985).
- [186] N. C. Handy, P. J. Knowles, and K. Somasundram, *Theor. Chem. Acc.* **68**, 87 (1985).
- [187] K. Hald, P. Jorgensen, J. Olsen, and M. Jaszunski, *J. Chem. Phys.* **115**, 617 (2001).
- [188] M. Kállay and P. Surján, *J. Chem. Phys.* **115**, 2945 (2001).
- [189] M. Kállay, P. G. Szalay, and P. R. Surján, *J. Chem. Phys.* **117**, 980 (2002).
- [190] C. L. Janssen and H. F. Schaefer, *Theor. Chem. Acc.* **79**, 1 (1991).
- [191] X. Li and J. Paldus, *J. Chem. Phys.* **101**, 8812 (1994).
- [192] F. E. Harris, *Int. J. Quant. Chem.* **75**, 593 (1999).
- [193] A. D. Bochevarov and C. D. Sherrill, *J. Chem. Phys.* **121**, 3374 (2004).
- [194] T. D. Crawford, T. J. Lee, and H. F. Schaefer, *J. Chem. Phys.* **107**, 7943 (1997).
- [195] P. J. Knowles and N. C. Handy, *Chem. Phys. Lett.* **111**, 315 (1984).
- [196] J. Olsen, B. O. Roos, P. Jorgensen, and H. J. A. Jensen, *J. Chem. Phys.* **89**, 2185 (1988).
- [197] R. J. Harrison and S. Zarrabian, *Chem. Phys. Lett.* **158**, 393 (1989).
- [198] C. D. Sherrill and H. F. Schaefer, *Adv. Quantum Chem.* **34**, 143 (1999).
- [199] M. Nooijen and V. Lotrich, *J. Mol. Structure (Theochem)* **547**, 253 (2001).
- [200] M. Wladyslawski and M. Nooijen, *Adv. Quantum Chem.* **49**, 1 (2005).
- [201] S. Hirata, *Theor. Chem. Acc.* **116**, 2 (2006).
- [202] M. Lutz and D. Ascher, *Learning Python* (O'Reilly Media, Inc, 2003), ISBN 10: 1-56592-464-9, ISBN-13: 978-0596002817.

- [203] G. Baumgartner, D. E. Bernholdt, D. Cociorva, R. Harrison, C. C. Lam, M. Nooijen, and J. Ramanujam, in *Proc. Int'l Workshop on High-Level Parallel Programming Models and Supportive Environments (held in conjunction with IEEE Int'l Parallel and Distributed Processing Symposium (IPDPS))* (2002), pp. 106–114.
- [204] ACES II is a program product of the Quantum Theory Project, University of Florida. Authors: J.F. Stanton, J. Gauss, S.A. Perera, J.D. Watts, A.D. Yau, M. Nooijen, N. Oliphant, P.G. Szalay, W.J. Lauderdale, S.R. Gwaltney, S. Beck, A. Balková, D.E. Bernholdt, K.K. Baeck, P. Rozyczko, H. Sekino, C. Huber, J. Pittner, W. Cencek, D. Taylor, and R.J. Bartlett. Integral packages included are VMOL (J. Almlöf and P.R. Taylor); VPROPS (P. Taylor); ABACUS (T. Helgaker, H.J. Aa. Jensen, P. Jørgensen, J. Olsen, and P.R. Taylor); HONDO/GAMESS (M.W. Schmidt, K.K. Baldridge, J.A. Boatz, S.T. Elbert, M.S. Gordon, J.J. Jensen, S. Koseki, N. Matsunaga, K.A. Nguyen, S. Su, T.L. Windus, M. Dupuis, J.A. Montgomery).
- [205] M. Nooijen and K. R. Shamasundar, *Coll. Czech. Chem. Commun* **70**, 1082 (2005).
- [206] MOLPRO is a package of ab initio programs written by H. J. Werner, P. J. Knowles, R. D. Amos, A. Berning, D. L. Cooper, M. J. O. Deegan, A. J. Dobbyn, F. Eckert, S. T. Elbert, C. Hampel, R. Lindh, A. W. Lloyd, W. Meyer, A. Nicklass, K. Peterson, R. Pitzer, A. J. Stone, P. R. Taylor, M. E. Mura, P. Pulay, M. Schutz, H. Stoll, and T. Thoorsteinsso.
- [207] T. H. Dunning, *J. Chem. Phys.* **90**, 1007 (1989).
- [208] K. Anderson, P.-A. Malmqvist, B. O. Roos, A. J. Sadlej, and K. Wolinski, *J. Phys. Chem.* **94**, 5483 (1990).
- [209] K. Anderson, P.-A. Malmqvist, and B. O. Roos, *J. Chem. Phys.* **96**, 1218 (1992).
- [210] P. G. Szalay and R. J. Bartlett, *Chem. Phys. Lett.* **214**, 481 (1993).
- [211] P. G. Szalay and R. J. Bartlett, *J. Chem. Phys.* **103**, 3600 (1995).
- [212] E. I. Solomon, M. J. Baldwin, and M. D. Lowery, *Chem. Rev.* **92**, 521 (1992).



- [213] N. Kitajima and Y. Moro-oka, *Chem. Rev.* **94**, 737 (1994).
- [214] W. Kaim and D.-C. J. Rall, *J. Angew. Chem. Int. Ed. Engl.* **35**, 43 (2003).
- [215] J. P. Klinman, *Chem. Rev.* **96**, 2541 (1996).
- [216] E. I. Solomon, U. M. Sundaram, and T. E. Machonkin, *Chem. Rev.* **96**, 2563 (1996).
- [217] E. I. Solomon, P. Chen, M. Metz, S.-K. Lee, and A. E. Palmer, *J. Angew. Chem. Int. Ed. Engl.* **40**, 4570 (2001).
- [218] H. Decker, R. Dillinger, and F. Tucek, *J. Angew. Chem. Int. Ed. Engl.* **39**, 1591 (2000).
- [219] P. Gamez, I. A. Koval, and J. Reedijk, *Dalton Trans.* **24**, 4079 (2004).
- [220] E. I. Solomon, F. Tucek, D. E. Root, and C. A. Brown, *Chem. Rev.* **94**, 827 (1994).
- [221] W. B. Tolman, *Acc. Chem. Res.* **30**, 227 (1997).
- [222] L. M. Mirica, X. Ottenwaelder, and T. D. P. Stack, *Chem. Rev.* **104**, 1013 (2004).
- [223] E. A. Lewis and W. B. Tolman, *Chem. Rev.* **104**, 1047 (2004).
- [224] A. P. Cole, V. Mahadevan, L. M. Mirica, X. Ottenwaelder, and T. D. P. Stack, *Inorg. Chem.* **44**, 7345 (2005).
- [225] J. Shearer, C. X. Zhang, L. N. Zakharov, A. L. Rheingold, and K. D. Karlin, *J. Am. Chem. Soc.* **127**, 5469 (2005).
- [226] L. Q. Hatcher, M. A. Vance, A. A. N. Sarjeant, E. I. Solomon, and K. D. Karlin, *Inorg. Chem.* **45**, 3004 (2006).
- [227] W. B. Tolman, *J. Biol. Inorg. Chem.* **11**, 261 (2006).
- [228] T. Lind, P. E. M. Siegbahn, and R. H. Crabtree, *J. Phys. Chem. B* **103**, 1193 (1999).
- [229] P. E. M. Siegbahn, *J. Biol. Inorg. Chem.* **8**, 577 (2003).
- [230] P. E. M. Siegbahn and M. Wirstam, *J. Am. Chem. Soc.* **123**, 11819 (2001).

- [231] M. F. Rode and H.-J. Werner, *Theor. Chem. Acc.* **114**, 309 (2005).
- [232] C. J. Cramer, M. Wloch, P. Piecuch, C. Puzzarini, and L. Gagliardi, *J. Phys. Chem. A* **110**, 1991 (2006).
- [233] C. J. Cramer, A. Kinal, M. Wloch, P. Piecuch, and L. Gagliardi, *J. Phys. Chem. A* **110**, 11557 (2006).
- [234] J. L. Lewin, D. E. Heppner, and C. J. Cramer, *J. Biol. Inorg. Chem.* **12**, 1221 (2007).
- [235] T. D. P. Stack, *Dalton Trans.* pp. 1881–1889 (2003).
- [236] M. Wloch, J. R. Gour, K. Kowalski, and P. Piecuch, *J. Chem. Phys.* **122**, 214107 (2005).
- [237] K. Kowalski and P. Piecuch, *Chem. Phys. Lett.* **344**, 165 (2001).
- [238] M. J. McGuire, K. Kowalski, and P. Piecuch, *J. Chem. Phys.* **117**, 3617 (2002).
- [239] M. J. McGuire, P. Piecuch, K. Kowalski, S. A. Kucharski, and M. Musiaã, *J. Phys. Chem. A* **108**, 8878 (2004).
- [240] K. Kowalski and P. Piecuch, *J. Chem. Phys.* **113**, 5644 (2000).
- [241] M. J. McGuire and P. Piecuch, *J. Am. Chem. Soc.* **127**, 2608 (2005).
- [242] A. Kinal and P. Piecuch, *J. Phys. Chem. A* **110**, 367 (2006).
- [243] A. Kinal and P. Piecuch, *J. Phys. Chem. A* **111**, 734 (2007).
- [244] S. Nangia, D. G. Truhlar, M. J. McGuire, and P. Piecuch, *J. Phys. Chem. A* **109**, 11643 (2005).
- [245] X. Li and J. Paldus, *J. Chem. Phys.* **119**, 5346 (2003).
- [246] [Http://www.molpro.net/infor/current/molpro\\_basis?element=Cu&basis=ECP10MWB&print=1](http://www.molpro.net/infor/current/molpro_basis?element=Cu&basis=ECP10MWB&print=1).
- [247] M. Dlog, U. Wedig, H. Stoll, and H. J. Preuss, *J. Chem. Phys.* **86**, 866 (1987).
- [248] P.-O. Widmark, P. Å. Malmqvist, and B. O. Roos, *Theor. Chim. Acta* **77**, 291 (1990).

- [249] Basis sets were obtained from the Extensible Computational Chemistry Environment Basis Set Database, Version 02/02/06, as developed and distributed by the Molecular Science Computing Facility, Environmental and Molecular Sciences Laboratory which is part of the Pacific Northwest Laboratory, P.O. Box 999, Richland, Washington 99352, USA, and funded by the U.S. Department of Energy. The Pacific Northwest Laboratory is a multi-program laboratory operated by Battelle Memorial Institute for the U.S. Department of Energy under contract DE-AC06-76RLO 1830. Contact Karen Schuchardt for further information.
- [250] M. J. Frisch, G. W. Trucks, H. B. Schlegel, G. E. Scuseria, M. A. Robb, J. R. Cheeseman, J. A. Montgomery, Jr., T. Vreven, K. N. Kudin, J. C. Burant, J. M. Millam, S. S. Iyengar, *et al.*, *Gaussian 03, Revision C.02*, Gaussian, Inc., Wallingford, CT, 2004.